UNIVERSITÀ
DEGLI STUDI
DI PADOVA

Università degli Studi di Padova
Dipartimento di Biologia

SCUOLA DI DOTTORATO DI RICERCA IN

BIOSCIENZE E BIOTECNOLOGIE

INDIRIZZO GENETICA E BIOLOGIA MOLECOLARE DELLO SVILUPPO

CICLO XXVIII

Antimicrobial peptide-mediated immune response in four *Bombyx mori* strains infected with Gram-positive and -negative pathogens

Direttore della Scuola: Ch.mo Prof. Paolo Bernardi

Coordinatore d'indirizzo: Ch.mo Prof. Rodolfo Costa

Supervisore: Ch.ma Prof. Federica Sandrelli

Dottoranda: Ottavia Romoli

Index

Abstract

The domesticated silkworm *Bombyx mori* is an important organism for its intrinsic economic and biotechnological value, but also for representing a model organism for *Lepidoptera* genetics.

Silkworm strains can be grouped into four geographical types (Japanese, Chinese, European and Tropical) characterized by a different resistance to infections, which is inversely correlated to the silk productivity. The aim of this project was to characterize which are the main elements of the immune response protecting *Bombyx mori* against pathogen infections, with the final purpose to obtain silkworms enhanced in their pathogen-resistance, but still maintaining good production capabilities. To achieve this objective, two main approaches have been used: 1) the characterization of the humoral immune response to oral infection of four *B. mori* strains originating from Japan, China, Europe and India, focusing on antimicrobial peptides (AMPs), important effectors of the innate immunity; 2) the production and characterization of transgenic silkworms over-expressing specific AMPs.

We first characterized the four strain under germ-free conditions for the structure of their peritrophic membranes and intestinal *epithelia*, which represent the first barriers for oral infection. Moreover, we evaluated the genetic variability of the four strains at the level of the 21 *B. mori* AMP genes, identifying several amino acid substitutions in the active portion of peptides.

To determine the possible differential sensitivity to microbial attack, we performed infection experiments in which each *B. mori* line was exposed to two silkworm pathogens, the Gram-positive *Enterococcus mundtii* or the Gram-negative *Serratia marcescens*. After a 24h oral infection, the differential response to pathogens of the four strains was determined by comparing 1) the survival profiles, 2) the presence of living pathogen cells in the hemolymph circulation, 3) the expression induction of 9 representative AMP genes in the tissues involved in the immune response (fat bodies and midgut), 4) the *in vitro* antimicrobial activity of the silkworm hemolymph, 5) the Lysozyme concentration in larvae plasma and 6) the rate of the melanization reaction.

Regarding the *E. mundtii* infection, the European line was found to be the most resistant, followed by the Chinese, the Indian and the Japanese strains. Our data suggest that the key resistance factor might consist in the AMP classes and/or isoforms produced in the European strain at both local and systemic levels.

Regarding the *S. marcescens* infection, the Indian strain was completely resistant, while none of the other three strains survived to the microbial exposure. We found a general correlation between the survival profile and the systemic AMP transcription

activation. In fact, the Indian line was the only one which showed a systemic induction of most AMPs and in which no viable bacteria were found in the hemolymph. Further analyses are required to explore whether this strain-specific resistance is due to more efficient mechanisms in the Gram-negative recognition process or in the signal transduction pathway activation.

In order to obtain transgenic silkworm strains with enhanced pathogen resistance, we generated three different piggyBac-based constructs to achieve the over-expression of *moricin*, *gloverin2* or *cecropinB* at the level of fat bodies. Currently, 2 independent lines over-expressing *moricin* have been obtained and are under evaluation for their resistance to infections.

Riassunto

Il baco da seta, *Bombyx mori*, oltre a possedere un'importanza economica intrinseca, è ampiamente utilizzato sia come sistema modello per i Lepidotteri, che nel campo delle biotecnologie.

In seguito alla domesticazione si sono originati numerosi ceppi, che possono essere classificati sulla base della loro origine geografica in giapponesi, cinesi, europei e tropicali. In genere, i ceppi che provengono dalle aree temperate mostrano una maggiore produttività, ma anche una più alta suscettibilità alle infezioni, mentre i ceppi di origine tropicale risultano essere più resistenti alle infezioni.

Lo scopo di questo progetto consisteva nell'identificare quali potessero essere gli elementi chiave della resistenza del *B. mori* alle infezioni. Il fine ultimo era di creare dei ceppi di baco da seta che fossero più tolleranti ai patogeni, ma che mantenessero comunque buone capacità produttive. Per raggiungere questi obiettivi, sono stati utilizzate due principali strategie: 1) la caratterizzazione della risposta immunitaria indotta da infezioni orali di quattro ceppi di baco da seta originatisi rispettivamente in Giappone, Cina, Europa ed India, ponendo particolare attenzione sui peptidi antimicrobici (AMP), i principali effettori dell'immunità innata; 2) la produzione e la caratterizzazione di linee transgeniche over-esprimenti i geni codificanti gli AMP.

In primo luogo abbiamo caratterizzato la morfologia delle membrane peritrofiche e degli epiteli intestinali dei quattro ceppi allevati in condizioni sterili. Queste strutture rappresentano la prima barriera fisica durante le infezioni orali. Successivamente, abbiamo valutato la variabilità genetica dei quattro ceppi a livello dei 21 geni codificanti per gli AMP di *B. mori*, identificando numerose sostituzioni amminoacidiche nella porzione attiva dei peptidi.

Abbiamo quindi sottoposto i quattro ceppi ad infezione orale con due batteri, specifici patogeni del baco da seta: *Enterococcus mundtii*, Gram-positivo, e *Serratia marcescens*, Gram-negativo. In seguito ad un'infezione di 24 ore abbiamo valutato la risposta differenziale dei quattro ceppi confrontando: 1) i profili di sopravvivenza, 2) la presenza di cellule batteriche vive nell'emolinfa, 3) l'induzione dell'espressione dei geni codificanti 9 AMP rappresentativi, 4) l'attività antimicrobica dell'emolinfa, 5) la concentrazione del Lisozima nel plasma, 6) la velocità di melanizzazione dell'emolinfa.

Per quanto riguarda l'infezione con *E. mundtii*, il ceppo europeo è risultato essere il più resistente, seguito dal cinese, dall'indiano e dal giapponese. I dati ottenuti indicano che le classi e i tipi di AMP prodotti dal ceppo europeo, sia a livello locale che a quello sistemico, possano essere l'effettiva causa della maggiore resistenza di questo ceppo.

A seguito dell'infezione con *S. marcescens,* il ceppo Indiano si è rivelato essere totalmente resistente a questo patogeno, mentre nessuno degli altri tre ceppi è sopravvissuto all'infezione. Abbiamo trovato una generale correlazione tra il profilo di sopravvivenza e l'attivazione sistemica degli AMP. Infatti nell'emolinfa dei bachi da seta indiani non sono state isolate cellule batteriche di *S. marcescens* e solamente questo ceppo ha mostrato un'induzione della trascrizione della maggior parte degli AMP. Sono necessarie ulteriori analisi per verificare se il ceppo indiano possieda meccanismi di riconoscimento o vie di trasduzione del segnale più efficaci per questo tipo di infezione.

Infine sono stati generati tre differenti costrutti basati sull'elemento trasponibile piggyBac per ottenere ceppi di baco da seta transgenici con una maggiore resistenza alle infezioni. Sono state ottenute due linee indipendenti over-esprimenti il gene per la Moricina. Al momento si stanno caratterizzando queste linee per verificare la loro resistenza alle infezioni.

Chapter 1: Introduction to *Bombyx mori* and Insect Immunity

The Silkworm *Bombyx mori* and the Sericulture

The Life Cycle of *Bombyx mori*

The silkworm *Bombyx mori* belongs to the Order of *Lepidoptera* and, together with its ancestor *Bombyx mandarina*, it is part of the *Bombycidae* family. The silkworm is a domesticated insect and its survival totally depends on human intervention on tightly controlled rearing conditions. Silkworms have been selected for centuries for their economic value, to the detriment of some characters essential to their survival in nature. In particular their monophagy (silkworms only eat mulberry leaves) and the moths inability to fly, make silkworms unsuited to autonomous survival the wild.

B. mori is a holometabolous insect, with a life cycle which lasts about 45 days and comprises different developmental stages: embryo, larva, pupa and adult. Figure 1 shows all the stages of the *B. mori* development.

First, eggs are deposited by the female moth. At this point, depending on the silkworm strain, two alternative scenarios may occur. Polyvoltine strains, which are able to reproduce continuously during the year, typically originate from tropical areas where mulberry leaves are constantly available. Therefore the embryo development inside the egg begins immediately, without facing any diapause period. Monovoltine lines, on the other hand, can reproduce their life cycle only one times per annum: they typically originate from temperate regions in which mulberry leaves are only seasonally available. For this reason, 48 h after laying their eggs in summer, these strains face a diapause period in which the embryo development is arrested, until the arrival of spring.

After the embryo development has been completed, the larva hatches from the egg and follows four molting periods: the first instar (which lasts 3-4 days), the second and the third instars (2-3 days each), the fourth larval stage (4 days) and the fifth instar (6-8 days). During the whole larval development, *B. mori* ingests high amounts of food. After the last instar, larvae prepare to metamorphosis: they completely empty their gut and their cuticle becomes translucent. At the same time, larvae cling to a support, such as branches, on which they start to spin the cocoon. Silk fibers are composed by two proteins, Sericin and Fibroin, which are assembled into one single thread inside the silk gland, and secreted through a small spinneret located in the larva mouth.

Once inside the protective cocoon shell, the silkworm undergoes two more molts which lead, after 4 days, to the pupa development and, after 10-12 days, to the reaching of the adult stage.

During the adult phase, moth mates and each female lays up to 500 eggs, which are fertilized during deposition. Since adult moths are unable to eat, they die few days after emerging from the cocoon.

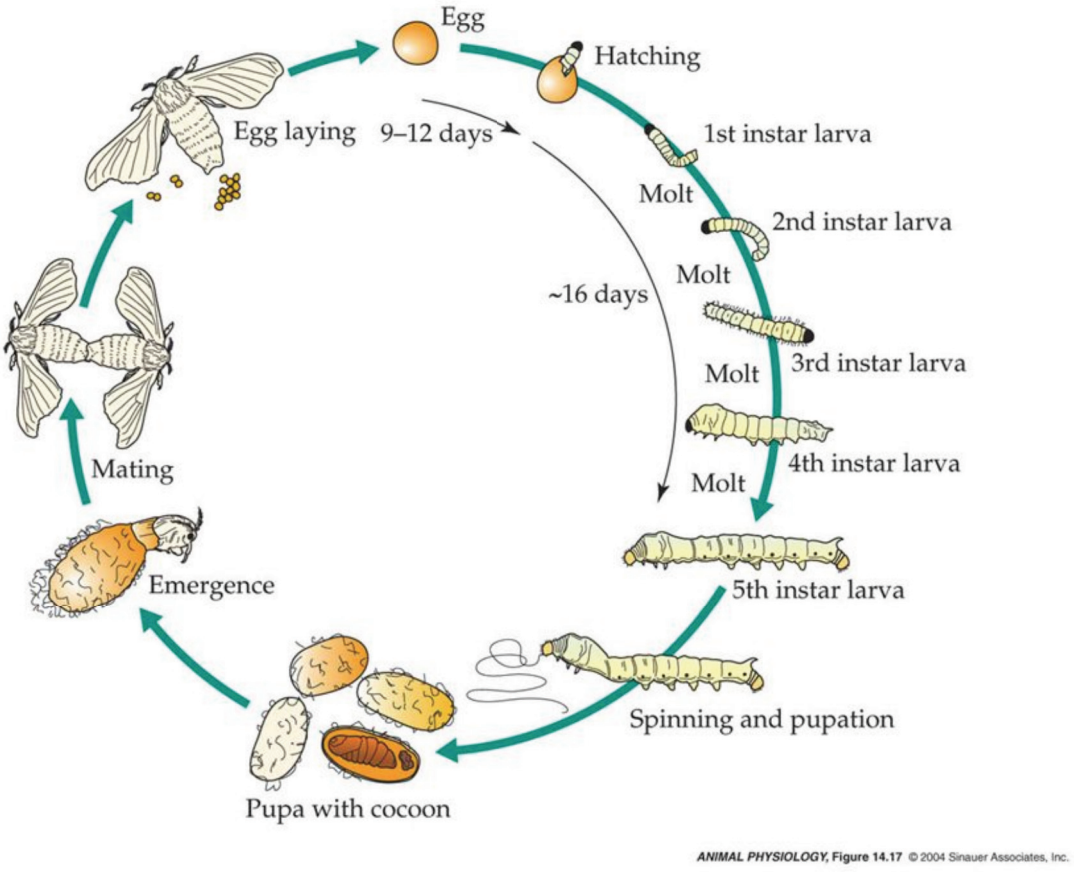

Figure 1. *Bombyx mori* life cycle. From Hill et al, 2004.

Brief Sericulture History

The silkworm rearing tradition has a prehistoric origin: first evidences of sericulture date back to the Neolithic period, around 2500 BC (Sun et al, 2012). Silk farming originated in Asian countries, even if it is difficult to precisely ascertain if this ancient tradition was first established in China or in India. However, the details of sericulture were kept secret for centuries by the Asian empires, since neither Greeks nor Romans knew that silk was produced by insects. In the Chinese empire severe laws

were promulgated to punish with the death penalty whoever tried to export silkworm eggs.

Procopious recounts that in 551 AD, two monks exported the first silkworm eggs from the Chinese empire, hiding them in their canes and bringing them to the Roman emperor Justinian.

Sericulture then spread to the Eastern Europe and, later, to Spain, south Italy, France and Austria. Between the XI and the XVII centuries, Italy effectively had the monopoly of European silk production and manufacturing, also thanks to the diffusion, in 1434, of the white mulberry *Morus alba.* This *Morus* species was able to grow in a wide variety of climatic regions and represented a more appropriate food for silkworms, favoring the diffusion of this species to the detriment of *Morus niger*.

Starting from the XVII century, the Italian primacy was replaced by the England, Germany and, above all, France, especially due to the industrialization of the silk manufacturing process that took place in those countries.

The gradual fall of the European silk production was first caused by great pébrine epidemics, which developed from 1850 and required the import of Japanese silkworm eggs. Furthermore the following Word Wars worsened the European silk industry. In recent history, Italian and European silk farming were strongly reduced for several reasons related to industrialization, including the abandonment of the countryside in favor of urbanized areas and the increasing pollution and insecticide uses that were found to be responsible for the inhibition of the silkworm spinning.

Currently, Asian countries and especially China are the leading players in the silk industry, basically due to their low labour costs. However, two factors have emerged and might lead to a come-back of sericulture in Europe: on one side, the increasing interest of the textile industry in restoring the ancient and high-quality European silk farming, with the development of new applications of silk as bio-compatible material; on the other hand, the growing migration of Chinese farmers from the countryside to urbanized areas, which increased the silk price (Ravaglioli and Bombacci, 1997).

Recent Silkworm Applications

Apart from the economic interest in the 4000 existing *B. mori* strains due to their silk production capabilities, many recent additional applications related to the use of silkworms, silk or silk manufacturing by-products have been developed. In fact, *B. mori* represents a model organism for *Lepidoptera* in genetics studies: more than 400 silkworm Mendelian mutations have been described, allowing the understanding of different physiological mechanisms such as epidermal pigmentation or sex

determination (Goldsmith et al, 2005). Moreover, the coexistence of both *B. mori* and its ancestor, the wild *B. mandarina,* permitted detailed analyses on the domestication phenomenon (Xia et al, 2009). *B. mori* is also used in the pharmaceutical-biomedical research field for the search for drug candidates or for the study of host-pathogen interactions (Nwibo et al, 2015). In addition, different techniques based on transposable elements have been developed to obtain transgenic strains that are used for both basic and applied research (Tamura et al, 2000). Thanks to their large sizes and to these transgenic techniques, silkworms are used as bioreactors for the production of many different compounds. In particular, several transgenic *B. mori* lines that produce molecules of interest in the silk glands have been generated (Xu, 2014). Silk is abundantly produced and naturally secreted by the larvae, therefore the purification process of the target molecule is made easier. Silkworm strains producing human collagens, feline interferon, mouse antibodies and human cytokines in the silk glands have been generated for both protein production and new bio-materials synthesis (Xu, 2014).

Finally, interest in by-products of the silk manufacturing process has recently emerged. In particular, silkworm pupae have been found to possess rich nutritional value, because rich in oils and proteins, and can be a source of fatty acids that can be used in food, medicines and cosmetics (Wei et al, 2009). On the other hand, Sericin, which envelops the Fibroin silk fibers and is removed during silk manufacturing, has been found to increase the bioavailability of Zn, Fe, Mg and Ca in rats, to possess antioxidant properties and to be a degradable biocompatible material. Therefore Sericin can be recovered from the silk industry wastewater and used in food, cosmetics and pharmaceutical products (Wu et al, 2007).

Aim of the Project

As mentioned above, an increasing interest of the textile industry in bringing back the high-quality silk farming in Europe has recently emerged. This interest is also moved by the raising of Chinese silk price, which is driven by the depopulation of country areas in favor of urbanized cities (Ravaglioli and Bombacci, 1997).

The Italian sericulture gradually disappeared during the XX century, mostly because of the silkworm and mulberry epidemics, the environmental pollution and the lacking of investments in industrialized technologies for the silk manufacturing process. Recently, an interest in the obtaining of a high quality silk with application in both textile and biomedical industry has arisen in Italy.

The Sericulture Unite of the Consiglio per la Ricerca in Agricoltura e l'Analisi dell'Economia Agraria (CREA-API) of Padova is an Italian institution which preserves around 200 silkworm strains. It represents the hugest sericulture center in Europe, fundamental for the basic research on *B. mori*, for the preservation of the genetic variability in domesticated silkworm lines and for providing productive strains for the industrial sector.

In the perspective to restore an Italian sericulture activity aimed to the development of a high-quality product, we begin a collaborative research project with CREA-API whose purpose was to examine in depth the silkworm capability to face infections. The final aim of the proposal was to obtain silkworms enhanced in their pathogen-resistance, but still maintaining good production capabilities. To achieve this objective, two main approaches were used: 1) the characterization of the humoral immune response to oral infections of distinct silkworm strains with different geographical origin, particularly focusing on antimicrobial peptides (AMPs), the most important effectors of the innate immunity; 2) the production of transgenic silkworms over-expressing specific AMPs.

The following sections provide an overview on the main mechanisms involved in the Insect immune response.

Insect Immunity

Insects represent the largest animal class on Earth: among the 1,62 billion of known species, almost 50% (~807,000) belongs to the *Insecta* class (catalog of life). The study of insects and, in particular, of their immune system, is not only justified by their great abundance on Earth, but it is also driven by economic and scientific reasons, that often intertwine with one another.

Many insects, like aphids (superfamily *Aphinoidea*) or tobacco hornworms (*Manduca sexta*), are extensively studied for the damage that they cause to crops, or because they are vectors for severe human diseases, like malaria or dengue, transmitted by mosquitos respectively of the genus *Anopheles* or *Aedes.*

The interest in some insect species as honeybees (*Apis millifera*) and silkworms (*Bombyx mori*) is driven by their importance as primary source of valuable products. This economic interest stimulated relatively early studies in the field of insect immunity: between 1865 and 1870, Louis Pasteur demonstrated that two important diseases, pébrine and flacherie, that were destroying silkworm livestock in France, had microbial origin and were caused, respectively, by a microsporidian and a virus (Pasteur, 1870). More recently, the study of insect immunity helped in the unraveling of many important aspects of the human innate immunity, as the discovery of Toll receptors in *Drosophila melanogaster* (Lamaitre et al, 1996) and the equivalent Toll-like receptors in humans (Medzhitov et al, 1997).

Insect defense against pathogens relies only on an innate immune system. In this class of organisms, the first defense-line is represented by the *epithelia* of the cuticle and of the gut, that are subjected to direct microbial exposure. Apart from the mechanical barrier that these *epithelia* represent, an efficient local immune response is activated at this level to prevent or to limit the entrance of microbes in the body circulation. In particular, reactive oxygen species (ROS) and antimicrobial peptides (AMPs) are produced in response to pathogen exposure at this level (Buchon et al, 2014). If pathogens escape these first defense barriers, a systemic response is activated. This is generally differentiated in cellular and humoral immunity. The cellular immunity is triggered by hemocytes, “blood cells” that circulate in the hemolymph, which are responsible for different immune mechanisms such as phagocytosis, encapsulation and nodule formation. The humoral response involves 1) the prophenoloxidase (PPO) cascade, that triggers the melanization reaction, and 2) the production of immune proteins like Lysozyme and AMPs, which are synthesized in both hemocytes and fat bodies, specific insect tissues that play a role analogous to that of the mammalian liver. All the humoral response components are released in the hemolymph, where they directly act against pathogens. The efficiency of this systemic

immunity relies on the open circulatory system characteristic of insects and on the relatively small volume of their hemocoel: these features permit antimicrobial molecules and effectors to accumulate rapidly in the hemolymph at concentrations sufficient to be effective against invading microbes and to reach rapidly all the sites of the infection. However, it should be taken into consideration that the distinction between “cellular” and “humoral” immunity employed to describe the complex and finely regulated innate immune system is somewhat simplistic. In fact, many humoral components are produced by hemocytes, which also play a role in cellular immune response in synergy with humoral effectors

In both local and systemic immunity, insects use different pathogen-recognition systems to sense the presence of potentially harmful microorganisms. In particular, distinct recognition proteins are involved in the specific sensing of Gram-positive and -negative bacteria, fungi, protozoa, as well as and viruses (Broderick at al, 2009). Among the many microbial sensors, the most important and characterized are Peptidoglycan Recognition Proteins (PGRPs), β-glucan recognition proteins (βGRPs), C-type lectins (CTLs) and Hemolin (Kurata, 2014). These molecules are involved in the activation of specific signaling cascades such as Toll, Immune deficiency (Imd), JUN N-terminal kinase (JNK) and Janus Kinase/Signal Transducer and Activator of Transcription (JAK/STAT) pathways. All these signaling cascades activate the production of a wide variety of immune effectors, often specific for the recognized pathogen. In particular, the Toll-pathway activates the immune response against Gram-positive bacteria and fungi, the Imd-pathway the one against Gram-negative bacteria, while the JAK/STAT pathway triggers the response against a general infection status or septic injury (Stokes et al, 2015).

In the next sections I will describe how innate immunity works in insects, drawing particular attention to the fruit fly *Drosophila melanogaster*, the most studied insect, and to the silkworm *Bombyx mori*, subject of this research.

Microbial Recognition

Several molecules are involved in the microbial recognition process. They are generally called Pathogen Sensors or Pattern Recognition Receptors (PRRs) and are able to detect very small amounts of pathogen specific molecules, generally absent in the host and commonly named Pathogen Associated Molecular Patterns (PAMPs; Kurata, 2014). Usually PAMPs are part of the microorganism cell wall or membrane: lipoteichoic acid from Gram-positive bacteria, lipopolysaccharide (LPS) from Gram-negative bacteria, different peptidoglycan (PGN) molecules from both Gram-negative

and -positive bacteria, β-1,3-glucans from fungi and yeasts. Also nucleic acids from bacteria and viruses are sensed by specific proteins (Buchon et al, 2014, Kurata, 2014), as well as molecules released by host cells that underwent injury or infection damages (Matzinger, 2002).

It is important to underline that the microbial recognition is carried out by a "redundant" pool of PRRs. Every specific class of pathogen is recognized by more than one protein. In this way, the recognition of invading microorganisms is not carried out by single elements, but it is the work of a multifaceted and efficient sensing system.

Many immune proteins are able to recognize and bind PGN. This molecule is one of the main component of bacterial cell walls and it strongly differs among bacteria, not only for the location in the cell envelope, but also in its molecular composition. While Gram-positive bacteria possess an external cell wall composed by a thick layer of PGN, the PGN layer of Gram-negative bacteria is located between two cell-membranes. PGN is a polymer of N-acetylmuramic acid and N-acetyl-glucosamine. Polymer chains are cross-linked by short peptides which differ among bacteria. In Gram-positive bacteria the third residue of these stem peptides is often lysine, while in Gram-negative bacteria and in *Bacillus* species is a meso-diaminopimelic acid (DAP) group (Schleifer and Kandler, 1972).

Among the multitude of proteins able to recognize PGN, Peptidoglycan Recognition Proteins (PGRPs) are the most studied in invertebrates. PGRPs were first identified in the hemolymph of *Bombyx mori*, as activators of the prophenoloxidase (PPO) response (Yoshida et al, 1986). *Drosophila* possesses 13 PGRP genes, the mosquito *Anopheles gambiae* 7, *B. mori* 12, humans and mice 4 (Tanaka et al, 2008). All PGRPs possess an amidase domain similar to bacteria amidases and bacteriophage Lysozymes, pointing to an ancestral origin for this protein family (Kurata, 2014).
However, only some members of the PGRP family have maintained this activity and are capable to hydrolyze PGN. These are called catalytic PGRPs. On the other hand, sensor PGRPs are those proteins which bind PGN without breaking it because they lack a functional amidase domain (Ferradon et al, 2007). Both catalytic and sensor PGRPs sense PGN fragments through a specific domain, even if the exact molecular mechanisms underlying this recognition process are still unclear (Yu et al, 2010).

Subsequently, catalytic PGRPs hydrolyze PGN, while both catalytic and sensor PGRPs interact with other PGRP molecules forming heterodimers, or with signaling proteins giving rise to a signal transduction pathway that ends with the production of immune effectors. PGRP genes' expression is induced upon infection in many tissues involved in the immune response, as hemocytes, fat bodies, gut and epidermis (Werner et al, 2000).

Insect PGRPs can also be classified on the basis of their transcript length in short PGRPs (PGRPs-S) and long PGRPs (PGRPs-L). PGRPs-S are thought to be

predominantly extracellular proteins because they often possess a signal peptide, while PGRPs-L can be localized both intracellularly and extracellularly. In addition, some PGRPs-L are transmembrane proteins (Kurata, 2014). *B. mori* possesses 6 PGRP-S, four of which are putative extracellular proteins and exhibit a conserved amidase domain. Of the 6 PGRP-L, one is thought to be cytoplasmatic, one transmembrane and four probably are secreted proteins (Tanaka et al, 2008).

A general mechanism of synergistic action among PGRPs has been hypothesized in *Drosophila*. After a septic injury, small amounts of PGN circulate in the hemolymph. It is thought that these fragments are released by both Gram-positive and -negative bacteria after their proliferation or during hemocytes and/or AMPs early action. The recognition process between PGN fragments and circulating PGRP fragments activates the production of AMPs, which fight the invading pathogens. After the direct action of AMPs, higher amounts of PGN are released in the hemocoel and are sensed even by membrane-bound PGRP receptors, which in turn trigger a massive effector production (Ferradon et al, 2007).

Data from *Drosophila* indicate that different PGRPs are involved in the specific recognition of different bacteria and are also fundamental in other defense mechanisms. For example, DPGRP-SA mutant flies are more sensitive to Gram-positive infection, because the Toll-pathway is blocked (Michel et al, 2001). On the other hand, *Drosophila* PGRP-LC mutants are more sensitive to Gram-negative infections, but their survival rate towards Gram-positive or fungi is not affected (Gottar et al, 2002). PGRP-LE appears to be an essential component in the hemocyte-mediated immunity in the recognition of intracellular pathogens as *Listeria monocytogenes* (Yano et al, 2008). PGRP-SC1b was found to be able to hydrolyze peptidoglycan through an amidase domain (Mellroth et al, 2003). Moreover it is thought that PGRPs contribute to pathogen phagocytosis, since RNA interference experiments on *Drosophila* cells showed that the inhibition of *PGRP-L* expression decreases the phagocytosis rate of *Escherichia coli* (Rämet et al, 2002).

β-Glucan Recognition Proteins (βGRPs) belong to a family including two different types of proteins with specific activities: one binds to β-1,3-glucan, the main component of fungi cell wall, the other, called Gram-negative Recognition Protein (GNRP), binds to Gram-negative and -positive bacteria (Tanaka et al, 2008). Both protein types were first isolated from the hemolymph of *B. mori* and were found to activate the Prophenoloxidase (proPO) cascade (Yoshida et al, 1986; Ochiai and Ashida, 1988; Lee et al, 1996).

βGRPs have a N-terminal domain that binds β-1,3-glucan chains, but also LPS and lipoteichoic acid (Mishima et al, 2009); this domain is responsible for the proPO cascade activation. The C-terminal domain is a glucanase-like domain but it is catalytically inactive (Ochiai and Ashida, 2000; Takahasi et al, 2009). *B. mori* possesses

4 genes encoding for βGRPs, which are thought to be secreted, given the presence of a putative signal peptide in their sequence. Of these four proteins, βGRPs 1 to 3 have been shown to lack the active catalytic residues at the glucanase domain, confirming the absence of a glucanase activity. On the other hand, βGRPs 4 was shown to possess the critical catalytic residues, but its glucanase activity has not been demonstrated yet (Tanaka et al, 2008). It has been hypothesized that βGRPs recognize the triple-helical structure of β-1,3-glucan through 3 specific residues. During a fungal infection, βGRPs accumulate on the cell wall of the invading microorganisms, exposing a negatively charged and acid surface which can possibly recruit downstream signaling molecules (Takahasi et al, 2009).

Another important protein group involved in pathogen recognition and conserved across plants, invertebrates and mammals is the C-type Lectin (CTL) family. CTLs recognize carbohydrates in a Ca^{2+}-dependent manner, generally exerting their function outside the cells as membrane-associated or secreted proteins. CTLs generally possess one or more carbohydrate recognition domains through which they are able to sense the presence of Gram-positive and -negative bacteria, as well as fungi and protozoa (Weis et al, 1998). In insects CTLs are responsible for the binding of both microorganisms and hemocytes, contributing to many immune responses as proPO activation, hemocyte nodule formation, phagocytosis and bacteria clearance (Yu and Kanost, 2000; Yu and Kanost, 2003; Koizumi et al, 1999). It has been hypothesized that hemocytes might interact with CTLs via a specific receptor (Ohta et al, 2006). In *B. mori,* 23 CTL genes have been identified (Rao et al, 2015). Among these, only 6 proteins have been thoroughly studied and have been found to have distinct binding activity and to recognize differentially Gram-positive and -negative bacteria and yeast cells (Koizumi et al, 1999; Kim et al, 2003; Watanabe et al, 2006; Takase et al, 2009).

Hemolin is a 48 KDa plasma protein found only in *Lepidoptera*. It belongs to the immunoglobulin superfamily and it was first discovered in *Hyalophora cecropia* (Rasmuson and Boman, 1979) and *Manduca sexta* (Ladendorff and Kanost, 1990). *M. sexta* hemolin was found to bind many components of the bacteria cell-envelope, such as LPS and lipoteichoic acid (Yu and Kanost, 2002) and hemocytes (Ladendorff and Kanost, 1990). *B. mori* possesses a single *hemolin* gene, but no evidence of an up-regulation of this gene after microbial challenge, nor the presence of a Hemolin protein has been demonstrated so far (Tanaka et al, 2008).

Signal Transduction Pathways

Pathogen PAMPs activate in different ways distinct defense signaling pathways that, in turn, induce the production of defined immune effectors.

In insects, invading microbes as fungi and Gram-positive bacteria with Lys-type peptidoglycan activate the Toll-pathway response, while Gram-negative bacteria with DAP-type peptidoglycan induce a response mediated by the Imd-pathway. On the other hand, general injury or stress signals are regulated by the JNK and the JAK/STAT pathways.

In addition to the different stimuli and the specific effectors that these signaling ways induce, the above mentioned transduction pathways differ also in the timing and localization of the activation. For example, while the Toll-pathway is specifically activated in fat body cells, the Imd-pathway was found to be initiated not only in fat bodies, but also in the midgut, tracheae and genital *epithelia*, in reaction to direct microorganism exposure before the systemic immune response (Broderick et al, 2009). These details will be discussed in the following sections.

Toll-Pathway

The *Drosophila* Toll-pathway is activated by serine protease cascades through two different mechanisms: the PRR-dependent pathway and the so called “danger pathway”. In the first case, PAMPs from fungi or Gram-positive bacteria are sensed by their specific PRRs and initiate a proteolytic cascade which involves the serine protease Grass. In the second situation, proteases secreted directly by fungi or Gram-positive bacteria are sensed as inducers of an abnormal proteolytic activity in the hemolymph.

A distinct proteolytic cascade, involving another serine protease named Persephone, is then responsible for the activation of the Toll-pathway in a PRR-independent way (Ashok, 2009; Stokes et al, 2015). A schematic summary of signaling cascades of the Toll-pathway in *Drosophila melanogaster* is shown in Figure 2.

Grass and Persephone are only two members of the large group of extracellular serine proteases, which not only activate the Toll-pathway, but also other immune responses such as melanization. However, to date, the links between all these proteases have not been fully characterized.

The extracellular serine proteases, also called clip domain serine proteases (CLIPs), share a common structure, composed by a N-terminal clip-domain probably involved in the regulation of the enzyme activity or in the localization of the protein,

and a C-terminal serine protease domain. CLIP proteases are first synthesized and released in the hemolymph as pro-enzymes; after a proteolytic cleavage, the clip-domain is separated from the protease domain, and it is thought to activate the PPO cascade and the melanization response (Jiang and Kanost, 2000). On the other hand, the serine protease domain is responsible for the beginning of the Toll signaling through the activation of the Spätzle-processing enzyme (SPE), which cleaves the cytokine Spätzle (Ashok, 2009).

The serine protease inhibitors or Serpins are negative regulators of the serine protease cascade that permit a very tight modulation of the immune response. In general, they covalently bind to serine proteases, blocking their activities. One example is the *Drosophila S*erpin Necrotic which in physiological conditions inhibits Persephone, blocking the activation of the Toll-pathway. However, after an immune challenge the N-terminus of Necrotic is cleaved, leading to the activation of the Toll-dependent immune response (Pelte et al, 2006).

B. mori possesses 15 genes encoding for CLIPs and 26 genes encoding for Serpins. No homologs of *Drosophila persephone*, *grass* or *necrotic* genes have been identified, suggesting that other CLIPs or Serpins are involved in the regulation of the Toll-pathway (Tanaka et al, 2008).

After serine proteases and Serpins regulation, the extracellular cytokine Spätzle is finally activated. Spätzle is first synthesized and released in the hemolymph as an inactive form composed of two dimers linked by a disulphide bridge. After a proteolytic processing, the Spätzle C-terminus active portion, named C106, binds the ectodomain of the Toll receptor (Ferrandon et al, 2007). Only one out of the six *spätzle* genes is involved in the *Drosophila* immunity, while *B. mori* possesses three genes, among which one has been demonstrated to up-regulate AMP genes after immune challenge (Tanaka et al, 2008).

The binding of Spätzle to the N-terminal ectodomain of the Toll receptor induces conformational changes in the latter, that permit the interaction with downstream components of the signaling. In particular, a complex of signaling elements assembles around the intracellular C-terminus of the Toll receptor. This complex is formed by the cytoplasmic adaptor Myeloid Differentiation Primary-response Gene 88 (MyD88), Tube and Pelle. MyD88 is highly conserved among vertebrates and invertebrates. It possesses a death domain (DD) and a Toll/ Interleukin-1 (TIR) domain. Pelle is a serine-threonine kinase, which also possesses a DD. Tube has a double DD through which is able to interact with both MyD88 and Pelle (Ferrandon et al, 2007; Stokes et al, 2015).

It is thought that in *Drosophila* MyD88 and Tube form a membrane-associated complex before the Spätzle signaling. When the Toll receptor is activated by Spätzle, it recruits the MyD88-Tube complex, which in turn binds Pelle. The MyD88-Tube-Pelle

complex, held together by the double DD of Tube, activates the kinase activity of Pelle, that leads to the final phosphorylation of Cactus. Cactus is an inhibitor of the transcriptional factor DIF (dorsal-related immunity factor): when Cactus is phosphorylated, it is rapidly polyubiquitylated and degraded in the lysosome, allowing DIF to translocate in the nucleus, to bind to an NF-κB response element and to induce the transcription of specific genes encoding AMPs that have to be produced against Gram-positive bacteria or fungi (Ferrandon et al, 2007; Broderick et al, 2009).

Spätzle activity has been demonstrated also in *B. mori* since the injection of the cleaved form of Spätzle is able to induce AMP transcription in silkworm larvae, while the injection of the inactive Spätzle form does not have any effect on AMP transcription (Wang et al, 2007).

B. mori possesses 14 *TLR* genes: the protein encoded by *Toll9-1* is thought to be the one which activates the Toll-pathway in the silkworm. Homolog genes encoding for all the downstream components of the Toll-pathway (MyD88, Tube, Pelle, Cactus) have been identified in *B. mori*, except for the *Dif* gene (Tanaka et al, 2008). Moreover, NF-κB regulatory elements have been found in the 5' up-stream regions of silkworm AMP genes, confirming that the general mechanisms through which the Toll-pathway regulates and activates AMP gene transcription is roughly conserved between *Drosophila* and *B. mori* (Tanaka and Yamakawa, 2011).

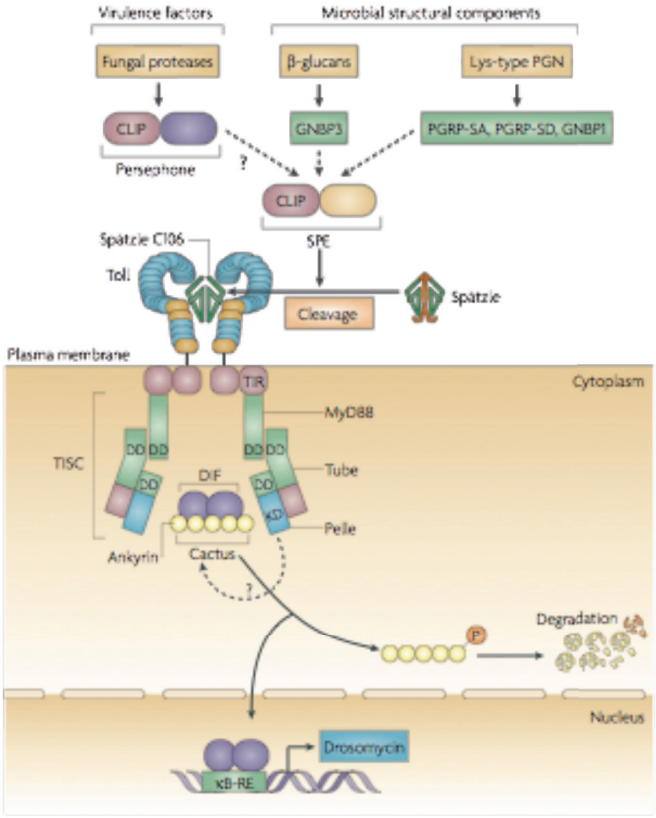

Figure 2. Schematic representation of Toll-signaling in *Drosophila melanogaster*. From Ferrandon et al, 2007.

Imd-Pathway

Another important signal transduction pathway is the Immune deficiency (Imd) pathway, which activates the immune response against Gram-negative bacteria. In *Drosophila* it is activated by the transmembrane PGRP-LC when the infection is systemic, and by the cytoplasmic PRCP-LE when the pathogen is intracellular. Both these PRRs recognize DAP-peptidoglycan and possess a RIP homotypic interaction motif (RHIM)-like domain which is essential for the downstream signaling (Yano et al, 2008). When PRRs sense the presence of Gram-negative bacteria, they induce the intracellular protein IMD to activate two distinct signaling pathways. The first leads to the phosphorylation of the transcriptional factor Relish, while the second ends with the cleaveage and activation of the phosphorylated Relish, allowing it to enter the nucleus and to promote AMP gene expression. In Figure 3 a representation of the signaling cascades of the Imd-pathway in *Drosophila melanogaster* is shown.

In the first process, IMD activates a class of enzymes involved in the K63-linked polyubiquitin conjugation mechanism, through which a chain of polyubiquitin linked through their lysine 63 is attached to a target protein. This group of enzymes comprehends DIAP2 (*D. melanogaster* inhibitor-of-apoptosis protein 2), the ubiquitin conjugating E2 enzyme Bendless and the ubiquitin conjugating E2 variant 1 enzyme (UEV1A). The polyubiquitin chain is probably the scaffold for the assemblage of two distinct protein complexes: 1) the IKK (inhibitory κB kinase) signaling complex, composed by IRD5 (immune-response deficient 5, the catalytic subunit) and Kenny (the regulatory subunit), which finally phosphorylates Relish; 2) the complex composed by the MAPKKK TAK1 (TGFβ-activated kinase 1) and its regulatory subunit TAB2 (TAK1-binding protein 2), which at the end phosphorylates and activates the IKK complex and stimulate the JUN N-terminal kinase (JNK) transduction pathway (Ferrandon et al, 2007; Stokes et al, 2015).

In the second signaling way, IMD recruits FADD (FAS-associated death domain) through its DD. Then, FADD interacts with the caspase DREDD (death-related ced-3/ Nedd2-like protein), which is thought to cleave the phosphorylated form of Relish, removing its C-terminal domain composed by an ankyrin-repeat/IκB-like structure. In this way the Rel DNA-binding domain (Rel68) translocates into the nucleus and activates AMP gene expression. Moreover, the FADD-DREDD complex was found to activate the IKK complex, before the regulation of TAK1 (Ferrandon et al, 2007, Broderick et al, 2009; Stokes et al, 2015). Although all these processes have been thoroughly characterized from a genetic stand point, there is lack of biochemical data in support of the predicted protein interactions in the Imd-pathway.

Tanaka et al identified putative ortholog genes for all components of the Imd-pathway in *B. mori*, suggesting a conservation of this pathway among insects (Tanaka et al, 2008).

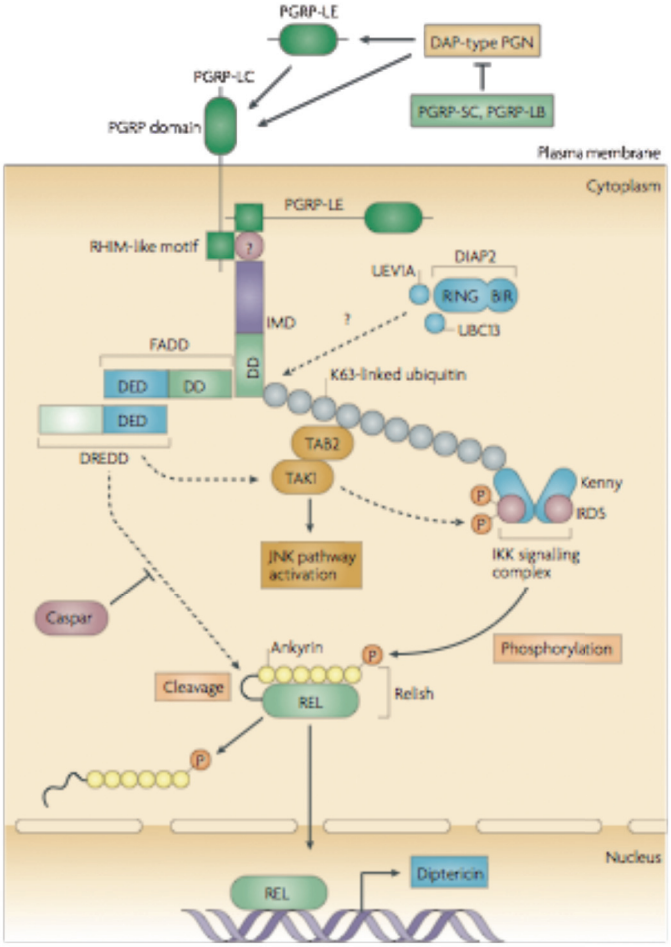

Figure 3. Schematic representation of Imd-signaling in *Drosophila melanogaster*. From Ferrandon et al, 2007.

Even if Toll and Imd signaling pathways have been described separately and were demonstrated to be activated independently, experimental data suggest that these two signaling ways might act synergistically during microbial infections (Ferrandon et al, 2007). For example, both pathways are activated at different levels when microbes are injected in *Drosophila* (Lamaitre et al, 1997) and mutant flies with a constitutive activation of the Toll-pathway are able to activate the Imd-pathway faster then wild-type flies (Lamaitre et al, 1996).

JAK STAT and JNK Pathways

The third transduction pathway of the innate immune response is the Janus Kinase/Signal Transducer and Activator of Transcription (JAK/STAT) pathway. The JAK/STAT pathway stimulates the production of important signaling molecules and effectors of the systemic immune response, even if it is not directly involved in the induction of AMP gene expression. The JAK/STAT pathway is activated after septic injury, during viral or bacterial infections. Moreover it is also involved in the hematopoiesis process.

In *Drosophila*, the receptor of the JAK/STAT pathway is the membrane receptor Domeless, which is thought to be present in fat body cell membranes. Unpaired cytokines, a family of cytokines linked to the human interleukin-6 (Santabárbara-Ruiz et al, 2015), are signaling molecules secreted upon injury or infection. They bind Domeless receptors, which dimerize and phosphorylate intracellular transcription factors such as Stat92E and Hopscotch. These enter the nucleus and induce gene expression of molecules involved in the inflammatory immune response and in the innate cellular defense, such as phagocytosis and melanization (Stokes et al, 2015). In the silkworm *B. mori*, many of the genes encoding important elements of the JAK/STAT pathway have not been found, suggesting the presence of differences among insects in this signaling way.

Finally, the JUN N-terminal kinase (JNK) pathway has been already mentioned as a collateral signal transduction way activated by the Imd-pathway, through TAK1, which is thought to phosphorylate the JNK kinase Basket. This signaling pathway was found to be involved in stress and wound repair/tissue damages responses, even if its precise role in the immune response is yet to be determined (Broderick at al, 2009). Since all orthologs of the genes involved in the JNK pathway have been found in *B. mori*, it is thought that this signaling way is conserved between *Drosophila* and the silkworm (Tanaka et al, 2008).

Immune Effectors

Antimicrobial Peptides

Antimicrobial peptides are a broad class of small proteins produced systemically in fat bodies and hemocytes, but also locally in tissues that are directly exposed to pathogens, such as gut or tracheal *epithelia.* AMPs are released in the hemolymph and in the site of the microbial exposure, where they display a direct activity against

bacteria, fungi, viruses and protozoa. Moreover, AMPs regulate many physiological functions, such as inflammation or wound healing, acting as chemotactic agents in the modulation of the innate immune system (Nakatsuji and Gallo, 2012).

It is generally thought that all known living species produce AMPs, including bacteria, fungi, plants, invertebrates, non-mammalian vertebrates and mammals (Lewis et al, 2015). This widespread distribution suggests an ancient evolutionary origin and reveals the crucial role of AMPs in the innate immune response (Zasloff, 2002). In particular AMPs play an essential function in those organisms that lack an adaptive immune system and that base their defense only on innate immune response, such as Insects. It is known that Insects are able to produce a variety of AMPs that share structural characteristics, but that are often specific for certain microorganisms (Bulet et al, 1999).

To date, more than 2500 AMPs have been isolated from a wide variety of sources, and from 2000 to 2014 about 100 new AMPs were entered in public databases each year (Wang et al, 2015). Among this large array of AMPs, at least 150 have been identified in Insects (Yi et al, 2014). Because of their variety, insect AMPs can be classified using many different criteria.

First of all, AMPs differ for their *final* size. In fact, these molecules are generally produced as pro-peptides or pre-pro-peptides, and they reach their final size and structure only after one or more proteolytic cleavages. Small AMPs possess around 10 -24 residues, medium AMPs about 25 -50 aa, and large AMPs between 50 and 100 aa. AMPs greater than 100 amino acids are often named antimicrobial proteins (Wang 2015).

AMPs can be divided on the basis of their net charge into anionic AMPs (AAMPs) and cationic AMPs (CAMPs). The first group is composed by peptides with a global negative charge between -1 to -7, rich in Aspartic and Glutamic acid residues. However, the more studied group of AMPs comprises peptides with a positive net charge from +2 to +9, with a composition rich in basic amino acids (Arginine, Lysine and/or Histidine; Lewis et al, 2015).

Finally AMPs can be classified for their sequence and secondary structure in four groups:

- α-helical peptides: these AMPs have a linear unstructured conformation in an aqueous environment, because they lack in cysteine residues. However, in a membranous environment they fold into α-helixes thanks to their hydrophobic residues and they assume an amphiphilic conformation (Lewis et al, 2015). Some of these AMPs have a proline- or glycine-induced kink in the middle of the α-helix (Nguyen et al, 2011). In Insects, this class is represented by Cecropins and Moricins (Yi et al, 2014).

- β-sheet peptides: these molecules contain 6 to 8 cysteine residues essential for the β-sheet structure, maintained by two or more disulphide bonds (Lewis et al, 2015). In Insects, Defensins and Drosomycins are cysteine-rich peptides that belong to this group (Yi et al, 2014).
- linear-extended peptides: these peptides do not assume any regular secondary structure and they are often composed by high proportions of particular amino acids as proline, arginine, tryptophan, glycine and histidine, but lack in cysteine residues (Lewis et al, 2015; Nguyen et al, 2011). Among insect AMPs, Apidaecins, Drosocins and Lebocins belong to the proline-rich class, while Attacins and Gloverins to the glycine-rich group (Yi et al, 2014).
- circular peptides: this class of AMPs includes all peptides that do not fit in the previous classes and that are often composed of mixed α-helix and β-sheet structures (Lewis et al, 2015).

Action Mechanism of Antimicrobial Peptides

Antimicrobial peptides generally assume an amphipathic conformation that is essential for the interaction with pathogen membranes or cell walls. However, AMPs not only act on membranes, but also on many different cellular targets. Moreover, sometimes the same peptide can deploy multiple action mechanisms in different cellular compartments: the variety of peptide types produced during an infection and the ability to target different cell components, make AMPs an extremely effective weapon against microbial attacks (Nguyen et al, 2011).

In general, AMPs act with a non-enzymatic mechanism, differently from other antimicrobial proteins, such as lysozyme, which have a catalytic site (Kirby, 1987). The ability of AMPs to target only microorganisms without interacting with host cells relies on the different composition of bacterial cell envelopes as compared to eukaryotic membranes. In fact bacteria membranes are predominantly composed by negatively charged hydroxylated phospholypids, such as phosphatidylglycerol, cardiolipin and phosphatidylserine, while eukaryotic cell membranes are positively charged for the presence of zwitterionic phospholipids and cholesterol (Yeaman and Yount, 2003). Moreover, Gram-negative bacteria possess an external membrane mainly made by negatively charged LPS, while Gram-positive bacteria possess a cell wall composed of peptidoglycan that is anchored to the inner membrane by negatively charged teichoic acids. It is thought that AMPs are also able to discriminate between fungi and eukaryotic host membranes because of the different sterols composition of these membranes (Yeaman and Yount, 2003). Therefore the electrostatic interaction between

cationic AMPs and pathogen cell envelopes precisely direct AMPs to their target. This interaction is essential not only for those peptides that act on bacterial membranes, but also for the translocation of AMPs that have intracellular targets.

The main action mechanism by which AMPs act against pathogens is membrane permeabilization. The general consequence of this membrane perturbation are lipid asymmetry and loss of electrochemical potential together with metabolites and cellular components (Teixeira et al, 2012). Different models have been proposed for AMP-membrane interaction mechanism and have extensively reviewed in Nguyen et al (2011), Teixeira et al (2012) and Lewis et al (2015) and are shown in Figure 4.

- Barrel-stave model: the AMP insert perpendicularly into the membrane forming a transmembrane pore, with the hydrophilic residues positioned towards the center of the pore and the hydrophobic chain/s interacting with the lipid bilayer. The result of these transmembrane pores is the loss of electrochemical potential of membranes (Figure 4A).
- Carpet model: this model hypothesizes a detergent-like membrane permeabilization. Amphipathic peptides accumulate parallel to the membrane, as in the toroidal model, covering the membrane like a carpet. Once the peptide reaches a threshold concentration , micelles and pores are formed (Figure 4B).
- Toroidal model: amphipathic AMPs interact with the double lipid layer in parallel with the membrane plane. In particular, charged residues interact with polar phospholipid head groups, while the hydrophobic amino acids arrange in a acyl tail core. Once a sufficient AMP concentration near the membrane is reached, AMP re-orienter themselves perpendicularly. Transient pores consisting of both peptides and lipids are formed as a consequence of the perturbation of the orientation and of the thickness of the double layer (Figure 4C).

Together with these models that attempt to explain membrane permeabilization and cell lysis, non-membranolytic AMP/membrane interaction mechanism have also been hypothesized. These latter mechanisms try to explain the action mechanisms of AMPs unable to cause depolarization but effective in killing microbes such as bovine Bactenecin or the chimeric artificial AMP named CP26 (Wu et al, 1999). For these peptides, the interaction with the microbial membrane is only the first obstacle that they encounter before reaching their final target. Once they translocate into the cytoplasm, these AMPs reach different internal targets, such as proteins involved in cell-wall synthesis, nucleic acids, enzymes inhibiting essential physiological cell functions.

- Aggregate channel model: AMPs form transient unstructured clusters on the membrane, associated with water molecules which allow the passage of AMPs inside the cell, where they interact with their possible intracellular targets.

- Molecular electroporation model: AMPs, when present at a threshold concentration near the membrane, are able to generate a weak electric field that promotes the formation of transient pores in the membrane if retained for a sufficient amount of time (Figure 4D).
- Sinking-raft model: this model hypothesizes a mass imbalance between the two sides of the membrane due to peptide association with particular lipid domains. This mass disproportion leads to peptide translocation inside the membrane by transient pores formation and by increasing the local membrane curvature (Figure 3E).

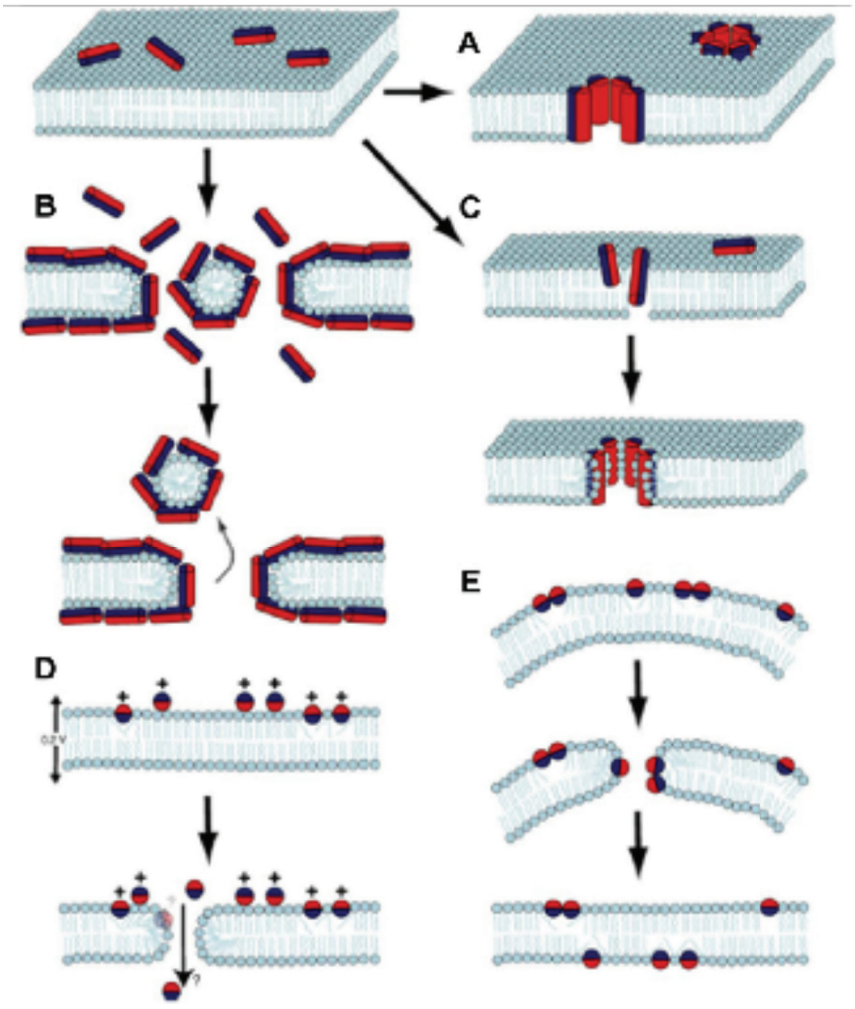

Figure 3. AMP-membrane interaction mechanisms. Different AMP mechanisms of action were hypothesized. Barrel-stave model proposes that peptides form a pore interacting with the hydrophobic phospholipids chains (A). The carpet model hypothesizes a detergent-like action for AMPs (B). The toroidal model differs from the barrel-stave for the proposed interaction between the hydrophilic part of AMPs and the phospholipids head-groups (C). The molecular electroporation model proposes that the electric potential induced by the accumulation of CAMPs near the cell membrane, creates molecular electroporation (D). The sinking-raft mechanism hypothesizes a mass imbalance between the two sides of the membrane that leads to peptide translocation inside the membrane by transient pores formation and by increasing the local membrane curvature (E). Adapted from Teixeira et al, 2012.

Bombyx mori Antimicrobial Peptides

In the silkworm *Bombyx mori*, at least 21 AMP and 13 AMP-like coding genes have been identified and classified in 6 families, belonging to 4 different groups (Tanaka et al, 2008):

1) Amphiphilic-α-helical peptides: Cecropins (13 genes) and Moricin.
2) Glycine-rich peptides: Attacin and Gloverins (4 genes).
3) Six cysteine containing peptides: Defensin.
4) Proline-rich, O-glycosilated peptides: Lebocin.

Summarizing information on *B. mori* AMPs are listed in Table 1.

Class	Name	Gene number	Induction	Main activity
Amphiphilic α-helical	Cecropin	13	Gram-negative (Imd-pathway ?)	Gram-positive and Gram-negative
	Moricin	1	Gram-positive, fungi (Toll-pathway ?)	Gram-positive and Gram-negative
Glycine-rich	Attacin	1	?	Gram-negative
	Gloverin	4	Gram-negative, Gram-positive, fungi	Gram-negative
Six cysteine containing	Defensin	1	?	Gram-positive (?)
Proline-rich, O-glycosilated	Lebocin	1	?	Gram-negative, Gram-positive, fungi

Table 1. Antimicrobial peptides from *B. mori*.

Cecropin family is a large group of 13 members, further divided in 6 classes: 2 Cecropin A, 6 Cecropin B, 2 Cecropin D, 1 Cecropin E, and 2 Enbocins. From a genetic stand point, 11 of these genes cluster on the same chromosome, while only *cecropin A* genes have been mapped on a different chromosome. The 6 *cecropin B* genes have the same deduced amino acid sequence, therefore they might be originated from gene duplication phenomena (Tanaka et al, 2008; Ponnuvel et al, 2010). *Bombyx mori cecropin A1* promoter was shown to be activated by *E. coli* and LPS through the binding

of Relish to the upstream NF-κB motif: therefore it is thought that Cecropin A, and possibly other Cecropins, are mainly induced by the Imd-pathway after challenge with Gram-negative bacteria (Hua et al, 2015).

Cecropin sizes range between 59 and 66 residues before maturation, while the active forms have between 31 and 39 residues. In general, they possess a polarized amphipathic helix at the N-terminus, a central portion with a β-turn and a hydrophobic region at the C-terminus (Christenses et al, 1988). Cecropins were first isolated from *Hyalophora cecropia* (Steiner et al, 1981), but have also been found in Lepidopteran, Dipteran and Coleopteran insects (Yi et al, 2013). Cecropin A from *H. cecropia* has been crystalized and is thought to act on microbial membranes through the carpet model mechanism (Marassi et al, 1999), even if previous experiments on the same peptide isolated from *H. cecropia* hemolymph suggested that this peptide might form ion channels on bacteria membranes (Christenses et al, 1988).

The precise structure of *B. mori* Cecropin B has only been hypothesized from preliminary X-ray analysis on crystals (Liu et al, 2010). However it is known that *B. mori* Cecropins display a wide and strong antimicrobial activity against Gram-positive and -negative bacteria (Yang et al, 2011). Moreover, there are many experimental evidences showing strong Cecropin A and B specific anti-tumoral activities (Suttmann et al, 2008; Zang et al, 2013). These researches pointed out the potential application of silkworm antimicrobial peptides in cancer therapy.

Enbocins share structure features and antibacterial activity with all other Cecropins, but they have been found only in *B. mori* (Kim et al, 1998).

Moricin was firstly isolated from the silkworm *B. mori* (Hara and Yamakawa, 1995) and to date it has only been found in Lepidoptera (Yi et al, 2014). *moricin* is present as a single gene in the silkworm genome, even if 11 *moricin*-like genes with a low identity in the amino acid sequences have been identified (Tanaka et al, 2008). The Moricin mature peptide is composed by 42 amino acids, it is highly basic and it is active against both Gram-positive and -negative bacteria, probably targeting their membranes (Hara and Yamakawa, 1995). Moreover, after incubation with Moricin, filamentous structures and electron dots have been observed inside bacteria cytoplasm, suggesting that Moricin might have also secondary intracellular targets, such as nucleic acids (Hu et al, 2013). Moricin is composed by a single α-helix containing 8 turns, except for 4 N-terminal and 6 C-terminal residues, which are not involved in the formation of the helix. Since the N-terminal part of the helix has a clear separation between hydrophobic and hydrophilic residues, it has been suggested that this region might be particularly important for the interaction with bacteria membranes. However, also the C-terminus is critical for Moricin antimicrobial activity (Hemmi et al, 2002). It is thought that the *moricin* gene might be regulated by the Toll-pathway. A 140 bp element with an enhancer activity on the *moricin* promoter has been identified in the upstream

region of the *moricin* gene: this enhancer has been named Moricin Promoter Activating Element (MPAE) and it might contain binding sites for Lepidoptera-specific transcription factors (Yi et al, 2014).

Attacin was identified in *B. mori* by similarity to the *H. cecropia attacin* nucleotide sequence (Sugiyama et al, 1995), but it was also found in many other Lepidoptera, as well in Diptera (Yi et al, 2014). One *attacin* gene has been identified in the silkworm genome: the analysis of the expression induction of *attacin* has revealed that the tissue-specific transcription of this gene might be regulated at a chromatin level (Tanaka et al, 2005). Attacin is a 20 KDa AMP synthesized as pre-pro-peptide: after the first proteolytic cleavage, the signal peptide is removed. Then, a second cleavage removes the so called Pro-domain. Therefore the active Attacin is composed by a N-terminal portion followed by two glycine-rich domains (G-domains). *Hyalophora* Attacin has be found to be particularly active against Gram-negative bacteria and in particular it was demonstrated that it was able to inhibit the synthesis of many *E. coli* outer membrane proteins (Carlsson et al, 1991). Also *B. mori* attacin is thought to inhibit Gram-negative bacteria growth by suppressing the synthesis of bacterial outer membrane components (Tanaka and Yamakawa, 2011).

Gloverins are basic, heat-stable and glycine-rich peptides first isolated from the giant moth *Hyalophora gloveri* (Axen et al, 1997) and only found in Lepidoptera (Yi et al, 2014). In *B. mori* the Gloverin family is composed by 4 members of highly similar peptides (Gloverins 1-4). The genes encoding Gloverin 2, 3 and 4 originated from duplication of *gloverin 1* (Tanaka et al, 2008). All the four genes were induced after fungi and Gram-positive and -negative challenge, but Gloverin peptides were demonstrated to have an antimicrobial activity only against Gram-negative bacteria (Yang et al, 2011). Moreover, it has been underlined that *B. mori* Gloverins are active against *E. coli* strains with rough LPS, while they are ineffective against smooth LPS containing *E. coli* (Yi et al, 2013), suggesting the importance of the interaction between Gloverins and this component of bacteria membranes. *H. gloveri* Gloverin was also found to inhibit the synthesis of bacterial outer membrane proteins and to increase membrane permeability in *E. coli* (Axen et al, 1997). *B.mori* Gloverins are firstly synthesized as pre-pro-peptides: the 14 KDa active portion is released only after the removal of the signal and pro-peptides (Kawaoka et al, 2008). Gloverins assume an α-helical structure in a membraneous environment, but the peptide exact structure has not been determined yet (Yi et al, 2013).

Bombyx mori possess one single **Defensin** (Tanaka et al, 2008), which belongs to a wide class of AMPs that includes peptides isolated from humans, plants and insects (Yi et al, 2014). The silkworm Defensin is a 4 KDa cationic/basic peptide composed by 36 residues, which possesses 6 cysteine residues essential for the formation of 3 pairs of disulfide bonds. Similarly to other AMPs, Defensin is first produced as pre-pro-

peptide. The active portion is released after the releasing of a 22 residues signal peptide and a 34 amino acids pro-peptide. In general, insect Defensins are composed by a N-terminal loop, an α-helix and an antiparallel β-sheet, with the α-helix and the β-sheet held together by 2 or 3 disulfide bonds (Yi et al, 2014). *B. mori* Defensin has been shown to be expressed not only after immune challenge, but also constitutively at high levels in many larvae tissues, such as silk gland, head and ovary. Therefore it has been suggested that it might play an important role not only in immunity, but also during development (Wen et al, 2009). Insect Defensins show antimicrobial activity especially against Gram-positive bacteria, probably targeting microbial membranes through the formation of channels (Yi et al, 2014). However, *B. mori* Defensin antimicrobial activity has not been demonstrated yet (Tanaka et Yamakawa, 2011).

Lebocin is a proline-rich peptide, first isolated from the silkworm hemolymph (Hara and Yamakawa, 1995), and then identified also in other Lepidoptera (Yi et al, 2014). *Bombyx mori* possess a single *lebocin* gene (Tanaka et al, 2008). The immature form of Lebocin possesses a 16 residues signal peptide, followed by a 104 amino acids pro-peptide and a 27 residues additional segment at the C-terminus. These are all removed with proteolytic cleavages (Chowdhury et al, 1995) giving rise to a 32 aa Lebocin mature peptide, which results O-glycosilated in a single threonine residue. It is thought that Lebocin targets microbial membranes of both Gram-positive and -negative bacteria, as well as fungi (Yi et al, 2014) and its O-glycosilation is essential for the full peptide activity. However, its *in vitro* antimicrobial activity has been found to be very low, in comparison to Cecropin B (Hara and Yamakawa, 1995).

Lysozyme

Beyond antimicrobial peptides, other humoral immune effectors are produced after microbial challenge and act against pathogens in the insect hemocoel. Among these, Lysozyme is one of the most known antimicrobial proteins, first identified by Alexander Fleming in 1922. Lysozyme acts primary on Gram-positive bacteria, such as *Micrococcus*, since it is able to break the bond between N-acetylglucosamine and N-acetylmuramic acid of peptidoglycan. Insect Lysozymes, however, have been reported to have a weak antimicrobial activity. In *B. mori* 1 *lysozyme* and 3 *lysozyme-like* genes have been identified (Lee and Brey, 1995; Tanaka et al, 2008). Lysozyme-like proteins (LLPs) lack the critical residues responsible for the muramidase activity, but have been reported to possess antimicrobial activity against Gram-positive and -negative bacteria, probably acting with mechanisms distinct from Lysozyme (Gandhe et al, 2007). Insect *lysozyme* genes are constitutively expressed, but they are often induced after microbial challenge (Morishima et al, 1995). In the silkworm, Lysozyme activity was found to

significantly differ among developmental stages, with mature larvae showing the highest Lysozyme concentrations (Morishima et al, 1994).

Prophenoloxidase and Melanization

Another important humoral immune response is an early reaction activated by the presence of invading microorganisms in the hemolymph or to tissue mechanical damages. The melanization reaction is not only a component of the humoral response, but it is also an important intermediary of cellular immunity, since it is involved in the encapsulation and sequestration of pathogens. The progression of this reaction is visible because the wound site or the surface of the pathogen becomes rapidly dark because of the presence of melanin (Kounatidis and Ligoxygakis, 2012).

Phenoloxidase (PO) is a circulating enzyme responsible for the melanization of hemolymph through the synthesis of melanin. Melanin deposits on damaged tissues or on foreign microbes, preventing or retarding their growth and mediating the activity of phagocytic cells. The reactions leading to melanin involve the synthesis of reactive oxygen species (ROS) and other toxic intermediates, which contribute to the counteraction to foreign microorganisms (Cerenius and Söderhäll, 2004).

PO is constitutively present in the hemolymph as inactive Pro-phenoloxidase (PPO). After an immune challenge, PAMPs are recognized by PGRPs and βGRPs and activate the CLIP serine protease cascade, which includes the so-called “pro-phenoloxidase cascade”. Therefore, PPO is cleaved in a specific site that is highly conserved throughout Insects, leading to the activation of PO. A negative regulation of these processes is carried out by Serpins, which finely control the activation of PO. Moreover, some insect pathogens are known to produce molecules that inhibit the PPO activation, blocking the melanin production (Clark and Strand, 2013). The active PO catalyzes the oxidation of Tyrosine-derived monophenols to ortho-diphenols and the further oxidation of ortho-diphenols to ortho-quinones, which are polymerized and form melanin (Cerenius and Söderhäll, 2004).

Moreover insect PPO possesses two conserved copper binding sites, which are thought to be involved in oxygen transportation, since they resemble the two copper sites of arthropod hemocyanins (Tanaka et al, 2008).

In the silkworm, PPO is synthesized by oenocytoids, a class of hemocytes (see below; Cerenius and Söderhäll, 2004). *B. mori* PPO is an heterodimer composed by two subunits encoded by two distinct genes, *PPO1* and *PPO2*. However, no signal peptide has been identified in *PPO* genes, suggesting that the PPO enzyme might be released in the hemolymph by cell lysis, as it occurs for hemocyanin (Tanaka et al, 2008).

Once *B. mori* PO is activated, it is thought to form a multi-protein complex with Serine Proteases, localizing near the wound site or in proximity to the foreign targets, where it synthesizes melanin. Wounded silkworm larvae were observed to activate the melanization reaction more rapidly than other insects as *Manduca sexta* or *Tenebrio molitor*, but the reasons of this early melanization have not been completely elucidated (Clark and Strand, 2013). In *Drosophila*, mutants for genes encoding the two PPO subunits are more sensitive to infections of Gram-positive bacteria and fungi, and are more susceptible to wounding, confirming the importance of this complex in the insect immune mechanism (Binggeli et al, 2014; Dudzic et al, 2015). A recent study showed that in silkworms PPO is also produced by the cells of the hindgut, the posterior part of the intestine. The hindgut PPO it is secreted into the lumen, where it induces feces melanization and reduction of bacteria content, representing an additional PO-mediated mechanism of the insect immune defense (Shao et al, 2012).

Cellular Immunity

The cellular component of insect immunity is represented by different blood cells that are able to identify foreign elements in the hemolymph and to actively remove them. The mechanisms through which these invading factors are cleared away from the hemolymph differ on the basis of their dimensions and dissemination.

B. mori, as other *Lepidoptera*, possess 5 different types of hemocyte cells, classified on the basis of their morphology and function:

- granulocytes are the most abundant hemocyte cell type. They resemble mammalian neutrophils, as they promptly adhere to invading elements, spread on their surface in a symmetric way, and finally phagocytize them.
- plasmatocytes are also involved in the phagocytosis, but also in capsule formation. They spread on foreign surfaces asymmetrically and are compared to mammalian macrophages.
- oenocytoids are the main responsible of hemocyte-mediated PPO synthesis, thus they are involved in the melanization response. They are not directly involved in the adhesion to foreign surfaces.
- spherule cells are thought to transport cuticular components, possibly participating in the repair events after cuticle mechanical damages.
- prohemocytes are the progenitor cells of all mentioned hemocyte types.

During larval developmental stage, granulocytes and plasmatocytes are the most abundant hemocyte type and are the only cells able to adhere to foreign surfaces (Lavine and Strand, 2002).

Hemocyte cells are responsible for three main immune mechanisms: phagocytosis, encapsulation and nodule formation.

Phagocytosis is the process through which foreign particles smaller than host cells, such as viruses, yeasts or bacteria, are engulfed by specialized hemocytes to form an intracellular phagosome. The engulfment of the target particles occurs through three phases: attachment, filopodial elongation through actin polymerization, and internalization. Once the target has been internalized, it forms a phagosome, which is subsequently fused to hemocyte lysosomes and endosomes. Finally the exogenous particle is destroyed by ROS, proteases and AMPs. Granulocytes are the hemocyte type mainly responsible of this mechanism (Strand, 2008; Tanaka and Yamakawa, 2011).

Foreign particles bigger than bacteria or yeast cells are eliminated from the hemolymph through encapsulation. In this case, the exogenous material is represented by parasitoids or nematodes, such as wasp larvae or eggs. It is thought that granulocytes are the first cells which interact with the target. After the releasing of cytokine molecules, they recruit plasmocytes. Granulocytes and plasmocytes bind the invaders and isolate them, inhibiting their growth and spread (Strand, 2008; Tanaka and Yamakawa, 2011).

The binding of many hemocytes to target particles in septic infection is called nodule formation. It has been observed that complexes of PPO and serine proteases localize on nodules, activating a strong local melanization response, which contributes to pathogen destruction (Tokura et al, 2013).

As for the humoral response, the activation of the cellular immunity is a multistep process, involving the recognition of the foreign element, a signal transduction activation and the production of effectors to counteract the invading pathogens.

It has been demonstrated that hemocytes are able to sense the presence of foreign elements through the already mentioned humoral PRRs (PGRPs, GNBPs, βGRP, Hemolin, C-type Lectins, Thioester Containing Proteins), as well as via hemocyte surface receptors. These latter membrane proteins are a wide group including scavenger receptors as *Drosophila* dSR-CI, Peste and Croquemort, membrane PGRPs (as *Drosophila* PGRP-LC) and other membrane proteins which have not been well characterized in Lepidoptera, as *Drosophila* Eater, Nimrod, Noduler, Draper, Down syndrome cell-adhesion molecule (Dscam), Integrins (Marmaras and Lampropoulou, 2009).

Signal transduction cascades in hemocytes comprise the Toll, Imd, JAK/STAT and JNK pathways described above, as well as the PO cascade. All these pathways induce

AMP synthesis, production of melanin and reactive oxygen and nitrogen species. It is thought that in Lepidoptera, granulocytes and plasmocytes synthesize AMPs, while spherule cells and oenocytoids are able to produce only Lysozyme (Strand 2008; Marmaras and Lampropoulou, 2009).

Both cellular and humoral immunities act in concert to protect insects to pathogen infections. The contribute of the cellular component appeared however to be less important with respect to that of the humoral immunity, since in *Drosophila* the inhibition of the hemocyte phagocyting activity does not modify the sensitivity to *E. coli* infections in wild-type flies (Elrod-Erickson et al, 2000).

Structure of the Thesis

The research project which I developed during my PhD is reported in the following chapters.

In Chapter 2 the characterization of the four silkworm strains selected for this study will be illustrated. In particular we focused on the production capabilities of the four lines and on some morphological and physiological aspects important in the response to infections. Moreover we analyzed the genetic variability of the four silkworm lines at the level of the 21 *B. mori* AMP genes, with the final aim to identify peculiar polymorphisms able to modify the peptide stability or efficiency.

In Chapter 3 the sensitivities to microbial attack of the four silkworm lines will be investigated. We performed infection experiments in which each *B. mori* line was exposed to two silkworm pathogens, the Gram-positive *Enterococcus mundtii* or the Gram-negative *Serratia marcescens*. After a 24 h oral infection, the differential response to pathogens of the 4 strains was determined by comparing 1) the survival profiles, 2) the presence of living pathogen cells in the hemolymph circulation, 3) the expression induction of 9 representative AMP genes in the tissues involved in the immune response (fat bodies and midgut), 4) the *in vitro* antimicrobial activity of the silkworm hemolymph, 5) the rate of the melanization reaction, and 6) the Lysozyme concentration in larvae plasma, among the different strains.

In Chapter 4 the effect of non-synonymous substitutions on AMP sequences will be evaluated. In particular we performed a first *in silico* analysis on the data obtained from the sequencing of the *B. mori* AMPs to determine the theoretical relevance of the detected amino acid substitutions. We attempted to obtain Gloverin 1 and 2 isoforms using both prokaryotic and eukaryotic heterologous systems. Then we compared the differential *in vitro* activities for two Cecropin B variants that showed a differential distribution in the four silkworm strains.

In Chapter 5 the characterization of two transgenic lines constitutively over-expressing *moricin* in fat bodies will be illustrated. We determined for both lines the position of the integrated transgene, the expression of *moricin* in fat bodies and the antimicrobial activity of hemolymph extracted from transgenic larvae.

All results obtained from these studies are globally discussed in Chapter 6.

Chapter 2: Characterization of the Four *Bombyx mori* Strains

Introduction

Silkworm Strains

More than 4000 silkworm strains are estimated to exist worldwide, including parental lines, hybrids and mutants (Zanatta et al, 2009). These strains are mainly maintained in germplasm banks of silk-producing countries (Goldsmith et al, 2005). Since silkworms have been completely domesticated and are no longer able to survive autonomously in natural environments, these Institutions represent the only source of *B. mori* biodiversity, besides being fundamental for sericulture preservation (FAO, 2003).

Through archaeological and genomic data, it was established that *B. mori* was domesticated more than 5000 years ago (Goldsmith et al, 2005). Silkworm strains originated from a common ancestor, the wild Chinese *Bombyx mandarina*, but the domestication events probably occurred simultaneously in different places and involved a large number of individuals, since domesticated silkworms exhibit high levels of inter-strain genetic variability (Xia et al, 2009). Domestication in silkworms led to a decrease in heterozygosity evaluated at a genome-wide level, probably because of inbreeding and/or bottleneck events occurring during rearing (Xia et al, 2009).

In general domestication gave rise to the loss of many traits, as the ability to fly or to avoid predators and diseases, but it also led to the acquisition of other important features, as the tolerance to human presence and manipulation and to crowded environments (Xia et al, 2009). Following domestication a large amount of strains arose and diversified in many productive features, such as the shape and color of the cocoon, the quality and quantity of the silk, as well as in many physiological traits, such as number of generations per year (the voltinism), growth rate, digestion efficiency and resistance to infections (Goldsmith et al, 2005). Currently silkworm strains can be roughly classified in four groups on the basis of their geographical origin: Chinese, Japanese, European and tropical (Zanatta et al, 2009). Monovoltine silkworms originated from temperate regions and belong to the Chinese, Japanese and European groups. On the other hand, polyvoltine lines originated from areas in which mulberry leaves are constantly present, therefore they belong mainly to the tropical group (FAO, 2003). Strains originating from tropical and temperate regions not only differ in their voltinism, but also for important economic traits: it is a general observation that silkworm lines from temperate regions possess the highest productivity, in terms of both silk quality and quantity, but are very susceptible to diseases. On the contrary

tropical strains produce low quantities of poor quality silk, but are tolerant to pathogen infections (FAO, 2003).

Bombyx mori Strains Selected for this Study

Since we were interested in the generation of silkworm strains with high tolerance to natural infections, we tried to establish if four *B. mori* lines with different geographical origin were effectively characterized by a differential sensitivity to pathogen oral exposure and if this different tolerance had a genetic basis. The four lines studied are part of the germplasm bank of the Sericulture Unite of the CREA-API of Padova, Italy, and originated, respectively, from China (strain "SCI 124"), Japan (strain "SGIII 129"), Europe (strain "Romagna bis") and India (strain "Nistari"). The Chinese, Japanese and European lines belong to the "temperate region" group, while the Indian one is classified as "tropical" (Figure 1).

The Indian strain is the only polyvoltine line: since it is able to reproduce continuously during the year and its life cycle is relatively short (41 days), it is suitable as "laboratory" line in biology and genetics research. Moreover, it is commonly used in India for silk production. This strain is part of the CREA-API collection since its transfer from the French National Institute for Agricultural Research (INRA) germplasm bank in 2009.

The Chinese and Japanese strains are monovoltine lines imported from Japan in 1997. These two strains are parental lines which are crossed to produce a particularly productive hybrid, currently sold to sericulturists for silk production. They complete their life cycle in 47-48 days.

The European strain is an Italian monovoltine line selected from the strain "Romagna" in 1990 for its bigger cocoons. Currently, it is not used for silk production but for particular decorative purposes, since its silk is fine and has a particular yellowish/golden color. Its life cycle is the slowest: it takes 53 days to reach the adult stage.

Experimental Overview

We characterized the four strains in germ-free conditions for some of their phenotypic and genotypic traits that are related both to their production capabilities and to their potential ability to respond to oral infections. In particular, we determined 1) their silk productivity, in terms of both quantity and quality; 2) the morphology of the intestinal *epithelia* and peritrophic membranes (PMs) as well as 3) the total number of hemocyte cells at the beginning of the fifth larval stage, when oral infections were planned to be performed. In addition, we investigated 4) the genetic variability at the level of antimicrobial peptide coding genes, to evaluate the possible presence of strain-specific AMP isoforms with modified activity or stability.

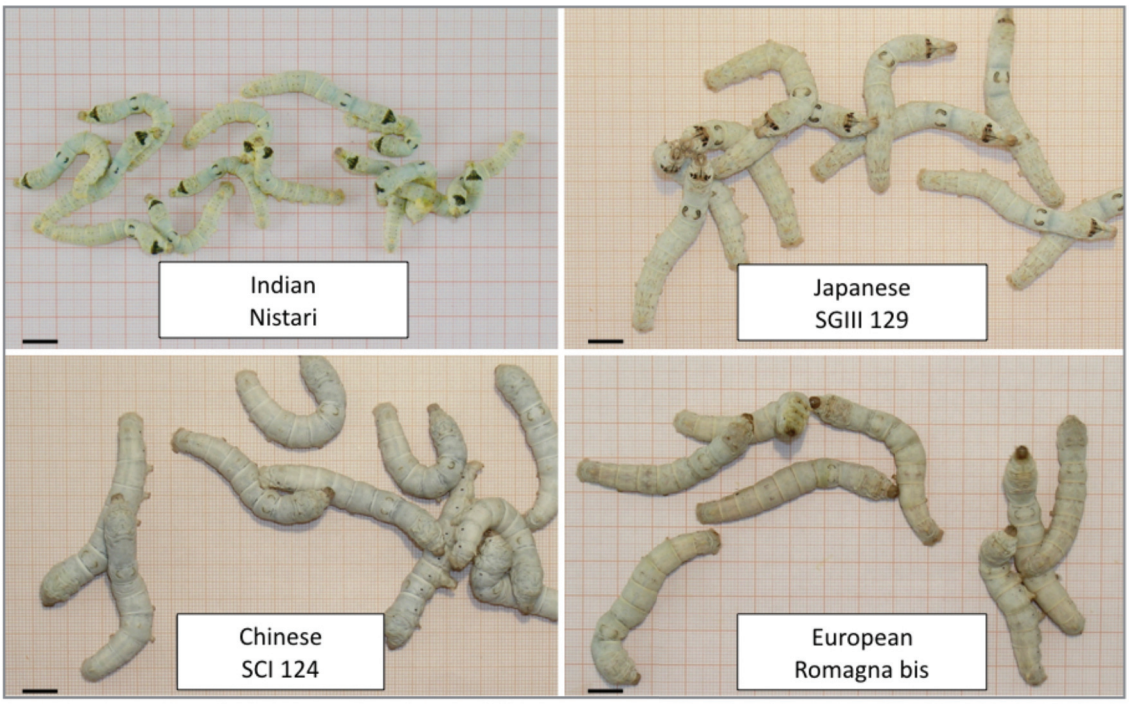

Figure 1. The four selected lines at the fifth larval stage. Bars: 1 cm.

Results

Estimation of the Four Strain Productivity

The four strains were analyzed evaluating their silk production efficiency, in terms of both silk quantity and quality. As to production capabilities, the silk percentage is generally calculated as the ratio between the weight of the empty silk shell and the weight of the whole cocoon (cocoon shell/whole cocoon weight ratio). Therefore, highly producing strains possess high values of silk ratios while scarcely producing lines have low silk ratios values. Figure 2 shows the median of the silk percentages produced by the four strains, evaluated on at least 45 organisms per line. The Japanese and Chinese strains showed similar silk productivity, significantly higher in comparison to both the Indian and European strains (One-way ANOVA: $F_{3,328}$ = 818.3, P < 0.001; Bonferroni *post hoc* test significant (P < 0.05) in all comparisons, except for the Japanese-Chinese and European-Indian comparisons).

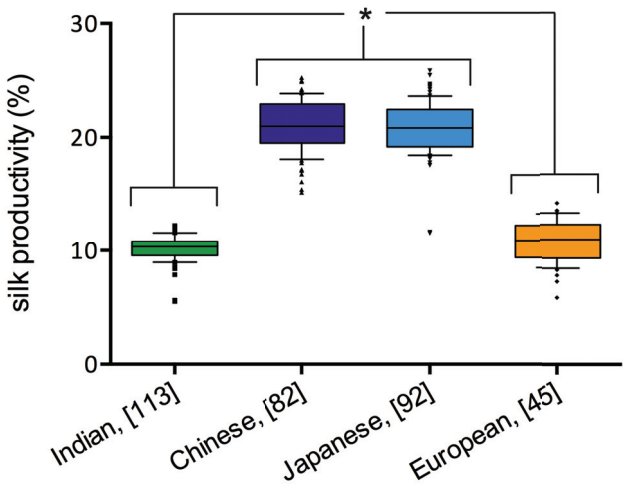

Figure 2. Quantity of silk fibers produced by the four silkworm strains. Silk percentage is calculated as the ratio between the cocoon shell weight and the whole cocoon weight (median, 10-90 percentile are shown). In square brackets the number of individuals used for the silk quantity determination. Significant differences in silk productivity: Chinese-Japanese > Indian-European (Bonferroni *post hoc* test, * P < 0.05).

To evaluate silk quality, we determined the fiber linear mass density. This parameter is measured in “deniers”, with one denier corresponding to 1 gram per 9000 meters of silk. Therefore, low denier values indicate a thin and fine silk fiber, while high denier values are typical of coarse and thick yarns. Table 1 reports the linear mass density values of silk fibers of the four silkworm strains, obtained from at least 45 individuals per strain. The European strain spun showed significant lower denier values

in comparison to the other strain yarns, representing therefore the finest silk fiber, followed by the Indian, the Chinese and the Japanese strains (One-way ANOVA: $F_{3,35}$ = 1012, $P < 0.0001$; Bonferroni *post hoc* test significant ($P < 0.05$) for all comparisons).

Strain	Linear Mass Density (deniers)
Indian (Nistari)	1.74 ± 0.02
Chinese (124)	1.94 ± 0.03
Japanese (129)	2.03 ± 0.01
European (Romagna)	1.55 ± 0.02

Table 1. Quality of silk fibers produced by the four silkworm strains. Silk quality is expressed in deniers (weight in grams of 9000 meters of fibre; mean ± SEM are shown). Significant differences in silk quality: European > Indian > Chinese > Japanese. Bonferroni *post hoc* test, $P < 0.05$ for all comparisons.

Morphology of Intestinal *Epithelia* and Peritrophic Membranes

Silkworm larvae begin to ingest food from their hatching from eggs. Therefore, one of the main route of naturally occurring infections during larval stage is the oral ingestion of pathogens.

The midgut is the first barrier that any microorganism encounters in oral infections. To identify possible differences in the morphology of this structure among the four *B. mori* strains, PMs and intestinal *epithelia* from germ-free larvae were sampled at the beginning of the fifth larval stage. Midgut samples were collected putting particular attention in the preservation of the corresponding inner PM. At least 6 individuals per strains have been analyzed.

The structure of the PMs in the different *B. mori* strains showed marked morphological differences, when analyzed under both light and TEM microscopes (Figure 3). In particular, the PM of the European strain had a felt-like appearance, with chitin fibrils aligned in thicker bundles. Conversely, in the Indian, Chinese and Japanese

strains this membranous structure was made of thin and separate layers of chitin fibrils.

Considering the morphology of the intestinal *epithelia*, no remarkable differences were observed among the lines, with midgut *epithelia* showing a comparable thickness and structure.

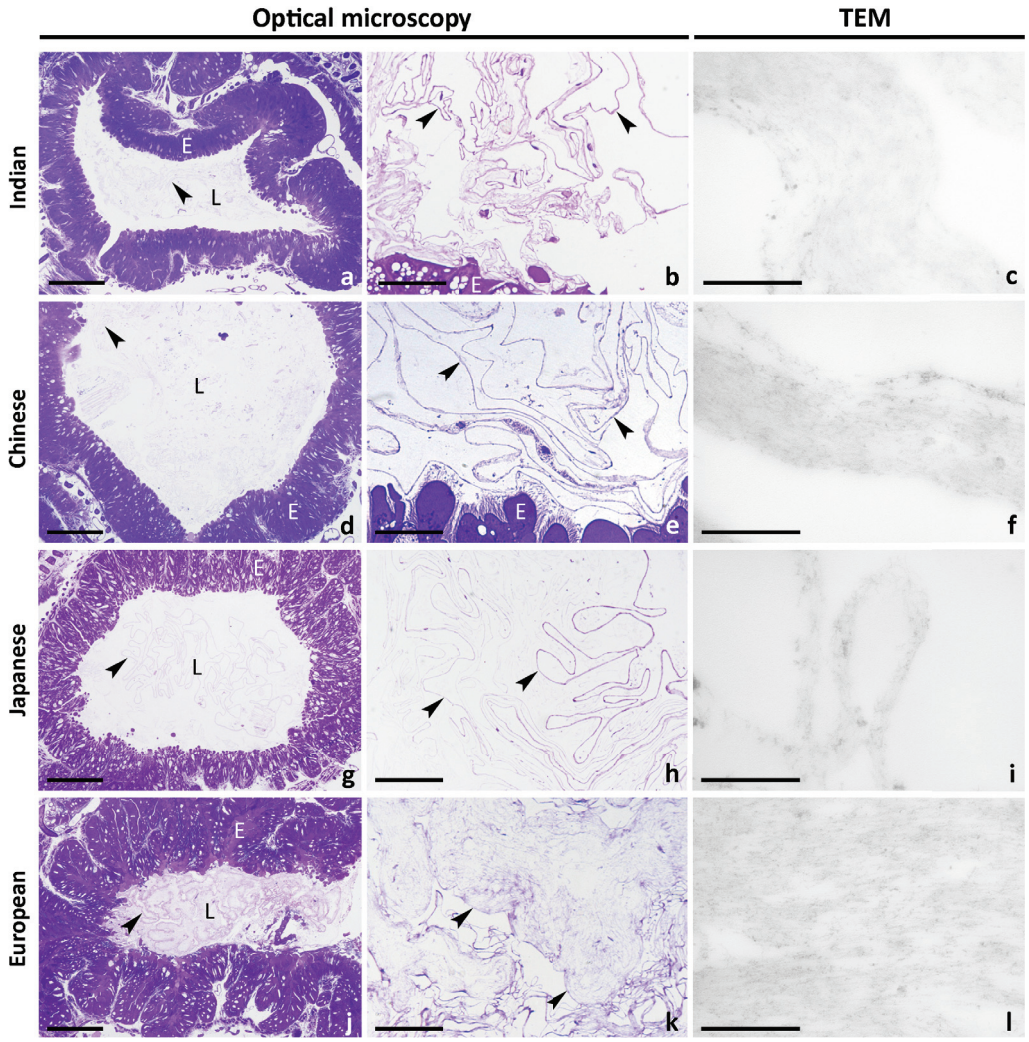

Figure 3. Morphology of the peritrophic membranes of fifth instar larvae of the four *B. mori* strains: Indian; Chinese; Japanese; European. Semithin cross-sections (a, b, d, e, g, h, j, k), TEM (c, f, i, l). Light and TEM analyses showed a marked morphological difference in the peritrophic membrane of the European strain (j-l) in which chitin fibrils are aligned in thicker bundles, and the peritrophic membrane has a felt-like appearance. In Indian (a-c), Chinese (d-f) and Japanese (g-i) strains, this membranous structure is made of thin and separate layers of chitin fibrils. b, e, h, k are details at higher magnification of a, d, g, j, respectively. Arrows: peritrophic membrane; E: midgut epithelium; L: midgut lumen. Bars: 200 µm (a, d, g, j), 10 µm (b, e, h, k), 500 nm (c, f, i, l).

Count of Hemocytes

Hemocytes represent the main players in the cellular immune response and the total number of hemocyte cells that the larvae possess before encountering any pathogen gives an indication of the possible differences that the four strains might have at cellular immunity level. Therefore, we determined the total number of hemocyte cells of the four strains at the beginning of the fifth larval stage, in germ-free conditions (Figure 4). For each line, hemocytes sampled from at least 10 individuals were analyzed. The Japanese strain showed a significantly higher number of hemocytes per mm^3 of hemolymph in comparison to the Indian, Chinese and European lines (One-way ANOVA: $F_{3,36} = 8.857$, $P < 0.001$; Bonferroni *post hoc* test significant ($P < 0.05$) only for the comparisons between the Japanese line and the other three strains).

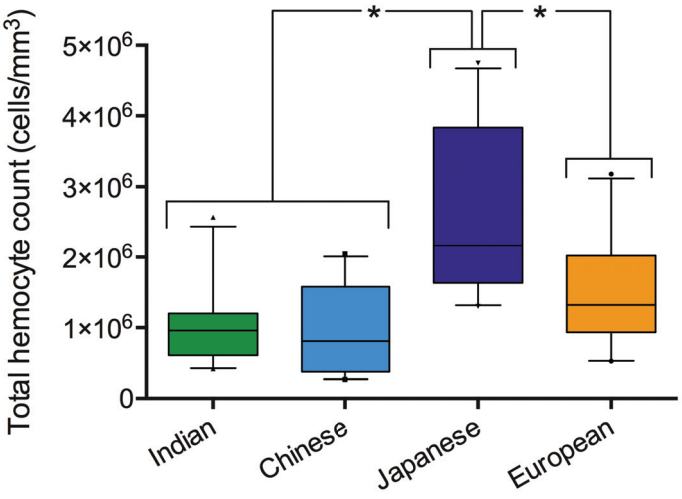

Figure 4. Total hemocyte count of fifth instar larvae of the four *B. mori* strains. The total hemocyte count is expressed as the number of hemocyte cells per mm^3 of hemolymph (median, 10-90 percentile are shown). Significant differences in total hemocyte count: Japanese > Indian-Chinese-European (Bonferroni *post hoc* test, * $P < 0.05$).

Analysis of AMP Coding Sequences

In order to investigate the genetic variability at antimicrobial peptides level in the four strains, we analyzed the coding sequences of all 21 *B. mori* AMP genes. AMP cDNA sequences were obtained from 10 individuals per strain and were first compared at nucleotide level. From the overall nucleotide sequences' comparison, several polymorphisms were identified in most AMP genes, except for *cecropin-A1*, *-A2*, *-D* and *moricin* (Table 2). Polymorphic alleles were detected within the Chinese, Japanese and European strains, while the Indian line was found to be almost monomorphic, with only 2 genes over 21 (*cecropin-B1* and *-B2*) displaying variability among the 10

individuals (Table 2 and Table A.1). Although our analysis was conducted on a limited number of individuals, some general considerations can be stated. In the inter-strain comparison, several alleles were found to be shared by different silkworm strains. In particular, the Chinese and the Japanese lines were found to have many alleles in common: among the 21 differential alleles found in the Japanese strain, 14 were shared with the Chinese line. Conversely, the European line seemed to carry the highest number of strain-specific alleles: this line carried 13 European-specific alleles over its 24 total alleles.

The conceptual translation of the identified AMP cDNAs showed that about one third of the polymorphisms were non-synonymous substitutions which modified the codified amino acids (Table 2). At amino acidic level, all AMPs were found to possess at least two protein isoforms, with the exception of *moricin, attacin*, *cecropin-B3*, *-B4*, *-B5, -B6* and *-E*. A summary of the information about the sequence analysis at the amino acid level is reported in Table A.2.

As to peptide sequences, most AMP variants were found to be present in more than one strain. However, strain-specific isoforms were also identified, for example for Cecropin-B1 and -B2 and for the four Gloverins.

In some cases, the amino acid substitutions mapped in the signal peptide which is removed during AMP processing, or in the peptide portion removed after an eventual second proteolytic cleavage. In those cases, it is unlikely that amino the acid modifications could have a direct effect on the AMP activity, even if those portions might be important for the regulation of AMP processing. On the other hand, modified residues were also found to be part of the active portion of certain AMPs. Focusing on these latter modifications, protein variants were identified for Cecropin-B1, -B2, Enbocin-1, -2, Gloverin-1, -2, and -3.

AMP	Gene length (cds)	Peptide length (full)	Peptide length (act)	N° alleles (DNA)	S	N	N (pre)	N (act)	N° isoforms (protein)	N° isoforms (active peptide)
Attacin	644 bp	214 aa	188 aa (27-214)	3	14	-	-	-	1	1
Cecropin A1	192 bp	63 aa	35 aa (27-61)	1	-	-	-	-	1	1
Cecropin A2	192 bp	63 aa	35 aa (27-61)	1	-	-	-	-	1	1
Cecropin B1	192 bp	63 aa	35 aa (27-61)	4	6	1	-	1	2	2
Cecropin B2	192 bp	63 aa	35 aa (27-61)	4	3	2	-	2	3	3
Cecropin B3	192 bp	63 aa	35 aa (27-61)	2	3	-	-	-	1	1
Cecropin B4	192 bp	63 aa	35 aa (27-61)	4	5	-	-	-	1	1
Cecropin B5	192 bp	63 aa	35 aa (27-61)	5	5	-	-	-	1	1
Cecropin D	186 bp	61 aa	37 aa (25-61)	1	-	-	-	-	1	1
Cecropin D2	200 bp	66 aa	?	3	1	2	1	1 (?)	3	2 (?)
Cecropin E	197 bp	65 aa	?	3	7	-	-	-	1	1
Defensin	287 bp	92 aa	36 aa (57-92)	2	-	1	1	-	2	1
Enbocin 1	179 bp	59 aa	37 aa (22-58)	2	6	4	-	4	2	2
Enbocin 2	179 bp	59 aa	37 aa (22-58)	3	8	4	-	4	2	2
Gloverin 1	539 bp	178 aa	135 aa (44-178)	5	13	5	3	2	4	3
Gloverin 2	521 bp	173 aa	131 aa (43-173)	4	13	4	3	1	3	2
Gloverin 3	524 bp	172 aa	131 aa (42-172)	5	15	6	5	1	5	2
Gloverin 4	518 bp	171 aa	131 aa (41-171)	3	7	3	3	-	3	1
Lebocin	542 bp	179 aa	32 aa (121-152)	2	2	4	4	-	2	1
Moricin	203 bp	66 aa	42 aa (25-42)	1	-	-	-	-	1	1

Table 2. Summarizing information on polymorphisms identified in AMP genes of the four *B. mori* strains. For each AMP the following information is indicated: length of the gene coding sequence (cds); length of the whole peptide (full); length of the active portion of the peptide (act), with indication of the starting and final residues that compose the mature portion; total number of alleles identified at the nucleotide level; number of synonymous substitutions (S); number of non-synonymous substitutions (N); number of non-synonymous substitutions in the pre-peptide or pre-pro-peptides (N pre), which are removed after the proteolytic cleavages; number of non-synonymous substitutions in the active portion of the peptide (N act); total number of protein isoforms deduced from the nucleotide sequences; number of protein isoforms with modification only in the active portion of the peptide.

Discussion

The four strains selected for this study were found to differ in their productive traits and in their physiology. Apart from voltinism, which is strictly related to the geographical origin, Chinese and Japanese lines were found to be the best silk producers, while the European strain was shown to produce the highest quality silk. These data confirmed one of the general observations which gave origin to this research: strains originating from temperate regions are better producers, both in terms of quality and quantity.

The four *B. mori* lines were found to possess similar intestinal *epithelia* but they were shown to differ in the morphology of their PMs, with the European strain possessing a significantly thicker chitinous matrix. PM protects intestinal *epithelia* from mechanical damages (Wang and Granados, 2001). However, it has not been established if a thick PM might be advantageous during oral infections (Weiss et al, 2014; Kuraishi et al, 2011).

The four *B. mori* strains also showed a certain degree of variability in the total number of hemocyte cells present in their hemolymph, with the Japanese line characterized by the highest numbers in comparison to all the other strains. Given that hemocytes are the main actors in the cellular immunity, these data might suggest that the Japanese line might be more prone to respond to pathogen infection with cellular immunity defense strategies when compared to the other strains.

Finally, the silkworm strains selected for this study were found to have a certain level of polymorphism at AMP coding sequence level. Although the set of the analyzed genes included only the immune effectors and then is limited in comparison to the whole genome, some general considerations about the genetic variability of the four strains can be made. The Indian strain resulted almost monomorphic. This is probably due to the fact that at the CREA-API seat this line is mainly maintained in small populations since it is mostly used as laboratory strain rather than a silk producer. Differently from the Indian line, the Japanese, Chinese and European strains were found to be more polymorphic in their AMP coding genes. This is probably due to their use as parental lines for the generation of hybrid strains for silk production and therefore they are reared in large populations. In addition, the Japanese and Chinese lines shared several AMP isoforms, while the European line possessed the highest number of strain-specific alleles, suggesting that the genetic distance between Japanese and Chinese lines is probably lower in comparison to the European strain.

Evaluations about the meaning of the amino acid substitutions found in the AMP variants of the four silkworm lines will be further discussed in Chapter 4.

Materials and Methods

Silkworm Germplasm Maintenance

Silkworm strains maintained in the germplasm bank of the CREA-API are reproduced annually during spring and late summer. For each line, at least 25 egg-masses, each made of about 400-600 eggs, give birth to more than 10,000 individuals every year. Larvae are fed on fresh mulberry leaves and reared until pupation. About 200 individuals (100 males and 100 females) are selected on the basis of the morphology of their cocoon and crossed to reconstitute the stock. Each stock is composed by 72 independent egg-masses, each originating from a single couple. Eggs are then subjected to a progressively decreasing temperature (aestivation) and then maintained at 5-2.5°C until the following year (hibernation).

Silkworm Strains Selected for the Study

The four silkworm strains originating from the four geographical areas and used in this study are: Nistari (Indian), SCI 124 (Chinese), SGIII 129 (Japanese) and Romagna bis (European). All these four *B. mori* lines belong to the CREA-API germplasm collection and are reproduced annually as described in the previous paragraph. For silk quality and quantity valuation, larvae fed on fresh mulberry leaves were used. On the other hand, larvae fed on artificial diet (Cappellozza et al, 2005) in germ-free conditions were used for the sampling of midgut specimens for the histological observation, for the hemocyte cell count and the evaluation of AMP genetic variability and.

Silk quantity and quality evaluations and hemocytes counts were all performed by Dr. Alessio Saviane of the CREA-API sericulture unit of Padova (Italy).

Silk Quantity and Quality Evaluations

Five to six days after spinning, cocoons were collected and individually weighed from at least 45 individuals per strain. Subsequently, cocoons were cut and the silk shell was individually weighed after pupa extraction; the silk ratio was calculated (silk ratio= weight of silk shell/weight of cocoon expressed in grams) according to the pupa sex. Pupae were numbered to maintain their production parameters identifiable.

At least 45 cocoons per line were analyzed for the silk quality evaluation. Five to six days after spinning, cocoons were boiled for 90 sec and then keep in hot water at 60°C until processing. From each cocoon a single silk bundle was spun, recording the length of the silk thread. The obtained bundles were weighted and the “denier” value was calculated considering that one denier correspond to 1 gram per 9000 meters of silk.

One-way Anova test were conducted on both silk quality and quantity data, with Neuman-Keuls *post hoc* analysis for the intra-strain comparisons.

Histological Sample Preparation and Observation

Larvae at the first day of the fifth instar were anesthetized with ice before dissection. They were cut dorsally and the midgut, including the inner PM, was immediately isolated and cut in small pieces. Midguts of at least six larvae per strain were processed for light microscopy and transmission electron microscopy (TEM) [Prof. Gianluca Tettamanti of Università degli Studi dell’Insubria, Varese (Italy)]. Midgut samples were fixed in 4% glutaraldehyde (in 0.1 M Na- cacodylate buffer, pH 7.4) overnight at 4 °C. Specimens were postfixed in 1% osmic acid for 1 h at room temperature and, after dehydration in an ethanol series, were embedded in an Epon/ Araldite 812 mixture. Semithin sections were stained with crystal violet and basic fuchsin and observed by using a Nikon Eclipse Ni-U microscope (Nikon, Tokyo, Japan). Images were acquired with a DS-5 M-L1 digital camera system (Nikon). Thin sections, stained with uranyl acetate and lead citrate, and observed with a JEOL JEM-1010 electron microscope. Images were acquired with an Olympus Morada digital camera.

Count of Hemocytes

For each of the four *B. mori* strains, hemolymph samples were collected from 10 individuals at the first day of the fifth larval stage. Before sacrifice larvae were anesthetized with ice. One of the abdominal proleg was cut with scissors and the outflowed hemolymph was collected in a centrifuge tube. An equal volume of 1% formaldehyde was added to the collected hemolymph samples, reaching a final formaldehyde concentration of 0.5%. The fixed solution was loaded into a counting chamber and the number of hemocyte cells was counted following the Bürker double ruling. This number was finally multiplied for 20000, which represented the dilution factor, and the number oh hemocytes per mL was obtained.

Analysis of AMP Coding Sequences

AMP coding genes were amplified via PCR from cDNA obtained from retro-transcribed RNA, except for the *cecropin A* and *cecropin B* genes, which were amplified from genomic DNA because of their high similarity at coding sequence level. For each silkworm strain, all 21 AMP genes were amplified from 10 individuals, Sanger-sequenced and analyzed.

Total RNA extraction: since most of the AMPs shows a pathogen-inducible expression, to obtain sufficient amounts of their mRNAs to allow their amplification, silkworm larvae were infected by contaminating their artificial diet with an overnight culture of the silkworm Gram-positive pathogen *Enterococcus mundtii* ($2.7*10^2$ CFU/mL) two days before sampling. Then the heads of 10 individuals per strain were homogenized in 500 µl of Trizol (Thermo Fisher Scientific) using an IKA T10 basic homogenizer and incubated at RT for 5 min. 100 µl of chloroform were then added. The mixture was vigorously shaken for 15 sec, incubated at RT for 2-3 min and centrifuged at 4°C for 15 min at 12000 x g. The aqueous phase was transferred in a new centrifuge tube and RNA was precipitated with 250 µl of RT isopropanol and incubated at -20°C for 1 h. Samples were then centrifuged at 4°C for 10 min at 12000 x g; supernatants were removed and pellets were washed with 1 mL of 75% ethanol. After a last centrifuge at 4°C for 5 min at 7500 x g, supernatants were removed, samples were air dried and resuspended in 80 µl of nuclease-free water. RNA quality and quantity were determined with NanoDrop 2000 (Thermo Fisher Scientific). RNA samples were stored at -80°C.

First-strand cDNA synthesis: RNA was retro-transcribed using EuroScript M-MLV Reverse Transcriptase (Euroclone). Reaction volumes were set between 10 and 20 µl, depending on the concentration of the RNA samples. First, 2.5 µg of total RNA were incubated with 1 µM oligo-dT_{18} at 65°C for 6 min and immediately put on ice. Then, 1mM dNTPs, Euroscript Buffer 1x, 10 mM DTT were added to the RNA-oligo-dT mixture. Finally 0.5 µl (100 units) of Reverse Transcriptase were added. After 1h at 42°C, additional 0.5 µl (100 units) of Reverse Transcriptase were added and incubated at 42°C for another h. The enzyme was heat-inactivated with a 10 min step at 70°C.

Genomic DNA extraction: genomic DNA was extracted from the midguts of 10 silkworms per strain. The midguts were homogenized an IKA T10 basic homogenizer in 500 µl of Grinding Buffer (0.2 M Sucrose, 0.1 M Tris pH 9, 50 mM EDTA, 0.5% SDS). After adding Potassium Acetate at a final 1 M concentration, samples were incubated at least 15 min on ice. Then, 500 µl of a phenol:chloroform mixture (1:1) were added. Samples were centrifuged for 15 min at 12000 x g at 4°C. The upper aqueous phase was transferred into a new centrifuge tube and DNA was precipitated with two iso-volumes of ethanol at -20°C for at least 1 h. After a centrifuge step at 12000 x g for 10 min at 4°C, supernatants were removed and pellets were washed with 750 µl of 70 %

ethanol. Samples were centrifuged at 7500 x g for 5 min at 4°C, supernatants were removed, pellets were air dried and finally resuspended in 50 µl of nuclease-free water. DNA quality and quantity were determined with NanoDrop 2000 (Thermo Fisher Scientific). DNA samples were stored at -20°C.

PCR amplification: AMP coding sequences were amplified in a total volume of 25 µl, containing 50 ng of cDNA or genomic DNA, 0.2 Units of Phusion® High-Fidelity DNA Polymerase (NEB), 200 µM dNTPs, 300 nM of each primer and the appropriate $MgCl_2$ containing buffer. The list of primers used for both amplification and sequencing of AMP genes are listed in Table 4. For all genes amplified from cDNA, for *cecropin-A1* (BGIBMGA006280), *cecropin-A2* (BGIBMGA014285) and *cecropin-B3* (BGIBMGA000024), a single PCR was carried out. Conversely, for the other 5 *cecropin-B* genes, a first PCR was carried out with outer primers (named "BIS"). Then, using this PCR as template, a second PCR was carried out using inner primers. This was necessary because of the high similarity at the level of both coding and non-coding sequences of the *cecropin-B* genes. The typical PCR cycle comprised an initial denaturing step at 98°C for 3 min, followed by 30 cycles of 98°C for 1 min, specific annealing temperature for 45 sec, 72°C for a period time varying from 15 sec to 2 min and 30 sec, depending on the amplicon length (see Table 3 for melting temperatures and extension times information). Amplicons were checked in 1 % agarose gel.

PCR purification and sequencing: PCR amplicons were purified using the Agencourt® AMPure® kit (Beckman Coulter) and sequenced with the Big-Dye Terminator Cycle Sequencing kit (Thermo Fisher Scientific) on an ABI 3730 platform (Thermo Fisher Scientific) at IGA Technologies Services (Udine, Italy). Sequencing primer was the same used for the amplification.

Sequence alignment: the software 4Peaks was used to visualize and determine the nucleotide sequences. The presence of double peaks of similar intensity in the same nucleotide position indicated heterozygosis for that site. The sequences obtained from the 10 individuals of the same *B. mori* strain were aligned using CLC Sequence Viewer. Sequences differing in at least one position, independently from the type of substitution, were considered different alleles. Then, all the detected intra-strain alleles were aligned, to assess if they were strain-specific alleles or if they were shared with one or more strains.

All identified alleles were then translated into their corresponding amino acid sequences. Sequences differing in at least one amino acid were considered different protein isoforms, independently from the type of substitution.

Gene (Gene id)	Primer name	Sequence (5'-3')	Template	Amplicon lenght (bp)	Tm	Ext. time
attacin BGIBMGA002747	ATT_FOR	AGATGTCCAAGAGTGTAGCGTTG	cDNA	790	60°C	45''
	ATT_REV	GGTTCTTTATTTGATAAGGCAGTACTGAC				
cecropin A1 BGIBMGA006280	CECA_6280_FOR	TATGCATTCCATCGTATAGCAATTT	gDNA	1002	58°C	1'
	CECA_6280_REV	GCTAAATGCGTCTTTGGTGCTA				
cecropin A2 BGIBMGA014285	CECA_14285_FOR	TCCTCCATACAGCGTATTTGTGAC	gDNA	1512	60°C	1'30''
	CECA_14285_REV	GAAGGCAATGACTGTGGTATTCTTA				
	CECA_14285_M_FOR	AACGCTCATCCTGTTGCCAT		698	60°C	45''
	CECA_14285_M_REV	ATGCGATGGCAACAGGATGA		832	60°C	1'
cecropin B1 BGIBMGA000021	CECB_21_BIS_FOR	TCAAAGCCCGCCTAGATGGC	gDNA	2364	63°C	2'30''
	CECB_21_BIS_REV	GCAATGTCCGCGGTGGAGT				
	CECB_21_FOR	TGTTAGCTCGTCCACCCAAC		1372	60°C	1'30''
	CECB_21_REV	CGTCACTGTAGATATTAAAAATGCGCT				
cecropin B2 BGIBMGA000023	CECB_23_BIS_FOR	GACGCAAATGAGTCATTGTTGTTGG	gDNA	1964	61°C	2'
	CECB_23_BIS_REV	GGTTGAGCTTTGTTAAAATGCGAGA				
	CECB_23_FOR	GGTTGAGCTTTGTTAAAATGCGAGA		911	60°C	1'
	CECB_23_REV	ACGAGTAGATTTATGGCGTACGTTT				
cecropin B3 BGIBMGA000024	CECB_24_FOR	CGTCTAACAACAAGCCACGC	gDNA	1485	60°C	1'30''
	CECB_24_REV	TGTTGTTCTCTTAGTGTGTTGGTTC				
cecropin B4 BGIBMGA000036	CECB_36_BIS_FOR	AAGGGACAGTTTACTTCGCTTGC	gDNA	1900	61°C	2'
	CECB_36_BIS_REV	GTTGATTGGCAGACTCCCTGC				
	CECB_36_FOR	AGGGAAGTACCCCTCTCGTG		1142	59°C	2'
	CECB_36_REV	AGGTAGTAGTGGTTTAAGGATTGATTA				
cecropin B5 BGIBMGA000037	CECB_37_BIS_FOR	CAGAGCGGGCGGTACTTC	gDNA	1317	60°C	1'30''
	CECB_37_BIS_REV	CGTGAATGGTGACGTCAATGTAG				
	CECB_37_FOR	ATCCGGCGAGAAACTCAGC		1264	59°C	1'30''
	CECB_37_REV	GATCATTTTCCTATAGCTTTAGCCG				
cecropin B6 BGIBMGA000038	CECB_38_FOR	CCAGTTTGGCTGTGAACTCC	gDNA	1497	59°C	1'30''
	CECB_38_BIS_REV	AACTAAGTGTGAAAGTGTCGTCAC				

Gene (Gene id)	Primer name	Sequence (5'-3')	Template	Amplicon lenght (bp)	Tm	Ext. time
	CECB_38_FOR	CCAGTTTGGCTGTGAACTCC		1286	59°C	1'30''
	CECB_38_REV	TCACTAAGAAAACTTTGGCAGACAT				
cecropin D NM_001043368.1	CECD_FOR	ATGAAAATCTCGAAAATTTTCGTTTTCG	cDNA	186	60°C	15''
	CECD_REV	CTATCCTTGTCCGAGAGCTTTTG				
cecropin D2 NM_001043459.1	CECD2_FOR	AGGCCGTAGAGCCCACAA	cDNA	261	59°C	15''
	CECD2_REV	CTCTGCTCTACTACGACACTCTATC				
cecropin E NM_001043927.1	CECE_FOR	GCCTCTCAACTAACGTATTCTTTGG	cDNA	306	60°C	30''
	CECE_REV	AAGTCTTTCACAGTCTATTGAGCG				
defensin NM_001043905.2	DEF_FOR	TGAGCAAGTTTCTGTATTTCTAGTCTG	cDNA	363	58°C	30''
	DEF_REV	TTTATTTGGCATTAACTAAAATGTATCCTT				
enbocin 1 NM_001044007.1	ENB1_FOR	GAGCTCGAACCCCGCTTTAG	cDNA	293	60°C	30''
	ENB1_REV	AATGCTGTTCCAAATAGTTGTGCG				
enbocin 2 NM_001098374.1	ENB2_FOR	TGTTCCTGACTCGGCACTC	cDNA	531	60°C	30''
	ENB2_REV	TGTCTCCAAAAGGCACTTTTATTGG				
gloverin 1 BGIBMGA013863	GLV1_FOR	GTCTCGAGCAGCGAAACCTG	cDNA	646	60°C	30''
	GLV1_REV	CATACTTCTAGGCTTACGAGGCAA				
gloverin 2 BGIBMGA005658	GLV2_FOR	GGTCTTGAGGAGCGAAACTTGA	cDNA	729	60°C	45''
	GLV2_REV	CGTCATAACAAAGCACGAGATCC				
gloverin 3 BGIBMGA013803	GLV3_FOR	CAACTCAAAATGAATTCCAAATTGCTG	cDNA	700	58°C	45''
	GLV3_REV	CAAGTTATCAGTAAGACATATTTCGTT				
gloverin 4 BGIBMGA013865	GLV4_FOR	AGGAGCGAAACCTGTCACAAG	cDNA	753	60°C	45''
	GLV4_REV	AGAGAAAGTGTAAAGTAGAATACTGTAGCTA				
lebocin BGIBMGA006775	LEB_FOR	TCAACATGTACAAGTTTTTAGTATTCA	cDNA	778	57°C	45''
	LEB_FOR	GAGAGAAATTTGTTGCAAAGCAA				
moricin BGIBMGA011495	MOR_FOR	TGTGGCAATGTCTCTGGTGTC	cDNA	305	61°C	30''
	MOR_REV	GAACTGACTATAAGTAAGTACTACAAAGGGG				

Table 3. List of primers used for the sequencing of AMP genes in the four *B. mori* strains. For each gene the following information is indicated: gene ID (Ensembl ID or Genbank Accession), name of primers used, 5'-3' sequence of primers, template on which the amplification was carried out, length of the amplicon, annealing temperature of primers, time of extension used in the PCR cycle.

Appendix

Gene	Length (cds)	Allele	Polymorphic loci	Strains			
				I	C	J	E
attacin	644 bp	1	105:G 108:T 162:A 234:G 240:T 262:C 322:C 334:T 379:G 391:T 472:C 514:G 538:T 580:T	+			
		2	105:G 108:C 162:G 234:A 240:C 262:T 322:C 334:C 379:G 391:T 472:G 514:G 538:T 580:T		+	+	
		3	105:A 108:C 162:G 234:G 240:T 262:C 322:T 334:T 379:T 391:C 472:G 514:C 538:G 580:C			+	+
cecropin A1	192 bp		-				
cecropin A2	192 bp		-				
cecropin B1	192 bp	1	6:C **112:A** 117:G 123:T 165:C 180:C 191:A	+			
		2	6:T **112:G** 117:A 123:T 165:T 180:T 191:G		+	+	
		3	6:C **112:G** 117:G 123:T 165:C 180:C 191:A		+	+	
		4	6:T **112:G** 117:G 123:C 165:T 180:T 191:G				+
cecropin B2	192 bp	1	6:T 63:T **112:G** 123:T **157:G**	+			
		2	6:C 63:C **112:A** 123:C **157:G**	+			
		3	6:C 63:T **112:G** 123:T **157:G**		+	+	
		4	6:T 63:T **112:G** 123:T **157:C**				+
cecropin B3	192 bp	1	75:A 180:T 191:G	+	+	+	
		2	75:G 180:C 191:A				+
cecropin B4	192 bp	1	63:C 123:C 165:C 171:A 180:C	+			
		2	63:T 123:C 165:C 171:A 180:C	+			
		3	63:C 123:C 165:C 171:G 180:T		+	+	+
		4	63:C 123:T 165:T 171:G 180:T		+	+	
cecropin B5	192 bp	1	6:T 87:G 117:G 123:C 165:T	+	+	+	
		2	6:T 87:G 117:G 123:C 165:C	+			
		3	6:T 87:A 117:A 123:T 165:T		+		
		4	6:C 87:G 117:G 123:C 165:T				+
		5	6:T 87:G 117:G 123:T 165:T				+
cecropin D	186 bp		-				
		1	**25:A 76:T** 132:C	+	+	+	

Gene	Length (cds)	Allele	Polymorphic loci	Strains			
				I	C	J	E
cecropin D2	200 bp	2	**25:G 76:T** 132:C		+		
		3	**25:G 76:C** 132:T				+
cecropin E	197 bp	1	43:C 108:G 117:G 156:C 165:A 189:T 197:G	+	+		
		2	43:T 108:A 117:G 156:T 165:G 189:C 197:A		+	+	+
		3	43:T 108:A 117:A 156:T 165:G 189:C 197:A				+
defensin	287 bp	1	**130:T**	+	+	+	+
		2	**130:C**				+
enbocin 1	179 bp	1	**73:T** 96:C 111:A 114:T 150:A **152:G** 153:C **160:G 163:G** 174:C	+	+		+
		2	**73:A** 96:T 111:C 114:C 150:G **152:C** 153:G **160:A 163:T** 174:T		+	+	+
enbocin 2	179 bp	1	9:C 48:G **73:T** 96:C 111:A 114:T 150:A **152:G** 153:C **160:G 163:G** 174:C	+	+		+
		2	9:C 48:A **73:T** 96:C 111:A 114:T 150:A **152:G** 153:C **160:G 163:G** 174:C		+		
		3	9:T 48:G **73:A** 96:T 111:C 114:C 150:G **152:C** 153:G **160:A 163:T** 174:T			+	+
gloverin 1	539 bp	1	27:T **31:C 47:A 110:A** 144:T 150:T **158:A 169:G** 219:T 231:C 255:C 300:G 309:C 312:C 348:T 405:A 444:C 459:C	+		+	
		2	27:C **31:C 47:G 110:G** 144:C 150:A **158:A 169:G** 219:C 231:C 255:C 300:A 309:T 312:C 348:C 405:C 444:C 459:T		+		
		3	27:T **31:T 47:A 110:G** 144:T 150:T **158:G 169:G** 219:T 231:T 255:T 300:A 309:T 312:C 348:T 405:C 444:C 459:C		+		
		4	27:T **31:C 47:G 110:G** 144:T 150:T **158:A 169:A** 219:T 231:C 255:C 300:G 309:C 312:T 348:T 405:C 444:C 459:C				+
		5	27:T **31:C 47:G 110:G** 144:C 150:T **158:A 169:G** 219:T 231:C 255:C 300:A 309:C 312:T 348:T 405:C 444:C 459:C				+
gloverin 2	521 bp	1	24:C 51:C **71:C** 81:A 90:C **99:C** 105:A **106:T** 123:C 195:C **221:A** 270:T 276:G 342:A 411:G 492:T 495:T	+			+
		2	24:A 51:T **71:T** 81:A 90:T **99:G** 105:G **106:C** 123:T 195:A **221:G** 270:C 276:A 342:A 411:G 492:T 495:T		+		
		3	24:C 51:C **71:C** 81:G 90:C **99:C** 105:A **106:T** 123:T 195:A **221:G** 270:C 276:A 342:A 411:G 492:A 495:C			+	
		4	24:C 51:C **71:C** 81:G 90:C **99:C** 105:A **106:T** 123:T 195:C **221:G** 270:T 276:G 342:T 411:T 492:T 495:T				+
gloverin 3	524 bp	1	**55:G 70:C** 78:C **82:G 92:T** 93:T **100:A** 108:C **146:G** 198:C 246:T 249:G 255:C 276:A 348:C 387:G 408:T 438:T 489:C 513:T 524:T	+			
		2	**55:G 70:T** 78:T **82:A 92:C** 93:C **100:G** 108:T **146:G** 198:A 246:T 249:G 255:C 276:G 348:T 387:G 408:T 438:C 489:T 513:T 524:T		+		
		3	**55:G 70:C** 78:C **82:G 92:C** 93:C **100:G** 108:T **146:A** 198:C 246:T 249:A 255:C 276:G 348:C 387:A 408:T 438:C 489:C 513:T 524:T		+	+	+
		4	**55:A 70:C** 78:C **82:G 92:C** 93:C **100:G** 108:T **146:G** 198:C 246:A 249:G 255:T 276:G 348:T 387:G 408:T 438:C 489:C 513:C 524:C			+	

Gene	Length (cds)	Allele	Polymorphic loci	Strains			
				I	C	J	E
		5	**55:G 70:C** 78:C **82:G 92:T** 93:T **100:A** 108:C **146:G** 198:C 246:T 249:G 255:C 276:A 348:C 387:G 408:G 438:T 489:C 513:T 524:T				+
gloverin 4	518 bp	1	**70:G 88:G** 96:T **99:G** 102:T 147:G 168:G 180:T 282:C 396:T	+		+	
		2	**70:T 88:A** 96:A **99:T** 102:C 147:A 168:G 180:C 282:T 396:C		+		
		3	**70:T 88:A** 96:T **99:T** 102:T 147:A 168:T 180:C 282:C 396:T				+
lebocin	542 bp	1	**83:A** 189:T **320:C 495:T 499:G** 525:C	+		+	+
		2	**83:T** 189:C **320:T 495:A 499:A** 525:T		+	+	
moricin	203 bp		-				

Table A.1. Polymorphic loci identified in AMP coding sequences of the four *B. mori* strains. For each AMP the following information is indicated: length of the gene coding sequence (cds); progressive number of alleles identified at the nucleotide level; polymorphic loci on each allele with indication of the position and the nucleotides identified (in bold: non-synonymous substitutions); strain in which each allele is present (I: Indian, C: Chinese, J: Japanese, E: European).

AMP	Length (full)	Length (active portion)	Isoform	Amino acid substitutions	Strains			
					I	C	J	E
Attacin	214 aa	188 aa (27-214)	1	-				
Cecropin A1	63 aa	35 aa (27-61)	1	-				
Cecropin A2	63 aa	35 aa (27-61)	1	-				
Cecropin B1	63 aa	35 aa (27-61)	1	**38:Ser**	+			
			2	**38:Gly**		+	+	+
Cecropin B2	63 aa	35 aa (27-61)	1	**38:Gly 53:Glu**	+	+	+	
			2	**38:Ser 53:Glu**	+			
			3	**38:Gly 53:Gln**				+
Cecropin B3	63 aa	35 aa (27-61)	1	-				
Cecropin B4	63 aa	35 aa (27-61)	1	-				
Cecropin B5	63 aa	35 aa (27-61)	1	-				
Cecropin D	61 aa	37 aa (25-61)	1	-				
Cecropin D2	66 aa	? (1-22: signal peptide)	1	9:Ile 26:Phe	+	+	+	
			2	9:Val 26:Phe		+		
			3	9:Val 26:Leu				+
Cecropin E	65 aa	? (1-20: signal peptide)	1	-				
Defensin	92 aa	36 aa (57-92)	1	44:Ser	+	+	+	+
			2	44:Pro				+
Enbocin 1	59 aa	37 aa (22-58)	1	**25:Phe 51:Gly 54:Ala 55:Ala**	+	+		+
			2	**25:Ile 51:Ala 54:Thr 55:Ser**		+	+	+
Enbocin 2	59 aa	37 aa (22-58)	1	**25:Phe 51:Gly 54:Ala 55:Ala**	+	+		+
			2	**25:Ile 51:Ala 54:Thr 55:Ser**		+	+	+
Gloverin 1	178 aa	135 aa (44-178)	1	14:Leu 19:Asn 41:Lys **54:Lys 58:Gly**	+		+	
			2	14:Leu 19:Ser 41:Arg **54:Lys 58:Gly**		+		+
			3	14:Phe 19:Asn 41:Arg **54:Arg 58:Gly**		+		
			4	14:Leu 19:Ser 41:Arg **54:Lys 58:Arg**				+
			1	24:Ser 33:Ser 36:Ser **74:Lys**	+			+

AMP	Length (full)	Length (active portion)	Isoform	Amino acid substitutions	Strains			
					I	C	J	E
Gloverin 2	173 aa	131 aa (43-173)	2	24:Phe 33:Arg 36:Pro **74:Arg**		+		
			3	24:Ser 33:Ser 36:Ser **74:Arg**			+	+
Gloverin 3	172 aa	131 aa (42-172)	1	19:Glu 24:Pro 28:Glu 31:Leu 34:Ser **49:Arg**	+			
			2	19:Glu 24:Ser 28:Lys 31:Pro 34:Gly **49:Arg**		+		
			3	19:Glu 24:Pro 28:Glu 31:Pro 34:Gly **49:Lys**		+	+	+
			4	19:Lys 24:Pro 28:Glu 31:Pro 34:Gly **49:Arg**			+	
			5	19:Arg 24:Pro 28:Glu 31:Lys 34:Ser **49:Arg**				+
Gloverin 4	171 aa	131 aa (41-171)	1	24:Asp 30:Val 33:Gln	+		+	
			2	24:Tyr 30:Ile 33:His		+		
			3	24:Tyr 30:Phe 33:His				+
Lebocin	179 aa	32 aa (121-152)	1	28:Tyr 107:Thr 165:His 167:Asp	+		+	+
			2	28:Phe 107:Ile 165:Gln 167:Asn		+	+	
Moricin	66 aa	42 aa (25-42)	1	-				

Table A.2. Protein variants identified in the four *B. mori* strains. For each AMP the following information is indicated: length of the whole peptide (full); length of the active portion of the peptide, with indication of the starting and final residues that compose the mature portion; progressive number of isoforms identified at protein level; modified residues that characterize each isoform (in bold: modified residues that map in the active portion of the peptide); strain in which each isoform is present (I: Indian, C: Chinese, J: Japanese, E: European).

Chapter 3: Sensitivity of the Four Strains to Infections

Introduction

Silkworm Pathogen-Associated Infections

Since *B. mori* domestication, pathogen infections seriously threatened silkworm keeping and were responsible for severe economic losses in sericulture (Zhang et al, 2013). The earliest report of silkworm diseases is dated 725-645 BC, when the Chinese chancellor Guan Zhong announced that any man who could produce disease-free silkworms would be awarded with 0.5 Kg of gold (Vega and Kaya, 2012). The first systematic scientific study on silkworm disease, however, dates back to 1807, when Agostino Bassi proposed a fungal origin for the white muscardine disease (Bassi, 1835). In the 19th century, a silkworm epidemic, called pébrine because of the characteristic aspect of sick larvae with brown dots on the cuticle, caused a great sericulture crisis in Europe and was the the start of sericulture decline in the Old Continent. Louis Pasteur was asked by the French Government to investigate on the pébrine etiology and he discovered that the disease was caused by infections by the microsporidian *Nosema bombycis* (Pasteur, 1870).

B. mori can be potentially infected by a variety of microorganisms such as fungi, viruses, bacteria and Protozoa. Apart from pébrine, other typical silkworm infective diseases which can compromise silkworm rearing are muscardine, grasserie and flacherie. The muscardine disease is a fungal infection characterized by sluggish larvae showing oil-colored specks. In the late stages cadavers become stiffen and "mummified", covered with a powder made of fungal conidia (Vega and Kaya, 2012). The grasserie is characterized by larvae showing defensive postures and swollen posterior abdominal segments. The cuticle of infected larvae is very fragile and breaks easily. Cadavers are flaccid and often show black spots on the cuticle (Vega and Kaya, 2012). Flacherie is one of the most serious silkworm infections. The term "flacherie" has a French origin and it is used to describe dysentery, which can have a non-infectious origin if larvae are exposed to high temperatures, or a viral or bacterial cause (Vega and Kaya, 2012). Infectious flacherie causes loss of appetite, retard in growth, oral and anal discharge, liquefaction of inner organs and finally cadaver rot (Zhang et al, 2013; Ayoade et al, 2014).

Nowadays, it is known that the fungus *Beauveria bassiana* is responsible for the white muscardine; viruses such as the Nuclear Polyhedrosis Virus or the Densovirus induce flacherie and grasserie in silkworms; bacteria belonging to *Enterococcus*, *Bacillus*, *Serratia, Streptococcus, Staphylococcus* and *Pseudomonas* genera are able to

induce flacherie, often in combination with viruses (Pasteur, 1870; Hou et al, 2014; Himeno et al, 1973; Huang et al, 2009; Kaufmann et al, 2011; Cappellozza et al, 2011; Zhang et al, 2013; Ishii et al, 2014; Ayoade et al, 2014).

As already stated in Chapter 2, silkworm strains with different geographical origin show an inverse correlation between production capabilities and susceptibility to diseases. Temperate region silkworms exhibit good silk production yields but higher sensitivity to pathogen infections, while tropical strains show good tolerance to microbial exposures but lower production capabilities (FAO, 2003).

The four *B. mori* strains selected for this study were already shown to differ in their production yields (Chapter 2). In order to test their sensitivity to infections preliminary infection experiments with different microorganisms were performed. Subsequently, we decided to thoroughly evaluate their response to oral infections with two silkworm specific pathogens, the Gram-positive *Enterococcus mundtii* and the Gram-negative *Serratia marcescens,* which are both responsible for the development of flacherie.

Enterococcus mundtii was found to be responsible for the flacherie disease in silkworms reared on artificial diet (Cappellozza et al, 2011; Nwibo et al, 2015). *E. mundtii* is phylogenetically closer to *E. faecium*, which has been reported to be the etiological agent of many nosocomial infections. However, genomic data analyses have shown that *E. mundtii* does not possess the virulence factors typical of clinical isolates belonging to the *Enterococcus* genus, suggesting that the pathogenicity of this strain is limited to insects (Repizo et al, 2014). The strain used in this study (HDYM-22) was isolated at the Sericulture Unit of the CREA-API of Padova, Italy, from silkworm larvae showing flacherie symptoms (Cappellozza et al, 2011).

Serratia marcescens is a pathogen for many host organisms, including plants, nematodes and mammals. It has also been identified as an opportunistic pathogen for humans and it is increasingly responsible for nosocomial infections (Kurz et al, 2003). *S. marcescens* has been isolated from silkworms showing flacherie disease (Zhang et al, 2013; Ayoade et al, 2014) and is a threat for silkworm rearing, especially in tropical regions (Sanchez et al, 2014). First evidences of *S. marcescens* infections in Indian silkworm livestocks date back to 1796, when it was reported that *S. marcescens* was the etiology cause of the common silkworm disease popularly known in India as “Rangi” (Vasantharajan and Munirathnamma, 1978). *S. marcescens* has already been used as pathogen model to analyze intestinal infections in *Drosophila* and *Bombyx* laboratory strains (Nehme et al, 2007; Ishii et al, 2014). These studies showed that this bacterium is susceptible to the intestinal *Drosophila* immune response (Nehme et al, 2007). Moreover, Ishii et al demonstrated that *S. marcescens* is able to produce a metalloprotease, called Serralysin, which induces silkworm bleeding and which inhibits the adhesion of hemocyte cells to bacterial targets (Ishii et al, 2014). The strain used in

our analyses (WW4) was isolated at the Forage-Livestock-Diary Unit of the CREA-FLC of Lodi, Italy.

Experimental Overview

Infection experiments were conducted on silkworms belonging to the four selected *B. mori* strains reared in germ-free conditions. After a 24 h oral exposure at the beginning of the last larval stage, we compared: 1) the survival profiles, 2) the presence of living pathogen cells in the hemolymph circulation, 3) the expression induction of 9 representative AMP genes in the tissues involved in the immune response (fat bodies and midgut), 4) the *in vitro* antimicrobial activity of the silkworm hemolymph, 5) the Lysozyme concentration in larvae plasma and 6) the rate of the melanization reaction, among the different strains.

Results

Experimental Set-Up

Oral infection is the most common and natural mechanism trough which silkworms are infected. All the experiments were carried out on larvae at the fifth larval stage. In fact, infections typically occur during this last larval instar, when silkworms eat abundantly and are reared in overcrowded conditions for silk production (Vega and Kaya, 2012). In addition, at this developmental stage silkworms are more tolerant to infections and have a large body size. This allows to observe the symptoms of nonlethal infections, and to extract enough amounts of biological samples for biochemical and molecular analyses.

To select the pathogens, preliminary experiments were conducted with *Escherichia coli* (DH5α), considered a model for Gram-negative bacteria, and three silkworm-specific pathogens: the Gram-negative *Serratia marcescens* (WW4), the Gram-positive *Enterococcus mundtii* (HDYM-22), and the fungus *Beauveria bassiana* (ATCC 74040). With the three bacteria *E. coli*, *E. mundtii*, *S. marcescens*, opportunely diluted cultures were homogeneously spread over silkworm artificial diet, while for the fungus *B. bassiana*, larvae were directly dipped into the fungal culture. For each *B. mori* strains, about 45 individuals at the beginning of the fifth larval stage were exposed for 24 h to the specific pathogen. Subsequently, larvae were put on a germ-free diet and followed until they reached the adult stage. During each infection experiment, germ-free controls were reared in parallel to assure the absence of any significant lethality not associated to the intentional larvae infection.

Since *E. coli* ($8*10^6$ CFU/mL) did not induce any significant mortality in any of the four *B. mori* strains (Figure 1A; Mantel-Cox test, $P > 0.05$, not significant (ns) for all comparisons) and did not show any significative activation of immune response in the selected *B. mori* strains (data not shown) it was excluded from the subsequent analyses. The infection with *B. bassiana* ($8*10^7$ conidia/mL) was also excluded from the analysis. Even if the pathogen induced a significant mortality on silkworms in comparison to their respective germ-free controls (Mantel-Cox test, $P < 0.0001$), the four *B. mori* strains were found to have similar sensitivity to this fungus and only a minimal difference was found between the survival curves of the Indian and the European lines (Figure 1B), suggesting the absence of strain-specific defense mechanisms against this infection.

For *E. mundtii*, two concentrations were tested: $2.7*10^6$ and $2.7*10^2$ CFU/mL. While the first was found to induce massive mortality (data not shown), the second induced a differential lethality among the four *B. mori* strains (see below) and was chosen for all subsequent analyses.

For *S. marcescens*, three concentrations were tested: $2.23*10^3$, $2.23*10^5$ and $2.23*10^7$ CFU/mL. The first two concentrations were found not to be pathogenic, while the $2.23*10^7$ CFU/mL dose was able to develop the disease in most of the *B. mori* strains (see below) and therefore it was selected for all subsequent experiments.

In each experiment, negative controls belonging to the four *B. mori* strains developed normally, and did not show any significant differences in survival rates (Mantel-Cox test, $P > 0.05$, ns for all comparisons, Figure 1C).

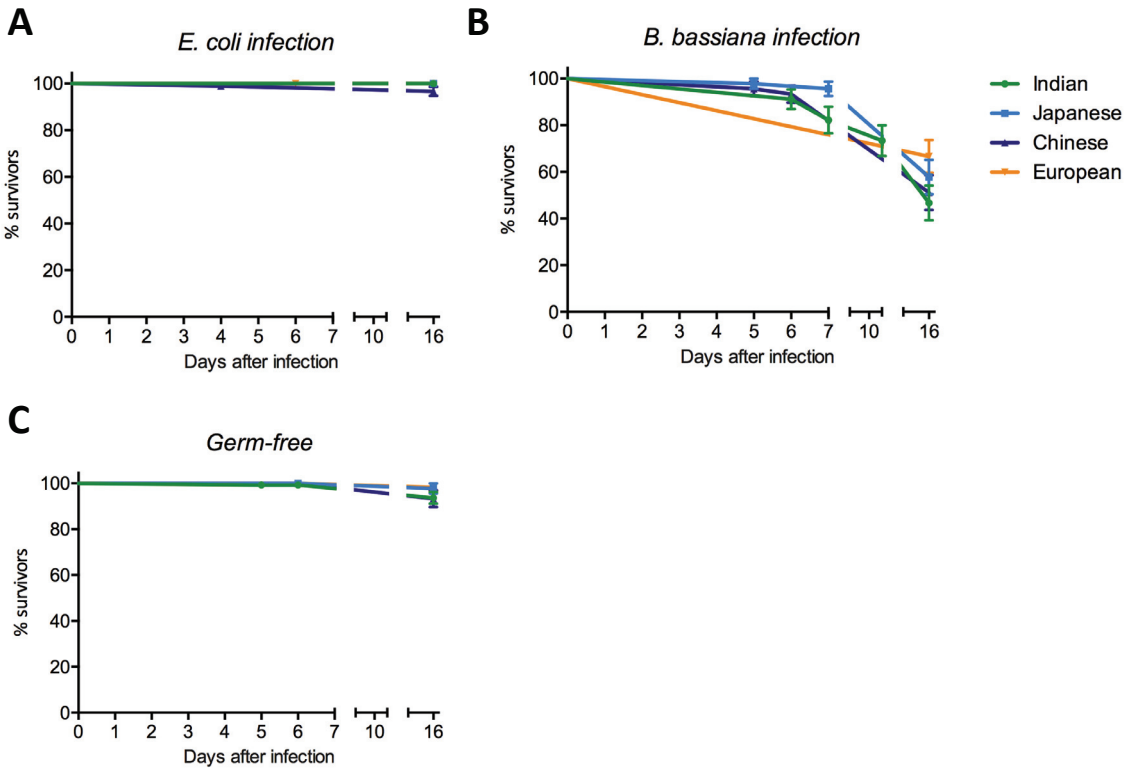

Figure 1. Survival curves of the four *B. mori* lines infected with *E. coli* (A), *B. bassiana* (B) and reared in germ-free conditions (C). For each line, 90 larvae in 6 replicates (*E. coli*) or 45 larvae in 3 replicates (*B. bassiana*) were infected with a 24 h oral exposure to *E. coli* ($8*10^6$ CFU/mL) or by dipping them in a fungal suspension ($8*10^7$ conidia/mL) and then transferred on a germ-free diet. For germ-free controls, 90 larvae for each line were reared in sterile conditions (mean ± SEM).

Sensitivity of the Four Strains to Gram-Positive and -Negative Infections

For each *B. mori* line, at least 90 larvae in 6 replicates were exposed to *E. mundtii*. The number of survivors was recorded every day throughout the 7 days of the fifth larval stage, before spinning (day 10) and after eclosion (day 16; Figure 2). All the four *B. mori* lines showed a significant mortality when compared to their germ-free controls (Figure A.1, Mantel-Cox test, $P < 0.0001$ for all comparisons). When comparing the survival profiles of the four infected silkworm strains, the Indian and the Japanese lines were shown to be the most sensitive to the Gram-positive infection, with 0-10% of larvae reaching the adult stage. The survival curves of these two lines did not significantly differ from each other (Mantel-Cox test, $P = 0.11$, ns), but were significantly different from those of the other two strains (Mantel-Cox test, $P < 0.0001$). The European strain was found to be the most resistant, with at least 60% of larvae reaching the adult stage (Figure 2; Mantel-Cox test, $P < 0.0001$ for all comparisons). The Chinese line showed a survival profile similar to that of the European one during the 7 days of the fifth larval stage. However, with the progression of the infection, it showed high levels of mortality before pupation, reaching a number of adult survivors comparable to that of the Indian strain. As consequence, its survival profile resulted significantly different in comparison to all the other lines (Mantel-Cox test, $P < 0.0001$ for all comparisons).

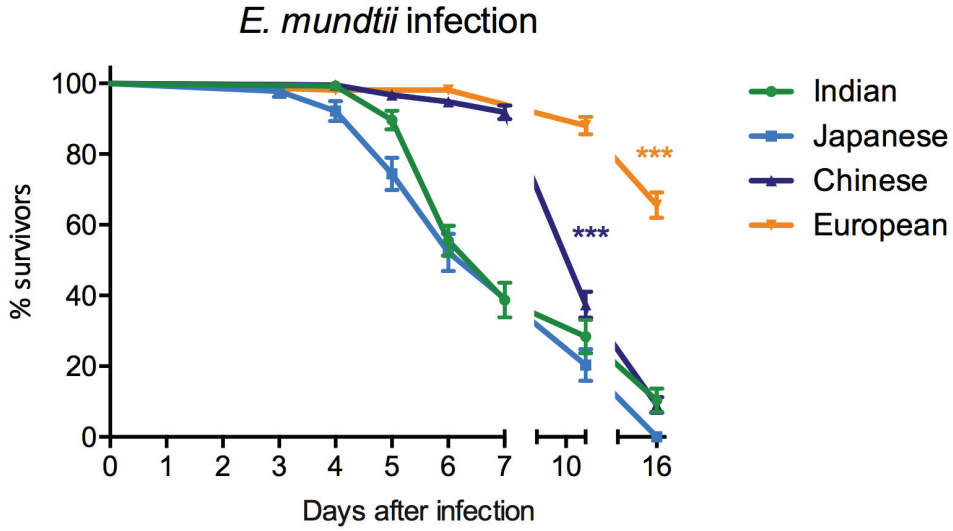

Figure 2. Survival curves of the four *B. mori* strains infected with *E. mundtii*. For each line, 90 larvae (in 6 replicates; mean ± SEM) were infected with a 24 h oral exposure to *E. mundtii* ($2.7*10^2$ CFU/mL) and then transferred on a germ-free diet. Strain sensitivity: European > Chinese > Japanese = Indian (Mantel-Cox test: ***: $P < 0.0001$).

Figure 3 reports the survival curves of the four *B. mori* strains exposed to the Gram-negative *S. marcescens.* At least 45 larvae in 3 replicates per strain were infected and followed to adult stage. The Indian line was found to be totally resistant to *Serratia* infection, showing a survival profile not different from that of germ-free controls (Figures 3 and A.1; infected *vs* germ-free Indian silkworms: Mantel-Cox test, $P = 0.087$ ns). On the contrary, the other three strains did not resist to *S. marcescens* infections , with only 0-5% of larvae reaching the adult stage. Among these three sensitive strains, the Chinese and Japanese lines had a significantly different survival profile (Mantel-Cox test, $P < 0.001$), while the comparisons between these two strains and the European one did not show significant differences (Mantel-Cox test, Chinese-European: $P = 0.26$, ns; Japanese-European: $P = 0.68$, ns).

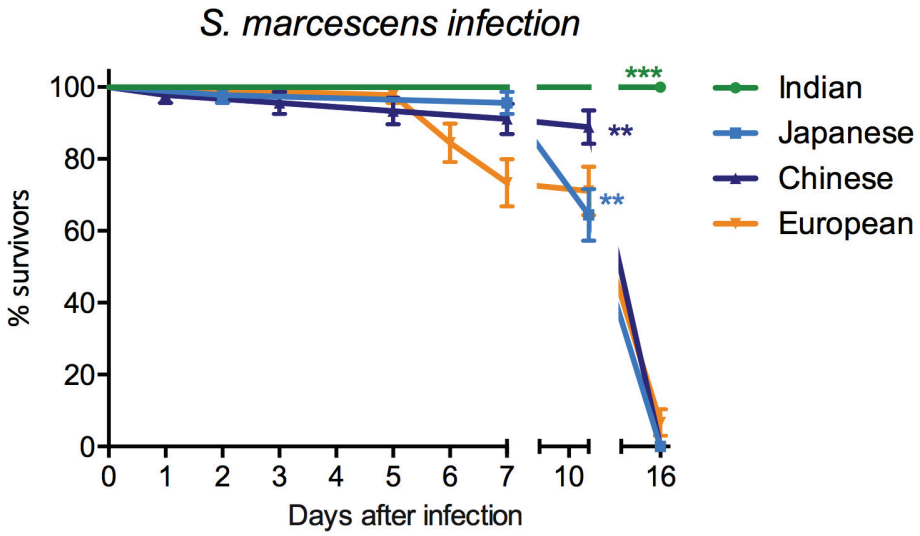

Figure 3. Survival curves of the four *B. mori* strains infected with *S. marcescens*. For each line, 45 larvae (in 3 replicates; mean ± SEM) were infected with a 24 h oral exposure to *S. marcescens* ($2.23*10^7$ CFU/mL) and then transferred on a germ-free diet. Strain sensitivity: Indian > Chinese-European-Japanese (Mantel-Cox test: ***: $P < 0.0001$, **: $P < 0.001$).

Isolation of Living Bacterial Cells in the Hemolymph

In Insects, a crucial aspect in the development of a septic infection following oral exposure is represented by the passage of bacterial cells from the localized and limited niche of the gut lumen, to the more widespread and unrestrained environment of the hemolymph circulation.

In order to evaluate if and when bacterial cells were able to pass the gastro-intestinal barrier and enter into the larvae circulation, hemolymph samples of infected larvae belonging to the four *B. mori* strains were collected each day after infection. Three replicates, each composed of hemolymph samples collected from at least 3 larvae, were plated in Plate Count Agar (PCA) plates, a common medium used to monitor the viable bacterial growth of a sample. Hemolymph extracted from larvae reared in germ-free conditions were also plated as negative control and did not show any bacterial growth (Table A.1). Living *E. mundtii* cells were isolated from the hemolymph of the four *B. mori* strains (Table 1), confirming that this pathogen was able to transit from the gut lumen to the circulation. In the Japanese strain, bacterial cells were consistently found from the second day since infection, with the bacterial load increasing in parallel with the disease development. In the other three lines, compelling numbers of bacterial cells were isolated at least one or two days later. It is interesting to note that the total bacterial load in the Chinese hemolymph was always lower compared to that of the other strains.

S. marcescens cells were shown to be present and viable in the hemolymph of the Japanese strain from the third day since infection, and from the fourth day after oral exposure in that of the Chinese and European strains (Table 1). Interestingly, in the hemolymph of the Indian line no living *S. marcescens* cell was found.

Day after infection	*E. mundtii* infection				*S. marcescens* infection			
	Indian	Chinese	Japanese	European	Indian	Chinese	Japanese	European
0	0	0	0	0	0	0	0	0
1	0	0	1.7 ± 3.5	0.75 ± 0.9	0	0	0	0
2	0	0.7 ± 1.5	155.7 ± 121.6	0	0	0	0	0
3	N.C.	2.2 ± 2.8	N.C.	N.C.	0	0	N.C.	0
4	N.C.	0	N.C.	N.C.	0	N.C.	n.d.	N.C.
5	N.C.	6 ± 7.3	N.C.	N.C.	0	N.C.	n.d.	N.C.
6	N.C.	39 ± 64	N.C.	N.C.	0	n.d.	N.C.	N.C.

Table 1. Presence of living *E. mundtii* or *S. marcescens* cells in the hemolymph of the *B. mori* lines after the oral infection. Hemolymph was collected from 9 individuals pooled in three replicates. The number of colonies grown after plating 70 µl of hemolymph on PCA plates (mean ± SEM) was recorded for each day of infection. N.C.: Non Countable; n.d.: Not Determined.

mRNA Expression of 9 Representative AMP Genes in Midgut and Fat Bodies

In order to investigate if the different sensitivity to both Gram-positive and -negative pathogens observed among the four *B. mori* strains could be explained by a differential expression of AMP genes at local (midgut) and/or systemic (fat bodies) levels, quantitative real-time PCR (qPCR) experiments were performed.

Midgut and fat body tissues were analyzed for three and six days respectively after pathogen exposure. At each time-point, mRNA samples were obtained from tissues of nine individuals, pooled in three replicates. The same number of samples extracted from germ-free larvae reared in parallel were analyzed as negative controls.

To obtain an overview of the capability of the different strains to activate AMP expression after pathogen exposure, we evaluated the nine most studied *B. mori* AMPs: *attacin*, *cecropin A*, *cecropin B*, *cecropin D*, *cecropin E*, *defensin*, *gloverin 2*, *lebocin*, *moricin*. For *cecropin A* and *cecropin B*, primers were designed to amplify all the genes that compose the multigene family, made of two and six elements respectively.

AMP expression profiles were initially evaluated in germ-free controls, to determine if there was a differential expression of these genes during the fifth larval stage development. In both midgut and fat body tissues, none of the AMP gene was found to have a significantly differential expression during the three (midgut) or six (fat bodies) days of monitoring (Figure A.2; Kruskal-Wallis test, $P > 0.05$, ns for all comparisons).

At the midgut level, all four strains were found to activate the expressions of the 9 AMP genes from the first 24 h after *E. mundtii* exposure (Figure 4A; Kruskal-Wallis test, $P < 0.05$ for all genes in all the four strains) even if with differences in the transcription levels of some genes. All the strains, except the Chinese one, immediately expressed high levels of *lebocin*. However, the Indian line expressed also high levels of *gloverin 2* and *defensin*, while the Japanese strain preferentially expressed *cecropin D* and *attacin*. The European line showed high levels of *gloverin 2*, *cecropin D*, and *cecropin E,* in addition to *lebocin.* The Chinese strain expressed preferentially *cecropin B,* which reached high expression values from the second day post-infection. In this line the other genes were significantly induced, even if at lower levels in comparison to the other three strains. These data suggested that the pathogen was immediately sensed at the midgut *epithelium* level by all four *B. mori* strains, since they all activated the AMP expression starting from the first day after infection.

Looking at the systemic AMP gene expression, the *E. mundtii* infection induced the transcription of all AMP genes in the fat bodies of all the four strains (Figure 4B;

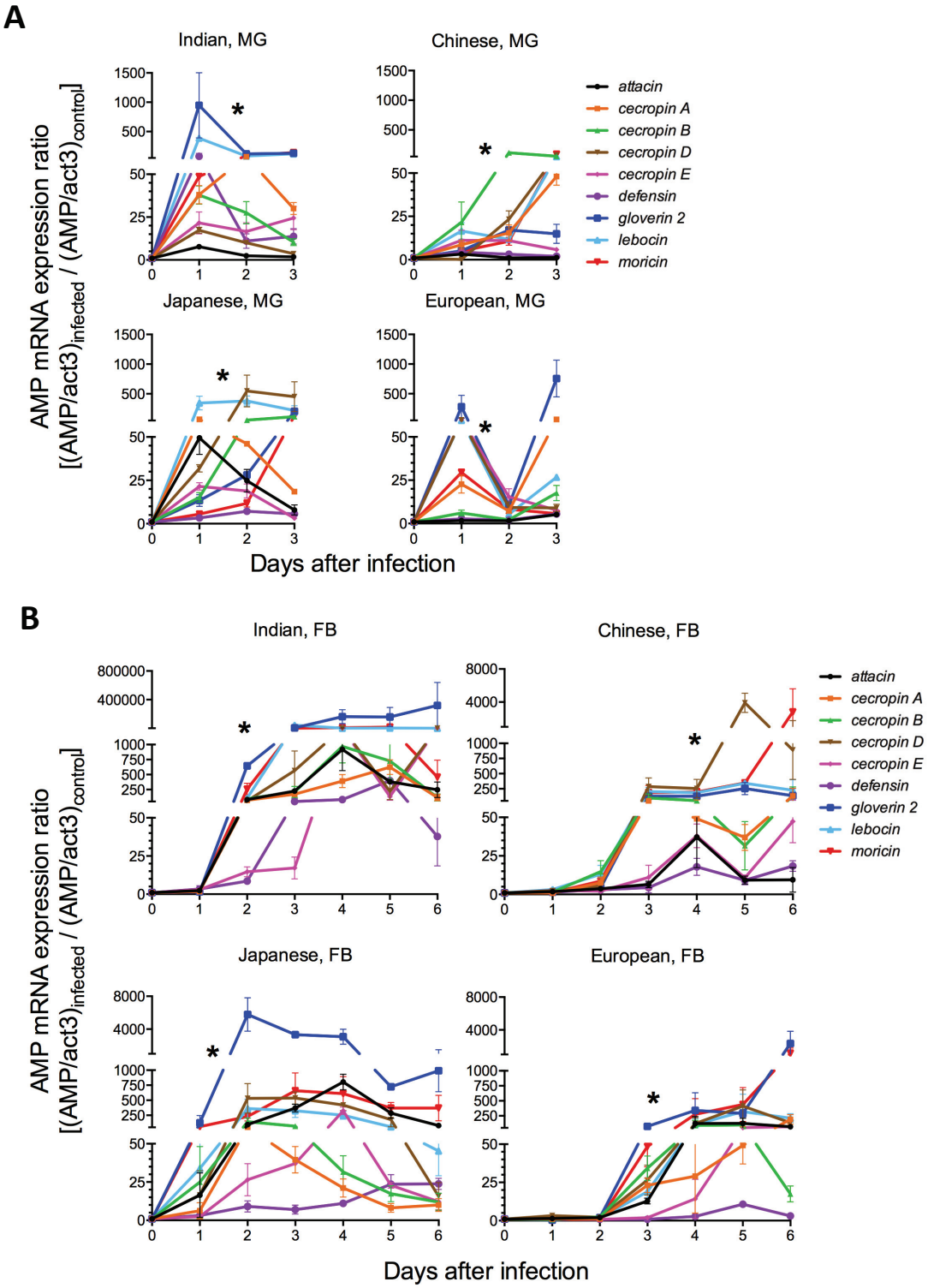

Figure 4. Time course expression of 9 AMP genes in midgut (A) and fat bodies (B) of fifth instar larvae belonging to the four *B. mori* strains infected with *E. mundtii*. The AMP mRNA expression was determined by quantitative RT-PCR on total RNA extracted for 6 (fat bodies) or 3 (midgut) days, after 24 h oral infection (9 individuals pooled in 3 replicates, mean ± SEM). AMP expression ratio represents the AMP/*actin3* mRNA levels of infected samples over those of their relative controls (Kruskal-Wallis test, *: at least 3 AMP genes with significant expression ratio, $P < 0.05$).

Kruskal-Wallis test, $P < 0.05$ for all genes in all four strains). In general, the Indian strain showed the highest level of AMP activation, with *gloverin 2*, *moricin*, and *lebocin* showing increments in their expression ratios of about 5 orders of magnitude in comparison with uninfected controls. The other three lines displayed similar AMP expression increments of 2 -3 orders of magnitude relatively to those of their relative germ-free controls. In particular, the Chinese strain preferentially induced *cecropin D* and *moricin*, the Japanese line *moricin, attacin* and *gloverin 2*, while the European strain showed high expression levels of *moricin* and *gloverin 2*. Interestingly, a difference in the timing of the activation was observed: in the Japanese strain, most of the 9 AMP genes (*gloverin 2*, *moricin*, *lebocin*, *cecropin B*, *attacin*) were immediately activated during the first 24 h after microbial exposure. Conversely, in the other three strains the expression of the vast majority of AMP genes was induced at least 24 h later, on the second day after microbial exposure.

The Gram-negative pathogen *S. marcescens* induced the expression of a restricted set of AMP genes in the midgut *epithelia* of the four *B. mori* strains (Figure 5A). In particular the Indian line was found to induce high levels of *attacin* and *moricin* respectively on the first and second day after infection (Kruskal-Wallis test, $P < 0.05$), while the Japanese strain activated the expression of *defensin* and *attacin* respectively on the first and second days (Kruskal-Wallis test, $P < 0.05$). The Chinese line up-regulated preferentially *moricin*, *cecropin B* and *attacin,* with peaks of expression on the second day (Kruskal-Wallis test, $P < 0.05$), while the European strain induced high levels of *gloverin 2* and *attacin* on the first day, and *moricin* starting from the second day after pathogen exposure (Kruskal-Wallis test, $P < 0.05$).

Considering the systemic AMP expression at fat body level, only the Indian strain was able to activate most of the AMP genes (Figure 5B). This line, which was shown to be the most resistant to the *S. marcescens* infection, expressed *cecropin E*, *attacin* and *cecropin D* starting from the first day of infection, and *moricin*, *defensin* and *lebocin* from the second day (Kruskal-Wallis test, $P < 0.05$ for all genes). The other three silkworm strains showed a late but significant increase in the transcriptional levels of many AMPs only between the fifth and the sixth days after infection.

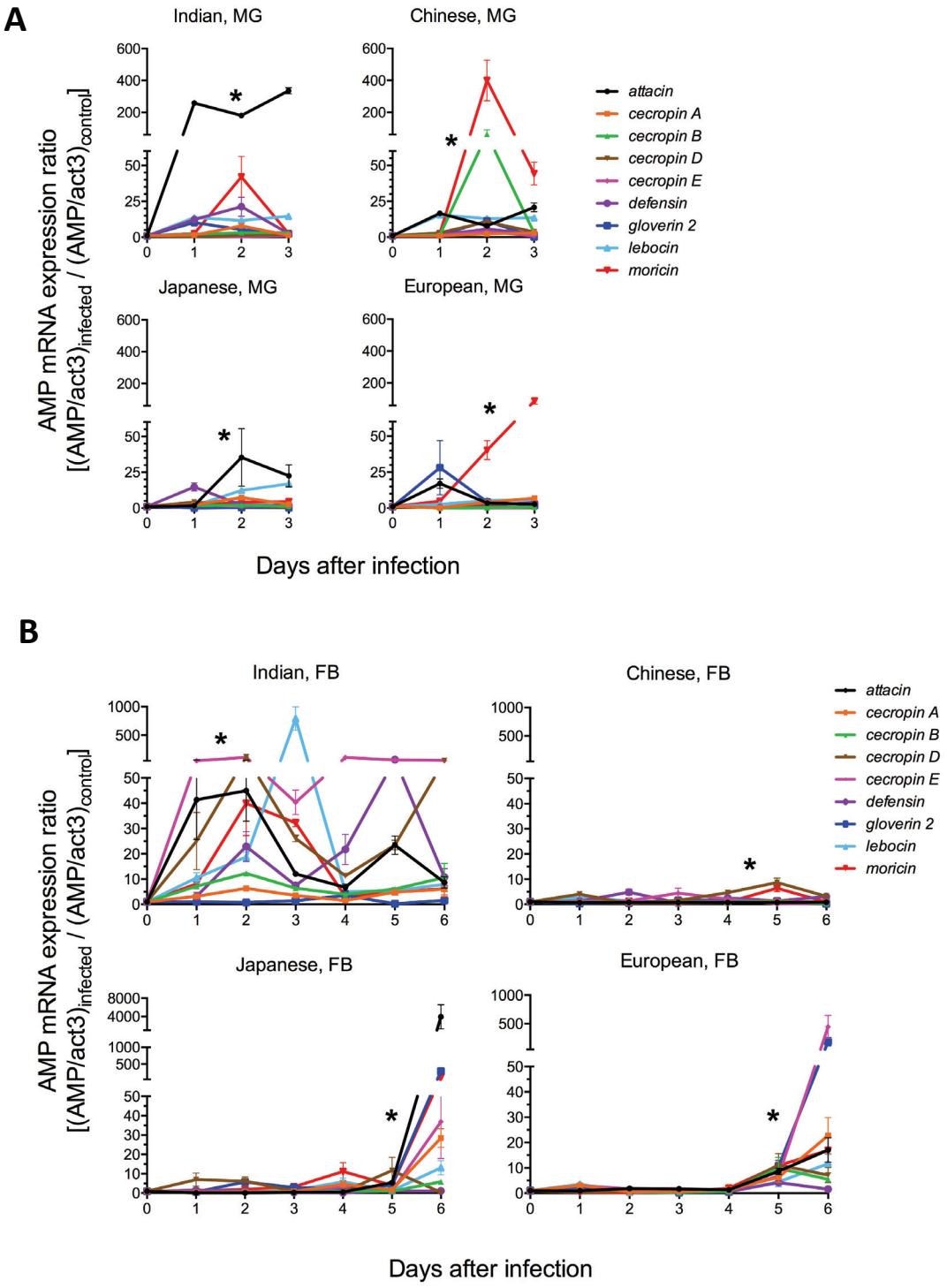

Figure 5. Time course expression of 9 AMP genes in midgut (A) and fat bodies (B) of fifth instar larvae belonging to the four *B. mori* strains infected with *S. marcescens*. The AMP mRNA expression was determined by quantitative RT-PCR on total RNA extracted for 6 (fat bodies) or 3 (midgut) days, after 24 h oral infection (9 individuals pooled in 3 replicates, mean ± SEM). AMP expression ratio represents the AMP/*actin3* mRNA levels of infected samples over those of their relative controls (Kruskal-Wallis test, *: at least 3 AMP genes with significant expression ratio, $P < 0.05$).

Plasma Antimicrobial Activity

The transcriptional induction of many AMP genes was detected after both *E. mundtii* and *S. marcescens* infections at local and systemic level, with differences in the timing of the expression and in the relative composition of the AMP mRNA pools induced among the four *B. mori* strains. However, the mRNA levels represent just an indication of the transcriptional activation of AMP genes, but do not give indications about the actual antimicrobial activity of hemolymph. Since AMPs produced by fat bodies, but also by hemocytes and midgut, are thought to be released in the hemolymph (Kuraishi et al, 2013), we developed a test to measure the global antimicrobial activity of silkworm plasma. This test could give a general overview on the effectiveness of the AMP pools produced by the four silkworm strains after the *E. mundtii* and *S. marcescens* infections.

The hemocyte-free plasma extracted from both germ-free and infected silkworms during the six days since infection was added to *E. mundtii* or *S. marcescens* cultures. The OD_{600} of the bacterial cultures was recorded every 2 h and the bacterial growth (μ) was calculated. Figure A.3 shows the growth rate curves of the two bacteria treated with germ-free and either *E. mundtii* or *S. marcescens* infected plasma. To compare the growth of bacteria treated with plasma samples collected on different days, the area under each μ curve was calculated in the time span between 3 and 9 h post-*inoculum*. For each bacterium in each growing condition, the numerical values of the areas under the curves were compared.

The germ-free plasma was found to provide a good substrate for microbial growth (Figure 6). In general, plasma extracted on different days of the fifth larval developmental stage did not show to differentially promote the *E. mundtii* growth, except for day 1 of the Japanese strain which induced a lower microbial growth (Kruskal-Wallis test, H at least < 11.06, $P > 0.05$).

Looking at the effect of the germ-free plasma on *S. marcescens*, samples extracted at different time-points of the fifth larval stage had a different influence on microbial growth for the Japanese, Chinese and European strains, with a general reduction of *S. marcescens* growth on the last days of the fifth instar (Figure 7; Kruskal-Wallis test, H at least > 12.38 and $P < 0.05$). On the other hand, plasma extracted from germ-free Indian larvae, did not show to promote a significant differential microbial growth on *S. marcescens* (Kruskal-Wallis test, H = 2.874, $P = 0.72$, ns).

In general, plasma extracted from *E. mundtii* infected silkworms belonging to the four *B. mori* strains showed high antimicrobial activity (Figure 6). In fact, most of the infected plasma significantly reduced the *E. mundtii in vitro* growth in comparison with their germ-fee controls (Two-ways ANOVA, time x condition, revealed a significant

effect only for the condition: germ-free vs infected: $F_{1,4}$ at least > 51.07 and $P < 0.05$ for all the four strains; see Figure 6 for Bonferroni multiple comparisons test results).

Interestingly, in all four strains the plasma extracted on the first day after infection almost invariably exhibited lower antimicrobial activity when compared to the plasma extracted at the other time-points. From qPCR data, it was shown that all four strains activated the AMP expression at midgut level since the first day after infection and should therefore possess high levels of AMPs in the hemolymph. However, a certain lapse of time is required to translate AMP mRNAs and to process the resulting immature peptides, therefore AMP effect in the hemolymph might increase with a certain delay in comparison with mRNA levels at midgut and fat bodies levels.

It is also remarkable that plasma samples collected at the sixth day after the infection from the European strain showed a general higher antimicrobial level in comparison with the sample collected from the other strains at the same time-point.

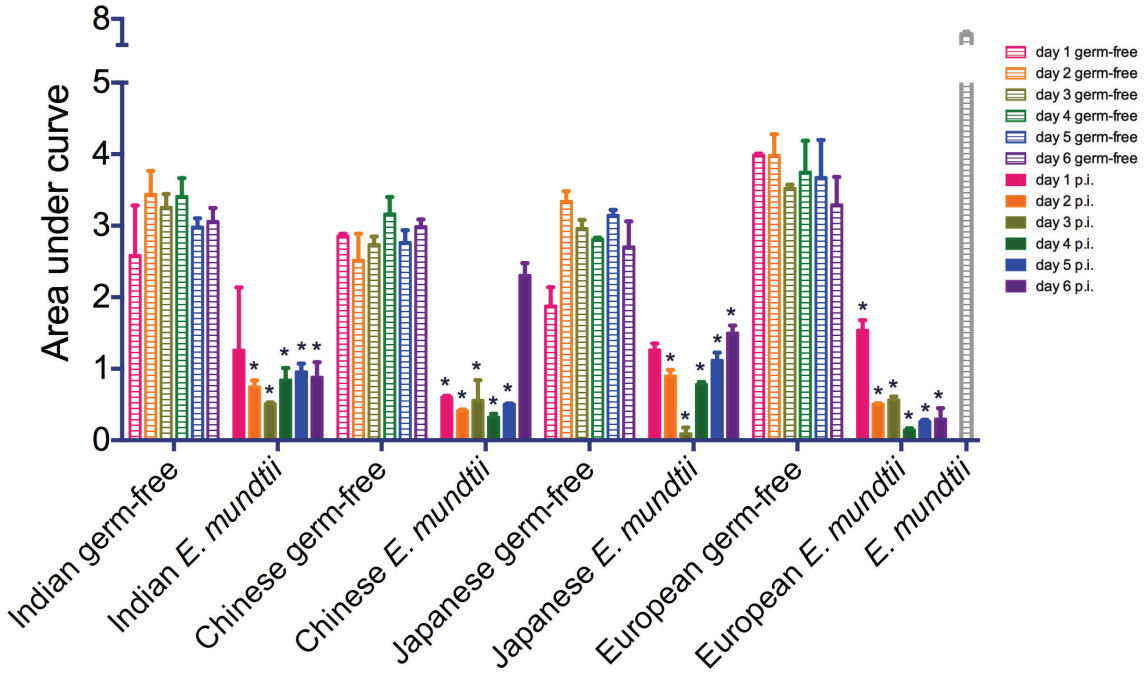

Figure 6. Comparison of the antimicrobial activity of germ-free and *E. mundtii* infected plasma. Hemolymph was collected from 9 individuals pooled in three replicates, from both control and infected larvae every 24 h after *E. mundtii* challenge. The hemocyte-free plasma was added to an *E. mundtii* culture ($5*10^5$ CFU/mL) and the optical density was measured to monitor the microbial growth. The areas under the growth rate (μ) curves were calculated for each condition (mean ± SEM). Bonferroni multiple comparisons tests: * indicates significant differences ($P < 0.05$) in the μ area between infected and germ-free plasma collected at the same time-point.

The plasma samples extracted from silkworms infected with *S. marcescens* showed a weak or absent antimicrobial activity (Figure 7). These data confirmed the qPCR data obtained for the Chinese, Japanese and European strains, which scarcely activated the transcription of AMP genes at both local and systemic levels. Therefore, low amounts of AMPs might have been released in the hemolymph of these three strains, as their plasma did not show any significant antimicrobial activity (Two-ways ANOVA, time x condition, $F_{1,4}$ (effect of the condition) at least < 3.064 and $P > 0.05$, ns; see Figure 5 for Bonferroni multiple comparisons test results).

Examining the Indian strain, which was completely resistant to the *S. marcescens* infection and which was the only strain showing a systemic AMP transcription, a weak but significant plasma antimicrobial activity was observed (Two-ways ANOVA, $F_{1,4}$ (effect of the condition) = 29.75, $P = 0.0055$). Considering the qPCR data, the number of AMPs induced after *S. marcescens* infection and the levels of mRNA expression were lower in comparison with the infection with *E. mundtii.* Therefore the global antimicrobial activity of plasma extracted from Indian silkworms infected with *S. marcescens* might be low because of the restricted AMP pool released in the hemolymph.

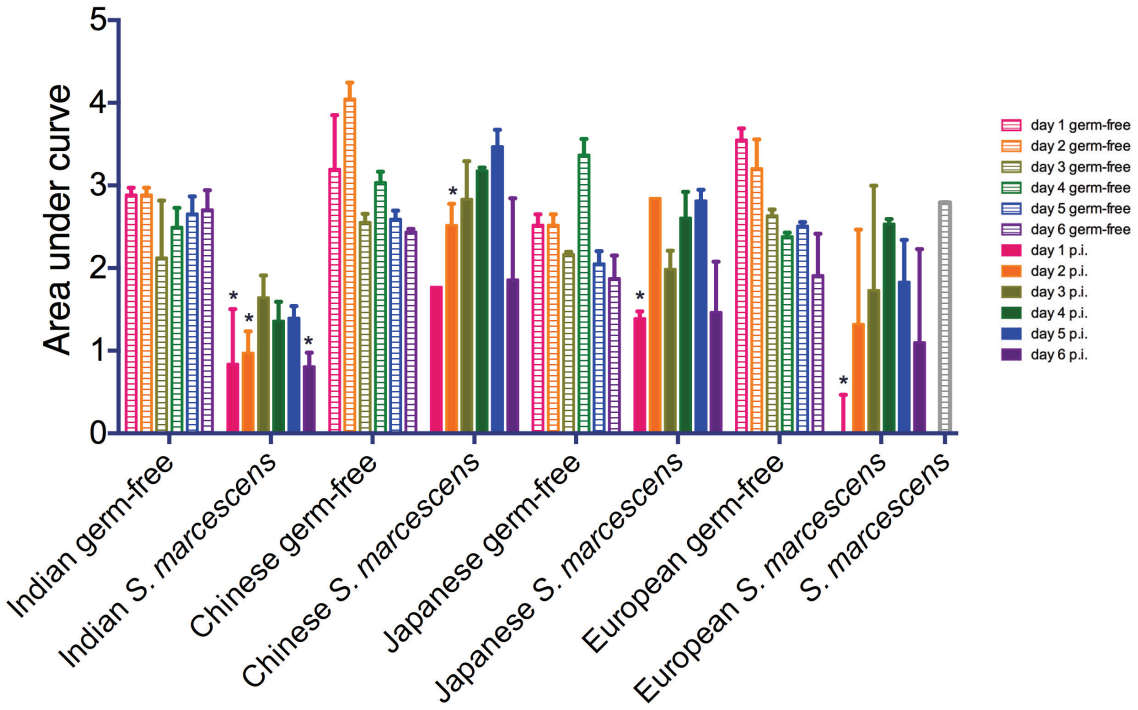

Figure 7. Comparison of the antimicrobial activity of germ-free and *S. marcescens* infected plasma. Hemolymph was collected from 9 individuals pooled in three replicates, from both control and infected larvae every 24 h after *S. marcescens* challenge. The hemocyte-free plasma extracted from both germ-free and infected silkworms during the six days after infection was added to an *S. marcescens* culture ($5*10^5$ CFU/mL) and the optical density was measured to monitor the microbial growth. The areas under the growth rate (µ) curves were calculated for each condition (mean ± SEM). Bonferroni multiple comparisons tests: * indicates significant differences ($P < 0.05$) in the µ area between infected and germ-free plasma collected at the same time-point.

Plasma Lysozyme Activity

In addition to AMPs, another important component of insect humoral immunity is represented by Lysozyme, an antimicrobial protein which acts primarily on Gram-positive bacteria breaking the bond between the N-acetylglucosamine and the N-acetylmuramic acid of peptidoglycan. Insect *lysozyme* genes are constitutively expressed, but they are often induced after microbial challenge (Morishima et al, 1995).

In order to directly measure the activity levels of Lysozyme in the silkworm plasma, we optimized a general Lysozyme detection protocol for silkworm plasma samples. The Lysozyme activities were found to be very variable among the germ-free silkworms of the four strains (Table 2). However, no significant differences were detected in the Lysozyme concentrations of the plasma samples extracted from the same *B. mori* strain on different days of the fifth larval stage (Kruskal-Wallis test, H at least < 9.525, $P > 0.05$ for all comparisons). Similarly, no significant differences were also found among plasma samples collected from different uninfected *B. mori* strains (Kruskal-Wallis test, H = 32.75, $P = 0.08$, ns).

In general, the concentration of active Lysozyme in silkworm plasma decreased after infection with *E. mundtii* (Table 2). None of the infected plasma showed a significantly different Lysozyme activity in comparison with its germ-free control (Two-ways ANOVA, $F_{1,4}$ (effect of the condition) at least < 0.9055 and $P > 0.05$, ns).

The Lysozyme activities measured in the *S. marcescens* infected plasma were in general at the same level of those of the germ-free controls for the Indian, Chinese and European strains (Table 2; Two-ways ANOVA, $F_{1,4}$ (effect of the condition) at least < 4.930 and $P > 0.05$, ns). Only the Japanese strain showed an increased Lysozyme activity of the infected plasma in comparison with its germ-free control (Two-ways ANOVA, $F_{1,4}$ (effect of the condition) = 8.357 and $P < 0.05$).

		Day 1	Day 2	Day 3	Day 4	Day 5	Day 6
Indian	Germ-free	65.9 ± 25.9	64.8 ± 8.9	64.8 ± 25.5	59.2 ± 21.9	56.8 ± 9.8	24 ± 2.6
	E. mundtii	16.7 ± 8.4	14.5 ± 14.5	25.4 ± 25.4	37.3 ± 37.3	35.5	0
	S. marcescens	37.6 ± 31.0	8.2 ± 4.1	50.4 ± 22.2	6.9 ± 6.9	10.9 ± 9.4	34.1 ± 6.4
Chinese	Germ-free	40.5 ± 8.8	37.1 ± 5.6	45.7 ± 25.4	31.7 ± 3.2	41.0 ± 2.7	2.0 ± 2.0
	E. mundtii	50.1 ± 8.8	0	0	3.3 ± 3.3	0	0
	S. marcescens	51.7 ± 7.2	28.3 ± 2.9	42.4 ± 12.0	25.1 ± 10.4	48.3 ± 8.1	37.9 ± 11.6
Japanese	Germ-free	33.3 ± 0.8	25.2 ± 13.1	58.1 ± 12.0	36.9 ± 18.8	56.8 ± 12.0	0
	E. mundtii	85.1 ± 46.4	21.1 ± 21.1	5.9 ± 5.9	17.1 ± 17.1	0	5.1 ± 5.1
	S. marcescens	50.7 ± 1.9	52.5 ± 7.0	45.3 ± 26.2	52.3 ± 6.2	48.8 ± 12.1	58.1 ± 13.9
European	Germ-free	56.0 ± 11.3	80.3 ± 23.8	24.3 ± 15.3	24.0 ± 7.9	33.4 ± 22.0	23.5 ± 20.5
	E. mundtii	96.8 ± 42.6	12.7 ± 7.9	71.9 ± 52.4	19.5 ± 2.5	17.9 ± 17.9	71.1 ± 49.0
	S. marcescens	26.4 ± 13.6	33.1 ± 15.5	19.7 ± 5.9	47.7 ± 11.3	50.9 ± 40.2	33.6 ± 6.7

Table 2. Lysozyme activity measured in the plasma of germ-free and *E. mundtii* or *S. marcescens* infected silkworm. Hemolymph was collected from 9 individuals pooled in three replicates, from both control and infected larvae every day after *E. mundtii* and *S. marcescens* challenges. The Lysozyme concentration expressed in Units/mL was calculated for each plasma (mean ± SEM).

Silkworm Melanization Response

The melanization reaction is a fundamental component of the silkworm humoral immune response. Melanin is a dark pigment which deposits on damaged tissues or on foreign microbes, preventing or retarding their growth and mediating the activity of phagocytic cells. When a pathogen or some of its components are recognized by PGRPs and βGRPs, the Phenoloxidase (PO), produced by hemocytes and present in the hemolymph as inactive Pro-Phenoloxidase (PPO) is activated and it

rapidly synthesizes melanin (Clark and Strand, 2013). However, some pathogens are able to interfere with melanin synthesis when present in the hemolymph, inhibiting the PPO activation (Ma et al, 2013). Since the melanin synthesis reaction is easily easily monitored, the analysis of the melanization rate can give an indication of the levels of PPO activation or inhibition and thus indirectly signal respectively the recognition of the pathogen by PGRPs and βGRPs or the presence of the pathogen in the hemolymph.

Hemolymph samples from both germ-free and infected larvae were collected every 24 h after immune challenge from at least 9 individuals pooled in 3 replicates. Hemocytes were removed via centrifugation, in order to observe the melanin synthesized only by the PO already present in the plasma, and not by POs subsequently released by hemocytes. To monitor the darkening of this hemocyte-free plasma, the optical density (OD) at 495 nm was measured every 10 min for 50 min (Figures A.4 and A.5). In order to compare the resulting melanization curves, linear regression analyses were performed and the slopes of the regression lines were plotted against the day of infection (Figure 8).

From the analysis of the melanization curves of plasma extracted from *E. mundtii* infected silkworms, it was found that this pathogen was in some way able to interfere with the PO activation when consistently present in the hemolymph of all four silkworm strains (Figure 8A). The melanization rates measured in infected plasma differed from those extracted from germ-free controls (Two-ways ANOVA, $F_{6,28}$ at least > 84.59, $P < 0.0001$). In particular, in the Indian and European strains, the melanization rates of infected plasma were higher than in germ-free controls on both the first and the second day after infection (Bonferroni multiple comparisons test, $P < 0.05$). However, starting from the third day after exposure to *E. mundtii*, the melanization rate went dramatically down ($P < 0.0001$ for all days). In the Chinese line, the melanization rate of infected plasma was significantly lower than in germ-free controls for all six days after infection, except for the second day (Bonferroni multiple comparisons test, $P < 0.05$ for all days except for day 2). However it was only after the third day that the difference in the melanization rate between infected and germ-free plasma was clearly noticeable (see also Figure A.4B). A similar profile was observed in the Japanese strain, with melanization rates of infected plasma always significant lower than in germ-free controls (Bonferroni multiple comparisons test, $P < 0.001$ for all days). In this case the inhibition of melanin synthesis was clearly detectable from the second day after infection.

The rates of melanization of plasma extracted from *S. marcescens* infected silkworms were generally lower than those extracted from germ-free larvae, suggesting that also *S. marcescens* was able to interfere with the PO activation of all four silkworm strains (Figure 8B; Two-ways ANOVA, $F_{6,28}$ at least > 20.96, $P < 0.0001$). However, the effect of this inhibition was not so evident or constant during the

infection as for the *E. mundtii* exposure. Specifically, in the Indian strain, the melanization rates of infected plasma were higher than germ-free controls until the third day after *S. marcescens* exposure (Bonferroni multiple comparisons test, $P < 0.001$ for all days). However, for the fourth and fifth day this trend was inverted, with germ-free melanization rates higher then infected ones ($P < 0.0001$ for both days). On the sixth day of infection, the two melanization rates were not significantly different ($P = 0.1894$, ns). In the European and Japanese lines, the melanization rate of *S. marcescens* infected plasma were generally lower than for germ-free plasma (Bonferroni multiple comparisons test, $P < 0.05$ for all days except for day 6 of the European strain and days 2 and 5 of the Japanese strain: $P > 0.05$, ns). In the Chinese line, the melanization rate of infected silkworms was lower than in germ-free controls only on the fourth and fifth days after infection (Bonferroni multiple comparisons test, $P < 0.0001$), while at the other time-points it was similar (day 1 and 2) or higher (days 3 and 6).

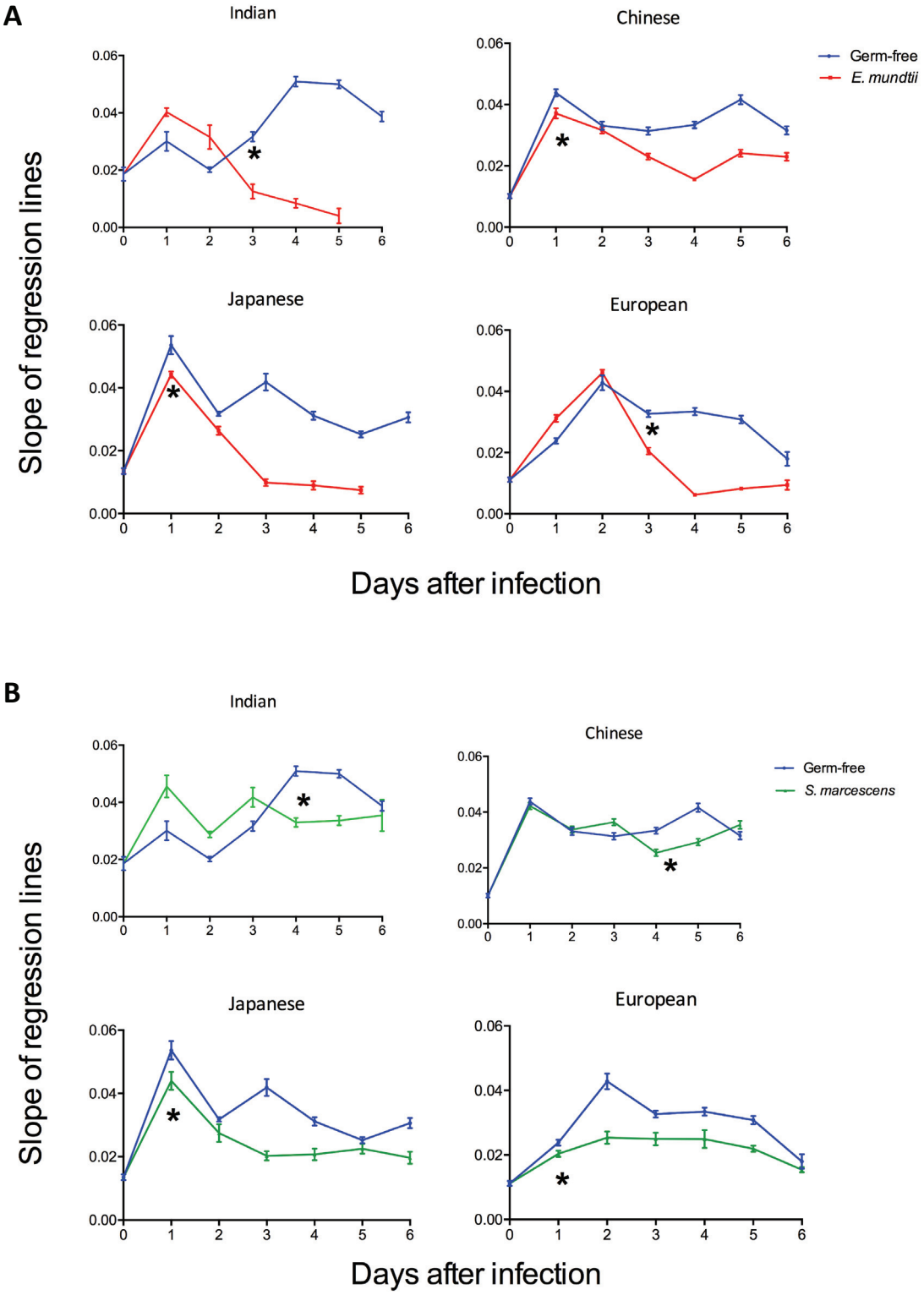

Figure 8. Melanization rate curves of plasma extracted from germ-free and *E. mundtii* (A) or *S. marcescens* (B) infected silkorms. Hemolymph was collected from 9 individuals pooled in three replicates. For each day of the experiment, the regression line of melanization curves was drawn and the slopes (mean ± SD) of these lines were plotted against the day of infection to give an indication of the melanization rate (Bonferroni multiple comparisons test: * indicates a significant lower melanization rate of infected plasma in comparison to the germ-free, $P < 0.05$).

Discussion

The four *B. mori* strains selected for this study were shown to have differential sensitivity to Gram-positive and -negative oral infections. In order to determine the factors that might explain this strain-specific sensitivity, different components of the silkworm humoral immunity were investigated, with particular attention to antimicrobial peptides, the most important players in the humoral immune response. The possible differential phagocytosis activity carried out by hemocytes among the four strains was not examined. In fact, a recent study indicated that different *Drosophila* laboratory strains with variable genetic backgrounds show different levels of hemocytes in uninfected conditions and that the number of hemocytes increases with the progression of infections with microorganisms such as *Escherichia coli* or *Enterococcus fecalis*. However, this increment was directly proportional so that the strains with higher number of hemocytes in uninfected conditions corresponded to those with higher number of immune cells also after microbial exposure, and *viceversa* (Eleftherianos at al, 2014). As reported in Chapter 2, similar levels of hemocytes were detected at the beginning of the fifth larval instar in germ-free individuals belonging to the Chinese, Indian and European lines, while the highest number of hemocytes was found in the Japanese strain. However, since this latter strain was the most sensitive to both infections, it appears unlikely that the cellular immune component might be involved in the differential silkworm strain-specific sensitivity to *E. mundtii* and *S. marcescens*.

The bacterial infections with *E. mundtii* and *S. marcescens* were found to have a totally different progression and are therefore discussed separately.

The oral infection of silkworms with the Gram-positive *E. mundtii* was particularly effective: only few bacterial cells (about 30 per larva) were sufficient to induce high mortality in all four *B. mori* strains. The European strain turned out to be the most resistant line, followed by the Chinese and, at a second stage, by the Japanese and the Indian strains. All four *B. mori* lines were found to activate the AMP transcriptional response at midgut level immediately after the ingestion of the bacterium, even if with differences in both the types of AMP transcribed and the levels of transcription. In *Drosophila* the local AMP gene expression at midgut level is thought to be activated through the Imd-pathway only (Nehme et al, 2007), which is also typically activated in response to a Gram-negative infection and controls the transcription of a limited number of AMPs. However, in the *B. mori* oral infection with *E. mundtii* we observed a massive AMP transcriptional activation of all the nine representative AMP genes examined in this tissue. These data might suggest that in *B.*

mori at midgut level the Imd-pathway had a wider activation spectrum in comparison with that acting at systemic level. Alternatively in the silkworm the *E. mundtii* induced AMP activation at midgut level might involve both Toll- and Imd-pathways.

Given this prompt local AMP transcription induction for all silkworm lines, we can hypothesize that *E. mundtii* cells or some of its components were in some way able to pass the peritrophic membrane (PM) and to stimulate the transcription in intestinal epithelial cells. It is therefore unlikely that the higher thickness of the PM observed in the European strain (Chapter 2) is able to retard the contact between the pathogen and the intestinal *epithelium*.

Data obtained from bacterial isolation from hemolymphs indicated that *E. mundtii* was able to pass both PM and intestinal *epithelium* and to proliferate in the larvae hemolymph of all four silkworm lines. However living bacterial cells were isolated from the hemolymph of the different silkworm lines at different time-points. In the Japanese strain, the pathogen was able to pass the gastro-intestinal barrier between the first and the second days after infection, while in the other three lines the massive entrance of *E. mundtii* in the hemolymph circulation took place at least 24 h later. Both the European and Indian lines showed hemolymphs with high bacterial load from the third day after pathogen exposure. These data suggest that the differential thickness of the PM among strains did not play a fundamental role in the timing of the bacterial transition. It was also interesting to note that the Chinese strain showed the lowest bacterial load in its plasma at all investigated time-points of the larval development.

A differential timing was also observed in the activation of the AMP expression at systemic level, with a general inverse correlation between the timing of the AMP induction and the susceptibility to *E. mundtii*: the Japanese strain, which was found to be the most sensitive line, activated immediately the AMP transcription in fat bodies, while the European strain, which showed the highest tolerance to *E. mundtii*, induced the AMP gene expression 24-48 h later. In general, Gram-positive bacteria are thought to stimulate the AMP transcription in fat bodies through the Toll-signaling (Ferrandon et al, 2007). Since these studies were carried out mainly in *Drosophila melanogaster,* we can not exclude that the Gram-positive driven systemic AMP transcriptional activation in *B. mori* might involve also the Imd-pathway. It is interesting to note that the transcription was activated in all four *B. mori* lines also for those genes which codify for AMPs that were previously demonstrated to be only active against Gram-negative bacteria, such as Gloverin 2, which was found to be active only against Gram-negative bacteria *in vitro* (Yang et al, 2011). Our data suggest therefore that Gloverin 2 might play a role also in the protection against Gram-positive oral infections.

The antimicrobial activity of silkworm plasma confirmed the qPCR data, indicating that AMPs might have been produced at both local and systemic levels and released in the hemolymph of all four *B. mori* lines.

The other components of the silkworm humoral immunity investigated appeared not directly linked to the increased resistance of the European strain, even if differences were found among the four lines. Lysozyme activity was found to be equal or reduced in the plasma of infected silkworms in comparison with germ-free controls. Since evidence of bacteria or viruses playing an active role in inhibiting Lysozyme activity has been found (Shelby et al, 1998; Mikonranta et al, 2014), it is possible that the infection with *E. mundtii* inhibited the silkworm Lysozyme activity, in particular in the Japanese and Chinese strains. However, since this possible inhibition did not correlate with the differential *B. mori* strain sensitivity, it is unlikely that Lysozyme might play a decisive role in the overall resistance to this Gram-positive infection.

The melanization reaction was found to be in some way inhibited in the late stages of the *E. mundtii* infection in all four *B. mori* lines. On the other hand, a significant activation of the PO activity at the first stages of the infection was found in both the European and the Indian strains, which however represent the most resistant and one of the more sensitive strains respectively. It is also remarkable that, on the first day of the fifth larval stage, the Japanese strain reared in germ-free conditions showed the highest levels of melanization. This is probably due to the highest number of hemocytes possessed by this strain at the beginning of the fifth larval stage, since the rate of the melanization reaction has been correlated to the amount of hemocytes actively producing PO (Eleftherianos et al, 2014). This feature, however, was not sufficient to provide protection against the *E. mundtii* infection, suggesting that the melanization reaction is not related to the differential sensitivity of the four *B. mori* strains.

Taken together, these data suggest the European strain might possess the most effective AMP-mediated immune response against this pathogen.

The AMP genetic variability analysis (Chapter 2) indicated that the European strain presents some AMP isoforms, such as those of Cecropin B2 and Gloverin 1, which might have a peculiar activity against *E. mundtii.* In order to evaluate this hypothesis, we initiate a study to analyze the *in vitro* antimicrobial power of the different AMP isoforms. Some preliminary results are reported in the following Chapter.

After oral infection with the Gram-negative *S. marcescens*, larvae belonging to the European, Chinese and Japanese strains were not able to reach adult stage, showing almost total mortality which was particularly high during the pupal stage. On the contrary, the Indian strain was found to successfully counteract the *S. marcescens* infection and its survival rate was not affected by this pathogen.

All four silkworm strains showed an activation of the AMP transcription at midgut level (even if weaker in comparison to that to *E. mundtii*) suggesting that *S. marcescens* was sensed by the gut *epithelia* of all four *B. mori* strains from the first day since pathogen exposure. It appeared that only specific AMPs were produced to counteract the pathogen at this level. Among this set of AMPs, *attacin* was found to be induced in all four strains, with the Indian one showing the highest expression levels. In Lepidoptera, this AMP was found to be particularly active against Gram-negative bacteria (Carlsson et al, 1991), therefore it might constitute an efficient strategy to counteract *S. marcescens*.

Since the European line induced the local AMP transcription at the same time as the other three strains, its thicker PM was not sufficient to block or hinder the passage of *S. marcescens* (or some of its components) to the gut *epithelium,* as noticed during *E. mundtii* infection.

The expression analysis at both local and systemic levels showed that the set of genes expressed by the Indian strain at local level is reduced in comparison with the ones induced at systemic level. Therefore, in the case of the *S. marcescens* infection, the regulation of AMP genes at systemic level might involve different transcriptional pathways or regulators in respect of the local response.

The AMP response activated at the midgut level was not sufficient to prevent the passage of the pathogen from the gut lumen to the hemolymph circulation for the Japanese, Chinese and European strains. For all these three *B. mori* lines, *S. marcescens* was found to be present and proliferating in the hemolymph of infected silkworms. No living pathogen cell was found in the hemolymph of infected silkworms belonging to the Indian line.

The three *S. marcescens*-sensitive strains activated few AMP genes at systemic level in the late stages of infection. Only the resistant Indian strain was able to induce a considerable and immediate systemic AMP response, with many of the investigated AMP genes found to be significantly over-expressed. The higher systemic AMP transcriptional level induced by the indian line in comparison to the other three *B. mori* strains was reflected by the antimicrobial activity of plasma extracted from indian infected silkworms against *S. marcescens.* The antimicrobial activity against this bacterium was significantly high also in samples collected during the late infection stage (sixth day). In the other three strains, the weak or late systemic transcription of the analyzed AMPs appeared not sufficient to give rise to an effective antimicrobial protection at the level of the hemolymph.

The Lysozyme activities were found to be in general unaltered after the infection in all four *B. mori* strains and therefore it is unlikely that this enzyme could influence the survival against *S. marcescens*.

The Indian line showed an activation of PO activity in the first stages of the infection. This higher capability to activate the melanization response, in addition to the activation of the systemic AMP transcription, might in part explain the higher tolerance of this line to *S. marcescens* and the absence of living pathogen cells in the hemolymph. With the progress of the infection, the melanization rates of the Indian strains lowered and were comparable to those of the other strains.

Taken together these data suggest that the peculiar resistance of the Indian strain to the *S. marcescens* infection might be due to a more efficient activation of recognition factors and/or signal transduction mechanisms that allow to efficiently and promptly respond to *S. marcescens* oral infections.

Materials and Methods

Germ-free Silkworm Rearing

Eggs belonging to the four strains and maintained in hibernation at 2.5-5°C were incubated at 6°C to hatch. When eggs were turning white, they were surface sterilized for germ-free rearing by soaking in 70% ethanol for 1 min and in 5% sodium hypochlorite for 20 min. The eggs were then rinsed with 95% ethanol, air-dried and closed in sterile plastic containers. Larvae were fed on artificial diet (Cappellozza et al, 2005) previously sterilized by autoclaving at 117°C for 40 min. The diet was prepared in a thin layer of around 2.5 cm of thickness, in a plastic container covered with a plastic wrap. Silkworms were grown at 26-28°C to the third larval stage, while during the fourth and the fifth larval instars they were kept at 24-26°C. Eggs and larvae were always manipulated under a laminar flow hood using sterile tweezers.

Bacterial Strains for Silkworm Infection

Single fresh colonies of *Escherichia coli* ATCC 25922, *Enterococcus mundtii* HDYM-22, *Serratia marcescens* WW4 and *Beauveria bassiana* ATCC 74040 were inoculated in Nutrient Broth Sucrose and grown overnight (ON) at 30°C at 250 rpm. To standardize bacterial cell numbers, the bacterial cultures optical density at 600 nm (OD_{600}) was measured. Serial dilutions of bacterial suspensions were plated in Plate Count Agar (PCA) medium petri dishes to determine the precise correlation between OD_{600} and Colony Forming Units (CFU). For the fungus *B. bassiana*, the number of conidia was determined with a counter chamber.

Silkworm Oral Infection

OD_{600} was measured in ON cultures of *Escherichia coli, Enterococcus mundtii* and *Serratia marcescens*. Bacterial cultures were diluted with sterile saline solution to a final theoretical OD_{600} of $1*10^{-2}$, $0.5*10^{-6}$ and $0.789*10^{-2}$, which correspond to a final concentration of $8*10^{6}$ CFU/mL for *E. coli*, $2.7*10^{2}$ CFU/mL for *E. mundtii* and of $2.23*10^{7}$ CFU/mL for *S. marcescens*, respectively. The *B. bassiana* concentration was instead determined by direct conidia count.

2 mL of each diluted bacterial suspension were homogeneously spread on the sterile artificial diet. Fifth instar silkworms, previously reared in germ-free conditions,

were fed for 24 h with the infected diet and then put on a new germ-free diet. For the *B. bassiana* infection, larvae were directly dipped into the fungal culture, reared for 24 h on sterile artificial diet and then moved to a new germ-free diet. Control animals were fed in parallel for 24 h with germ-free diet previously soaked with 2 mL of sterile saline solution. In total, at least 400 silkworms were infected with each pathogen or reared as germ-free controls.

Determination of Silkworm Sensitivity to Oral Infections

Fifth instar larvae belonging to the four strains were infected with the two pathogens or kept in germ-free conditions as uninfected controls. From 3 to 6 replicates of 15 individuals were tested for each strain and condition. The number of dead larvae was recorded every 24 h during the 7 days of the fifth larval stage. Since bacterial infections often result in a delay in larval development and in spinning failure, the number of larvae which did not spin the cocoon and died on different days, were considered dead before spinning (day 12). Since it was not possible to monitor the survival status of pupae which were enclosed in their cocoons, the number of individuals which did not reach adult stage was considered dead during pupation (day 16).

Sample Collection

The sample collection was conducted with the same procedures as used to collect all biological samples analyzed (hemolymph, midgut, fat bodies). For each of the four *B. mori* strains, samples from infected and germ-free larvae were collected for 6 days after infection, every 24 h. Three replicates, each composed by hemolymphs or tissues of three larvae, were collected at each time-point. All operations were conducted under a laminar flow hood.

Isolation of Bacteria from Silkworm Hemolymph

Before sacrifice, the surface of the larval body was disinfected to prevent contamination of hemolymph samples by bacteria present on silkworm integument: larvae were anesthetized with ice, dipped in 70% ethanol for 5 sec, then in 5% sodium hypochlorite for 5 sec and again in 70% ethanol for 5 sec. Larvae were dried with sterile

tissue paper. One of the abdominal proleg was cut with sterile scissors and the outflowed hemolymph was collected in a sterile centrifuge tube. For each pool, 70 µl of hemolymph were plated in PCA medium Petri dishes. Plates were sealed with parafilm and incubated at room temperature (RT) for at least 2 days for colony count.

Total RNA Extraction

Larvae were anesthetized with ice and dissected using sterile scissors and tweezers. Midgut and fat bodies samples were immediately placed in RNAlater solution (Thermo Fisher Scientific) to prevent RNA degradation and stored at -20°C.

Tissues were homogenized in 500 µl of Trizol (Thermo Fisher Scientific) an IKA T10 basic homogenizer and incubated at room temperature for 5 min. 100 µl of chloroform were added. The mixture was vigorously shaken for 15 sec, incubated at RT for 2-3 min and centrifuged at 4°C for 15 min at 12000 x g. The aqueous phase was transferred to a new centrifuge tube and RNA was precipitated with 250 µl of room temperature isopropanol and incubated at -20°C for 1 h. Samples were then centrifuged at 4°C for 10 min at 12000 x g, the supernatants were removed and the pellets were washed with 1 mL of 75% ethanol. After a last centrifuge at 4°C for 5 min at 7500 x g, supernatants were removed, samples were air dried and resuspended in 80 µl of nuclease-free water. RNA quality and quantity were determined with NanoDrop 2000 (Thermo Fisher Scientific). RNA samples were stored at -80°C.

Quantitative Real-Time PCR

The expression ratios of 9 representative AMP genes were determined in the two tissues (fat bodies and midgut) by quantitative PCR (qPCR) using Power SYBR Green RNA-to-CT 1-Step Kit (Thermo Fisher Scientific) and an ABI 7900HT Fast Real-Time PCR System (Thermo Fisher Scientific). The PCR cycle consisted of an initial 30 min of retro-transcription step at 48°C, a 10 min denaturation step at 95°C and 40 cycles of 15 sec at 95°C (denaturation) and 60 sec at 60°C (annealing and extension).

In order to ensure the specificity of the qPCR reactions, the correct starting amounts of RNA and primers were determined as following: qPCR reactions were performed on serially diluted RNA amounts (500, 100, 20, 4, 0.8 ng) using two different primer concentrations (100 or 200 nM). For each primer couple, cycle threshold (Ct) values were graphed against the $\log_{10}$ of the RNA amounts. The slopes of the resulting linear curves were determined and the amplification efficiency (E) was calculated as follows : $E = 10^{-1/slope}$. The optimal RNA and primer concentrations were considered to

be the ones which gave a linear correlation between Ct and RNA amounts and which showed single peaks in the dissociation curves. QPCR reactions were performed in duplicate in a total volume of 10 µl, on 20 ng of total RNA using *actin3* as housekeeping gene (see Table 3 for primer sequences and concentrations).

Data were analyzed using the $2^{-\Delta\Delta CT}$ method. For each sample, the AMP mRNA expression ratio (R) was calculated as following:

$$R = \frac{E_{AMP}^{\text{Ct } AMP \text{ germ-free - Ct } AMP \text{ infected)}}}{E_{act3}^{\text{Ct } act3 \text{ germ-free - Ct } act3 \text{ infected)}}}$$

Expression ratios for each AMP gene were graphed against the day of infection.

Gene	Primer name	Sequence (5' - 3')	Amplicon length (bp)	Concentration
actin3	ACT3_RT_FOR	CGGGAAATCGTTCGTGAT	181 bp	100 nM
	ACT3_RT_REV	ACGAGGGTTGGAAGAGGG		
attacin	ATT_RT_FOR	CAGGGCTCGCTCTGGACAAT	68 bp	100 nM
	ATT_RT_REV	GAAGCCGGGAATGCGGGTC		
cecropin A *	CECA_RT_FOR	CCTGAGCCCAGGTGGAAACTC	93 bp	200 nM
	CECA_RT_REV	GACGGCTATAGCTGGACCCG		
cecropin B *	CECB_RT_FOR	TTCGCTCTGGTGCTGGCTTTG	118 bp	200 nM
	CECB_RT_REV	GGCCCGCTTTGACGATGCC		
cecropin D	CECD_RT_FOR	CGCCACGGCTTCGGTCTC	109 bp	100 nM
	CECD_RT_REV	GGTGTCGACTGCTGGAGCC		
cecropin E	CECE_RT_FOR	GTGTGTGCGAGCGTTATGGC	147 bp	100 nM
	CECE_RT_REV	CCCATGAGCGATGGTCGCC		
defensin	DEF_RT_FOR	CGTTGCCGAGAGACGCAAC	116 bp	100 nM
	DEF_RT_REV	TCGCACCATATCCGCCCAG		
gloverin 2	GLV2_RT_FOR	GCGAACAAGAATGCACAAGCCAC	207 bp	100 nM
	GLV2_RT_REV	GTGTTGAGGTGATCACCAATCATG		
lebocin	LEB_RT_FOR	CCAGAGGTTCATCCAGCCGAC	85 bp	200 nM
	LEB_RT_REV	CGGTTCCTGGCCAGCTTGTC		
moricin	MOR_RT_FOR	CATGTAGTACAGCCGCTCCAGC	108 bp	200 nM
	MOR_RT_REV	CGTTGGCTGTACTGGCGATATT		

Table 3. List of primers used for qPCR on AMP genes. For each gene the following information is indicated: gene name, name of primers used, 5'-3' primer sequences, length of the amplicon, optimal primer couple concentration. * indicates that the primer was designed to amplify the whole gene family.

Plasma Antimicrobial Activity Test

Hemolymph samples were collected as for the bacterial isolation analysis, with the only difference that the outflowed hemolymph was immediately mixed with 2.5 mM of filter sterilized phenylthiourea to prevent melanization. Hemocytes were removed by centrifugation at 1000 x g for 5 min at 4° C. Plasma samples were snap-frozen in liquid nitrogen and thawed on ice just before the test.

Single fresh colonies of *E. mundtii* and *S. marcescen*s were inoculated in PCA and Muller Hinton (MH) broth respectively. Bacterial *inocula* were grown for 12-16 h at 30°C at 250 rpm and therefore used during their exponential growth phase. OD_{600} was measured and bacterial cultures were diluted with the appropriate culture media (MH or PCA broths) to a final theoretical concentration of $0.5 * 10^5$ CFU/mL just before the test.

The assay was performed on sterile polystyrene 96-well plates (Costar). For each sample, 25 µl of plasma were tested in triplicate against 200 µl of bacterial cultures. Plasma extracted from *E. mundtii* infected silkworm was tested against *E. mundtii*, while plasma from *S. marcescens* larvae was tested against *S. marcescens*. Non-infected plasma was tested against both bacteria. As negative control of growth, ampicillin at a final concentration of 50 µg/mL was added to bacterial suspension in three wells. No-treated bacterial suspension were grown as positive control. Plates were incubated at 30°C with soft shaking (50 rpm) and the OD_{600} was measured at different time-points (0, 3, 5, 7, 9, 24 h) using a DTX 880 Multimode Detector (Beckman Coulter).

Since the number of bacterial cells is proportional to the OD_{600}, this value was used to calculate the specific bacterial growth rate (µ) as described in Widdel 2010:

$$\mu = \frac{2.303\ (\lg OD_n - \lg OD_{n-1})}{(t_n - t_{n-1})}$$

For each bacterium, its growth rate was calculated separately for each treatment (plasma extracted from germ-free silkworms or from *E. mundtii* or *S. marcescens* infected ones). Since the correlation between µ and time was not linear, in order to compare the µ of bacteria treated with different plasma samples, the area under each µ curve was calculated in the time span comprised between 3 and 9 h *post-inoculum*. In this way, a single value representing the whole growth trend of each bacterium treated with the different plasma samples, was obtained.

Plasma Lysozyme Activity

Plasma samples were obtained as for the Antimicrobial Activity test. *Micrococcus luteus* was used for this test as Gram-positive standard to determine Lysozyme activity. A single fresh *M. luteus* colony was inoculated in Nutrient Broth Sucrose and incubated at 30°C and 250 rpm overnight. The culture was centrifuged at 5000 x g for 5 min and the bacterial pellet was resuspended in sterile Reaction Buffer (66 mM potassium phosphate, pH 6.24) at a final OD_{450} of 0.6. A fresh Lysozyme (Sigma-Aldrich) solution was prepared in cold Reaction Buffer just before use at a final concentration of 1800 Units/mL.

The assay was performed on sterile polystyrene 96-well plates (Costar). For each sample, 25 µl of plasma were tested in triplicate against 200 µl of *M. luteus* cell suspension. As positive control, a Lysozyme solution at a final concentration of 200 Units/mL was added to the bacterial suspension in three wells. As negative control, 25 µl of Reaction Buffer were added to a *M. luteus* suspension in other three wells. The OD_{450} was measured at time zero and after 5 min using a DTX 880 Multimode Detector (Beckman Coulter).

For each sample, the OD_{450} measured at time zero was subtracted from the values obtained after 5 min. Since one Lysozyme Unit is defined as the amount of enzyme necessary to produce a decrease in ΔOD_{450} of 0.001, the Lysozyme concentration expressed in Units/mL was calculated as follows:

$$U = \frac{- \Delta OD_{450} / 5 \text{ min}}{(0.001) * (0.025 \text{ mL})}$$

Lysozyme concentration was set to zero when the U value was negative, that is when the OD_{450} measured after 5 min was higher than the one measured at time zero.

Silkworm Melanization Response

Hemolymph samples were collected in pre-cooled centrifuge tubes, as described in the previous sections. All operations were performed on ice, since hemolymph samples tend to get darker quickly due to the rapid synthesis of melanin by the Phenoloxidase (PO) enzyme. Hemocytes were removed by centrifugation at 1000 x g for 5 min at 4° C, to remove the effect of the PO enzyme synthesized by hemocytes. The hemocyte-free plasma samples were snap-frozen in liquid nitrogen.

Samples were thawed on ice just before the absorbance test. The assay was performed on sterile polystyrene 96-well plates (Costar). The 495 nm optical density

(OD_{450}) of 100 µl of plasma was measured to quantify the levels of melanization every 10 min using a DTX 880 Multimode Detector (Beckman Coulter). In parallel, as negative control, 2.5 mM of filter-sterilized phenylthiourea was added to each pool to prevent melanization. Three replicates were tested for each plasma pool.

The OD_{450} measured at time zero was subtracted from all other values obtained at the following time-points (10, 20, 30, 40 and 50 min). These ΔOD_{450} values were graphed versus time. In order to compare the speed of melanization of plasma samples collected at different time-points after bacterial exposure, a linear regression was performed for each ΔOD_{450} versus time line. The slopes of these regression lines were graphed against the day of infection. Germ-free plasma curves were compared with those of infected plasma.

Statistical analysis

Survival curve analysis: log-rank (Mantel-Cox) tests were first conducted on replicates of each treatment condition (germ-free, *E. mundtii*, *S. marcescens*), to assess their homogeneity. Then, Mantel-Cox analyses were performed comparing germ-free and infected survival curves separately for each bacterial infection and for each strain. Finally, Mantel-Cox tests were conducted on the survival data of the four silkworm strains infected with the same pathogen.

qPCR: considering separately the R values for each *B. mori* strain, non parametric Kruskal-Wallis one-way analyses of variance were performed for each infection (*E. mundtii*, *S. marcescens*) and for the germ-free controls on the R values of the 9 AMP genes during the 6 days of infection, in order to assess if there was a significantly different expression of these genes within the time frame of the experiment.

Antimicrobial activity and Lysozyme tests: non parametric Kruskal-Wallis one-way analyses of variance were conducted among germ-free plasma extracted from the same silkworm strain to determine the presence of any significant difference at different days during the fifth larval stage. Two-ways ANOVA followed by the Bonferroni *post-hoc* test was performed to evaluate the time x condition statistical significant interaction, between germ-free and infected plasma of the same *B. mori* strain during larval development.

Melanization response: Two-ways ANOVA tests were performed on calculated slope values and corresponding standard deviations. Bonferroni multiple comparisons tests were performed to compare the slopes of melanization reaction curves of germ-free and infected plasma.

Appendix

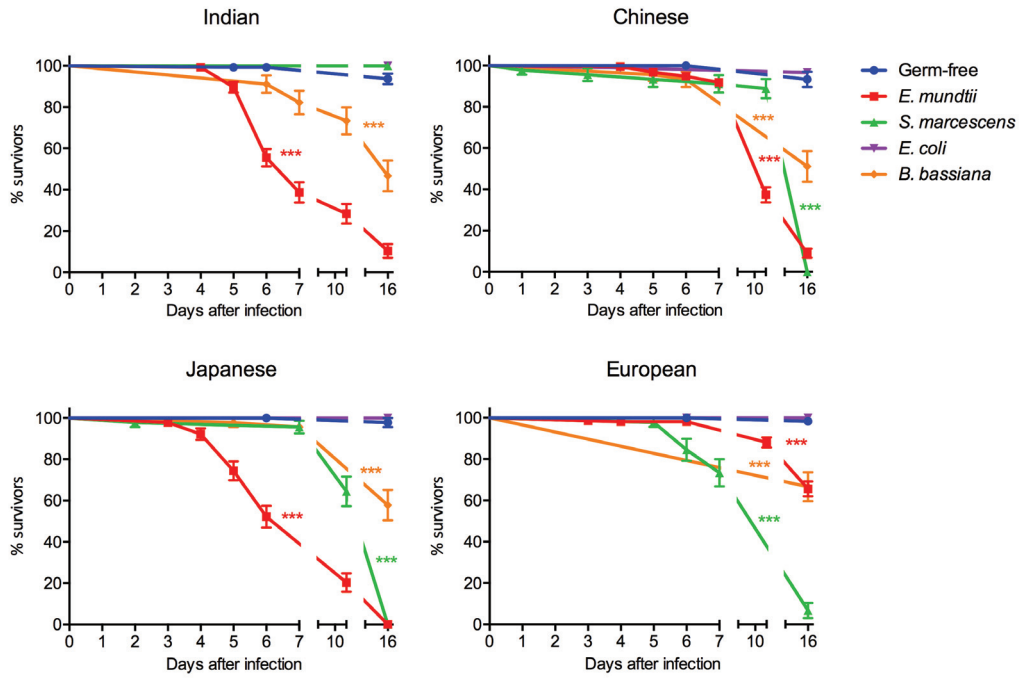

Figure A.1. Survival curves of the four *B. mori* strains infected with the four tested pathogens. For each line, germ-free survival curves were compared to those of larvae infected with *E. mundtii*, *S. marcescens, E. coli* and *B. bassiana* (mean ± SEM; Mantel-Cox test: ***: $P < 0.0001$).

Day of the fifth larval stage	Indian	Chinese	Japanese	European
0	0	0	0	0
1	0	0	0	0
2	0	0	0	0
3	0	0	0	0
4	0	0	0	0
5	0	0	0	0
6	0	0	0	0

Table A.1. Hemolymph bacterial load of the four *B. mori* lines reared in germ-free conditions. Hemolymph was collected from 9 individuals pooled in three replicates. The number of colonies grown after plating 70 µl of hemolymph on PCA plates was recorded for each day of the fifth larval stage. No bacterial cells were found in the circulation of the four strains' silkworms.

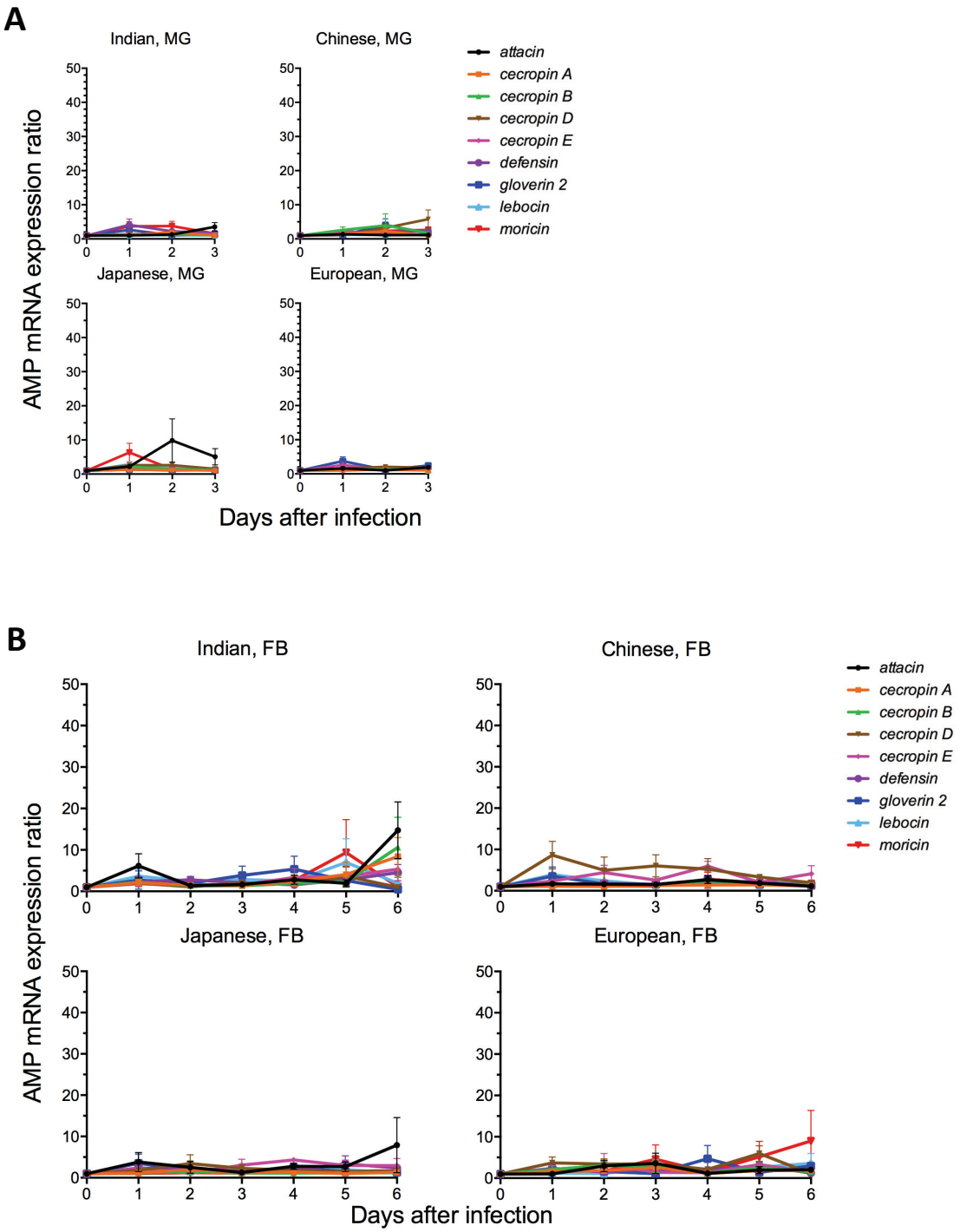

Figure A.2 Time course expression of 9 AMP genes in midgut (A) and fat bodies (B) of fifth instar larvae belonging to the four *B. mori* strains reared in germ-free conditions. The AMP mRNA expression was determined by quantitative RT-PCR on total RNA extracted for 6 (fat bodies) or 3 (midgut) days, after 24 h oral infection (9 individuals pooled in 3 replicates, mean ± SEM). AMP expression ratio represents the AMP/*actin3* mRNA levels of every control sample over the other two controls. None of the AMP gene was found to have a significantly differential expression during the three o six days analyzed (Kruskal-Wallis test, $P > 0.05$ for all comparisons).

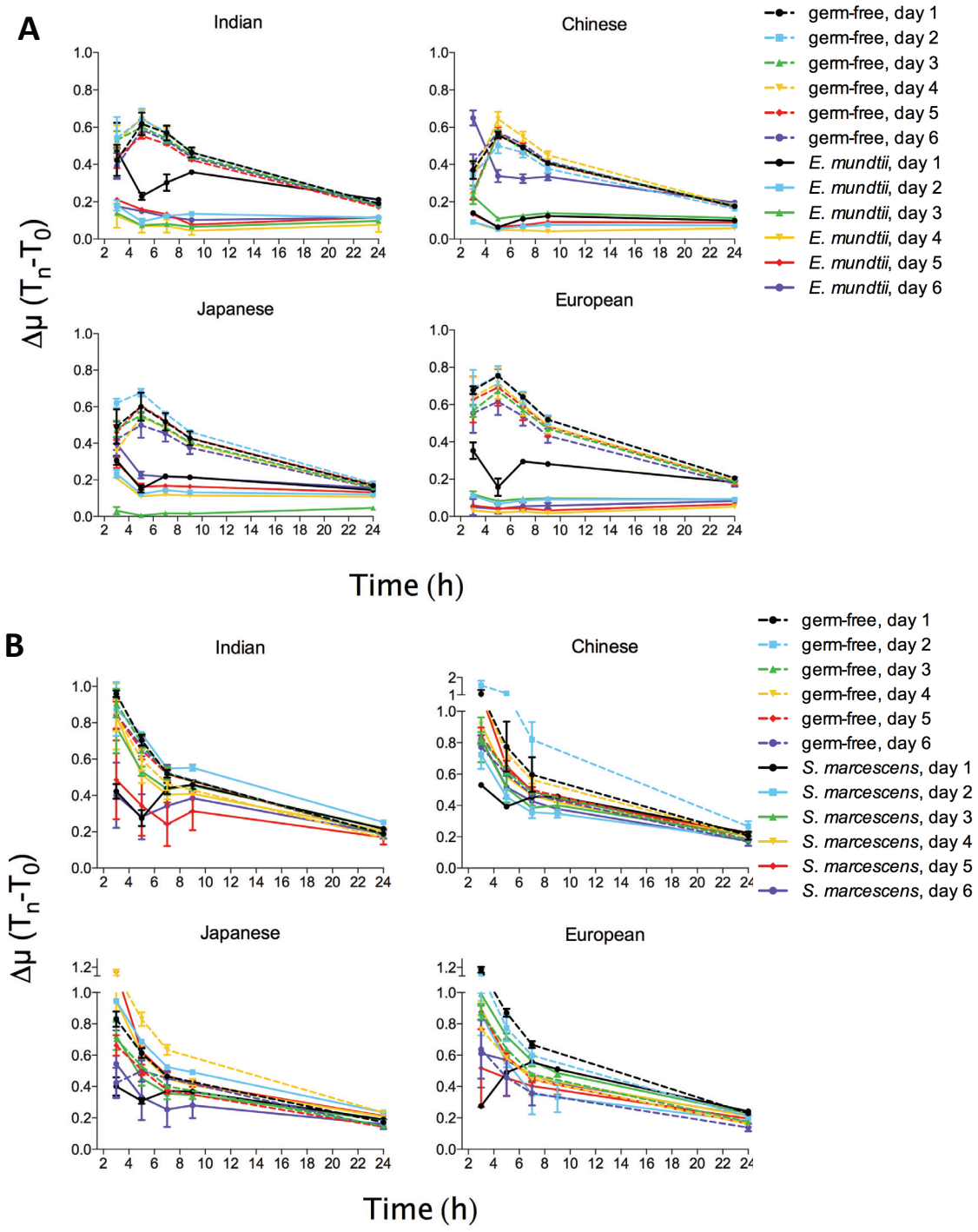

Figure A.3. Growth rates of *E. mundtii* (A) and *S. marcescens* (B) with germ-free and *E. mundtii* (A) or *S. marcescens* (B) infected plasma. Hemolymph was collected from 9 individuals pooled in three replicates, from both control and infected larvae every 24 h after *E. mundtii* or *S. marcescens* challenge. The hemocyte-free plasma was added to an *E. mundtii* or *S. marcescens,* culture ($5*10^5$ CFU/mL) and the optical density was measured to monitor the microbial growth. The growth rate was calculated and plotted against time (mean ± SEM).

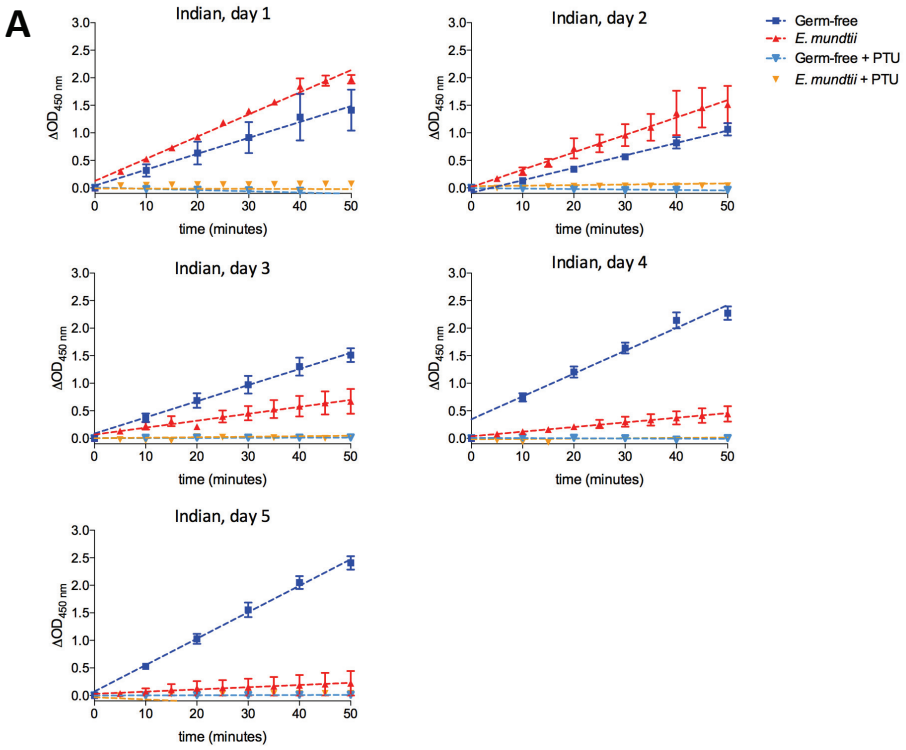
A
Indian, day 1
Indian, day 2
Indian, day 3
Indian, day 4
Indian, day 5
Germ-free
E. mundtii
Germ-free + PTU
E. mundtii + PTU
ΔOD450 nm
time (minutes)

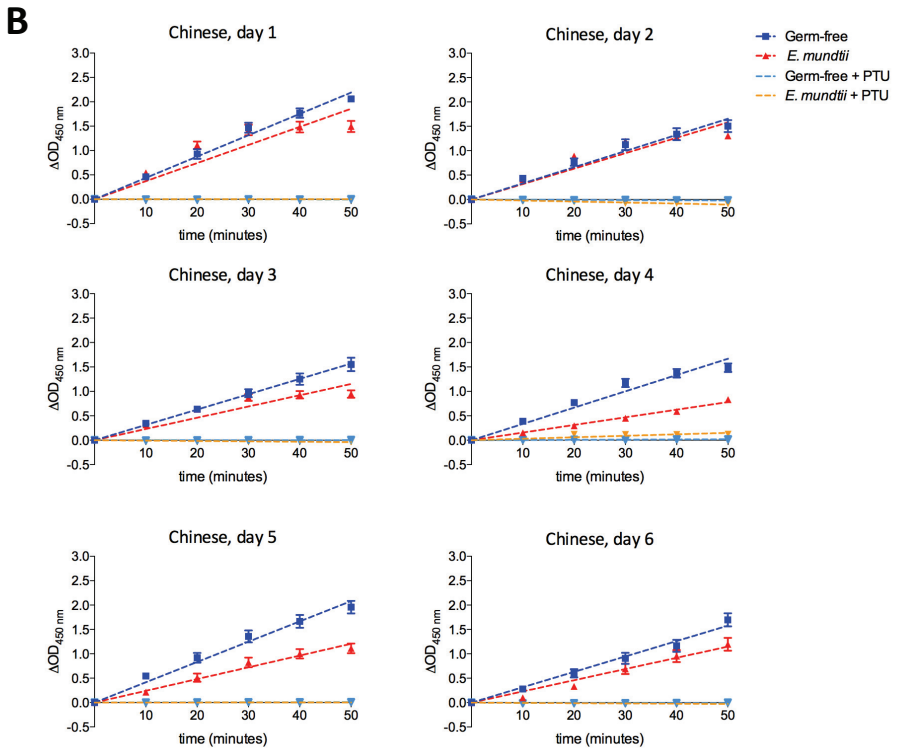
B
Chinese, day 1
Chinese, day 2
Chinese, day 3
Chinese, day 4
Chinese, day 5
Chinese, day 6
Germ-free
E. mundtii
Germ-free + PTU
E. mundtii + PTU
ΔOD450 nm
time (minutes)

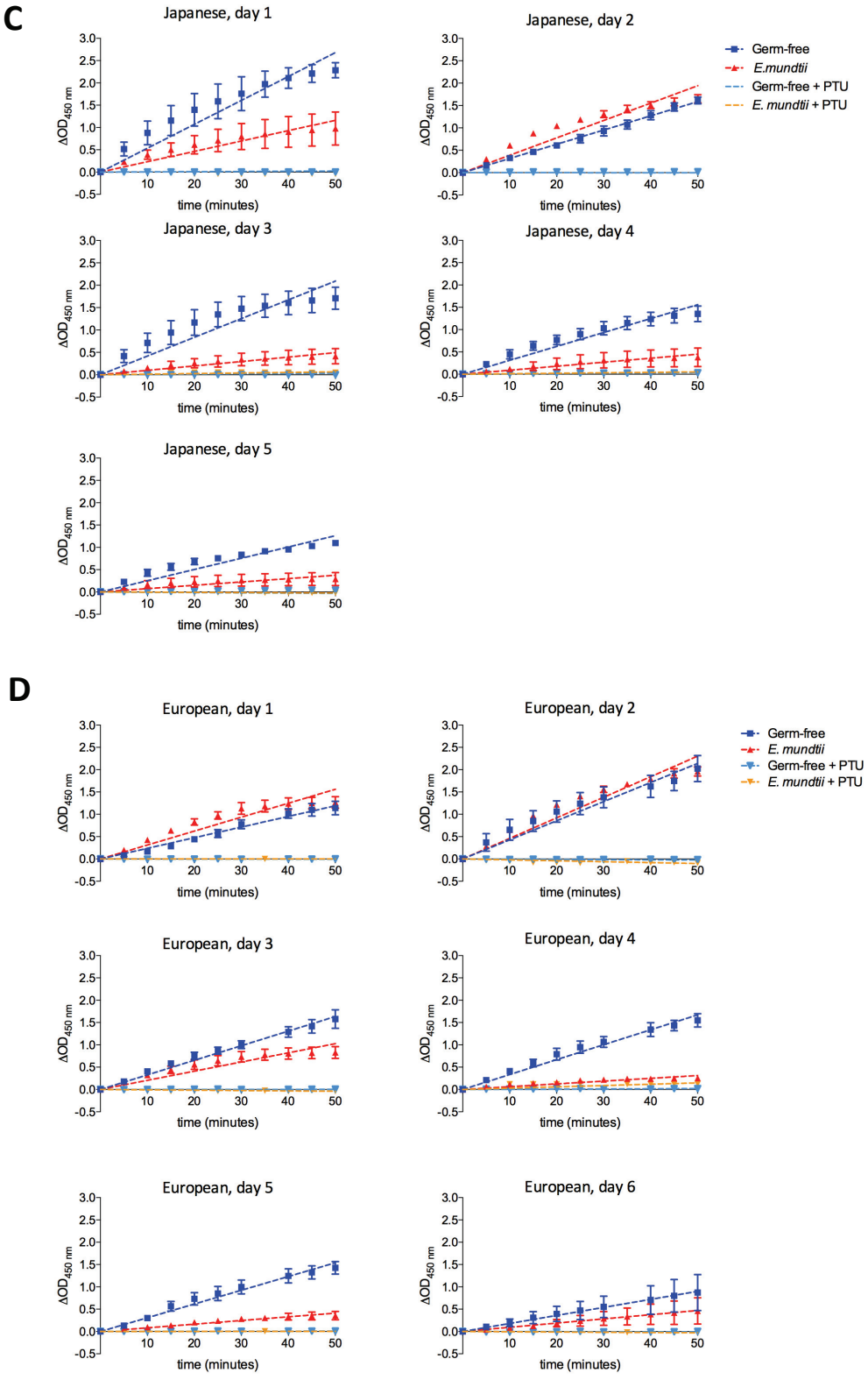

Figure A.4 Melanization curves and regression lines of germ-free and *E. mundtii*-infected plasma extracted from Indian (A), Chinese (B), Japanese (C) and European (D) silkworms. Hemolymph was collected from 9 individuals pooled in three replicates. The optical density (OD) at 495 nm of the hemocyte-free plasma was measured every 10 min to quantify the rate of melanization. As negative control, phenylthiourea (PTU) was added to a final concentration of 2.5 mM. The OD_{450} measured at time zero was subtracted from all other values obtained at the following time-points (10, 20, 30, 40 and 50 min). These ΔOD_{450} values were graphed versus time (mean ± SEM).

A

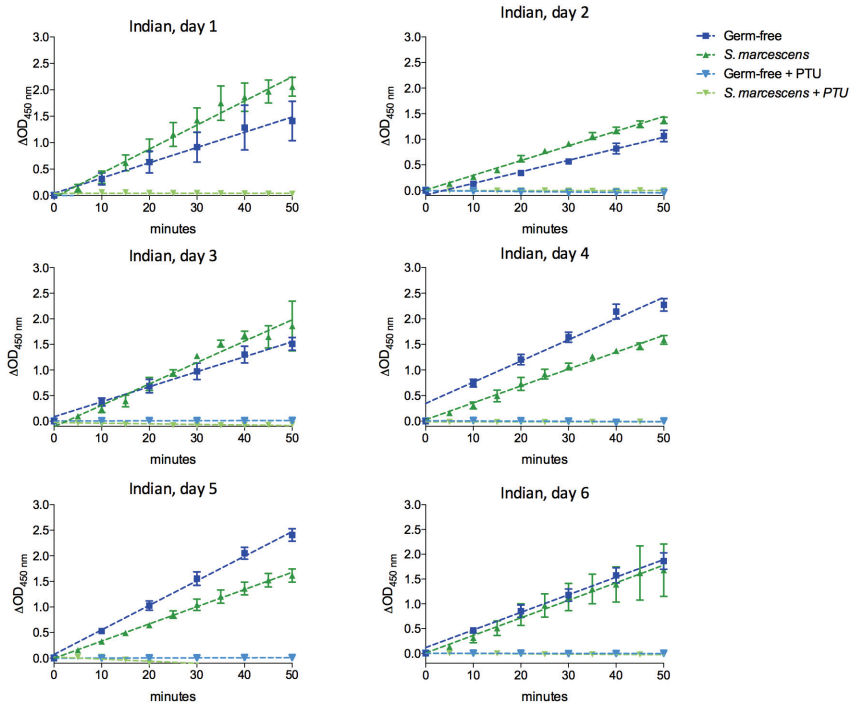
Indian, day 1
Indian, day 2
Indian, day 3
Indian, day 4
Indian, day 5
Indian, day 6
ΔOD450 nm
minutes
Germ-free
S. marcescens
Germ-free + PTU
S. marcescens + PTU

B

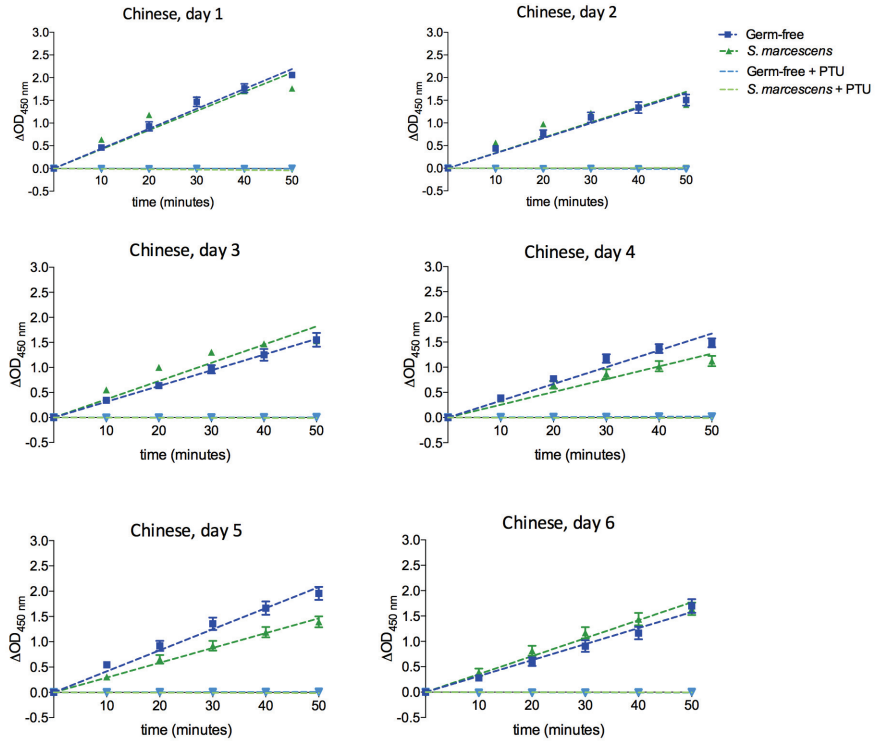
Chinese, day 1
Chinese, day 2
Chinese, day 3
Chinese, day 4
Chinese, day 5
Chinese, day 6
ΔOD450 nm
time (minutes)
Germ-free
S. marcescens
Germ-free + PTU
S. marcescens + PTU

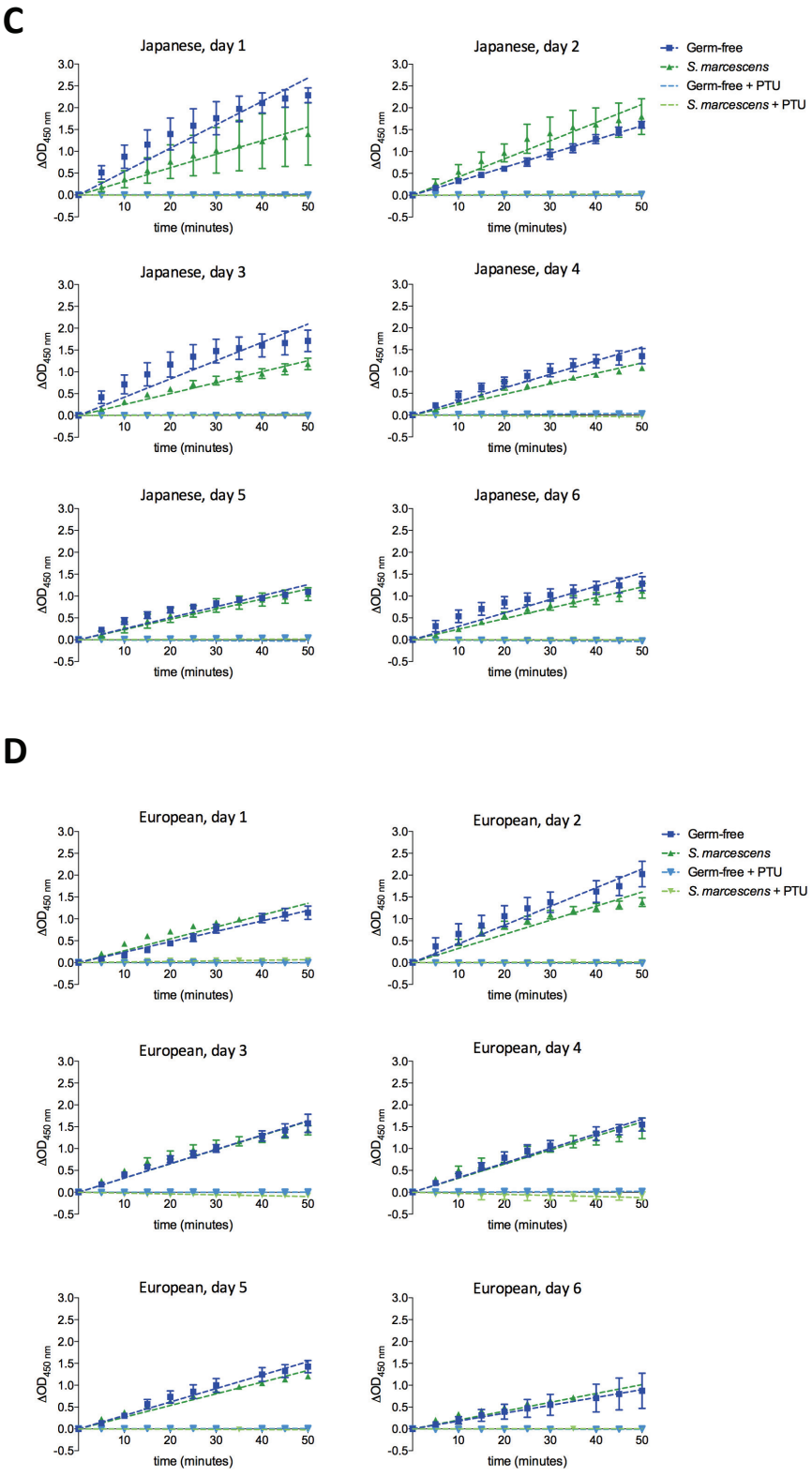

Figure A.5 Melanization curves and regression lines of germ-free and *S. marcescens*-infected plasma extracted from Indian (A), Chinese (B), Japanese (C) and European (D) silkworms. Hemolymph was collected from 9 individuals pooled in three replicates. The optical density (OD) at 495 nm of the hemocyte-free plasma was measured every 10 min to quantify the rate of melanization. As negative control, phenylthiourea (PTU) was added to a final concentration of 2.5 mM. The OD_{450} measured at time zero was subtracted from all other values obtained at the following time-points (10, 20, 30, 40 and 50 min). These ΔOD_{450} values were graphed versus time (mean ± SEM).

Chapter 4: Characterization of the AMP isoforms

Introduction

Different studies indicate that a moderate positive selection occurred on genes codifying for some AMPs in a wide variety of organisms, promoting a certain level of amino acid variability in response to pathogen pressure (Lazzaro and Clark, 2003; Tennessen, 2005). Both synonymous and non-synonymous polymorphisms at the level of regulatory and effector immune genes in *Drosophila* have been found to correlate with the differential total bacterial load isolated from different organisms and with overall survival to infections (Lazzaro et al, 2004 and 2006). In addition it has been reported that in many organisms, modifications in single AMP residues lead to a differential *in vitro* antimicrobial activity (Velliyagounder et al, 2003; Fine et al, 2013; Iijima et al, 2003; Lauth et al, 2001).

The four *B. mori* strain selected for this study were found to have differential sensitivities to infections with both Gram-positive and -negative silkworm specific pathogens (Chapter 3). From the analysis of the coding sequences of the 21 AMP genes in the four silkworm lines, many non-synonymous substitutions mapping in the active portion of the peptide were found (Chapter 2). In particular, Gloverin 1, 2 and 3, Cecropin B1 and B2 and Enbocin 1 and 2 were found to have different peptide variants in the four silkworm lines. Even if *B. mori* has been completely domesticated and thus entirely relies on humans for its maintenance in strictly controlled environments, a positive selection might have determined the preservation of different AMP isoforms in silkworm lines which has originated from distinct geographical areas and which were exposed to different types of pathogens.

In order to determine if the sequence modifications identified in the AMP active portion of the four *B. mori* strains might possibly alter the AMP stability or their antimicrobial activity and therefore influence the overall silkworm immune response, a first *in silico* analysis was conducted on peptide sequences of the variants of Gloverin 1, 2 and 3 (Glv1, Glv2 and Glv3), Cecropin B1 and 2 (CecB1 and CecB1) and Enbocin 1 and 2 (Enb1 and Enb2). Moreover, repeated attempts were made to produce the different AMP isoforms, with the final aim to perform *in vitro* experiments on AMP activities. Since the purification of AMPs from their original source is neither economical nor efficient, both heterologous systems and chemical synthesis were tried for the AMP production (Müller et al, 2014). The Gram-negative *Escherichia coli* and the methanotrophic yeast *Pichia pastoris* were used to produce the AMP variants of Glv1 and Glv2, while two isoforms of CecB2 were chemically synthesized. For these two latter peptide variants Minimal Inhibitory Concentrations (MIC) were determined against the silkworm pathogens *Enterococcus mundtii* and *Serratia marcescens*.

Results

In Silico Analysis of AMP Variants

From the analysis of the 21 AMP genes in the four silkworm lines, 11 genes were found to have non-synonymous substitutions in their coding sequence. Among these, the genes encoding for Gloverin 1, 2 and 3, Cecropin B1 and B2 and Enbocin 1 and 2 showed amino acid substitutions that mapped in the active portion of the peptide (Chapter 2).

To have a preliminary indication of the effects that the detected non-synonymous substitutions might have on overall peptide activity, the AMP variants carrying amino acid substitutions in their active portion were analyzed *in silico*. Three different AMP prediction tools were used: CAMP (Collection of Antimicrobial Peptides, Whagu et al, 2013), APD2 (Antimicrobial Peptide Database 2, Wang et al, 2009) and AMPA (Torrent et al, 2012).

CAMP and APD2 make predictions on several biochemical parameters based on simple calculations on amino acidic sequences and on their homology with characterized AMP sequences and structures deposited in their databases (8164 sequences deposited in CAMP and 2651 in APD2). AMPA evaluates the propensity of each amino acid to be part of an antimicrobial sequence. In the Material and Methods section detailed information of parameters calculated from the AMP prediction tools are reported. Summary information on parameters predicted from this *in silico* analysis is listed in Table 1. Since isoforms 1 and 2 of CecB1 are completely identical to isoforms 2 and 1 of CecB2 respectively, results for CecB1 are omitted. The same applies for Enb1 and 2, which share the same coding sequence and the same isoforms.

Taking into account the output of the three predicting tools, the isoform 3 of CecB2, specific for the European strain was predicted to be more stable (instability index: 47.96) and with a higher propensity to be antimicrobial (Figure 1A), compared to the other two isoforms. Moreover this isoform had a more positive net charge (+8), important factor in the interaction between cationic AMPs and negatively charged bacterial membranes.

As to Enb1, the isoform 2 was predicted to be more soluble and hydrophilic (Boman index: 0.97; hydropathy index: 0.38), more thermostable (aliphatic index: 95.26), and with a higher antimicrobial potential (Figure 1B), while the isoform 1 was suggested to be more hydrophobic and generally more stable (instability index: 21.55).

The isoform 3 of Glv1 was predicted to have a higher predisposition to be antimicrobial (Figure 1C), a less negative net charge (-3), to be more soluble (Boman index: 1.96) and

more stable, and to have a higher number of hydrophobic residues on the same surface (24).

The two variants of Glv2 and 3 showed only little changes in the Boman index and in the instability index, with no differences in the other predicted parameters.

We focused our attention on the different isoforms of Glv1, 2 and Cecropin B2, some of which appeared to be specific for the European strain. A further analysis of their frequency distributions performed with the methodologies reported in Chapter 2 and conducted on a wider sample population (60 individuals), revealed that the European line possessed the Glv1-iso3 (f = 0.52) and Glv2-iso1 (f = 0.48) alleles at higher frequencies in comparison to all the other strains (Indian and Japanese: f (Glv1-iso1) = 1; Chinese: f (Glv1-iso1) = 0.58; f (Glv1-iso2) = 0.35; f (Glv1-iso3) = 0.07). In addition it resulted monomorphic for the CecB2-iso3 allele (f = 1, evaluated on 10 individuals). Therefore these variants were further analyzed as good candidates for a differential antimicrobial activity.

AMP	Length (active portion)	Iso.	Amino acid substitutions	Strains				Net charge	Boman Index (Kcal/ mol)	Aliphatic Index	Instability Index	Hydro-pathy	N° hydroph. res. on same surface
				I	C	J	E						
Cecropin B2	35 aa	1	**38:Gly 53:Glu**	+	+	+		+7	1.45	100.27	61.88	-0.24	12
		2	**38:Ser 53:Glu**	+				+7	1.57	100.27	78.96	-0.25	12
		3	**38:Gly 53:Gln**				+	+8	1.42	100.27	47.96	-0.24	12
Enbocin 1	37 aa (22-58)	1	**25:Phe 51:Gly 54:Ala 55:Ala**	+	+		+	+ 1	0.79	87.63	21.55	0.41	12
		2	**25:Ile 51:Ala 54:Thr 55:Ser**		+	+	+	+ 1	0.97	95.26	41.53	0.38	12
Gloverin 1	135 aa (44-178)	1	**54:Lys 58:Gly**	+	+	+	+	-4	1.84	62.89	15.33	-0.61	23
		2	**54:Arg 58:Gly**		+			-4	1.91	62.89	15.41	-0.62	23
		3	**54:Lys 58:Arg**				+	-3	1.96	62.89	12.88	-0.64	24
Gloverin 2	131 aa (43-173)	1	**74:Lys**	+			+	0	2.11	55.11	23.34	-0.80	18
		2	**74:Arg**		+	+	+	0	2.18	55.11	21.53	-0.80	18
Gloverin 3	131 aa (42-172)	1	**49:Arg**	+	+	+	+	-1	2.24	58.85	23.59	-0.75	21
		2	**49:Lys**		+	+	+	-1	2.17	58.85	26.08	-0.75	21

Table 1. *In silico* analysis of the AMP isoforms with modification in the active portion of the peptide. For each AMP the following information is indicated: length of the active portion of the peptide, with indication of the starting and final residues that compose the mature portion; progressive number of isoforms identified at protein level; modified residues that characterize each isoform (only modified residues that map in the active portion of the peptide are shown); strain in which each isoform is present (I: Indian, C: Chinese, J: Japanese, E: European); net charge; Boman index; aliphatic index; instability index hydropathy; number of residues on the same surface. See text for explanation of these parameters.

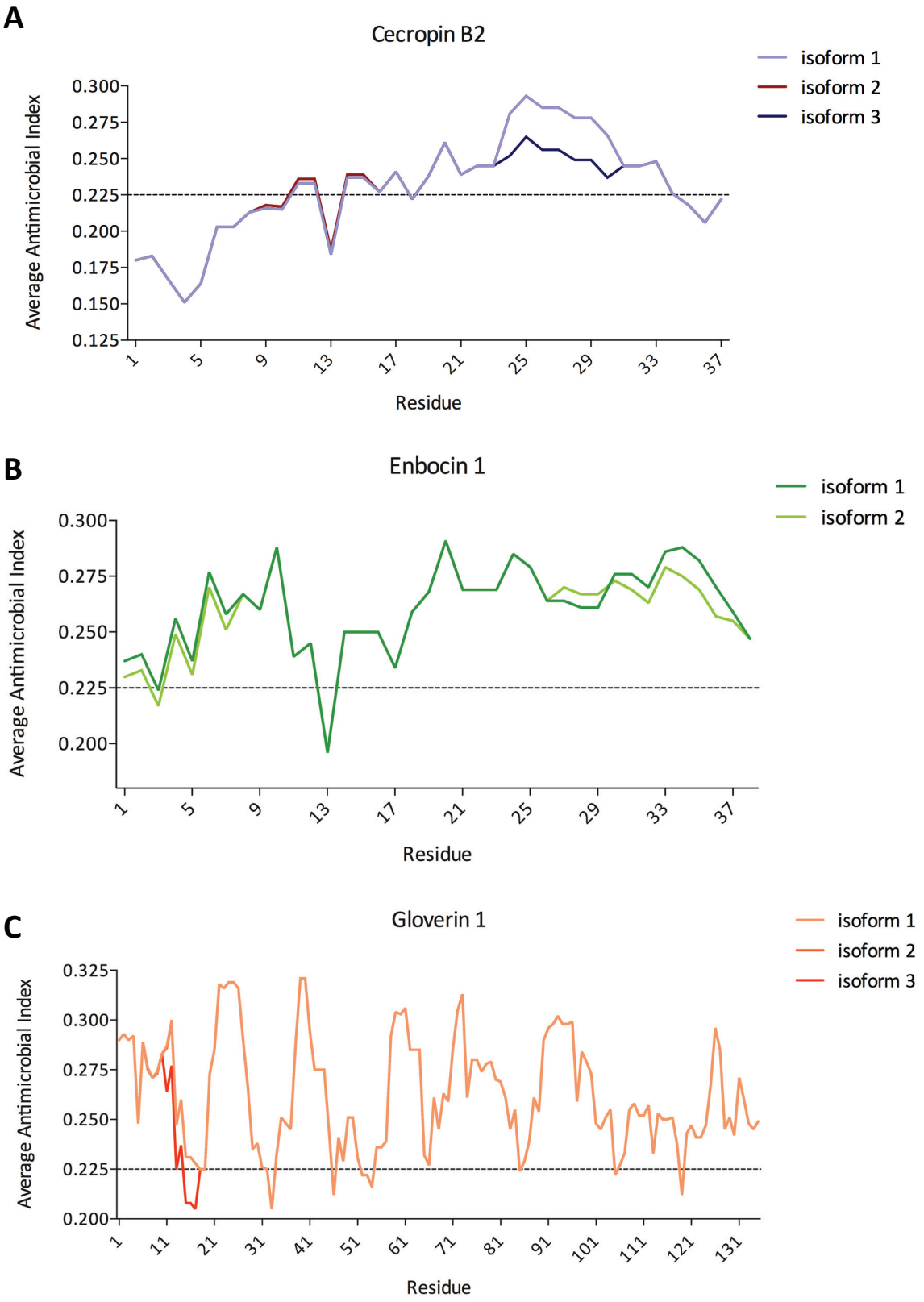

Figure 1. Average antimicrobial indexes calculated with AMPA. Only results for peptides showing a modification in the antimicrobial index are reported. For each residue (x-axis) the antimicrobial index (y-axis) is plotted. Threshold value for significant antimicrobial index was set at 0.225 (dotted line). **A**: Cecropin B2; **B**: Enbocin 1; **C**: Gloverin 1.

Production of AMP Variants Using *E. coli* and pETM-22

The cDNAs coding for the active portion of the isoform 2 and 3 of Glv1 and the isoform 1 and 2 of Glv2 were successfully cloned in the pETM-22 vector, under the control of the T7 RNA Polymerase promoter and in frame with the gene of Thioredoxin A (TrxA), the six Histidine (6xHis) tag and the 3C proteolytic site (Figure 2). TrxA is a globular protein which should mask the AMP activity and solubilize the entire fusion protein. The release of the native AMP is made possible by the 3C site specific for the Human Rhinovirus (HRV)-3C Protease. The theoretical molecular weights of both Glv1 and Glv2 fusion proteins were calculated with the Expasy pI/Mw tool (http://web.expasy.org/compute_pi/) and were found to be around 28 KDa, while native Glv1 and GLV2 should weight about 14 KDa.

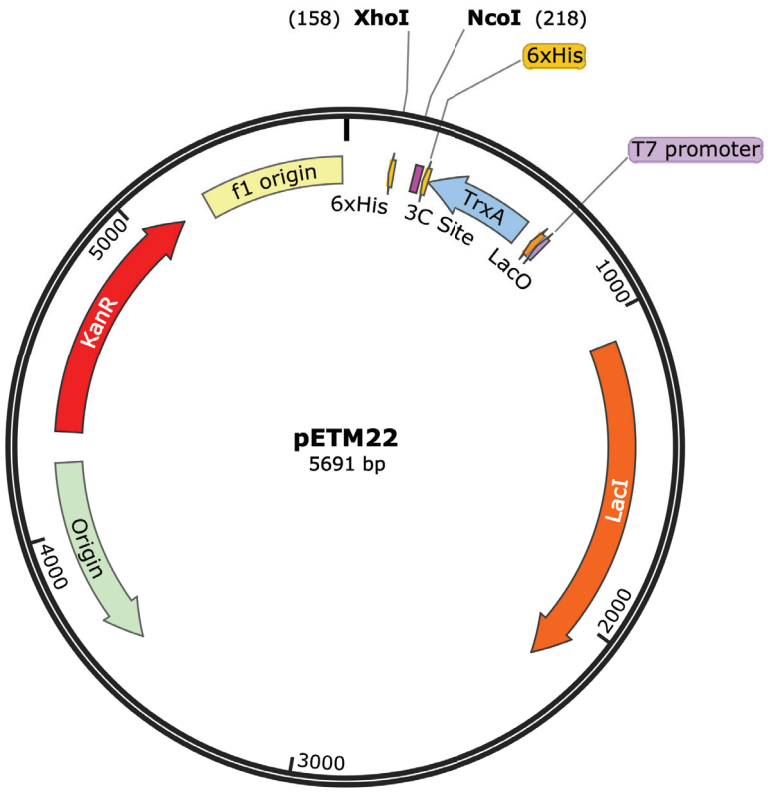

Figure 2. pETM-22 sequence map. The AMP sequences were cloned in the pETM-22 vector, using *Xho*I and *Nco*I restriction sites. The cloned sequences were under the control of the IPTG-inducible T7 RNA Polymerase promoter and in frame with the gene of Thioredoxin A (TrxA), the six Histidine (6xHis) tag and the 3C proteolytic site. TrxA is a globular protein which should mask the AMP activity and solubilize the entire fusion protein. The release of the native AMP is made possible by the 3C site specific for the Human Rhinovirus (HRV)-3C Protease. The His tag permit the affinity purification with Ni^{2+} charged resins.

E. coli Rosetta Strain

Small-Scale Protein Induction

The *E. coli* Rosetta strain was transformed with the four constructs and small-scale induction experiments were performed. This particular strain co-expresses tRNAs for rare *E. coli* codons which are common in eukaryotic translational systems. Moreover it carries the gene for the T7 RNA Polymerase, which allows a very efficient transcription of genes under the control of the T7 RNA Polymerase promoter. The transcription of the recombinant proteins was induced when the *E. coli* transformed cultures showed an OD_{600} of 0.6 adding 0.1 mM IPTG. *E. coli* cultures were then grown for at least 8 h at 30°C. Cell lysates collected at different time-points were analyzed with both SDS-PAGE and Western-blot analysis using an anti-His tag antibody to detect recombinant proteins (Figure 3). A significant induction of the target protein was observed for Glv1-iso2 (Figure 3A-B) and Glv2-iso1 (Figure 3E-F), with small amounts of recombinant protein produced also before induction and larger amounts produced between 1-8 h. A lower but still clearly detectable expression of Glv1-iso3 (Figure 3C-D) was observed. For Glv2-iso2, only small amounts of recombinant protein (Figure 3G-H) were detected with Western-blot. Aspecific low (~12 KDa) and high (> 40 KDa) Western-blot signals were observed for all the tested cultures.

Large-Scale Protein Induction and Purification

Largescale experiments were conducted setting up a 1 L culture of *E. coli* Rosetta expressing Glv2-iso1. This particular isoform was selected for the large-scale trials because of the high yields obtained in the small-scale pilot experiments. The cell-lysate was loaded into a Ni^{2+} charged column, for which the six Histidine tag had a high affinity. The detachment of the His-tagged protein from Ni^{2+} ions was carried out with imidazole, which bounds more efficiently to the Ni^{2+} column than His-tagged proteins. The first eluted fraction (E1) mainly contained the Glv2 fusion protein (Figure 4A). However, aspecific peptides carrying Histidines stretches and weighting about 12 and 60 KDa were also present in this E1 fraction (Figure 4B). The purified Glv2-iso1 was then digested with the HRV-3C Protease, to release the native Glv2-iso1 from the TrxA-6xHis fragment. This protease also had a 6xHis tag, therefore it should be retained in the Ni^{2+} column together with the TrxA-6xHis fragment. Then, the digestion was further purified by affinity chromatography and both the flow-through and the eluted

fractions were loaded in two different amounts in 12% acrylamide gels for SDS-PAGE (Figure 4A) and Western-blot (Figure 4B). The flow-through fraction (Figures 4A and B, D1 and D2 lanes) should include the native Glv2-iso1, while the eluted part should contain the TrxA-6xHis fragment and the HRV-3C Protease. However in both fractions the fusion protein and the Protease signals were detected, suggesting that the proteolysis reaction was not complete and that the purification step did not efficiently separate the Glv2-iso1 from the TrxA-6xHis fragment and the HRV-3C Protease.

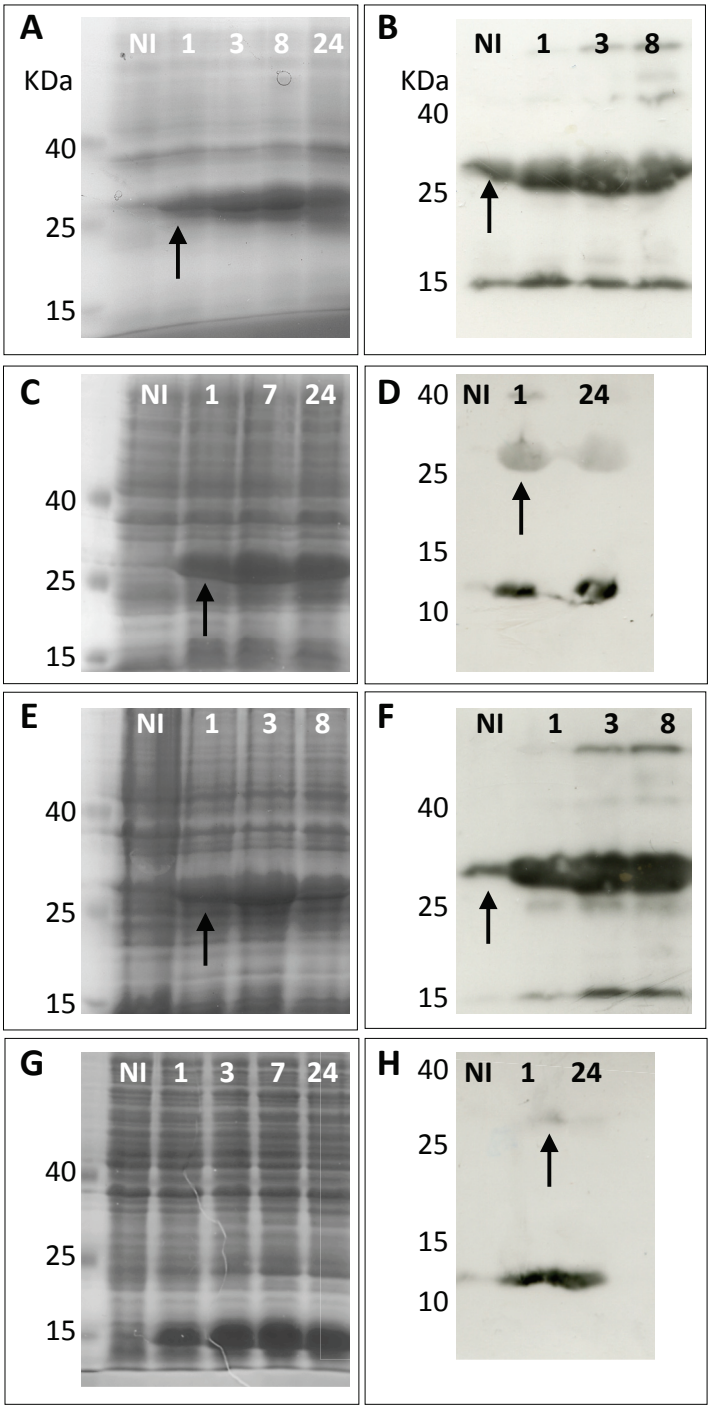

Figure 3. Small-scale protein induction using pETM-22 and *E. coli* Rosetta. Bacterial cultures (30 mL) were grown until an OD_{600} of 0.6. The transcription of the recombinant protein was induced with 0.1 mM IPTG. Cells were grown for 24 h at 37°C at 250 rpm. Small aliquots of bacterial cultures were sampled at different time-points (0, 1, 3, 7, 8, 24h) and loaded into 12% acrylamide gel for SDS-PAGE (**A-C-E-G)** or anti-His Western-blot analysis (**B-D-F-H**). *E. coli* Rosetta expressing pETM-22-Glv1-iso2 (**A-B**), pETM-22-Glv1-iso3 (**C-D**), pETM-22-Glv2-iso1 (**E-F**) and pETM-22-Glv2-iso2 (**G-H**). Black arrows indicate the recombinant induced protein; NI: not induced.

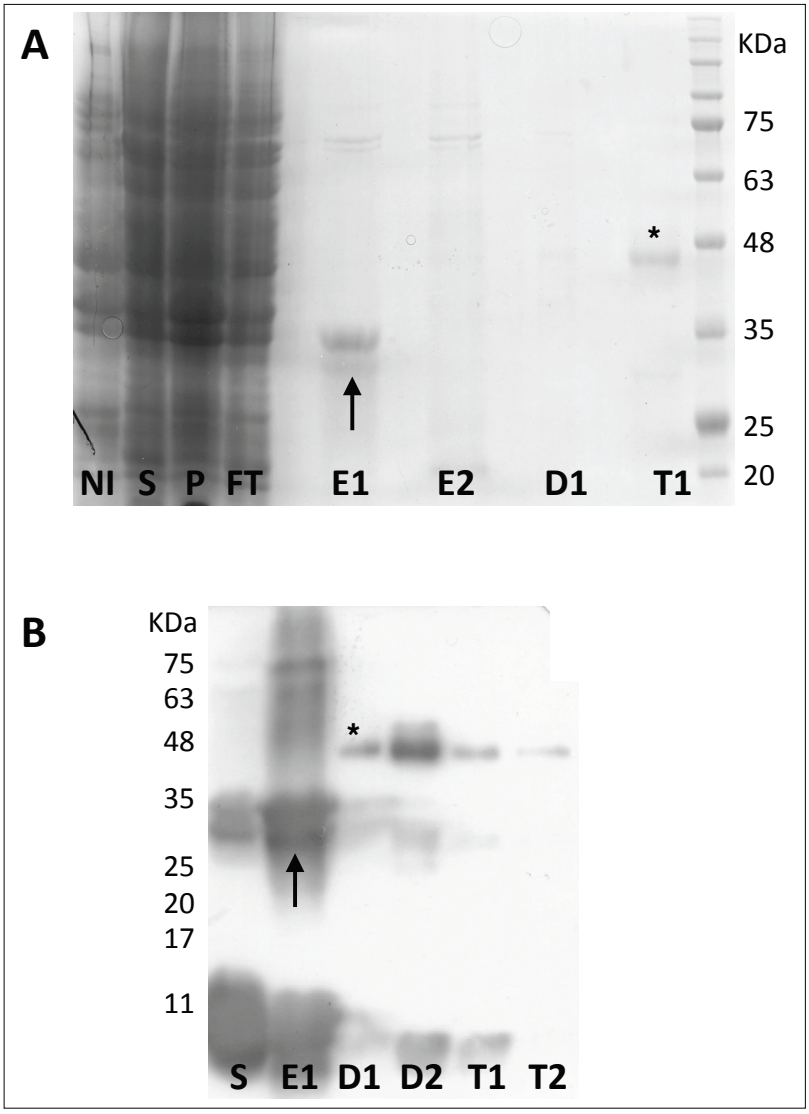

Figure 4. High-scale Glv2-iso1 induction and purification using pETM-22 and *E. coli* Rosetta strain. Bacterial culture (1 L) was grown until an OD_{600} of 0.6. The transcription of the recombinant protein was induced with 0.1 mM IPTG. Cells were grown for 16 h at 30°C at 250 rpm. The cell-lysate was purified by affinity chromatography using a Ni^{2+} resin. The TrxA-6xHis portion was removed from the fusion protein through proteolysis with 2 Units of HRV-3C Protease at 4°C for 24 h. The product of the digestion was loaded into the Ni^{2+} column. The flow through should contain the Glv2-iso1 protein, while the retained portion should have both TrxA-6xHis fragment and 6xHis-containing HRV-3C Protease. **A**: 12% SDS-PAGE; NI: not induced; S: supernatant after cell lysis and centrifugation; P: pellet after cell lysis and centrifugation; FT: flow-through; E1: first elution; E2: second elution; D1: flow-through after digestion; T1: TrxA-6xHis fragment and HRV-3C Protease retained in the column. **B**: Western-blot on 12% acrylamide gel with anti-His tag antibody; S: supernatant after cell lysis and centrifugation; E1: first elution; D1: flow-through after digestion; D2: flow-through after digestion (double amount loaded); T1: TrxA-6xHis fragment and HRV-3C Protease retained in the column after digestion; T2: TrxA-6xHis fragment and HRV-3C Protease retained in the column after digestion (double amount loaded). Black arrows indicate the recombinant induced protein, black asterisks indicate the 6xHis-containing HRV-3C Protease.

E. coli Artic Strain

Small-Scale Protein induction

Since the low efficiency of the proteolytic reaction might have been due to some mis-folding in the fusion protein and to a further low exposure of the 3C site to the HRV-3C Protease, the *E. coli* Artic strain was used for the expression of the recombinant protein through the pETM-22 construct. This strain possessed all the features of the Rosetta strain, but it also carried an inducible Chaperonin useful for the correct tridimensional conformation of exogenous proteins at low temperatures. The procedure for the expression induction was identical to that used for the Rosetta strain, with the only exception that the growth after IPTG induction took place at 12°C rather than at 30°C, to allow the correct Chaperonin activity.

Small-scale induction experiments were performed on Glv1-iso2, Glv1-iso3 and Glv2-iso1, with good results for both isoforms of Glv1 (Figure 5). On the contrary, Glv2-iso1 was not successfully induced at this level: in the SDS-PAGE, only bands corresponding to the induced Chaperonin were clearly detected (Figure 5C), while the Western-blot hybridized with the anti-His tag antibody showed a strong signal only at ~11 KDa (Figure 5D).

Large-Scale Protein Induction and Purification

Large-scale experiments were then carried out on Glv1-iso3, because of the high yields obtained in the small-scale pilot experiments. After 10 days of induction at 12°C, the bacterial cells grown from this 1L culture were disrupted with French press and the cell-lysate was purified using the Ni^{2+} charged column (Figure 6A-B). The eluted E1-E5 fractions contained predominantly the Glv1-iso3 fusion protein and were therefore pooled. In order to remove the small aspecific peptides that were eluted with the target protein, an additional gel filtration chromatographic step was performed (Figure 6C-D). Gel filtration allows to separate peptides on the basis of their dimension, with high molecular weight proteins released before small peptides or fragments. The fractions containing the fusion protein were pooled (Figure 6C), concentrated and loaded into a gel, in order to assess the absence of small amounts of contaminant peptides (Figure 6E, lane 1). Even if Glv1-iso 3 was not completely pure, the fusion protein was digested in different proportions with HRV-3C Protease to determine the best reaction conditions. Using 2 Units of Protease, 130, 65 and 6 µg of protein were

digested at 4°C for 72 h, obtaining the completely release of the native Glv1-iso3 protein only in the last reaction (Figure 6E, lane 2, 3 and 4). The digestion was purified by affinity chromatography and both the flow-through (Figure 6F, lane 3) and the eluted fractions (Figure 6F, lane 4) were loaded into 4-12% acrylamide gels for SDS-PAGE. Both these fractions, however, showed the HRV-3C Protease, the TrxA-6xHis fragment and the native Glv1-iso3, indicating the low efficiency and the low yield of this expression and purification system.

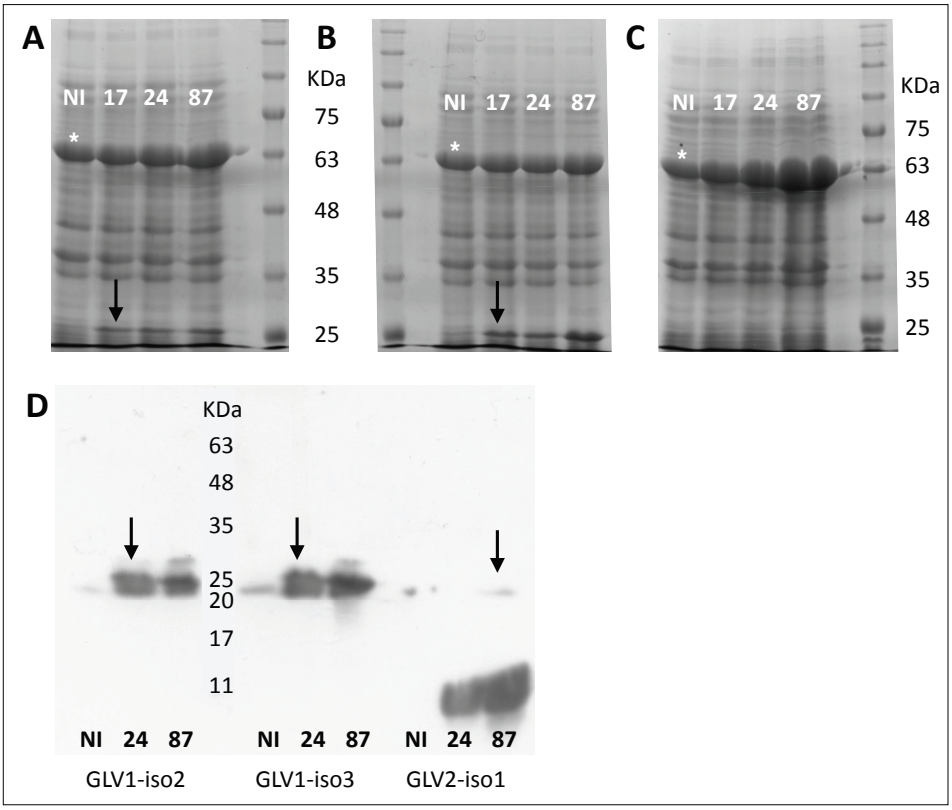

Figure 5. Small-scale protein induction using pETM-22 and *E. coli* Artic strain. Bacterial cultures (30 mL) were grown until an OD_{600} of 0.6. The transcription of the recombinant protein was induced with 0.1 mM IPTG. Cells were grown for 87 h at 12°C at 250 rpm. Small aliquots of bacterial cultures were sampled at different time-points (0, 17, 3, 7, 8, 24h) and loaded into 12% acrylamide gel for SDS-PAGE (**A-B-C**) or anti-His Western-blot analysis (**D**). **A-B-C:** SDS-PAGE on total cell lysates of *E. coli* Artic expressing pETM-22-Glv1-iso2 (**A**), pETM-22-Glv1-iso3 (**B**), pETM-22-Glv2-iso1 (**C**). D: Western-blot with anti-His antibody on cell extracts of *E. coli* Artic expressing the three recombinant proteins. Black arrows indicate the recombinant induced protein, white asterisks indicate the co-induced Chaperonin; NI: not induced.

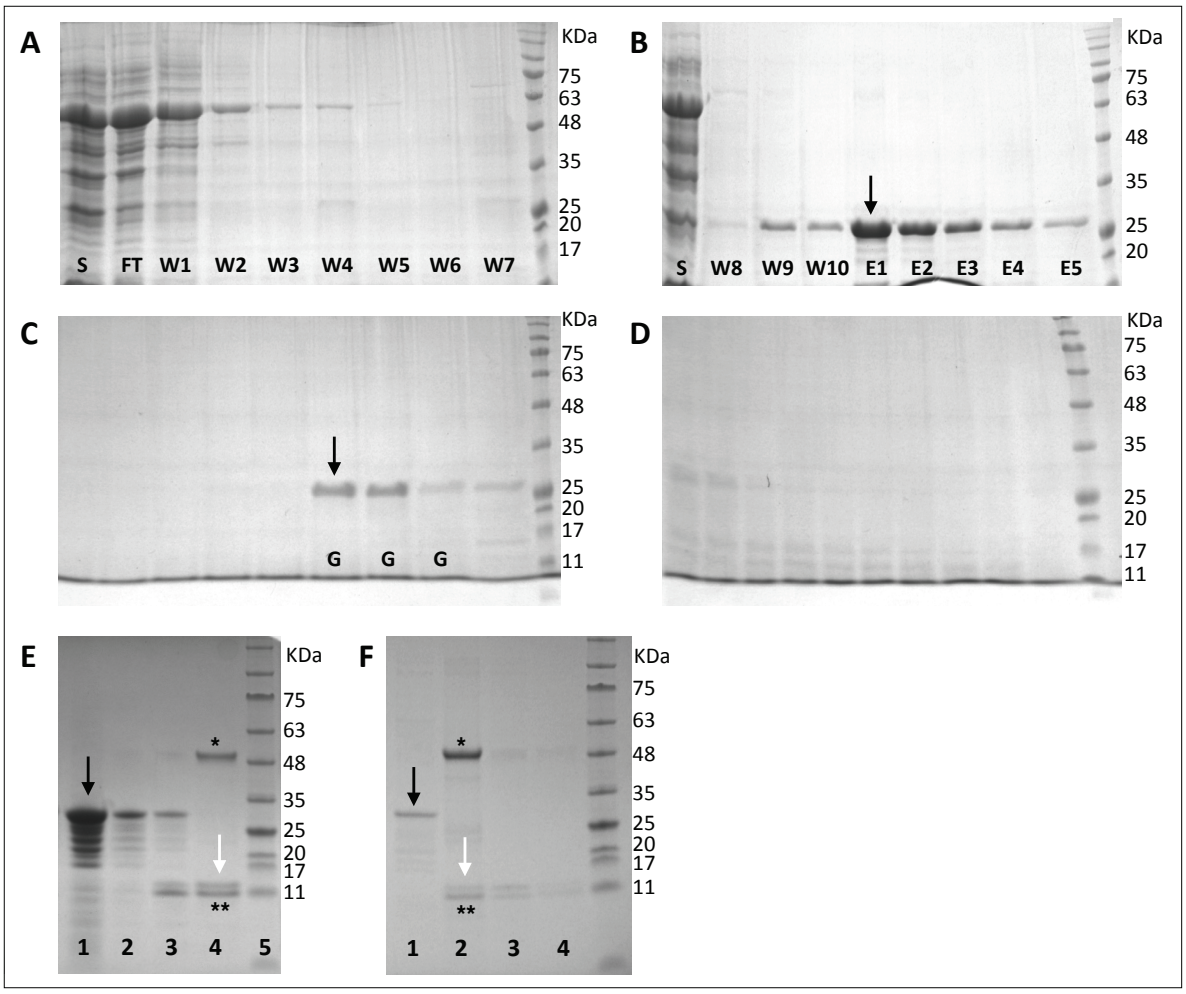

Figure 6. High-scale Glv1-iso3 induction and purification using pETM-22 and *E. coli* Artic strain. Bacterial culture (1 L) was grown until an OD_{600} of 0.6. The transcription of the recombinant protein was induced with 0.1 mM IPTG. Cells were grown for 240 h at 12°C at 250 rpm. The cell-lysate was purified by affinity chromatography using a Ni^{2+} resin (**A-B**). The eluted protein was further purified by gel filtration using a FPLC system and a 16/600 Superdex column (**C-D**). The TrxA-6xHis portion was removed from the fusion protein through proteolysis with 2 Units of HRV-3C Protease at 4°C for 72 h (**E**). The product of the digestion was loaded into the Ni^{2+} column. The flow through should contain the Glv2-iso2 protein, while the retained portion should have both TrxA-6xHis fragment and 6xHis-containing HRV-3C Protease (**F**). **A-B**: 12% SDS-PAGE of the fractions recovered after Ni^{2+} affinity purification; S: supernatant after cell lysis and centrifugation; FT: flow-through; W1-W6: column washes with Equilibration Buffer; W7-W8: column washes with Equilibration Buffer and 10 mM imidazole; W9-W10: column washes with Equilibration Buffer and 25 mM imidazole; E1-E5: elutions. **C-D**: 12% SDS-PAGE of the fractions recovered after gel filtration; G: pooled fractions containing Glv1-iso3. **E**: 4-12% SDS-PAGE on digestion reactions carried out with different proportions between Glv1-iso3 and HRV-3C Protease; 1: purified and concentred Glv1-iso3; 2: digestion with 2 Units of HRV-3C Protease and 130 µg of Glv1-iso3; 3: digestion with 2 Units of HRV-3C Protease and 65 µg of Glv1-iso3; 4: digestion with 2 Units of HRV-3C Protease and 6 µg of Glv1-iso3. **F**: 4-12% SDS-PAGE on digestion reactions purified by affinity chromatography; 1: purified Glv1-iso3; 2: digestion HRV-3C Protease; 3: flow-through after the digestion; 4: TrxA-6xHis fragment and HRV-3C Protease retained in the column after digestion. Black arrows indicate recombinant Glv1-iso3, single black asterisks indicate the 6xHis-containing HRV-3C Protease, double black asterisks indicate the TrxA-6xHis fragment; white arrows indicate the released native Glv1-iso3.

Production of AMP Variants Using *P. pastoris* and pPICZα

The active portion nucleotide sequences of Glv1-iso1, -iso2 and -iso3 and of Glv2-iso1 and -iso2 were successfully cloned in the pPICZα vector, under the control of the methanol induced Alcohol Oxidase 1 (AOX1) promoter and in frame with the signal sequence of the *Saccaromyces cerevisiae* α-Factor which should direct the secretion of the target protein from the yeast cells into the culture medium (Figure 7). Between the α-Factor signal and the AMP cloned cDNAs, two sites for two different *P. pastoris* proteases, Kex2 and Ste13, were present, in order to cleave the α-Factor signal and to release the native target protein. To limit the number of additional amino acids, only a six-Histidine tag coding sequence and two stop codons were added via PCR at the 3' of the AMP gene, and therefore the C-Myc and 6xHis tags originally present in the plasmid were not used. The predicted molecular weight of the Glv1 secreted in the culture media by *P. pastoris* should be similar to that of the native protein, about 14 KDa.

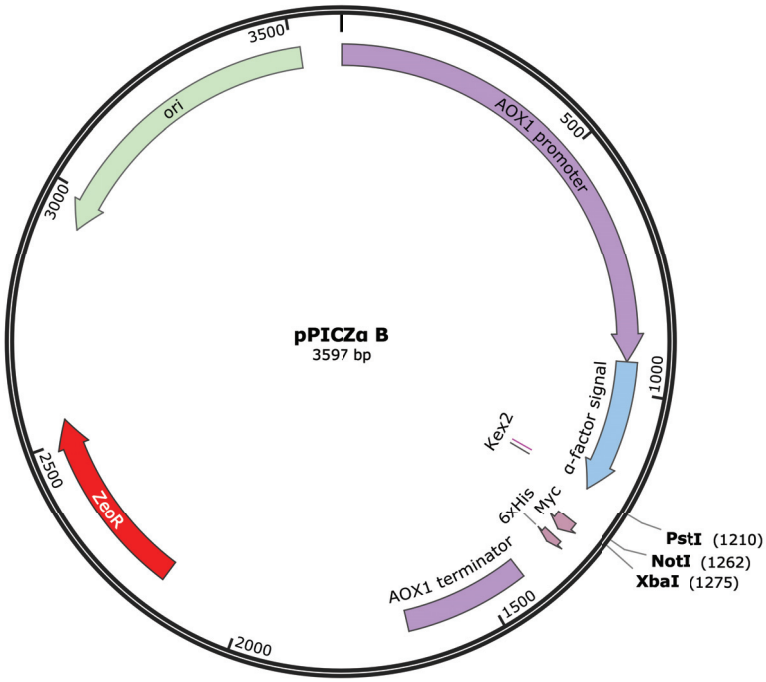

Figure 7. pPICZα sequence map. The AMP sequences were cloned in the pPICZα vector, using *Pst*I or *Not*I and *Xba*I restriction sites, under the control of the methanol induced AOX1 promoter and in frame with the signal sequence of the *Saccaromyces cerevisiae* α-Factor which should direct the secretion of the target protein. Between the α-Factor signal and the AMP genes, two sites for two different *P. pastoris* proteases, Kex2 and Ste13, were present, in order to cleave the α-Factor signal and to release the native target protein. To reduce the number of additional amino acids to a minimum, a six-Histidine tag and two stop codons were added via PCR to the 3' of the cloned AMP gene, and thus the C-Myc and 6xHis tags originally present in the plasmid, were not used.

Small-Scale Protein Induction

Small scale experiments were carried out on Glv1-iso1. In order to compare the productivity of different clones, five independent *P. pastoris* colonies were grown in BMGY medium for 24 h and then induced with methanol. Fractions of the supernatants were loaded into 12% acrylamide gels for SDS-PAGE, but no bands were visible (data not shown). Only with anti-His tag Western-blotting the productivity of the five clones was detectable and was found to be very variable among different colonies (Figure 8A). The clone number 4 was selected for the large-scale production for its higher protein yield (Figure 8A, lane 4).

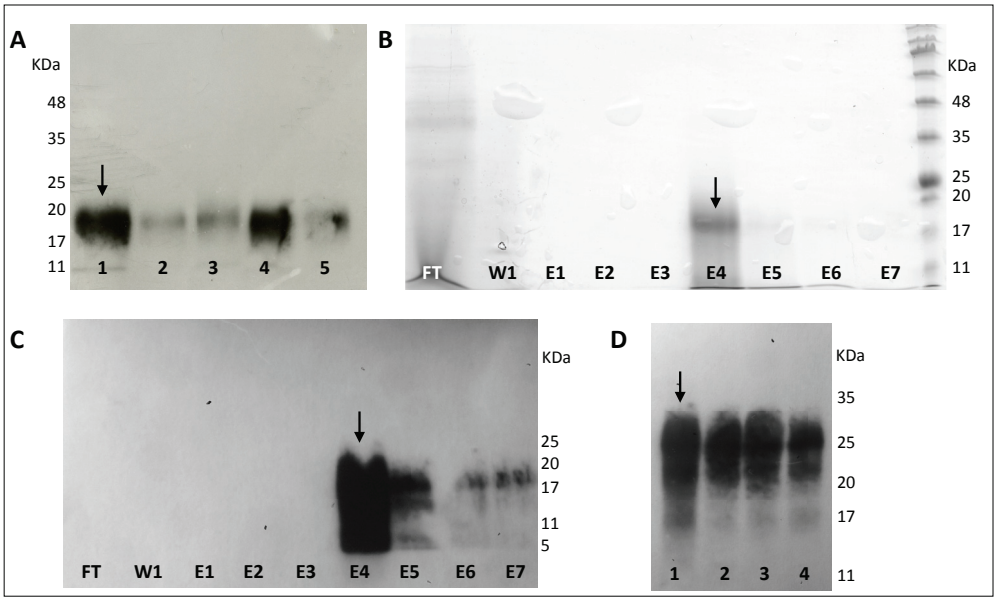

Figure 8. Small- and high-scale Glv1-iso1 induction and purification using pPICZα and *P. pastoris* X-33 strain. Five independent *P. pastoris* clones transformed with the linearized pPICZα-Glv1-iso1 were cultured in 2 mL of BMGY medium for 24 h at 28°C. The transcription of the recombinant protein was induced by removing the culture media and growing yeasts on methanol-containing BMMY medium. Cells were grown for 42 h at 28°C at 250 rpm. The cell-free supernatant was loaded into 12% acrylamide gel for Western-blot (**A**). The most productive clone was grown in BMGY overnight and then in BMMY for 42 h at 28°C and 250 rpm. After precipitation with ammonium sulphate the culture supernatant was purified by affinity chromatography using a Ni^{2+} resin (**B-C**). To assess if the higher observed molecular weight of the recombinant protein was due to hyperglycosylation, the purified Glv1-iso1 was deglycosylated with PNGase and O-Glycosylase (**D**). **A**: Western-blot on 12% acrylamide gel with anti-His tag antibody on the supernatant of small-scale cultures of five independent *P. pastoris* clones transformed with the linearized pPICZα-Glv1-iso1. Clone 4 was selected for the high-scale protein production. **B-C**: 12% SDS-PAGE and anti-His tag Western-blot of the fractions recovered after Ni^{2+} affinity purification; FT: flow-through; W1: first column wash; E1-E7: elutions. D: Western-blot on 12% acrylamide gel with anti-His tag antibody on Glv1-iso1 (1) deglycosylation reactions with PNGase F (2), O-Glysosydase (3) and both PNGase F and O-Glysosydase (4).

Large-Scale Protein Induction and Purification

Clone number 4 was grown in 250 mL of BMGY overnight and then in 2 L of methanol-containing medium BMMY for 42 h at 28°C and 250 rpm. The whole protein content of the culture supernatant was precipitated with ammonium sulphate, resuspended in Phosphate Buffer 0.1 M and purified by affinity chromatography using the Ni^{2+} resin. A fraction containing the majority of the recombinant Glv1-iso1 was eluted (Figure 8B-C, E4).

Protein Deglycosylation

The resulting purified protein showed a higher molecular weight than predicted (> 17 KDa instead of 14 kDa). Because *P. pastoris* is known to hyperglycosilate proteins and because glucidic chains increase the protein molecular weight, different trials of deglycosylation were carried out with PNGase F, O-Glycosylase or with both enzymes, in both denaturing and native reaction conditions. However, no differences in the weight of Glv1-iso1 were found among the diverse reactions (Figure 8D). The molecular weight of the recombinant protein was also confirmed by 6M Urea denaturing gel (data not shown).

Glv1-iso1 Antimicrobial Activity Test

The antimicrobial activity of recombinant Glv1-iso1 was tested against different bacteria, to assess if the *P. pastoris* heterologous system could be a valid method to produce high amounts of active AMPs. Glv1-iso1 at an approximative final concentration of 2 µM was added to *E. mundtii*, *S. marcescens*, *E.coli* and *S. aureus* cultures and the OD_{600} was measured at different time-points to monitor the microbial growth. The Glv1-iso1 tested concentration was not sufficient to prevent bacterial growth, but it had however an anti-proliferative effect on *S. marcescens*, *S. aureus* and, to a lesser degree, on *E. coli* (Figure 9).

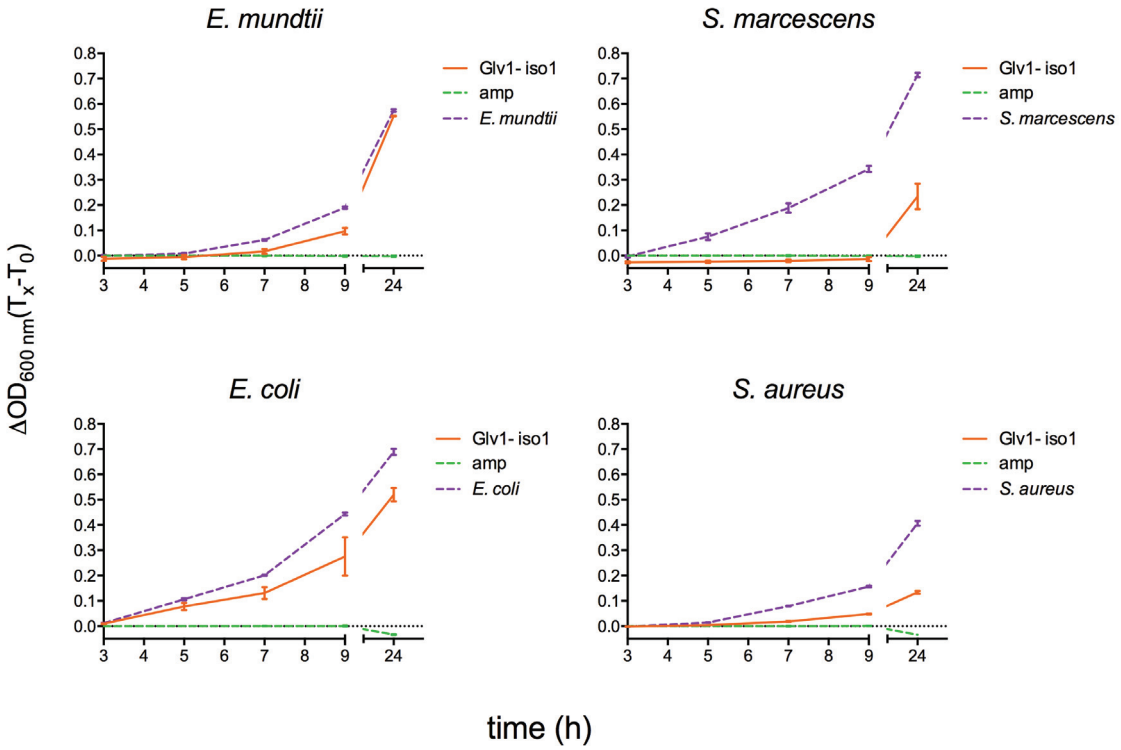

Figure 9. Glv1-iso1 antimicrobial activity against *E. mundtii*, *S. marcescens*, *E. coli* and *S. aureus*. Glv1-iso1 was added at a final concentration of 2 µM to bacterial cultures (0.5 * 10^5 CFU/mL) and the optical density at 600 nm was measured to monitor the microbial growth. The OD_{600} measured at time zero was subtracted from the OD_{600} of each time-point and the resulting ΔOD_{600} values were plotted against time (mean ± SEM).

Minimal Inhibitory Concentration Assay of two Variants of CecB2

The Minimal Inhibitory Concentration (MIC) value was assessed for isoform 1 and isoform 3 of CecB2 against *E. mundtii* and *S. marcescens*. Serial dilutions of the two peptide suspensions were added to bacterial cultures and the optical density at 600 nm was measured to monitor the microbial growth. The MIC value was represented by the lowest concentration that totally inhibited the bacterial growth after 24 h.

As for *E. mundtii*, CecB2-iso1 MIC value corresponded to the 0.8 µM dilution, since at 0.4 µM a microbial growth was still observed (Figure 10A). For CecB2-iso3, the MIC value was lower and corresponded to 0.4 µM. At a final concentration of 0.2 and 0.1 µM, both peptides did not prevent bacterial growth, even if isoform 3 had a qualitative higher anti-proliferative effect on the first 9 h when compared to isoform 1.

The two peptides tested against *S. marcescens* did not show any effect on the microbial growth (Figure 10B). To point out a parallelism with *E. mundtii*, only peptide concentration values between 0.1 and 0.8 µM are shown, but any relevant inhibitory effect was found also at 20 µM (data not shown).

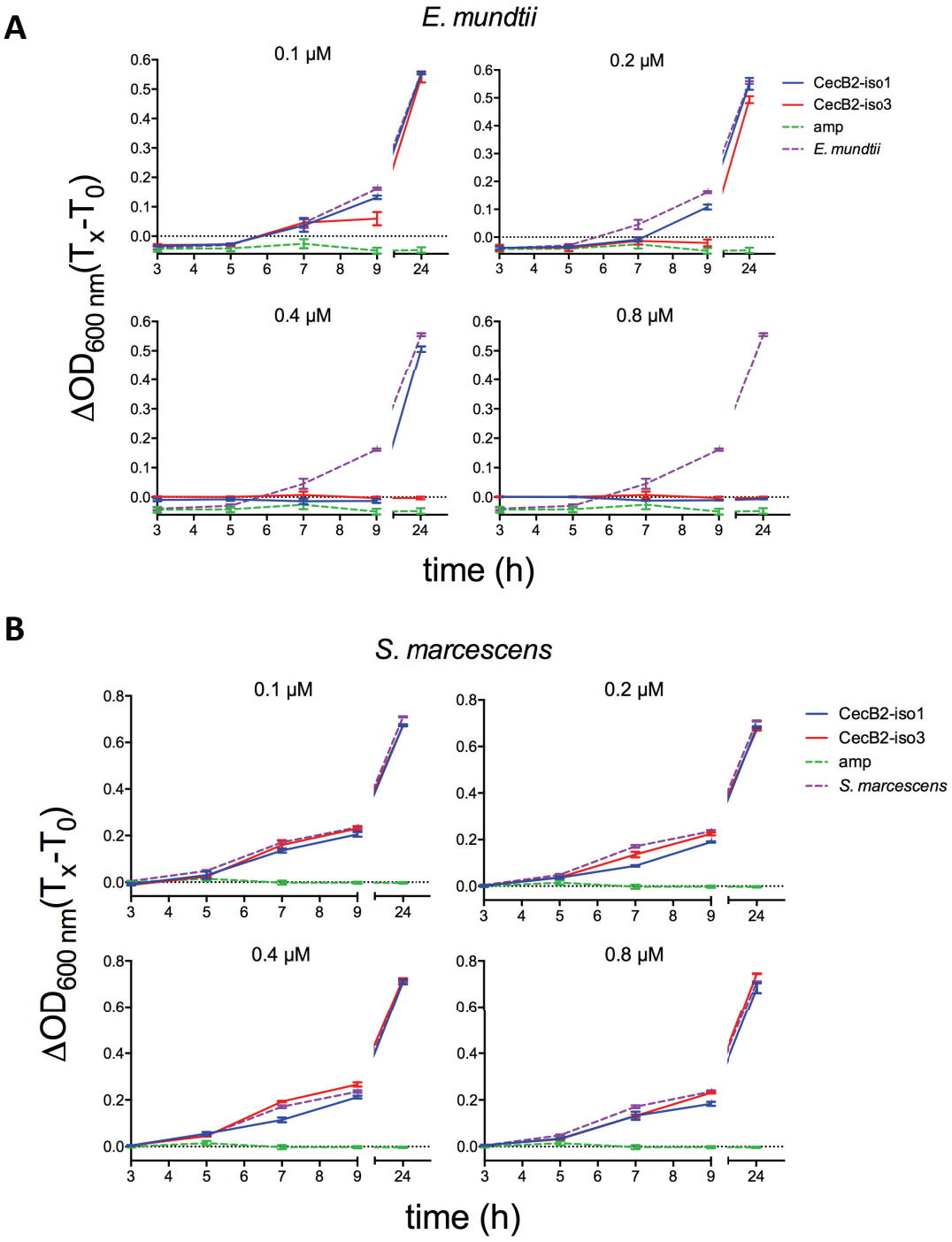

Figure 10. MIC for CecB2-iso1 and -iso3 against *E. mundtii* (A) and *S. marcescens* (B). Serial dilutions of the two peptide suspensions were added to bacterial cultures (0.5 * 10^5 CFU/mL) and the optical density at 600 nm was measured to monitor the microbial growth. The OD_{600} measured at time zero was subtracted from the OD_{600} of each time-point and the resulting ΔOD_{600} values were plotted against time (mean ± SEM).

Discussion

The *in silico* analysis revealed that the identified non-synonymous substitutions found in the *B. mori* AMPs might have a direct influence on their antimicrobial activity or stability. In particular, CecB2-iso3, Enb1-iso2 and Glv1-iso3 showed the highest propensity to be antimicrobial when compared to their respective variants. Moreover, the different isoforms of Glv1, Glv2 and Glv3 showed the Lysine-Arginine modification that has been already reported to alter the peptide antimicrobial activity of other AMPs, like the human Lactoferrin (Velliyagounder et al, 2003) and the red sea bream Chrysophsin (Iijima et al, 2003). In particular, the Lactoferrin Lysine isoform was found to have a higher antimicrobial activity against *Streptococcus mutants,* frequently associated to dental caries and the presence of this Lysine isoform was found to be associated to a low risk to develop dental caries (Fine et al, 2013).

Since Glv1, Glv2, and CecB2 isoforms were found to be present with different frequencies among the four *B. mori* strains, the possibility that the detected isoforms might have differential antimicrobial activity and therefore contribute to the strain-specific sensitivity was investigated. Different strategies for peptide production were taken into consideration, evaluating which was the most convenient for each peptide. The sizes of all mature Glv1 and Glv2 isoforms range between 131 and 135 residues, therefore the chemical synthesis does not represent an appropriate or economical strategy. For this reason, we attempted to produce them using heterologous expression systems. Since mature CecB2 variants are only 37 residues long, the chemical synthesis was chosen to obtain two isoforms using a custom peptide synthesis service (Genescript, USA).

The simplest prokaryotic system, *E. coli*, was first used to produce the Glv1 and Glv2 isoforms. Peptide production with prokaryotic organisms like bacteria, in general, lead to the highest yields and is the more economical option (Müller et al, 2014). However, the different codon usage between Prokaryotes and Eukaryotes and the absence of the post-translational machinery in bacteria represent a limit for this strategy. Moreover, one of the main problems occurring in the production of molecules with an intrinsic antimicrobial activity using bacteria is the potential damage that the produced peptides may cause to host cells, which might affect the overall protein yield. To overcome these problems, bacterial strains expressing rare prokaryotic tRNAs were used. The plasmid chosen for the recombinant AMP production had a strictly regulated promoter which controlled the transcription of the target AMP and which was activated only after the growth of a sufficient bacterial biomass. Furthermore, AMPs

were fused to a globular protein, TrxA, which masked and neutralized their activity and which could be removed through a specific proteolytic cleavage.

The results obtained with this strategy were satisfactory considering the yields of AMPs produced: the Rosetta strain showed high levels of recombinant protein production. However some critical steps induced us to change strategy. In particular, since the His-tag sequence was placed between TrxA and the AMP, also incomplete transcriptional or translational products containing the His-tag but not the AMP, were also purified together with the full-length recombinant protein. Moreover, the proteolytic cleavage necessary to release the AMP from its fusion partner was found to be inefficient. To overcome these problems, the Artic strain co-expressing a Chaperonin was used. The AMP yields obtained with this strain were satisfactory, the amounts of a-specific products was lower and, after an additional gel filtration step, the fusion protein was obtained in good quantities. The removal of the TrxA fusion partner was also obtained, but the limiting step was represented by the final purification of the native AMP.

Therefore we opted for the eukaryotic heterologous system with the methylotrophic yeast *P. pastoris*. The synthesis of proteins using eukaryotic organisms, such as yeasts or insect-cells, show high yields and allow the correct insertion of the majority of post-translational modifications, such as glycosylation or disulfide-bonds (Müller et al, 2014). The plasmid chosen for this system carried the target AMP gene downstream to an inducible promoter and to a secretion signal. Therefore the production of the target protein was activated only after the reaching of a sufficient yeast biomass making it possible to recover the AMP from the culture supernatant. Sufficient amounts of Glv1-iso1 were obtained, but with a higher molecular weight than predicted. In the first instance the possibility of a glycosylation was explored, since *P. pastoris* is known to produce glycosylated proteins and since glucidic chains are known to increase peptide molecular weight. However, after digestion with two different deglycosylases, no differences in the weight of Glv1-iso1 were observed. One hypothesis is that the α-factor secretion signal was not removed from the recombinant AMP: in fact the theoretical molecular weight of Glv1 fused to the α-factor secretion signal is 24 KDa, which is approximately the weight of the obtained protein. When tested against different bacteria, however, the recombinant protein was found to have a biological activity, reducing the growth of *S. marcescens*, *S. aureus* and *E. coli*. These data were only qualitative, since different Glv1-iso1 concentrations were not tested. However they demonstrated that the *P. pastoris* heterologous system could be a valid method for the production of high amounts of active AMPs.

Chemical synthesis was used to produce CecB2-iso1 (which showed a similar predicated antimicrobial activity with respect to -iso2) and -iso3. This strategy is generally quick and does not require particular setting-up. Yields with this production

system are lower than those achieved by heterologous systems, but the purity of the synthesized peptides is often higher (Müller et al, 2014). The majority of the post-translational modifications are not achievable with chemical synthesis, with some exceptions like amidation, which is fundamental for the activities of many AMPs, including Cecropin B, (Callaway et al, 1993).

The two CecB2 isoforms tested against *E. mundtii* showed a small but relevant differential *in vitro* activity. They both inhibited bacterial growth at a final concentration of 0.8 µM, but only isoform 3 was able to suppress *E. mundtii* growth at 0.4 µM, while isoform 1 was not effective at this concentration. At lower peptide amounts, both isoforms were ineffective, even if CecB2-iso3 showed a higher microbial inhibition during the first hours of microbial growth. When tested against *S. marcescens*, the two peptides did not show any effect. Higher peptide amounts should be tested against this bacterium to assess the MIC value for both CecB2 isoforms. These experiments give just a first indication of the differential activities showed by these two isoforms against *E. mundtii* and should be repeated to demonstrate their reproducibility.

Overall, these results suggested that the modifications identified in the active portions of silkworm AMPs could affect their *in vitro* antimicrobial activity and might in some way contribute to the differential sensitivities observed among of the four *B. mori* strains. In fact, CecB2-iso3, which showed a higher activity than CecB2-iso1 against *E. mundtii*, was identified only in the European strain, the more resistant line to this Gram-positive infection. Although the presence of specific AMP alleles should be only one of the possible reasons which explains the differential resistance to microbial exposure of the different *B. mori* strains, it is interesting to mention that the presence of an amino acid polymorphism in *Drosophila* Diptericin was recently found to be highly predictive of resistance to bacterial infections (Unckless et al, 2016).

Materials and Methods

In Silico Analysis of AMP Variants

AMP peptide isoforms which showed modified residues in their active portion were analyzed with three different online tools: CAMP (Collection of Antimicrobial Peptides, Whagu et al, 2013; http://www.camp.bicnirrh.res.in/), APD2 (Antimicrobial Peptide Database 2, Wang et al, 2009; http://aps.unmc.edu/AP/main.php) and AMPA (Torrent et al, 2012; http://tcoffee.crg.cat/apps/ampa/do).

In particular, the following parameters were obtained:

- *net charge*: overall charge of the peptide, particularly important for cationic AMPs which interact with negatively charged bacteria membranes because of their positive charge.
- *Boman index*: it measures the protein-binding potential. It is calculated as the sum of the free energy of the respective side chains for transfer from cyclohexane to water taken from Radzeka and Wolfenden (1988) and divided by the total number of residues in an antimicrobial peptide. A more hydrophobic peptide tends to have a negative index, while a more hydrophilic peptide tends to have a more positive index. The more an AMP is hydrophobic, the more it will be able to interact with microbial membranes, while the more it is hydrophilic, the more it will be soluble.
- *Aliphatic index*: it represents the relative volume occupied by aliphatic side chains. High values indicate increased thermostability. This parameter is particularly important for large AMPs.
- *Instability index*: this parameter estimates the stability of a protein. A protein whose instability index is smaller than 40 is predicted stable, a value above 40 indicates that the protein may be unstable.
- *Hydropathy*: it is the sum of the hydrophaty values of all amino acids, divided by the number of residues in the sequence. Positive values indicate hydrophobic and negative values indicate hydrophilic peptides. As already stated, the hydrophobicity of an AMP determines its ability to interact with microbial membranes, while the hydrophilicity determines its solubility.
- *Number of hydrophobic residues on the same surface*: the interaction of AMPs with microbial membranes is facilitated by peptide amphipathic structures, because charged residues interact with polar phospholipid head groups, while hydrophobic amino acids arrange themselves in the acyl tail core. Therefore, an amphipathic AMP will have a high number of hydrophobic residues on the same surface and will

interact more easily with bacteria membranes. For those AMPs for whose tridimensional structure has not been determined yet, this parameter should be considered preliminary only.

- *Antimicrobial index*: value assigned to each residue that represents the tendency of such amino acids to be found within an AMP sequence. Amino acids with a low antimicrobial index are the most favored to be part of an AMP. The commonly accepted threshold is 0.225, therefore residues with an antimicrobial index lower than 0.225 are considered to be likely to be found within an AMP.

Production of AMP Variants Using *E. coli* and pETM-22

Amplification of *glv1* and *glv2* Genes

To amplify the different active portions of the AMP variants, cDNA samples retrotranscribed from RNA extracted from Indian, Chinese and European larvae were used as templates. For *glv1*, isoform 1, 2 and 3 were amplified respectively from Indian, Chinese and European cDNA samples, while for *glv2*, isoform 1 and 2 were obtained from Indian and Chinese cDNAs.

Amplification reactions were carried out in a total volume of 25 µl, containing 50 ng of cDNA, 0.2 Units of Phusion® High-Fidelity DNA Polymerase (New England BioLabs), 200 µM dNTPs, 300 nM of each primer and the appropriate $MgCl_2$ containing buffer. The PCR cycle comprised an initial denaturing step at 98°C for 3 min, followed by 5 cycles of 98°C for 30 sec, 52°C for 30 sec and 72°C for 40 sec and 35 cycles of 98°C for 30 sec, 62°C for 30 sec and 72°C for 40 sec, with a final elongation step at 72°C for 5 min. Amplicons were checked in 1 % agarose gel. The list of primers used for amplification are listed in Table 2. All forward and reverse primers included, respectively, an *Nco*I and an *Xho*I site, for the directional cloning in the pETM-22 vector. The isoform identity was checked by sequencing.

Gene	Primer name	Sequence (5'->3')	Tm	Amplicon length
glv1	Glv1_NcoI_FOR	TAT**CCATGG**ATATTCACGACTTTGTCACT	5 cycles x 52°C 35 cycles x 62°C	408 bp
	Glv1_XhoI_REV	TAT**CTCGAG**TTACCACTCGTGAGTAATCT		
glv2	Glv2_NcoI_FOR	TAT**CCATGG**ACGTCACTTGGGACAAAC	5 cycles x 52°C 35 cycles x 62°C	396 bp
	Glv2_XhoI_REV	TAT**CTCGAG**TCACCAATCATGGCGGATC		

Table 2. List of primers used for the amplification of *glv 1* and *gl2* genes and the cloning in pETM-22. For each gene, the sequences of both forward and reverse primers, the annealing temperature of primers (Tm) and the length of the amplicon are indicated. In the sequence of each primer, the restriction site used for the directional cloning is indicated in bold.

Plasmid Construction

The pETM-22 plasmid was kindly provided by the Protein Expression and Purification Core Facility of the European Molecular Biology Laboratory (EMBL) of Heidelberg (Germany) on the basis of a Material Transfer agreement. The cDNAs coding the different *glv1* and *2* isoforms were cloned in pETM-22 using the *Nco*I and *Xho*I unique sites, downstream and in frame with the *Thioredoxin A* (TrxA) gene, the six Histidines (6xHis) tag and the 3C site for the Human Rhinovirus (HRV)-3C Protease (Figure 2). In this way, an unique fusion protein made of TrxA, 6xHis, 3C site and the target protein, would be produced. The open reading frame coding for this fusion protein, was under the control of the T7 RNA Polymerase Promoter and Lac operator. Therefore, the transcription of the mRNA encoding the target protein would be possible only in those *E. coli* strains carrying the gene for the T7 RNA Polymerase, such as BL21, Rosetta or Artic, and in presence of Isopropyl β-D-1-thiogalactopyranoside (IPTG).

Restriction of inserts and plasmid: the *glv1* and *2* amplicons were purified using the PureLink® PCR Purification Kit (Thermo Fisher Scientific) and restricted using 20 Units of both *Nco*I and *Xho*I (New England BioLabs) and the appropriate reaction buffer. In parallel, 2 µg of pETM-22 were restricted with the same amounts of both *Nco*I and *Xho*I. Restriction reactions were all carried out in a total volume of 50 µl, incubated at 37°C for 1 h and heat-inactivated at 80°C for 10 min.

Ligation: ligation reactions were carried in a total volume of 20 µl using 50 ng of linearized plasmid, 3 Weiss Units of T4 DNA Ligase (New England BioLabs) and the appropriate reaction buffer. Ligations were carried out with an insert:vector ratio of 3:1. Ligation reactions were incubated overnight at 4°C and inactivated for 10 min at 65°C.

Preparation of E. coli competent cells: JM109 competent cells were prepared with the CCMB method. Briefly, 10 µl of JM109 glycerol stock were pre-inoculated into 5 mL of LB broth an incubated overnight at 37°C on a shaker. 500 µL of the pre-*inoculum* were inoculated in 50 mL of LB broth and grown at 37°C until reaching an OD_{600} of 0.3. Culture was cooled on ice for about 10 min and centrifuged at 1000 x g for 15 min at 4°C. Supernatant was removed and cell pellet was resuspended in 16.6 mL of CCM Buffer, one third of original culture media. Cells were put on ice for 20 min and then centrifuged at 1000 x g for 10 min at 4°C. Supernatant was removed and cell pellet was resuspended in 4.1 mL of CCM Buffer, one twelfth of original culture media. Cells were split in pre-cooled centrifuge tubes, 200 µL for each aliquot, and immediately used or stocked at -80°C.

Transformation of E. coli and screening of recombinants: competent cells were transformed using 1 µl of the ligation reaction. After ligation adding, cells were incubated on ice for 30 min. After a heat-shock step at 42°C for 90 sec, cells were put

on ice for 10 min. 800 µL of SOC broth were added to bacteria and the culture was incubated 1h at 37°C. Finally, *E. coli* cells were plated on Luria-Bertani (LB) plates added with kanamycin (50 µg/mL). Plates were incubated overnight at 37°C. At least 10 colonies for each transformation were checked by colony PCR. Colonies were picked with a sterile filter tip and put in the PCR reaction mixture composed of 1 Unit of GoTaq® DNA Polymerase (Promega), 160 µM dNTPs, 240 nM of each primer used for the *gloverin* gene amplification and the appropriate $MgCl_2$ containing buffer. The PCR cycle comprised an initial denaturing step at 95°C for 3 min, followed by 30 cycles of 95°C for 30 sec, 62°C for 30 sec and 72°C for 40 sec, and a final elongation step at 72°C for 5 min. Positive colonies were inoculated in 5 mL of LB broth with kanamycin (50 µg/mL) and incubated overnight at 37°C at 250 rpm. Plasmids were extracted from overnight *E. coli* cultures using the Wizard® Plus Minipreps DNA Purification System (Promega) and checked by direct sequencing at BMR Genomics Center (Padova, Italy).

Transformation of E. coli Rosetta™2(DE3) and Artic strains: competent *E. coli* cells belonging to Rosetta and Artic strains were prepared and transformed with the CCMB method as described above. The Artic strain possessed an additional plasmid which carried Gentamicin resistance and the gene for a Chaperonin active at low temperatures. Therefore, when growing the Artic strain, gentamicin (50 µg/mL) was always added to the culture broth. About 30 to 50 ng of the pETM-22 plasmids containing the different allele variants of *glv1* and *2* and previously sequence-checked were used for the transformation. *E. coli* cells were plated in LB plates with the appropriate/s antibiotic.

Small-Scale Protein Induction

Transcription induction: at least two independent clones for each pETM-22 transformation were pre-inoculated in 5 mL of LB broth with the appropriate antibiotic/s, and inoculated overnight at 37°C on a shaker. 500 µl of the pre-*inoculum* were inoculated in 30 mL of LB broth with antibiotic/s and grown until reaching an OD_{600} of 0.6. Cultures were split-up in two aliquots: one was left un-induced as negative control, while the other one was induced with 0.1 mM IPTG. When using the Artic strain, cultures were grown at 12°C after induction, while for the Rosetta strain the growth was continued at 37°C. 2 mL aliquots of the cultures were sampled at different time-points: OD_{600} was measured and then samples were pelleted and stored at -20°C until SDS-PAGE or Western-blotting analysis.

SDS-PAGE: bacterial pellets were resuspended in Sample Buffer (SB, 10 % glycerol, 40 mM Tris-HCl pH 6.8, 3 % SDS, 30 mM DTT). To normalize the amount of total proteins among different samples, the SB volume was proportional to the OD_{600} of the original sample. Samples were vortexed, incubated at 95°C for 5 min and centrifuged at 4°C for 15 min at 10000 x g. Supernatants were transferred in new

tubes, heat-denatured at 75°C for 10 min, loaded into 12% acrylamide gel and run at 4°C. Gels were stained for 2 h in Blue Coomassie solution containing 0.1 % Coomassie Blue R-250, 50% methanol and 10% acetic acid, destained with a 40% methanol and 10% acetic acid solution for at least 2 h and stored in a 5% acetic acid solution.

Western-blot: after the run, gel was incubated for 20 min in Transfer Buffer containing methanol. Nitrocellulose membrane (GE Healthcare) was soaked in deionized water and incubated for 5 min in Transfer Buffer. The transfer from gel to nitrocellulose membrane was run at 4°C for 1h at 30 V. Membrane was then blocked with Tris-Buffer Saline with 0.05 % Tween (TBST) and 5 % non-fat milk for 1 h at room temperature at 40 rpm. 1:500 primary anti-Histidine antibody (GE Healthcare) was hybridized overnight at 4°C at 40 rpm in TBST and 1 % non-fat milk. The membrane was washed with TBST at least 5 times and hybridized with 1:3000 secondary Horseradish Peroxidase (HRP)-linked antibody in TBST and 1 % non-fat milk for 2 h at room temperature at 40 rpm. After other 5 TBST washes, membrane was incubated for 5 min with 2 mL of Enhanced chemiluminescence (ECL) Buffer (10 µl luminol, 4.4 µl p-coumaric acid, 0.6 µl H_2O_2 in Tris-HCl 0.1 M ph 8.6). After the removal of the ECL Buffer, the chemiluminescence of the membrane was impressed in X-ray films (GE Healthcare) using Developing and Fixing Solutions (Sigma-Aldrich).

Large-Scale Protein Induction and Purification

Transcription induction: once the most productive *E. coli* Rosetta or Artic clones were selected, they were pre-inoculated in 5 mL of LB broth with the appropriate antibiotic/s, and inoculated overnight at 37°C on a shaker. 2 mL of the pre-*inoculum* were inoculated in 100 mL to 1 L of LB broth with antibiotic/s and grown at 37°C until reaching of OD_{600} of 0.6. The transcription was induced with 0.1 mM IPTG. When using the Artic strain, cultures were grown at 12°C after induction, while for the Rosetta™ strain the growth was continued at 30°C. After 12 or 4 h of induction respectively, cultures were cooled on ice and centrifuged at 4°C for 15 min at 10000 x g.

Cell lysis and protein purification: cell pellets were resuspended in 6-8 mL of Equilibration Buffer (50 mM Na_3PO_4 pH 8.0, 0.3 M NaCl) with an protease inhibitor cocktail (Sigma-Aldrich) and disrupted using a cell disruption system (Constant) set to a pressure of 1.90 Kbar. Bacterial debris were pelleted at 4°C for 15 min at 18000 x g and the supernatant was purified by affinity chromatography by directly loading the cell lysate into a Ni-NTA Agarose resin (Sigma-Aldrich) previously equilibrated with Equilibration Buffer. The His-tag containing fusion protein should preferentially bind to Nickel ions and be retained by resin, while all other *E. coli* proteins should pass in the flow through. After this first step, the Ni-column was washed with Equilibration Buffer and with Equilibration Buffer with 10 and 25 mM imidazole and finally eluted with the same buffer containing 500 mM imidazole. Different eluted fractions were collected

separately. Flow-through, wash and elution fractions were all loaded in acrylamide gels for SDS-PAGE or Western-blotting. When affinity purification showed a low efficiency an additional chromatographic step was carried out. In particular a gel filtration with a HiLoad 16/600 Superdex 200 pg column was performed using a Fast Protein Liquid Chromatography (FPLC) system. The different fractions containing the target protein were pooled, concentrated with an Ultraspin filter with a cutoff of 10 KDa and loaded into an acrylamide gel for SDS-PAGE or Western-blotting.

Removal of the TrxA-6xHis portion from the target protein: once the fusion protein was purified, 2 Units of HRV-3C Protease (Thermo Fisher Scientific) were added to at least 10 µg of fusion protein, in the appropriate buffer. The reaction was incubated at 4°C overnight and a small aliquot was loaded into an acrylamide gel for SDS-PAGE to check the result of the proteolysis. The product of the digestion was loaded into the Ni^{2+} column and both flow through and retained proteins were analyzed through SDS-PAGE and Western-blot.

Production of AMP Variants Using *P. pastoris* and pPICZα

Amplification of *glv1* and *glv2* Genes

The different active portions of the AMP variants were amplified from the pETM-22 plasmids previously obtained. Amplification reactions were carried out in a total volume of 25 µl, containing 10 ng of pETM-22 with the specific allele variants, 0.2 Units of Phusion® High-Fidelity DNA Polymerase (New England BioLabs), 200 µM dNTPs, 300 nM of each primer and the appropriate $MgCl_2$ containing buffer. The PCR cycle comprised an initial denaturing step at 98°C for 3 min, followed by 5 cycles of 98°C for 15 sec, 52°C for 30 sec and 72°C for 30 sec and 25 cycles of 98°C for 15 sec, 65°C for 30 sec and 72°C for 30 sec, with a final elongation step at 72°C for 5 min. Amplicons were checked in 1 % agarose gel. The list of primers used for amplification are listed in Table 3. All forward primers included a *Pst*I site, while all reverse primers had a sequence coding for a 6xHis tag, two stop codons and a *Not*I or *Xba*I site, for the directional cloning in the pPICZα B vector of, respectively, *glv1* and *glv2*.

Gene	Primer name	Sequence (5'->3')	Tm	Amplicon length
glv 1	Glv1_PstI_FOR	CCT**CTGCAG**ATATTCACGACTTTGTCACT	5 cycles x 52°C 25 cycles x 65°C	405 bp
	GLV1_NotI_6His_REV	TAT**GCGGCCGC**TCATCAATGATGATGATGATGATGCCACTCGTGAGTAATCT		
glv2	GLV2_PstI_FOR	GCGT**CTGCAG**ACGTCACTTGGGAC	5 cycles x 52°C 25 cycles x 65°C	393 bp
	GLV2_XbaI_6His_REV	TAT**TCTAGA**TCATCAATGATGATGATGATGATGCCAATCATGGCGGAT		

Table 3. List of primers used for the amplification of *glv1* and *glv2* genes and the cloning in pPICZα B. For each gene, the sequences of both forward and reverse primers, the annealing temperature of primers (Tm) and the length of the amplicon are indicated. In the sequence of each primer, the restriction site used for the directional cloning is indicated in bold, the stop codons and the 6xHis coding sequences in the reverse primers are indicated, respectively, in grey and green.

Plasmid Construction and Yeast Electroporation

The pPICZα B plasmid was kindly provided by Elisabetta Bergantino (Biology Department of the University of Padova, Italy). The different variant alleles of *glv1* and *2* were cloned in pPICZα B using the *Pst*I and *Not*I or *XbaI* unique sites, downstream and in frame with the *Saccaromyces cerevisiae* α-Factor secretion signal and with sites for Kex2 and Ste13, two proteases that are responsible for the removal of the α-Factor signal and for the secretion of the target protein (Figure 7). The 6xHis tag and two stop codons were then directly inserted via PCR downstream the cloned gene. The open reading frame coding for the target protein was under the control of the Alcohol Oxidase 1 (AOX1) promoter, which activates the methanol-induced transcription. All the clones were checked for errors by sequencing.

Restriction of inserts and plasmid: the *glv1* and *2* amplicons were purified using the PureLink® PCR Purification Kit (Thermo Fisher Scientific) and restricted using 20 Units of both *Pst*I and *Not*I or *Xba*I (New England BioLabs) and the appropriate reaction buffer. In parallel, 2 µg of pPICZα B were restricted with the same amounts of both *Pst*I and *Not*I or *Xba*I. Restriction reactions were all carried out in a total volume of 50 µl, incubated at 37°C for 1 h and heat-inactivated at 80°C for 20 min.

Ligation: ligation reactions were carried in a total volume of 20 µl using 100 ng of linearized plasmid, 3 Weiss Units of T4 DNA Ligase (New England BioLabs) and the appropriate reaction buffer. Ligations were carried out with an insert:vector ratio of 10:1. Ligation reactions were incubated overnight at 4°C and inactivated for 10 min at 65°C.

Transformation of E. coli and screening of recombinants: *E. coli* TOP10 competent cells prepared and transformed as previously described. After transformation *E. coli* cells were plated on low-salt LB plates added with Zeocin (25 µg/ mL). Plates were incubated overnight at 37°C. At least 10 colonies for each transformation were checked by colony PCR with AOX1 primers (AOX1_F: 5'-GACTGGTTCCAATTGACAAGC-3'; AOX1_R: 5'-GCAAATGGCATTCTGACATCC-3'). The PCR cycle comprised an initial denaturing step at 95°C for 3 min, followed by 30 cycles of 95°C for 30 sec, 58°C for 30 sec and 72°C for 60 sec, and a final elongation step at 72°C for 5 min. Plasmids were extracted from positive colonies and checked by direct sequencing.

Preparation of linearized vector: the pPICZα B plasmids containing the different allele variants of *glv1* and *2* and previously sequence-checked were linearized with *Sac*I, which had a single restriction site in the AOX1 promoter. This step was fundamental for the integration of the construct in the *P. pastoris* genome through homologous recombination with the native AOX1 promoter. Therefore, 5 µg of each pPICZα B plasmid were digested with 100 Units of *Sac*I and the appropriate reaction buffer. Restriction reactions were all carried out in a total volume of 50 µl, incubated at 37°C for 2 h and heat-inactivated at 80°C for 20 min. The complete linearization of the vectors was checked through agarose gel electrophoresis. Linearized plasmids were purified using the PureLink® PCR Purification Kit (Thermo Fisher Scientific) and quantified with NanoDrop 2000 (Thermo Fisher Scientific).

Preparation of P. pastoris competent cells: a single fresh colony of *P. pastoris* X-33 was pre-inoculated in 5 mL of YPD broth. Yeast cells were grown overnight at 28°C at 250 rpm. Then 1 mL of this pre-*inoculum* was inoculated in 250 mL of YPD and incubated overnight at 28°C at 200 rpm. When the culture reached an OD_{600} of 1.3-1.5, cells were harvested by centrifugation at 1519 x g for 5 min at 4°C. Supernatant was removed and cells were resuspended in 200 mL LiAc/DTT solution (100 mM Lithium Acetate, 10 mM DTT, 0.6 M sorbitol, 10 mM Tris-HCl, ph 7.5). The cell suspension was incubated at room temperature for 30 min while gently shaking at 100 rpm and then centrifuged at 1519 x g for 5 min at 4°C. Supernatant was removed, cells were resuspended in 35 mL of ice cold 1 M sorbitol and kept on ice. Cells were collected by centrifugation at 1811 x g for 5 min at 4°C and then they were further resuspended in 35 mL of ice cold 1 M sorbitol and centrifuged at 1811 x g for 5 min at 4°C. This last step was repeated one more time. Cells were finally resuspended in 1.875 mL of ice cold 1 M sorbitol and stored on ice until electroporation.

Electroporation of P. pastoris X-33 and screening of recombinants: 80 µL of competent *P. pastoris* cells were mixed with 500 ng of linearized DNA plasmid in a pre-chilled electroporation cuvette and incubated of ice for 5 min. Electroporation was carried out in a Gene Pulser II (BioRad) using the following conditions: 1.5 kV,

capacitance of 25 µF and resistance of 200 Ω. After pulsing, 1 mL of 1 M ice cold sorbitol was immediately added to cells and the suspension was incubated for 1 h at 28°C without shaking. Each transformation was plated in YPD plates containing Zeocin at a final concentration of 100 µg/mL and incubated for 48 h at 28°C. At least 10 colonies per transformation were analyzed for the presence of the construct. Genomic DNA samples were obtained with standard procedures, quantified using NanoDrop 2000 (Thermo Fisher Scientific). PCR was carried out on 100 ng of genomic DNA, 1 Unit of EuroTaq DNA Polymerase (Euroclone), 160 µM dNTPs, 240 nM of each primer (Table 3) and the appropriate $MgCl_2$ containing buffer. The PCR cycle comprised an initial denaturing step at 95°C for 3 min, followed by 30 cycles of 95°C for 1 min, 58°C for 1 min and 72°C for 1 min, and a final elongation step at 72°C for 5 min. Positive colonies were inoculated in 5 mL of YPD with Zeocin (100 µg/mL) and incubated overnight at 28°C at 250 rpm.

Small-Scale Protein Induction

At least five different clones of *P. pastoris* X-33 transformed with pPIZα B containing Glv1-iso1 sequence were inoculated in 2 mL of BMGY medium and growth for 24 h at 28°C at 250 rpm. Cells were harvested by centrifugation at 1811 x g for 5 min at 4°C, supernatant was removed and pellets were resuspended in 5 mL of BMMY. This step was repeated one more time. Cells were finally resuspended in 2 mL of BMMY medium and grown at 28°C at 250 rpm. 1% methanol was added every 24 h to maintain induction. 50 µL of supernatants were sampled at different time-points and loaded into 12% acrylamide gel for SDS-PAGE or Western-blot analysis as previously described. The most productive clone was selected for the large-scale production.

Large-Scale Protein Induction and Purification

The selected yeast colony was pre-inoculated in 10 mL of BMGY medium. Yeast cells were grown overnight at 28°C at 250 rpm. Then 8 mL of this pre-*inoculum* were inoculated in 200 mL of BMGY and incubated overnight at 28°C at 200 rpm. The OD_{600} was measured and the culture was centrifuged at 3000 x g for 5 min at room temperature. The pellet was resuspended in BMMY to have a final OD_{600} of 1. The culture was grown at 28°C at 250 rpm for 48 h. Cells were harvested by centrifugation at 10000 g for 10 min at 4°C. The supernatant was filtered using a Nalgene filter unit (Thermo Fisher Scientific). The whole protein content of supernatant was precipitated using ammonium sulphate. About 590 g of ammonium sulphate were added to 1.2 L of supernatant, reaching a final saturation of 75%. The mixture was mixed for at least 1 h at 4°C and centrifuged at 10000 x g for 15 min at 4°C and the pellet was resuspended in 12 mL of Phosphate Buffer 0.1 M pH 6.0. This suspension was purified by affinity chromatography by directly loading the concentred supernatant in a Ni^{2+} column

previously equilibrated with Phosphate Buffer. Ni-column was then washed with Phosphate Buffer with 10 mM imidazole and finally eluted with the same buffer containing 500 mM imidazole. Different eluted fractions were collected separately. Flow-through, wash and elution fractions were all loaded in acrylamide gels for SDS-PAGE or Western-blotting.

Protein Deglycosylation

Since following the purification from of the supernatant Glv1-iso1 was found to have a molecular weight higher than predicted, an aliquot of the purified protein was treated with both PNGase F and O-Glycosidase. *P. pastoris* is known to hyperglysosylate secreted proteins and the linking of glycan chains to a protein leads to an increase of the protein weight. At least 10 µg of purified protein were treated in denaturing or native conditions with PNGase F (New England BioLabs), O-Glycosidase (New England BioLabs) or with both glycosidases together. All reactions were carried out in a total volume of 20 µL. For the denaturing conditions, 10 µg of Glv1 were added to a 10X Denaturing Buffer containing SDS, mixed, heated at 95°C for 5 min and put on ice. Then, 10X reaction buffer and NP-40 were added and finally 500 Units of PNGase F, 40000 Units of O-Glycosidase or both Glycosidases in the same amounts were added. Reactions were incubated at 37°C for 1 h and heat inactivated at 75°C for 10 min. For native conditions 10 µg of Glv1 were added to 10X reaction buffer and 500 Units of PNGase F, 40000 Units of O-Glycosidase or both Glycosidases in the same amounts were added. Reactions were incubated at 37°C for 4 h and heat inactivated at 75°C for 10 min. All reactions were loaded in acrylamide gels for SDS-PAGE or Western-blotting.

Glv1-iso1 Antimicrobial Activity Test

An antimicrobial activity test was conducted on Glv1 produced with *P. pastoris* and purified from its supernatant to confirm its activity. The microorganisms used for this test were the two Gram-positive bacteria *Enterococcus mundtii* HDYM-22 and *Staphylococcus aureus* ATCC BAA-44 and the two Gram-negative bacteria *Serratia marcescens* WW4 and *Escherichia coli* ATCC 25922. To standardize the bacterial cell number, the OD_{600} of cultures was first measured and correlated to CFU by plating serial dilutions of bacterial suspensions in PCA plates. Single fresh colonies of the four bacteria were inoculated in PCA (*E. mundtii*) or Muller Hinton (MH) broth (*S. marcescens*, *E. coli*, *S. aureus*). Bacterial *inocula* were grown for 12-16 h at 30°C at 250 rpm and then used during their exponential growth phase. OD_{600} was measured and bacterial cultures were diluted with the appropriate culture media (MH or PCA broths) to a final theoretical concentration of $0.5 * 10^5$ CFU/mL just before the test. The assay was performed on sterile polystyrene 96-well plates (Costar). Glv1-iso1 was tested in triplicate against 200 µl of bacterial cultures with a final concentration of 2 µM. As a

negative control for growth, Ampicillin at a final concentration of 50 µg/mL was added to bacterial suspension. No-treated bacterial suspensions were grown as positive control. Plates were incubated at 30°C with soft shaking (50 rpm) and the OD_{600} was measured at different time-points (0, 3, 5, 7, 9, 24 h) using a DTX 880 Multimode Detector (Beckman Coulter). The OD_{600} measured at time zero was subtracted from the OD_{600} of each time-point and the resulting ΔOD_{600} values were plotted against time.

Minimal Inhibitory Concentration Assay of two Variants of Cecropin B2

Two isoforms of Cecropin B2 identified from the AMP sequencing analysis were compared for their antimicrobial activity with an *in vitro* Minimal Inhibitory Concentration (MIC) assay. In particular isoform 1, which was found in all the four *B. mori* strains, and isoform 3, were chemically synthesized at Genescript (USA) with a purity higher than 97%. Both peptides had the final amidation modification which is reported to be characteristic of insect Cecropins for the antimicrobial activity (Callaway et al, 1993). Serial dilutions of the two peptides were tested against exponential growth cultures of the Gram-positive *Enterococcus mundtii* HDYM-22 and the Gram-negative bacteria *Serratia marcescens* WW4. Bacterial culture dilutions were prepared as described in the previous section.

The MIC assay was performed on sterile polypropylene 96-well plates (Costar). The serial dilution tested for both peptides were 20, 10, 6, 3, 2.2, 1.8, 1.2, 0.8, 0.4, 0.2 and 0.1 µM. 10 µL of each dilution were tested in triplicate against 200 µl of bacterial cultures. As negative control of growth, Ampicillin-treated bacterial cultures were followed during the 24h experiment. No-treated bacterial suspension were grown as positive control. Plates were incubated at 30°C with soft shaking (50 rpm) and the OD_{600} was measured at different time-points (0, 3, 5, 7, 9, 24 h) using a DTX 880 Multimode Detector (Beckman Coulter). The OD_{600} measured at time zero was subtracted from the OD_{600} at each time-point and the resulting ΔOD_{600} values were plotted against time. The MIC value was considered the lowest concentration sufficient to completely inhibit the bacterial growth.

Chapter 5: Transgenic lines over-expressing AMPs

Introduction

Insect Transgenesis

One of the aim of the project was the production of silkworm lines able to constitutively over-express specific AMPs, with the final purpose to study the effect of the AMP over-expression on *B. mori* physiology and to obtain silkworm lines with an enhanced resistance to infections. In order to obtain these lines we took the advantage of the insect transgenesis technique.

Insect transgenesis has been developed over the past 20 years with the aim of manipulating insect genomes for both basic and applied research purposes (Fraser, 2012). Transgenic *Drosophila* strains are commonly used as models for the study of insect physiology but also of basic biological and human diseases (Venken et al, 2007). Furthermore, transgenic techniques are often applied to an ever greater variety of insects such as the cotton-pest *Pectinopora gossypiella* in the pest-control field, in order to impair their detrimental effect on crops, but also to human health research, as with the *Anopheles* malaria-vectors (Hoy, 2003). More recently, transgenesis has been applied to the silkworm *Bombyx mori* to employ larvae as bioreactors for the production of different bioactive compounds (Xu, 2014).

Transposon vector systems are the most common technology used for insect transgenesis (Fraser, 2012). At least four different transposon vectors have been used for the genetic manipulation of nondrosophilid species: the vectors based on the *mariner* family elements, *Mos1* and *Minos*, systems which use the *hAT*-related element *Hermes* and vectors which take advantage of *piggyBac* transposable elements (Fraser, 2012). Among those, piggyBac (pBAC) is the most studied and used transposon vector for insect transgenesis. GermLine transformation frequencies with this type of vector range from 1-2% to greater than 40% (Handler, 2002).

*piggyBa*c is a baculovirus-derived DNA transposon first discovered in *Trichoplusia ni* which is able to autonomously transpose into TTAA sites using a self-encoded Transposase. The *piggyBac* mobile element is characterized by two inverted-terminal repeat sequences (ITRs) specifically recognized by the Transposase, which is responsible for the excision of the *piggyBac* element and for its insertion into TTAA chromosomal sites. Generally pBAC-based transgenesis vectors are made of the two external *piggyBac*-specific ITR sequences, called “arms”, which surround a target gene and the marker gene for the selection of transformants. Since the Transposase-coding sequence is not included in the pBAC vector, an helper plasmid encoding for this

enzyme is always co-injected with the pBAC construct. The pBAC transgenesis system allows to obtain germLine transformations and stable transgenic insect lines.

Experimental Overview

In 2000 Tamura and co-workers developed a robust system for the germLine transformation of *Bombyx mori* using a pBAC-based vector (Tamura et al, 2000). Starting from this technology, Deng *et al*. generated a construct for the specific expression of target genes in silkworm fat bodies, using the promoter of a 30K lipoprotein (Deng et al, 2013).

In order to study the effect of a stable over-expression of AMP genes in silkworm fat bodies, we created three different pBAC-based constructs, each carrying the *moricin*, *gloverin 2* or *cecropin B* genes under the control of the 30K promoter, reported to be mainly active in fat bodies. Injection experiments have been performed using the *B. mori* Indian strain (Nistari) as host organism.

Nowadays, we obtained two fertile independent transgenic lines for the construct carrying the *moricin* coding sequence. These lines are currently under molecular and physiological characterization. Figure 1 shows a schematic representation of the different steps carried out to obtain and characterize transgenic silkworms (A), with examples of DsRed positive transgenic embryos (B) and pupa (C).

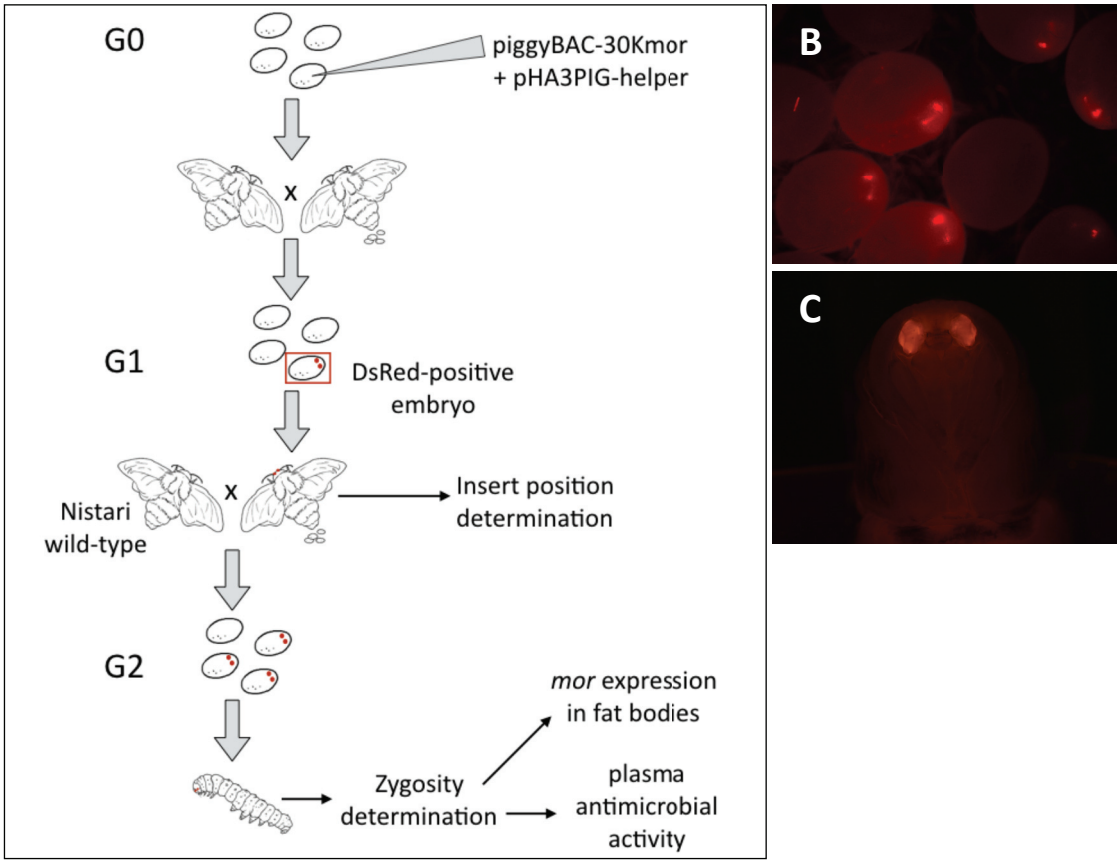

Figure 1. Flow diagram of pBac-30Kmor silkworm transgenesis (A) and examples of G2 transgenic embryos (B) and pupa (C). The G0 generation of larvae hatched from the microinjected eggs were crossed between siblings. The resulting G1 eggs were screened and positive embryos were detected for the red fluorescence at the level of ocelli. The positive G1 individuals were backcrossed to wild-type Nistari, obtaining the G2 transgenic generation. The two G1 adults belonging to the two independent transgenic lines were analyzed for the determination of insert position. After zygosity determination, G2 larvae carrying two copies of the transgene were analyzed for *moricin* expression at the level of fat bodies and for plasma antimirobial activity tests.

Results

Construct Generation

To generate the constructs for the AMP over-expression in *B. mori*, we obtained the [30K-GAL4/3xP3DsRed] plasmid by the National Institute of Agrobiological Sciences (NIAS-Japan) on the basis of a Material Transfer agreement. This *pBAC* plasmid contained: 1) the ITR sequences (left and right arms) to guarantee the insertion of the construct in the host genome when injected in presence of a Transposase, 2) the 30K promoter cloned upstream to the yeast transcriptional factor GAL4 3) the *DsRed* gene encoding the reporter Red Fluorescent Protein under the control of the artificial promoter 3xP3, which directs the *DsRed* transcription into silkworm ocelli and developing eyes at all developmental stages and which allows an early and easy detection of positive transgenic insects (Figure 2).

The three AMPs chosen for the generation of pBAC constructs were selected for their known high and wide antimicrobial activity. Moricin and Cecropin B display a broad and strong antimicrobial activity against both Gram-positive and Gram-negative bacteria (Hara and Yamakawa, 1995; Yang et al, 2011), while Gloverin 2 was demonstrated to have an antimicrobial activity only against Gram-negative bacteria (Yang et al, 2011). These genes or cDNA were obtained via amplification from Nistari larvae genome or RNA (see Material and Methods) and cloned in place of the of *GAL4* sequence, under the control of the 30K promoter in the *pBAC* vector.

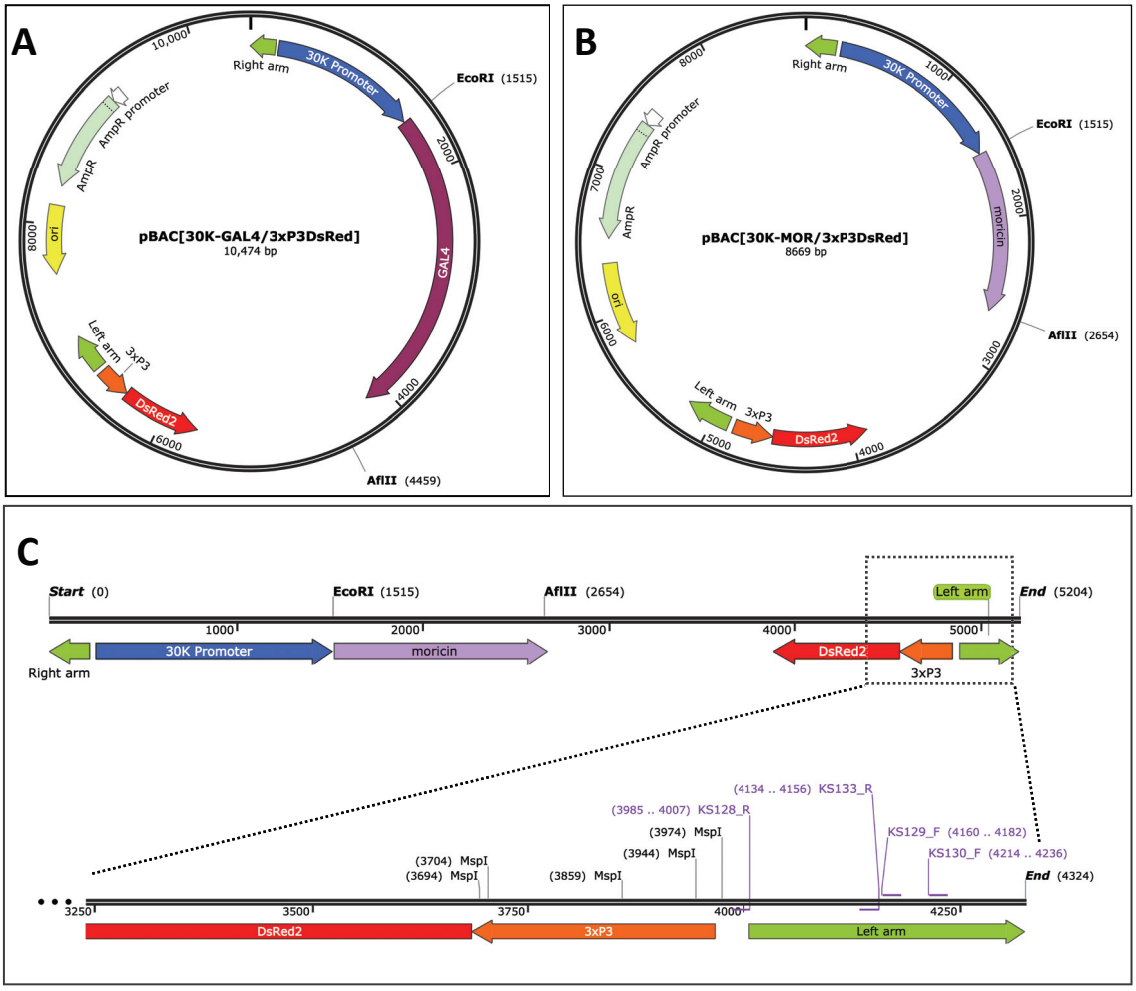

Figure 2. Map of pBAC[30K-GAL4/3xP3DsRed] (A) and pBAC[30K-MOR/3xP3DsRed] (B) plasmids and pBAC[30K-MOR/3xP3DsRed] region integrated in the genome of transgenic individuals, with magnification of Left-arm (C). The *moricin* gene was cloned in the pBAC[30K-GAL4/3xP3DsRed] plasmid in place of *GAL4,* using *Eco*RI and *Afl*II restriction sites (A-B). The plasmid region between left and right arms is the portion which integrates in the silkworm genome. It comprises the *moricin* gene under the control of the 30K fat body specific promoter and the *DsRed* gene under the control of the ocelli-specific promoter 3xP3 (C). In the magnified section, the position and the orientation of primers used for the inverse PCR and the location of *Msp*I sites are shown.

Microinjection of *Bombyx mori* Eggs

The polyvoltine Indian (Nistari) strain was selected for the transgenesis for its peculiar characteristics: larvae showed a good adaptation to artificial diet, they were able to reproduce continuously throughout the year and they deposited eggs with a transparent chorion, allowing to monitor the development of the transgenic embryos.

Currently, the two constructs, containing *moricin* and *gloverin 2* respectively, have been uses for microinjection experiments. For both constructs at least four

injection sessions were conducted on at least 1300 embryos, and for the *moricin* construct only, three independent transgenic and viable individuals were obtained. Of these, however, only two individuals were fertile and have been used as founders for two independent transgenic lines (30K-*moricin* line 1 and line 2) Table 1 gives summary information on the injection experiments. The percentage of germ-line successful integration was very low (0.37 %).

Construct	N° injected embryos	N° hatched embryos	Hatching %	N° transgenic embryos (G2)	N° fertile and viable larvae (G2)
pBAC[30K-mor/3xP3DsRed]	2,072	1,070	51.64	4	2
pBAC[30K-glv2/3xP3DsRed]	1,344	376	27.98	/	/

Table 1. Information on injection experiments of pBac vectors in Nistari embryos.

Characterization of the two 30K-moricin Transgenic Lines

At the time of these analyses, the two 30K-*moricin* lines were at their second generation (G2), which was made of individuals that were both homozygous and hemizygous for the transgene. A prior experiment was conducted to determine the zygosity of each individual, and the analyses of the expression of *moricin* in fat bodies and of the antimicrobial activity of hemolymph were conducted.

A population of 29 fifth instar larvae was sampled for each 30K-*moricin* transgenic lines. Midgut, fat body and hemolymph samples were collected from each individual separately, for both transgenic lines. Genomic DNAs extracted from midguts were used to determine the zygosity and to map the insert position in the host genome.

Determination of Zygosity

Genomic DNA samples extracted from midguts collected separately from transgenic larvae belonging to the 30K-*moricin* line 1 and line 2 were used to analyze the transgene zygosity trhough qPCR, following the method of Weng et al (2004). The

number of copies of the *DsRed* gene was determined by relative quantification with a reference gene, *Or2*, which occurs in one single copy per haploid genome.

For line 1, 9 individuals were found to possess two copies of the transgene per diploid genome, and were considered homozygous for the insertion (Table 2).

As to line 2, 18 individuals were found to have two or more copies of the transgene per diploid genome (Table 2). It was therefore inferred that this line had at least two independent integrations in the genome.

Line 1			**Line 2**		
	Larva	**N° *DsRed* copies (mean ± SEM)**		**Larva**	**N° *DsRed* copies (mean ± SEM)**
Pool 1	AA	2.38 ± 0.60	**Pool 1**	B	1.96 ± 0.56
	C	1.98 ± 0.20		E	2.54 ± 0.28
	D	1.40 ± 0.36		J	2.08 ± 0.04
Pool 2	J	1.60 ± 0.40	**Pool 2**	D	7.04 ± 2.20
	K	1.9 ± 0.44		P	4.62 ± 0.70
	M	1.56 ± 0.20		W	6.28 ± 2.62
Pool 3	N	2.16 ± 0.44	**Pool 3**	C	3.08 ± 0.42
	S	1.92 ± 0.04		U	3.30 ± 0.52
	V	1.86 ± 0.26		Y	3.34 ± 0.46
			Pool 4	A	2.50 ± 0.64
				H	2.30 ± 0.42
				AB	2.54 ± 0.28
			Pool 5	I	3.04 ± 0.12
				K	2.40 ± 0.22
				L	1.96 ± 0.38
			Pool 6	O	2.34 ± 0.26
				S	3.28 ± 0.40
				Z	2.80 ± 0.44

Table 2. Determination of the *DsRed* copy number in 9 (line 1) and 18 (line 2) larvae belonging to the two transgenic lines. The number of copies of the *DsRed* gene was determined by relative quantification with a reference gene, *Or2*, which is present in one single copy per haploid genome. For each single G2 larva, the *DsRed* copy number was determined. For each line, pools of fat body and hemolymph samples extracted from three larvae were created as indicated.

Insert Position

The genome extracted from moths belonging to the G1 generation was digested with the four-cutter enzyme *Msp*I and ligated. Because *Msp*I restriction sites should theoretically be present in a generic genome every 256 bp and because the pBAC construct included many *Msp*I sites, there was a high probability that the left or right arm portions circularized on the genome regions flanking the integration sites.

Specific primers were used to amplify the circularized fragments. Different amplification products were obtained for each line, therefore PCR fragments were cloned in pGEM and the resulting plasmids were sequenced to determine the sequences flanking the inserts. Two pGEM plasmids showing different insert sizes were sequenced for each line. From the sequence analysis it was found that the two pGEM plasmids of the same transgenic line contained the same flanking genome sequence and that the larger dimension of the insert was due to an independent *Msp*I-*Msp*I fragment ligated into the circularized genome.

The genomic DNA sequences flanking the pBAC left arm are shown in Figure 3. The analysis of these sequences confirmed that pBAC constructs integrated into TTAA sites.

Moreover the precise integration site was identified for both lines, with line 1 showing a single intergenic integration in chromosome 11 and line 2 possessing an intergenic integration in chromosome 13 (Table 3). Since the zygosity analysis showed that line 2 possessed at least a double integration, a higher number of colonies should be analyzed in order to identify the multiple insertion sites.

```
Line-1 ---piggyBac---TTAAATTTGCTTAGAGCCTGTAACGTACCCTAGTTACATGCATTTTGCTAATTCA
AGGCGATTTCGCAATTAACAACCAGTGGCGTACGTGACTACAAATTGTCGACGCAGCAACCTCATTCCATGTTCAT
GGAATACGCGACTGGCGTCAAGTGCTGACACTGCAGCGTCGCTATGCCGCCCGG

Line-2 ---piggyBac---TTAATGAATGAATGCCCTTTTTAAAGTTCCATATGGTGCCGTGCTGTGTCTTACT
CAGTGGGTCCGG
```

Figure 3. Genomic DNA sequences flanking the pBAC left arm. In bold, the TTAA sequence characterizing the transposon insertion site has been underlined. The restriction sites for *Msp*I are shown in grey.

Line N°	N° of inserts	Scaffold ID	Scaffold position	Chromosome	Chromosome position	Gene involved
1	1	Bm_scaf16	853550–853374	chr11	13109417–13109593	None
2	≥2	Bm_scaf1	1391258–1391316	chr13	16600514–16600456	None
		?	?	?	?	?

Table 3. Insert position information for the two transgenic lines. The PCR fragments obtained with the inverse PCR on left-arm sequence were cloned in pGEM and sequenced. The resulting sequences were mapped on *B. mori* genome using KAIKObase. Line 2 probably possessed a multiple integration, even if this was not confirmed by insert position analysis.

Expression of *moricin* in Fat Bodies

To assess if the integration of the pBAC construct was associated with a higher expression of *moricin* in fat bodies, transcriptional levels were determined in fifth instar larvae homozygous for the transgene and belonging to the G2 generation. For the transgenic *K30-mor* line 1 fat bodies samples of the nine homozygous larvae were pooled in three replicates, each composed of fat bodies extracted from three individuals. For the transgenic *K30-mor* line 2, fat body samples from the eighteen larvae showing more than two copies of the transgene were pooled in six replicates, each composed of the samples extracted from three larvae which showed similar number of inserts.

Through qPCR, *moricin* mRNA levels were compared between the two transgenic lines and with wild-type Nistari larvae.

Figure 4 shows the *moricin* expression levels for both Nistari wild-type and the two transgenic lines. Both lines 1 and 2 significantly over-expressed *moricin* in comparison with the wild-type strain (Kruskal-Wallis test, $P < 0.001$; Bonferroni multiple comparisons test: wild-type/line 1: $P < 0.05$; wild-type/line 2: $P < 0.0001$). Line 2 showed apparent higher expression levels when compared to line 1, but this difference was not significant (Bonferroni multiple comparisons test line 1/line 2, $P = 0.29$, ns).

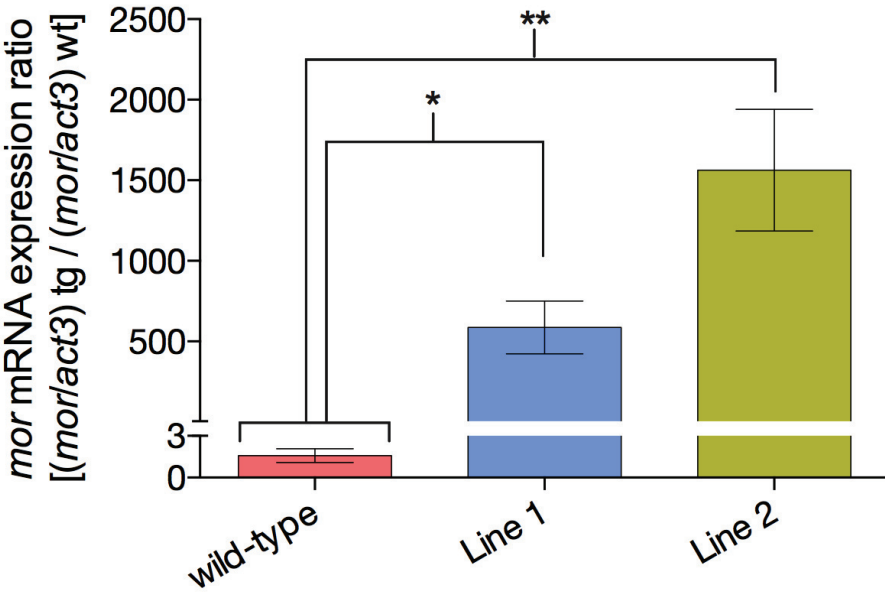

Figure 4. *Moricin* expression levels in fat bodies of wild-type and transgenic larvae at the fifth larval stage. The *moricin* mRNA expression was determined by quantitative RT-PCR on total RNA extracted from fat bodies of 9 individuals pooled in 3 replicates (wild-type and line 1) or from 18 individuals pooled in 6 replicates (line 2). *Moricin* expression ratio represents the *mor*/*actin3* mRNA levels of transgenic samples over those of wild-type individuals (mean ± SEM). Kruskal-Wallis test: * $P < 0.05$; **: $P < 0.01$.

Plasma Antimicrobial Activity

In order to establish if the constitutive expression of the *moricin* gene was associated to higher hemolymph antimicrobial activity of, hemocyte-free plasma samples extracted from the same larvae used for the *moricin* expression analysis were tested against different bacteria. The test was conducted using the silkworm specific pathogens *Enterococcus mundtii*, Gram-positive, and *Serratia marcescens*, Gram-negative. This wide variety of microorganisms was tested to investigate the effect of Moricin-rich plasma on bacteria with different characteristics.

The hemocyte-free plasma extracted from both transgenic and wild-type negative control larvae reared in germ-free conditions was added to the bacterial cultures. The OD_{600} of cultures was measured every 2 h and bacterial growth (μ) was calculated. Figure A.1 shows the growth rate curves of all six bacteria treated with the different plasma samples. To compare the bacterial growth of microorganisms treated with different plasma samples, the area under each μ curve was calculated in the time span between 3 and 9 h post-*inoculum*.

Figure 5 shows the global effect of plasma extracted from wild-type and transgenic lines. A strong antimicrobial activity was found only against *Enterococcus mundtii.* Both transgenic lines showed higher antimicrobial activity against *E. mundtii* when compared to the wild-type strain (Figure 5A; Kruskal-Wallis test, $P < 0.001$; Bonferroni multiple comparisons test: wild-type/line 1 and wild-type/line 2 comparisons: $P < 0.0001$). As to *Serratia marcescens*, non out the two *moricin* over-expressing lines showed any inhibitory effect on the bacterial growth in comparison to the negative control (Figure 5B and A.1).

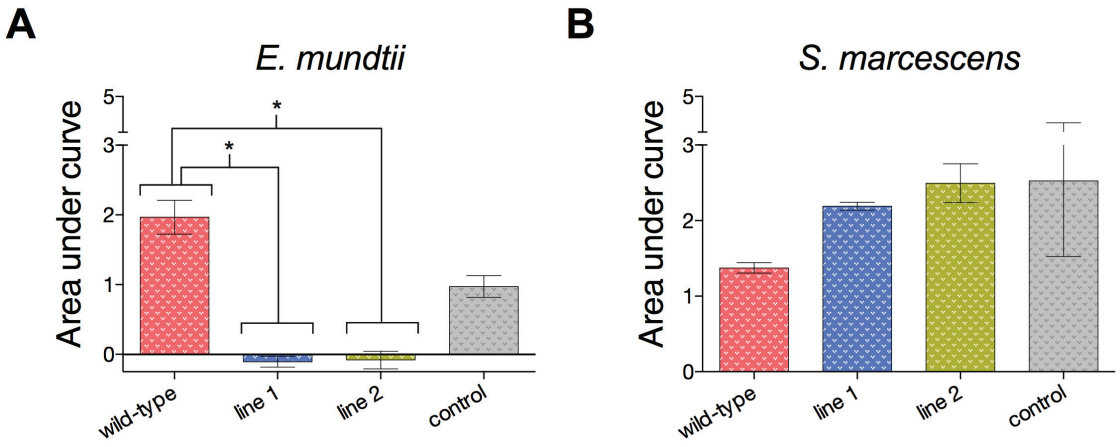

Figure 5. Comparison of the antimicrobial activity of plasma extracted from wild-type and transgenic fifth instar larvae against *E. mundtii* (A) and *S. marcescens* (B). Hemolymph was collected from 9 individuals pooled in 3 replicates (wild-type and line 1) or from 18 individuals pooled in 6 replicates (line 2). The hemocyte-free plasma was added to the two bacterial culture ($5*10^5$ CFU/mL) and the optical density at 600 nm was measured to monitor the microbial growth. The areas under the growth rate (µ) curves were calculated for each condition (mean ± SEM). Bonferroni multiple comparisons tests: * indicates significant differences ($P < 0.05$) in the µ areas.

Discussion

PiggyBac based transgenesis was successfully applied for the generations of stable silkworm transgenic lines constitutively expressing *moricin* at fat body level. However, the percentage of G0 transformants (4/1070, 0.37% positive embryos) was lower in comparison to the efficiencies reported by both Tamura *et al.* (2.12 %; 2000) and Deng *et al.* (3.97%; 2013) and for the *gloverin 2* construct, no positive embryo was obtained over the 1300 injected eggs. These low transformation efficiencies were probably due to a general inexperience on the injection technique rather than to intrinsic construct features. Therefore, there is vast room for improvement for this transgenesis technology.

Tamura also reported highly frequent multiple independent integrations of the *piggyBac* construct in the genome of the same transgenic individual (Tamura et al, 2000). Among the two independent lines obtained in our experiment, line 2 showed evidences of at least a double integration of the construct.

The *piggyBac* vectors were found to precisely target TTAA sites in both transgenic lines. Moreover, both lines showed intergenic integration, even if results for line 2 are only preliminary. The intergenic integration could be preferable when generating transgenic animals, because of the lower probability of interfering with the organism physiology. On the other hand, the integration of the transgene in a silenced intergenic region could be problematic for its expression (Fraser, 2012). However, from the analysis of the transgene expression at the level of fat bodies, it appeared that in the two obtained *moricin* lines the integration site/s did not compromise the level of the transgene mRNA production. In fact, it was confirmed that both transgenic strains showed a *moricin* fat body over-expression in comparison with the wild-type strain. Since silkworms were reared in germ-free conditions, this *moricin* induction was independent from exposure to microorganisms. The expression levels of line 2 were in general higher than for line 1, even if the difference was not statistically significant. These higher expression ratios might be due to the putative multiple insertion of the *moricin* transgene in line 2.

As to the antimicrobial activity of the hemolymph, a strong effect was observed only on *E. mundtii* growth after the treatment with plasma extracted from both lines, with no significant differences in the antimicrobial activities of the two transgenic strains. Therefore, Moricin rich plasma was found to efficiently reduce the growth of this important Gram-positive silkworm pathogen. Interestingly, no effect was observed on the *S. marcescens* growth when treated with hemolymph samples extracted from the *moricin* over-expressing lines. There are many evidences showing that Moricin has an antimicrobial activity on both Gram-positive and -negative bacteria (Hara and

Yamakawa, 1995; Yang et al, 2011). Moreover *moricin* was one of the few genes induced at midgut level after *S. marcescens* infection (Chapter 3). Probably the concentrations reached by Moricin in silkworm hemolymph are not sufficient to arrest *S. marcescens* proliferation.

These results raise hopes that the AMP constitutive systemic expression exhibited by transgenic silkworms may have a significant effect on their resistance to pathogens .

Since genetic markers and balancer chromosomes are not available for the silkworm *B. mori,* the screening and maintenance of the multiple insertions on line 2 could be difficult. The presence of a multiple integration in this line did not correlate with a higher antimicrobial power of plasma, suggesting that the number of integrated constructs was not associated with a significantly higher Moricin activity in the hemolymph. Therefore, line 1 could be the best candidate for more in-depth studies.

Experiments are planned to clarify important aspects of this particular genetic modification in silkworms. In particular, we intend to determine the survival profiles of transgenic silkworms after infection with the Gram-positive pathogen *E. mundtii*. Moreover, we intend to determine the levels of the transgene expression and protein production at the different silkworm developmental stages (embryo, five larval stages, pupa and adult) and in different tissues, to assess the precise expression pattern of Moricin driven by the 30K promoter.

Even if the pBAC system was found to have lower efficiency than expected, transgenic silkworms with constitutive AMP production could increase the knowledge on *B. mori* AMP physiology and *in vivo* functions. These silkworms might turn out to be an important resource in the fight against *B. mori* diseases which are threatening sericulture. Moreover, transgenic strains over-expressing AMPs might be used as bioreactors for the massive production of AMPs. The main advantage of producing silkworm AMPs in their original host is that, after setting up the purification procedure, active AMPs would be obtained with all their native post-translational modifications. These AMPs could be therefore purified and employed in many pharmacological applications. Furthermore, *B. mori* pupae over-expressing AMPs could be used as food additives rich in oils and proteins and containing natural preservatives.

Materials and Metods

Amplification of *moricin*, *cecropin B* and *gloverin 2* Genes

Genomic DNA and total RNA were extracted from Nistari larvae and RNA was retrotranscribed as described in Chapter 2. The *moricin* gene was amplified from genomic DNA and cloned with its 833 bp intron, while *gloverin 2* and *cecropin B* genes were amplified from cDNA. Amplification reactions were carried out in a total volume of 25 µl, containing 50 ng of genomic DNA or cDNA, 0.2 Units of Phusion® High-Fidelity DNA Polymerase (New England BioLabs), 200 µM dNTPs, 300 nM of each primer and the appropriate $MgCl_2$ containing buffer. The PCR cycle comprised an initial denaturing step at 98°C for 3 min, followed by 30 cycles at 98°C for 30 sec, 60°C for 30 sec and 72°C for 1 min, and a final elongation step at 72°C for 5 min. Amplicons were checked in 1 % agarose gel. The list of primers used for amplification are listed in Table 4. All forward and reverse primers included an *Eco*RI and an *Afl*II site respectively, for the directional cloning in the pBAC[30K-GAL4/3xP3DsRed] vector.

Gene	Primer name	Sequence (5'->3')	Template	Tm	Amplicon length
moricin	MOR_EcoRI_FOR	**GAATTC**AAACCGCGCAGTTATTTAAAA	gDNA	60°C	1133 bp
	MOR_AflII_REV	**CTTAAG**CTAATACCATTCACTCAATTTCTTTTC			
cecropin B	CECB_EcoRI_FOR	**GAATTC**ATGAATTTCGCAAAGATCCTATC	cDNA	60°C	192 bp
	CECB_AflII_REV	**CTTAAG**TCATTTTCCTATAGCTTTAGCCG			
gloverin 2	GLV2_EcoRI_FOR	AT**GAATTC**ATGAACTCAAATCTGTTTTATATATTC	cDNA	60°C	744 bp
	GLV2_AflII_REV	AT**CTTAAG**CATAACAAAGCACGAGATCC			

Table 4. List of primers used for the amplification of *moricin*, *cecropin B* and *gloverin 2* genes. For each gene, the sequences of both forward and reverse primers, the type of template, the annealing temperature of primers (Tm) and the length of the amplicon are indicated. In the sequence of each primer, the restriction site used for the directional cloning is indicated in bold. For *gloverin 2*, the Cytosine highlighted in grey in the forward primer, has been modified in respect of the original gene sequence, which contained a Thymine, to remove an *Eco*RI site initially present in the Gloverin 2 coding sequence. The substitution was, however, synonymous, since the codified amino acid was not changed.

Plasmid Construction

The pBAC[30K-GAL4/3xP3DsRed] and the pHA3PIG-helper plasmids were kindly provided by the National Institute of Agrobiological Sciences (NIAS) of Japan. The *moricin*, *cecropin B* and *gloverin 2* genes were cloned in pBAC[30K-GAL4/3xP3DsRed] using the *Eco*RI and *Afl*II unique sites to remove the *GAL4* gene which was inserted downstream the fat bodies specific 30K promoter (Figure 2).

Restriction of inserts and plasmid: the *moricin*, *cecropin B* and *gloverin 2* amplicons were purified using the PureLink® PCR Purification Kit (Thermo Fisher Scientific) and restricted using 20 Units of both *Eco*RI and *Afl*II (New England BioLabs) and the appropriate reaction buffer. In parallel, 2 µg of pBAC[30K-GAL4/3xP3DsRed] were restricted with the same amounts of both *Eco*RI and *Afl*II. Restriction reactions were all carried out in a total volume of 50 µl, incubated at 37°C for 1 h and heat-inactivated at 65°C for 10 min.

The restricted pBAC[30K-GAL4/3xP3DsRed] plasmid was run on a 0.8% agarose gel. The band corresponding to the 7500 bp linearized vector was cut, purified using an Ultrafree®-DA Centrifugal Filter Unit (Merck Millipore) and quantified with NanoDrop 2000 (Thermo Fisher Scientific).

Ligation: ligation reactions were carried in a total volume of 10 µl using 50 ng of linearized plasmid, 3 Weiss Units of T4 DNA Ligase (New England BioLabs) and the appropriate reaction buffer. Ligations were carried out with an insert:vector ratio of 10:1, therefore 75 ng, 13 ng and 50 ng of restricted amplicons were used for, respectively, *moricin*, *cecropin B* and *gloverin 2*. Ligation reactions were incubated overnight at 4°C and inactivated for 10 min at 65°C.

Transformation of E. coli and screening of recombinants: *E. coli,* High Efficiency Competent Cells JM109 (Promega) were transformed using 1 µl of the ligation reactions and following the manufacturer's instruction. *E. coli* cells were plated on Luria-Bertani (LB) plates added with ampicillin (50 µg/mL). Plates were incubated overnight at 37°C. At least 10 colonies for each transformation were checked by colony PCR. Colonies were picked with a sterile pipette tip and put in the PCR reaction mixture composed of 1 unit of GoTaq® DNA Polymerase (Promega), 160 µM dNTPs, 240 nM of each of the primers used for the first amplification and the appropriate $MgCl_2$ containing buffer. The PCR cycle comprised an initial denaturing step at 95°C for 3 min, followed by 30 cycles at 95°C for 30 sec, 60°C for 30 sec and 72°C for 1 min, and a final elongation step at 72°C for 5 min. Amplicons were checked in 1 % agarose gel. Positive colonies were inoculated in 5 mL of LB broth with ampicillin (50 µg/mL) and incubated overnight at 37°C at 250 rpm.

Plasmids were extracted from overnight *E. coli* cultures using the Wizard® Plus Minipreps DNA Purification System (Promega) and checked by direct sequencing at the BMR Genomics Center (Padova, Italy).

Preparation of the Injection Solution

Midi preparations of the pBAC[30K/3xP3DsRed]-mor, -cecB and -glv2 plasmids were extracted using the QIAGEN Plasmid Midi Kit (Qiagen). The vector DNA was resuspended in Injection Buffer (5 mM KCl and 0,5 mM Phosphate Buffer, pH 7.0) and quantified. A 1:1 mixture of each pBAC[30K/3xP3DsRed] construct and the helper plasmid pHA3PIG were diluted to the final concentration of 400 ng/µL in Injection Buffer and stored at -20°C until use.

Experimental Animals and Preparation of Eggs for Microinjection

Nistari larvae were maintained, reared and microinjected at the Sericulture Unite of the CREA-API of Padova, Italy.

Eggs were surface sterilized with 0.5% sodium hypochlorite. Larvae were reared on artificial diet until spinning. After mating, female moths deposited eggs on a paper covered with a flour glue (50 g of flour per L of water) and moved to a new paper sheet every h, to obtain eggs synchronized in their embryo development.

Eggs were then detached from paper sheets and washed with deionized water. Malformed, damaged or sterile eggs were removed. The selected eggs were deposited on a slide and sterilized with formaldehyde vapors.

Transgenesis and Screening

Plasmid microinjections were performed between 4-6 h after oviposition using a binocular microscope, an IM-300 microinjector, a M-152 manipulator and a HD-20 pipette holder (Narishige). Microinjection needles were made from 5 µL capillary (Drummond Scientific Company) using a PC-10 puller (Narishige) and sterilized in heater at 160°C for 2 h.

Eggs were punched with a tungsten needle in the ventral part, were the germinal line would develop. The pBAC-helper mixture previously loaded in the capillary needle was microinjected pushing the plunger for 30-60 ms and at a pressure of 20-25 psi. The

injection perforations were sealed with glue. Eggs were sterilized with formaldehyde vapors and incubated at 25°C in a sterile plastic container.

All transgenic larvae were reared in germ-free conditions. The G0 generation of larvae hatched from the microinjected eggs were reared on artificial diet until adult stage. After sibling mating, the resulting G1 eggs were screened with a Leica MZ16 F fluorescence stereomicroscope with an appropriate filter for DsRed detection. Positive embryos were detected for the red fluorescence the ocelli level.

The positive G1 individuals were backcrossed to wild-type Nistari, obtaining the G2 transgenic generation.

Characterization of the two 30K-moricin Transgenic Lines

Determination of Zygosity

In order to determine the zygosity of each individual, quantitative PCR reactions were carried out on genomic DNA extracted from midgut samples (see Chapter 2 for the protocol). Both the transgene and a reference gene were amplified in two independent reactions on the same template. *Or-2,* which encodes for Odorant Receptor, it is known to be present in a single copy in the *B. mori* genome (Sakudoh et al, 2011), therefore it was selected as the reference gene. On the other hand, *DsRed* was the transgene. Primer sequences are: OR2-1 5'-GCTGGATGTCATTTT CTGTTCGTGG-3'; OR2-2 5'-AACTCGGAACAACTCAGCCGTATTG- 3'; DsRed2_FOR 5'-CCGCTACAGGAACAGGTGGT-3'; DsRed2_REV 5'-TACTACGTGGACGCCAAGCTG-3' (Sakudoh et al, 2011).

According to the protocol *Creating Standard Curves with Genomic DNA or Plasmid DNA Templates for Use in Quantitative PCR* (PN 4371090), available at www.appliedbiosystems.com, the number of copies of *Or-2* in different amounts of genomic DNA were calculated. In particular, it was established that 0.52 pg of genomic DNA would contain one haploid *B. mori* genome and therefore one copy of *Or-2*.

Standard curves were created for both *DsRed* and *Or-2* on serially diluted DNA amounts (156, 15.6, 1.56, 0.156 ng), each carrying $3*10^5$, $3*10^4$, $3*10^3$, $3*10^2$ and 30 copies of the *Or-2* gene. For each transgenic line, two random individuals were used to draw a standard curve. For both *DsRed* and *Or-2*, cycle threshold (Ct) values were graphed against the $\log_{10}$ of DNA amounts. The slopes and the intercepts of the resulting linear curves were determined.

The number of transgene copies were calculated as described in Weng et al (2004) using the following equation:

$$N = 10^{\wedge}\left\{ \frac{[(Ct_{DsRed}\text{-}I_{DsRed})]}{S_{DsRed}} - \frac{[(Ct_{Or\text{-}2}-I_{Or\text{-}2})]}{S_{Or\text{-}2}} \right\}$$

in which I and S are respectively intercepts and slopes and Ct is the detected threshold cycle for a tested sample.

qPCR reactions were performed in a total volume of 10 µl using GoTaq® qPCR Master Mix (Promega), 200 nM of each primer and 70 ng of genomic DNA in an Applied Biosystem 7900 RealTime system with the following thermal cycle: 98°C for 3 min, 40 cycles at 98°C for 15 sec and 60°C for 60 sec.

Insert Position

Genomic DNA was extracted as described in Chapter 2 from the heads of adult moths belonging to the G1 generation of the two independent transgenic lines. The following operations were conducted on both lines: 3 µg of gDNA were digested with 60 Units of *Msp*I (New England BioLabs) in the appropriate reaction buffer, in 50 µL of total volume, at 37°C for 1 h. 10 µL of the digested DNA were circularized in a total volume of 20 µL, with 3 Weiss Units of T4 DNA Ligase at 4°C overnight. After heat-inactivation at 65°C for 10 min, 10 µL of the ligated genomic DNA was subjected to inverse PCR using 0.25 Units of Phusion® High-Fidelity DNA Polymerase (New England BioLabs), 200 µM dNTPs, 300 nM of each primer and the appropriate $MgCl_2$ containing buffer. Left arm primers were used for inverse PCR. The orientation and the position of primers are shown in Figure 2C. The primers KS129_F (5'-AAATCAGTGACACTTACCGC ATT- 3') and KS133_R (5'-ACTATAACGACCGCGTGAGT CAA-3') were used in the first amplification. The PCR cycle consisted of an initial denaturing step at 98°C for 3 min, followed by 30 cycles at 98°C for 30 sec, 59°C for 45 sec and 72°C for 10 min, and a final elongation step at 72°C for 10 min.

A 10-fold dilution of this first PCR was subjected to a second PCR with the primers KS130_F (5'-CGACTGAGATGTCCTAA ATGCAC-3') and KS128_R (5'-TTATCGATACCGTCGAC CTCGAG-3'). The PCR cycle included an initial denaturing step at 98°C for 3 min, followed by 30 cycles at 98°C for 15 sec, 59°C for 15 sec and 72°C for 1 min 30 sec, and a final elongation step at 72°C for 5 min. Amplicons were checked in 1 % agarose gel.

The amplicons were cloned in pGEM®-T Easy Vector (Promega) using a TA cloning. Before ligation, amplicons from both transgenic lines were subjected to A-tailing, since Phusion® High-Fidelity DNA Polymerase releases blunt-ends: 0.1 Units of EuroTaq DNA Polymerase (Euroclone) and 200 µM dNTPs were added to PCR amplicons and incubated at 95°C for 3 min and at 72°C for 10 min.

Ligation reactions were carried in a total volume of 10 µl using 50 ng of pGEM, 3 Weiss Units of T4 DNA Ligase (New England BioLabs), 50 ng of A-tailed amplicons and the appropriate reaction buffer. Ligation reactions were incubated overnight at 4°C and inactivated for 10 min at 65°C.

1 µl of ligations were used to transform *E. coli* TOP10 competent cells as described in Chapter 4 and plated on Luria-Bertani (LB) plates added with ampicillin (50 µg/mL), X-gal (80 µg/mL) and IPTG (200 µM). Plates were incubated overnight in the dark at 37°C. At least 10 white colonies for each transformation were checked by colony PCR. Colonies were picked with a sterile filter tip and put in the PCR reaction mixture constituted of 1 unit of EuroTaq DNA Polymerase (Euroclone), 160 nM dNTPs, 240 nM of M13 universal primers and the appropriate $MgCl_2$ containing buffer. The PCR cycle consisted of an initial denaturing step at 95°C for 3 min, followed by 30 cycles at 95°C for 30 sec, 55°C for 30 sec and 72°C for 1 min, and a final elongation step at 72°C for 5 min. Amplicons were checked in 1 % agarose gel. Positive colonies which showed inserts of different sizes were inoculated in 5 mL of LB broth with ampicillin (50 µg/mL) and incubated overnight at 37°C at 250 rpm.

Plasmids were extracted from overnight *E. coli* cultures using the Wizard® Plus Minipreps DNA Purification System (Promega). Two pGEM plasmids for each line showing different insert sizes were checked by direct sequencing at BMR Genomics Center (Padova, Italy).

The resulting sequences, which represent the sequences flanking the insertion site, were analyzed using KAIKObase (http://sgp.dna.affrc.go.jp/KAIKObase/) and mapped in the silkworm genome to determine the precise insertion site.

Expression of *moricin* in Fat Bodies

Total RNA was extracted and retro-transcribed from pools of three fat body samples extracted from larvae homozygous for the insertion. For the transgenic line 1, three pools were obtained, while for transgenic line 2, fat body tissues were pooled in six replicates. In parallel, RNA was extracted and retro-transcribed also from Nistari wild-type larvae. RNA extraction and retro-transcription methods are described in Chapter 2.

Both transgenic and wild-type larvae were reared in germ-free conditions to avoid *moricin* activation due to immune reactions to microorganisms possibly present in the rearing environment.

The expression ratios of *moricin* were determined by comparing the expression ratios between the two transgenic lines and Nistari wild-type larvae. Quantitative real-time PCR reactions were performed in a total volume of 10 µl using GoTaq® qPCR Master

Mix (Promega), 200 nM of each primer and 20 ng of cDNA in an Applied Biosystem 7900 RealTime system with the following thermal cycle: 95°C for 2 min, 40 cycles at 95°C for 15 sec and 60°C for 60 sec. See Table 3 in Chapter 3 for *moricin* and *actin3* primer sequences.

Data were analyzed using the $2^{-\Delta\Delta CT}$ method. For each sample, the *moricin* mRNA expression ratio (R) was calculated as following:

$$R = \frac{E_{mor}^{\text{Ct } mor \text{ wild-type - Ct } mor \text{ transgenic)}}}{E_{act3}^{\text{Ct } act3 \text{ wild-type - Ct } act3 \text{ transgenic)}}}$$

Plasma Antimicrobial Activity

Hemolymph samples were collected from single larvae at the fifth day of the fifth larval stage belonging to the two transgenic lines and to the Nistari wild-type strains. After zygosity analysis, hemolymph samples were pooled as described for fat bodies RNA extraction.

Hemolymph samples were collected as described in Chapter 3, mixing the outflowed hemolymph with 2.5 mM of filter sterilized phenylthiourea to prevent melanization. Hemocytes were removed by centrifugation at 1000 x g for 5 min at 4° C. Plasma samples were snap-frozen in liquid nitrogen and thawed on ice just before the test.

The microorganisms used for this test were both the two silkworm specific pathogens used for the previous infection experiments and bacteria commonly used as standards in antimicrobial activity determination. In More specifically, the three Gram-positive bacteria *Enterococcus mundtii* HDYM-22, *Staphylococcus aureus* ATCC BAA-44 and *Staphylococcus epidermidis* ATCC 700565 and the three Gram-negative bacteria *Serratia marcescens* WW4, *Escherichia coli* ATCC 25922 and *Pseudomonas aeruginosa* ATCC 25668 were used. To standardize bacterial cell numbers , the OD_{600} of cultures was previously measured and correlated to CFU by plating serial dilutions of bacterial suspensions in PCA plates.

The plasma antimicrobial activity test and the data analysis were performed as described in Chapter 3.

Statistical Analyses

Kruskal-Wallis tests were performed on calculated *moricin* R values and on the areas under the μ curves, to assess if there were significant differences between the values of the two transgenic lines and those of the wild-type strain. Bonferroni multiple comparisons tests were used for the single comparisons.

Appendix

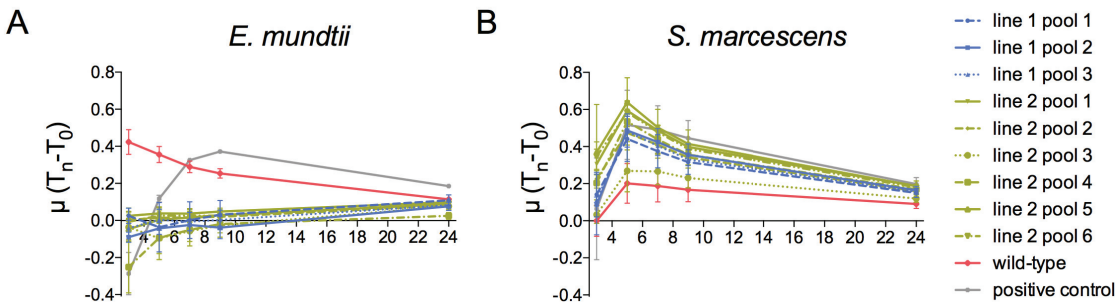

Figure A.1. Growth rates of *E. mundtii* (A) and *S. marcescens* (B) with plasma extracted from wild-type and transgenic larvae. Hemolymph was collected from 9 individuals pooled in three replicates (line 1 and wilk-type) or from 18 individuals pooled in six replicates (line 2). The hemocyte-free plasma was added to microbial cultures ($5*10^5$ CFU/mL) and the optical density was measured to monitor the microbial growth. The growth rate was calculated and plotted against time (mean ± SEM).

Chapter 6: Final Considerations

The aim of my PhD project was to characterize which are the main elements of the immune response protecting *Bombyx mori* against pathogen infections. This thesis is part of a wider project which has the final purpose to obtain silkworms enhanced in their pathogen-resistance, but still maintaining good production capabilities. To achieve this objective, two main approaches were used: 1) the characterization of the humoral immune response to oral infections of distinct silkworm strains with different geographical origin, particularly focusing on antimicrobial peptides (AMPs), the most important effectors of the innate immunity; 2) the production and characterization of transgenic silkworms over-expressing specific AMPs.

We started from the general observation that silkworm domesticated strains belonging to different geographical areas often show a differential sensitivity to pathogens. In particular, lines originating from temperate regions possess the highest productivity, in terms of both silk quality and quantity, but are very susceptible to diseases. On the contrary tropical strains produce low quantities of poor quality silk, but are more tolerant to pathogen infections (FAO, 2003). During domestication process, *B. mori* strains have been artificially selected for their productive traits. However, *B. mori* strains might have been also "unintentionally" selected for their ability to counteract infections particularly common in that specific geographical area. The characterization of their immune response would point-out which are the key factors that lead to an increased resistance to infections in silkworms.

Therefore we selected four silkworm strains originating respectively from India, China, Japan and Europe and we characterized them for some of their phenotypic and genotypic traits that are related both to their production capabilities and to their potential ability to respond to oral infections. Then we tested the response of these four strains to oral infections with two silkworm specific pathogens, the Gram-positive *Enterococcus mundtii* and the Gram-negative *Serratia marcescens,* which are both responsible for the development of flacherie in different geographical areas. We investigated different humoral immune mechanisms that could influence the silkworm response to pathogens, particularly focusing on AMPs.

Finally, we generated silkworm transgenic lines carrying a constitutive over-expression of the gene encoding the specific *B. mori* AMP Moricin to study the effect of the AMP over-expression on *B. mori* physiology and to obtain silkworm lines with an enhanced resistance to infections.

Looking at the differential intrinsic characteristics that the four selected strain have, the principal was the voltinism, which is strictly related to the geographical origin. While the Indian line is a polyvoltine tropical strain and it is able to reproduce continuously throughout the year, the Chinese, Japanese and European strains are all monovoltine. The Chinese and Japanese lines were found to be the best silk producers

in terms of quantity, while the European strain was shown to produce the highest quality silk.

B. mori possess at least 21 different AMP genes. Examining the genetic variability at the level of their coding regions, the four lines were shown to have a certain level of polymorphism, with many synonymous and non-synonymous substitutions mapping both in the pre-peptide region and in the active portion. The Indian strain was found to be almost monomorphic in AMP genes, while the other three strains were found to have a higher level of heterozygosity. Although it is expected that the domestication process is associated to a general reduction in heterozygosity (Xia et al, 2009; Bellucci et al, 2014), our data can be explained considering the different rearing conditions which the different strains have been experienced at the CREA-API sericulture center. In fact the Indian line is mainly maintained in small populations since it is mostly used as laboratory strain rather than a silk producer, while the Japanese, Chinese and European strains are used for commercial purposes and therefore reared in large populations.

The infection experiments with *E. mundtii* and *S. marcescens* showed that the four selected *B. mori* lines have differential sensitivity to Gram-positive and -negative oral infections, with the European and Indian lines most resistant to the *E. mundtii* and *S. marcescens* exposures, respectively. For both pathogens the melanization reaction and the Lysozyme concentrations were found not to be directly correlated with the differential pathogen sensitivities of the four *B. mori* strains.

Heterogeneous morphologies in the four strains were observed at the level of the first physical barrier that the pathogen encounters during oral infections and represented by the peritrophic membrane (PM). The European line showed the thickest PM in comparison to those of all the other strains. PM is an essential structure of the insect digestive tract, which protects intestinal *epithelia* from mechanical damages (Wang and Granados, 2001). In *Lepidoptera*, it is continuously formed by the anterior part of the midgut, it moves posteriorly with the food bolus and it is in part released with larval feces (Wang and Granados, 2001). Since insects invest many energy resources in the synthesis and maintenance of this structure, it is clear that it represents an essential component of the larval gastrointestinal tract. However, it is not clear if a thick PM might have a positive or negative effect on pathogen infection progression. For example it was shown that tsetse flies with a disrupted PM were more resistant to oral infection by *Serratia marcescens* (Weiss et al, 2014). In this case, authors hypothesized that a thick and intact PM can be a niche for bacteria stack and proliferation, therefore it is not an advantageous factor when considering oral infections. On the other hand, *Drosophila* was shown to be more susceptible to *Pseudomonas entomophila* and *S. marcescens* when the PM is altered (Kuraishi et al, 2011), suggesting the importance of maintaining intact this structure to protect the gut

lumen from pathogen attack. From our data a thicker PM seemed unrelated to a higher protection against neither *E. mundtii* not *S. marcescens* infections because the European strain showed an AMP expression activation at midgut level and a passage of pathogen cells in the hemolymph circulation at the same time than other strains.

Since the Japanese strain was found to be very sensitive to both infections, it is unlikely that the higher number of phagocytizing hemocytes possessed by this strain at the beginning of the fifth larval stage might be correlated to a higher chance to survive to bacterial infections.

After the infection with the Gram-positive *Enterococcus mundtii* the European strain turned out to be the most resistant line, followed by the Chinese and, at a second stage, by the Japanese and the Indian strains. All four *B. mori* lines were found to activate the AMP transcriptional response at midgut level immediately after the ingestion of the bacterium. Moreover, a massive induction of AMP systemic transcription was observed among the four lines, even if with different profiles. This general transcriptional activation can explain the antimicrobial activity of the *E. mundtii* infected hemolymph for all the four strains.

In addition, the plasma extracted from the European strain showed the highest antimicrobial power in the late stage of infection. Since all the strains actively transcribed AMP genes at this time-point, our data suggest that the key resistance factor for the *E. mundtii* infection might consist in the AMP classes and/or isoforms produced in the European strain at both local and systemic levels.

Different AMP classes are known to show variable antimicrobial *in vitro* activity (Hara and Yamakawa, 1995), a further comparative analysis on the antimicrobial power of the specific AMP types mainly activated in the different strains will shed light on the possible link on the AMP gut activation and the differential behavior of the four strains to infections. In addition, considering AMPs within the same classes, the analysis of the genetic variability identified different AMP isoforms with a predicted higher antimicrobial activities. These variants have been found to be present with higher frequencies (Glv1-iso3, Glv2-iso2) or exclusively (CecB2-iso3) in the European strain. By *in vitro* analysis the CecB2-iso3 showed two-fold higher antimicrobial activity against *E. mundtii* in comparison to CecB2-iso1. The differences in antimicrobial power might be characteristic also of the Glv1 and 2 isoforms and future experiments are planned to evaluate this hypothesis. Interestingly, a recent study showed that the presence of an amino acid polymorphism in *Drosophila* Diptericin was highly predictive of resistance to specific bacterial infections (Unckless et al, 2016). It is also important to underline that the difference revealed *in vitro* might be amplified in physiological conditions *in vivo.* In fact it is believed that the peptide concentration sufficient to inhibit the bacterial growth *in vitro* is probably considerably higher than in physiological conditions (Phoenix et al, 2013).

Regarding the *S. marcescens* infection, there is a general correlation between the survival profile and the systemic AMP transcription activation. Of the four *B. mori* strains only the Indian one efficiently responded to the pathogen and survived to the infection. None of the infected individuals of the other three strains, reached the adult stage and, in general, the AMP transcriptional activation was low or delayed during larval stage. In addition only this resistant line was able to induce a considerable and immediate systemic AMP response, with many of the investigated AMP genes found to be significantly over-expressed. The peculiar resistance of the Indian strain might be due to a more efficient activation of recognition factors as well as other elements involved in the *B. mori* physiology, such as the Juvenile hormone (JH)/Ecdysone hormone balance and the nitric oxide (NO) levels.

The flacherie disease induced by *S. marcescens* is a recurrent infection in tropical areas silkworm livestocks. Therefore, the Indian strain, might possess more efficient recognition factors for this pathogen, rapidly inducing a prompt and effective immune response against this infection.

A second possibility might be linked to the hormone dosages. Hormones are the main regulators of insect life cycle, from embryogenesis to egg hatching, from larval molting to metamorphosis. In particular, these two latter events are triggered through Ecdysone and JH activities (Riddiford, 2008; Tian et al, 2010). In *Drosophila* adult flies, Ecdysone is essential for the activation of the Imd-pathway against Gram-negative bacteria infections (Buchon et al, 2014). On the other hand, RNAi and hormone treatment experiments in *B. mori* suggested that JH might act as activator of immune defenses, while Ecdysone might be an inhibitor of such responses (Tian et al, 2010). Infection of *B. mori* larvae with both *Bacillus bombyseptieus* and *Nosema bombycis* lead to alterations in the transcription levels of many elements of the JH signaling cascade, suggesting an involvement of these signaling cascades in the regulation of the immune response (Huang et al, 2009; Ma et al, 2013). In addition, topical applications of the JH analog Methoprene are able to induce AMP production in fat bodies of *B. mori* larvae, confirming the role of this hormone in the activation of the systemic immunity (Tian et al, 2010). Since the Indian strain was the only polyvoltine line, its general hormone levels might be different with respect to the other monovoltine strains and this difference might be also responsible of its enhanced AMP production capability.

A third possible scenario might be hypothesized considering that, in Insects, a inter-tissue communication plays a role in the stimulation of the systemic immune response. It has been demonstrated that during oral infections, in *Drosophila* a systemic response can be activated independently from bacteria physical crossing of the gastric barrier, suggesting the presence of a communication from gut to fat bodies (Broderick et al, 2009). One of the important factor in this phenomenon is the NO, a

soluble molecule synthesized by NO Synthase (NOS). In *B. mori*, the ingestion of both Gram-negative and -positive bacteria induces NOS transcription at the level of both gut and hemocytes. As a result, NO levels are increased in the gut and contribute to the local defense against the bacterial infection (Zhang et al, 2015). Moreover, NO is responsible for the up-regulation of AMPs in the fat bodies of both *Drosophila* and *Bombyx*, since the treatment of flies with NO donors is sufficient to trigger the AMP systemic response (Imamura et al, 2002; Foley and O'Farrell, 2003).

These candidates will be further investigated for their differential expression/ activity in the four strains.

Regarding the generation of AMP over-expressing *B. mori* strains, currently two independent transgenic lines over-expressing Moricin were obtained. The uninfected plasma of both lines showed higher antimicrobial activity against *E. mundtii* but not versus *S. marcescens*. Future experiments are planned to analyze the sensitivities of these lines against an *E. mundtii* infection. On the basis of these results, the *moricin* transgene could be transferred in other *B. mori* lines used for silk production.

Finally the AMP over-expressing transgenic lines might be used also to obtain high amounts of silkworm AMPs, since both chemical synthesis and production using heterologous systems are challenging technologies. Therefore, the use of the silkworm as bioreactor for the production of native AMPs could accelerate the study on these molecules, which possess an intrinsic pharmacological interest.

References

Axen A, Carlsson A, Engström A, Bennich H (1997) *Gloverin, an Antibacterial Protein from the Immune Hemolymph of Hyalophora Pupae,* European Journal of Biochemistry 247: 614-619.

Ayoade F, Oyejide NE, Fayemi SO (2014) *Isolation, Identification, Antibiogram and Characterization of Bacterial Pathogens of the Silkworm, Bombyx mori in South-West Nigeria*, Journal of Biological Sciences, doi: 10.3923/jbs.2014

Bassi A (1835) *Del mal del segno, calcinaccio o moscardino*.

Bellucci E, Bitocchi E, Ferrarini A, Benazzo A, Biagetti E, Klie S, Minio A, Rau D, Rodriguez M, Panziera A et al (2014) *Decreased Nucleotide and Expression Diversity and Modified Coexpression Patterns Characterize Domestication in the Common Bean*, The Plant Cell 26: 1901-1912.

Binggeli O, Neyen C, Poidevin M, lemaitre B (2014) *Prophenoloxidase Activation Is Required for Survival to Microbial Infections in Drosophila*, PLoS Pathogens 10(5): e1004067.

Broderick NA, Welchman DP, Lamaitre B (2009) *Recognition and Response to Microbial Infection in Drosophila,* Insect Infection and Immunity. Evolution, Ecology, and Mechanisms, Oxford (NY): Oxford University Press.

Buchon N, Silverman N, Cherry S (2014) *Immunity in Drosophila melanogaster - from Microbial Recognition to Whole-Organism Physiology*, Nature Reviews Immunology, 14: 796-810.

Bulet P, Hetru C, Dimarcq J-L, Hoffmann D (1999) *Antimicrobial Peptides in Insects; Structure and Function*, Developmental and Comparative Immunology 23: 329-344.

Callaway JE, Lai J, Haselbeck B, Baltain M, Bonnesen SP, Weickmann J, Wilcox G, Lei SP (1993) *Modification of the C Terminus of Cecropin Is Essential for Broad-Spectrum Antimicrobial Activity*, Antimicrobial Agents and Chemotherapy, 37(8): 1614-1619.

Cappellozza L, Cappellozza S, Saviane A, Sbrenna G (2005) *Artificial Diet Rearing System for the Silkworm Bombyx mori (Lepidoptera: Bombycidae): Effect of Vitamin C Deprivation on Larval Growth and Cocoon Production*, Applied Entomology and Zoology 40: 405-412.

Cappellozza S, Saviane A, Tettamanti G, Squadrin M, Vendramin E, Paolucci P, Franzetti E, Squartini A (2011) *Identification of Enterococcus mundtii as a pathogenic agent involved in the ''flacherie'' disease in Bombyx mori L. larvae reared on artificial diet*, Journal of Invertebrate Pathology 106: 386-393.

Carlsson A, Engström P, Palva ET, Bennich H (1991) *Attacin, an Antibacterial Protein from Hyalophora cecropia, Inhibits Synthesis of Outer Membrane Proteins in Escherichia coli by Interfering with omp GeneTranscription*, Infection and Immunity 59(9): 3040-3045.

Cerenius L, Söderhäll K (2004) *The Prophenoloxidase-Activating System in Invertebrates*, Immunological Reviews 198: 116-126.

Chowdhury S, Taniai K, Hara S, Kadono-Okuda K, Kato Y, Yamamoto M, Xu J, Choi SK, Debnath NC, Choi HK, Miyanoshita A, Sugiyama M, Asaoka A, Yamakawa M, *cDNA Cloning and Gene Expression of Lebocin, a Novel Member of Antimicrobial Peptides from the Silkworm, Bombyx mori*, Biochemical and Biophysical Research Communicarions 214(1): 271-278.

Christensen B, Fink J, Merrifield RB, Mauzerall D (1988) *Channel-Forming Properties of Cecropins and Related Model Compounds Incorporated into Planar Lipid Membranes*, Proceedings of the National Academy of Science 85: 5072-5076.

Clark KD, Strand MR (2013) *Hemolymph Melanization in the Silkmoth Bombyx mori Involves Formation of a High Molecular Mass Complex that Metabolizes Tyrosine*, Journal of Biological Chemistry 288, doi: 10.1074/jbc.M113.459222.

Deng DJ, Xu HF, Wang F, Duan X, Ma SY, Xiang ZH, Xia Q (2013) *The Promoter of BmLp3 Gene can Direct Fat Body-Specific Expression in the Transgenic Silkworm, Bombyx mori*, Transgenic Research 22: 1055-1063.

Diaz Sanchez AA, Corzo Lopez M, Baez Arias M, Espinosa Castaño I, Prieto Abreu M, Fiallo Madruga RC (2014) del Carmen Perez Hernandez M, Martinez Zubiaur Y, *Pathogenic bacteria of Bombyx mori L. larvae in breeding areas of Cuba,* Revista de protección vegetal 29(3): 216-219.

Dudzic JP, Kondo S, Ueda R, Bergman CM, Lemaitre B (2015) *Drosophila Innate Immunity: Regional and Functional Specialization of Prophenoloxidases*, BMC Biology 13: 81, DOI 10.1186.

Eleftherianos I, More K, Spivack S, Paulin E, Khojandi A, Shukla S (2014) *Nitric Oxide Levels Regulate the Immune Response of Drosophila melanogaster Reference Laboratory Strains to Bacterial Infections*, Infection and Immunity 82(10): 4169-4181.

Elrod-Erickson M, Mishra S, Schneider D (2000) *Interactions Between the Cellular and Humoral Immune Responses in Drosophila*, Current Biology 10: 781-784.

FAO (2003) *Conservation status of sericulture germplasm resources in the world. I. Conservation status of silkworm genetic resources in the world*, compiled by Sohn KW, Rural Infrastructure and Agro-Industries Division. FAO, Rome. http://www.fao.org/3/a-ad108e/ad108e0a.htm#bm10

Ferrandon D, ImLer JL, Hetru C, Hoffmann JA (2007) *The Drosophila Systemic Immune Response: Sensing and Signaling During Bacterial and Fungal Infections*, Nature Reviews Immunology 7: 862–874.

Fine DH, Toruner GA, Velliyagounder K, Sampathkumar V, Godboley D, Furgang D (2013) *A Lactotransferrin Single Nucleotide Polymorphism Demonstrates Biological Activity That Can Reduce Susceptibility to Caries*, Infection and Immunity 81(5): 1596-1605.

Fine DH, Toruner GA, Velliyagounder K, Sampathkumar V, Godboley D, Furgang D (2013) *A Lactotransferrin Single Nucleotide Polymorphism Demonstrates Biological Activity That Can Reduce Susceptibility to Caries*, Infection and Immunity 81(5): 1596-1605.

Foley E, O'Farrell PH (2003) *Nitric Oxide Contributes to Induction of Innate Immune Responses to Gram-Negative Bacteria in Drosophila*, Genes and Development 17: 115-125.

Fraser MJ (2012) *Insect Transgenesis: Current Applications and Future Prospects*, Annual Review of Entomology 57: 267-289.

Gandhe A, Janardhan G, Nagaraju J (2007) *Immune Upregulation of Novel Antibacterial Proteins from Silkmoths (Lepidoptera) that Resemble Lysozymes but Lack Muramidase Activity*, Insect Biochemistry and Molecular Biology 37(7): 655-666.

Goldsmith MR, Shimada T, Abe H (2005) *The Genetics and Genomics of the Silkworm, Bombyx mori*, Annual Review of Entomologies 50: 71-100.

Gottar M, Gobert V, Michel T, Belvin M, Duyk G, Hoffmann JA, Ferrandon D, Royet J (2002) *The Drosophila Immune Response Against Gram-negative Bacteria is Mediated by a Peptidoglycan Recognition Protein*, Nature 416, 640-644.

Handler AM (2002) *Use of the piggyBac Transposon for Germ-line Transformation of Insects*, Insect Biochemistry and Molecular Biology 32: 1211-1220.

Hara S, Yamakawa M (1995) *A Novel Antimicrobial Peptide Family Isolated form the Silkworm, Bombyx mori*, Biochemistry Journal 310: 651-656.

Hara S, Yamakawa M (1995) *Moricin, a Novel Type of Antibacterial Peptide Isolated from the Silkworm, Bombyx mori*, Journal of Biological Chemistry 270(50): 29923–29927.

Hemmi H, Ishibashi J, Hara S, Yamakawa M (2002) *Solution Structure of Moricin, an Antibacterial Peptide, Isolated from the Silkworm Bombyx mori*, FEBS Letters 518: 33-38.

Himeno M, Matsubara F, Hayashiya K (1973) *The Occult Virus of Nuclear Polyhedrosis of the Silkworm Larvae*, Journal of Invertebrate Pathology 22(2): 292-295.

Hou C, Qin G, Liu T, Geng T, Gao K, Pan Z, Qian H, Guo X (2014) *Transcriptome Analysis of Silkworm, Bombyx mori, during Early Response to Beauveria bassiana Challenges,* PLoS ONE 9(3): e911

Hoy MA (2003) *Transgenic Insects for Pest Management Programs: Status and Prospects*, Environmental Biosafety Research 2(1): 61-64.

http://www.catalogueoflife.org/col/browse/tree?d3a2b84cd742df79b09306d72e46959e

Hu H, Wang C, Guo X, Li W, Wang Y, He Q (2013) *Broad Activity against Porcine Bacterial Pathogens Displayed by Two Insect Antimicrobial Peptides Moricin and Cecropin B*, Molecules and Cells 35, 106-114.

Hua XT, Ma XJ, Xue RJ, Cheng TC, Wang F and Xia QY (2015) *Characterization of the Bombyx mori Cecropin A1 promoter regulated by IMD pathway*, Insect Science 0: 1-8.

Huang L, Cheng T, Xu P, Cheng D, Fang T, Xia Q (2009) *A Genome-Wide Survey for Host Response of Silkworm, Bombyx mori during Pathogen Bacillus bombyseptieus Infection*, PLoS ONE 4(12): e8098.

Iijima N, Tanimoto N, Emoto Y, Morita Y, Uematsu K, Murakami T, Nakai T (2003) *Purification and Characterization of Three Isoforms of Chrysophsin, a Novel Antimicrobial Peptide in the Gills of the Red Sea Bream, Chrysophrys major*, European Journal of Biochemistry 270: 657-686.

Imamura M, Yang J, Yamakawa M (2002) *cDNA Cloning, Characterization and Gene Expression of Nitric Oxide Synthase from the Silkworm, Bombyx mori*, Insect Molecular Biology 11(3): 257-265.

Ishii K, Adachi T, Hara T, Hamamoto H, Sekimizu K (2014) *Identification of a Serratia marcescens virulence factor that promotes hemolymph bleeding in the silkworm, Bombyx mori*, Journal of Invertebrate Pathology 117: 61-67.

Jiang H, Kanost MR (2000) *The Clip-Domain Family of Serine Proteinases in Arthropods*, Insect Biochemistry and Molecular Biology 30: 95–105.

Kaufmann B, El-Far M, Plevka P, Bowman VD, Li Y, Tijssen P, Rossmann MG (2011) *Structure of Bombyx mori Densovirus 1, a Silkworm Pathogen*, Journal of Virology 85(10): 4691-4697.

Kawaoka S, Katsuma S, Daimon T, Isono R, Omuro N, Mita K, Shimada T (2008) *Functional Analysis of Four Gloverin-like Genes in the Silkworm, Bombyx mori*, Archives of Insect Biochemistry and Physiology 67: 87-96.

Kim SH, Park BS, Yun EY, Je YH, Woo SD, Kang SW, Kim KY, Kang SK (1998) *Cloning and Expression of a Novel Gene Encoding a New Antibacterial Peptide from Silkworm, Bombyx mori*, Biochemical and Biophysical Research Communications 246, 388-392.

Kim SR, Lee KS, Kim I, Kang SW, Nho SK, Sohn HD, Jin BR (2003) *cDNA Sequence of a Novel Immulectin Homologue from the Silkworm Bombyx mori*, International Journal of Industrial Entomology 6(1): 99-102.

Kirby AJ (1987) *Mechanism and stereoelectronic effects in the lysozyme reaction*, Critical Reviews in Biochemistry and Molecular Biology 22(4): 283-315.

Koizumi N, Imamura M, Kadotani T, Yaoi K, Iwahana H, Sato R (1999) *The lipopolysaccharide-binding protein participating in hemocyte nodule formation in the silkworm Bombyx mori is a novel member of the C-type lectin superfamily with two different tandem carbohydrate-recognition domains*, Federation of European Biochemical Societies Letters 443: 139-143.

Kounatidis I, Ligoxygakis P (2012) *Drosophila as Model System to Unravel the Layers of Innate Immunity to Infection*, Open Biology 2: 120075.

Kuraishi T, Hori A, Kurata S (2013) *Host-microbe Interactions in the Gut of Drosophila melanogaster,* Frontiers in Physiology 4, doi: 10.3389.

Kurata S (2014) *Peptidoglycan Recognition Proteins in Drosophila immunity,* Developmental and Comparative Immunology 42: 36-41.

Kurz CL, Chauvet S, Andres E, Aurouze M, Vallet I, Michel GP, Uh M, Celli J, Filloux A, De Bentzmann S et al (2003) *Virulence Factors of the Human Opportunistic Pathogen Serratia marcescens Identified by in Vivo Screening,* EMBO Journal 22: 1451-1460.

Ladendorff NE, Kanost MR (1990) *Isolation and Characterization of Bacteria-Induced Protein P4 from Hemolymph of Manduca sexta*, Archives of Insect Biochemistry and Physiology 15: 33-41.

Lamaitre B, Nicolas E, Michaut L, Reichhart JM, Hoffmann JA (1996) *The Dorsoventral Regulatory Gene Cassette spätzle/Toll/cactus Controls the Potent Antifungal Response in Drosophila Adults*, Cell 86: 973-983.

Lamaitre B, Reichhart J, Hoffmann JA (1997) *Drosophila Host Defense: Differential Induction of Antimicrobial Peptide Genes After Injection by Various Classes of Microorganisms*, Proceedings of the National Academy of Science 94, 14614-14619.

Lauth X, Shike H, Burns JC, Westerman ME, Ostland VE, Carlberg JM, Van Olst JC, Nizet V, Taylor SW, Shimizu C, Bulet P (2001) *Discovery and Characterization of Two Isoforms of Moronecidin, a Novel Antimicrobial Peptide from Hybrid Striped Bass*, Journal of Biological Chemistry, 277(7): 5030-5039.

Lavine MD, Strand MR (2002) *Insect Hemocytes and Their Role in Immunity*, Insect Biochemistry and Molecular Biology 32: 1295-1309.

Lazzaro BP, Clark G (2003) *Molecular Population Genetics of Inducible Antibacterial Peptide Genes in Drosophila melanogaster*, Molecular Biology Evolution 20(6): 914-923.

Lazzaro BP, Sackton TB, Clark G (2006) *Genetic Variation in Drosophila melanogaster Resistance to Infection: a Comparison Across Bacteria*, Genetics 174: 1539-1554.

Lazzaro BP, Sceurman BK, Clark AG (2004) *Genetic Basis of Natural Variation in D. melanogaster Antibacterial Immunity*, Science 303: 1873-1876.

Lee WJ, Brey PT (1995) *Isolation and Characterization of the Lysozyme-Encoding Gene from the Silkworm Bombyx mori*, Gene 161: 199-203.

Lee WJ, Lee JD, Kravchenko VV, Ulevitch RJ, Brey PT (1996) *Purification and Molecular Cloning of an Inducible Gram-negative Bacteria-Binding Protein from the Silkworm, Bombyx mori*, Proceedings of the National Academy of Science 93: 7888-7893.

Lewies A, Frederik WJ, Garmi J, Du Plessis LH (2015) *The Potential Use of Natural and Structural Analogues of Antimicrobial Peptides in the Fight against Neglected Tropical Diseases*, Molecules 20: 15392-15433.

Ma Z, Li C, Pan C, Li Z, Han B, Xu J, Lan X, Chen J, Yang D, Chen Q et al (2013) *Genome-Wide Transcriptional Response of Silkworm (Bombyx mori) to Infection by the Microsporidian Nosema bombycis*, PLoS ONE 8(12): e84137.

Marassi FM, Opella SJ, Juvvadi P, Merrifield RB (1999) *Orientation of Cecropin A Helices in Phospholipid Bilayers Determined by Solid-State NMR Spectroscopy*, Biophysical Journal 77: 3152-3155.

Marmaras VJ, Lampropoulou M (2009) *Regulators and Signalling in Insect Hemocyte Immunity*, Cellular Signalling 21: 186-195.

Matzinger P (2002) *The Danger Model: A Renewed Sense of Self*, Science 296(5566): 301-305.

Medzhitov R, Preston-Hurlburt P, Janeway CA (1997) *A Human Homologue of the Drosophila Toll protein signals activation of adaptive immunity*, Nature (388):394-397.

Mellroth P, Karlsson J, Steiner H (2003) *A Scavenger Function for a Drosophila Peptidoglycan Recognition Protein*, Journal of Biological Chemistry, 278(9): 7059-7064.

Michel T, Reichhart JM, Hoffmann JA , Royet J (2001) *Drosophila Toll is Activated by Gram-Positive Bacteria Through a Circulating Peptidoglycan Recognition Protein*, Nature 414, 756-759.

Mikonranta L, Mappes J, Kaukoniitty M, Freitak D (2014) *Insect Immunity: Oral Exposure to a Bacterial Pathogen Elicits Free Radical Response and Protects from a Recurring Infection*, Frontiers in Zoology 11:23.

Mishima Y, Quintin J, Aimanianda V, Kellenberger C, Coste F, Clavaud C, Hetru C, Hoffmann JA, Latgé JP, Ferrandon D, Roussel A (2009) *The N-terminal Domain of Drosophila Gram-negative Binding Protein 3 (GNBP3) Defines a Novel Family of Fungal Pattern Recognition Receptors*, Journal of Biological Chemistry 284(42): 28687-28697.

Morishima I, Horiba T, Iketani M, Nishioka E, Yamano Y (1995) *Parallel Induction of Cecropin and Lysozyme in Larvae of the Silkworm, Bombyx mori*, Developmental and Comparative Immunology 19(5): 357-363.

Morishima I, Horiba T, Yamano Y (1994) *Lysozyme Activity in Immunized and Non-Immunized Hemolymph During the Development of the Silkworm, Bombyx mori,* Comparative Biochemistry and Physiology 108A(2/3): 311-314.

Müller H, Salzig D, Czermak P (2014) *Considerations for the Process Development of Insect-Derived Antimicrobial Peptide Production*, Biotechnology Progress 31: 1-11, doi: 10.1002/btpr.2002.

Nakatsuji T, Gallo RL (2012) *Antimicrobial Peptides: Old Molecules with New Ideas*, Journal of Investigative Dermatology 132: 887-895.

Nehme TN, Liégeois S, Kele B, Giammarinaro P, Pradel E, Hoffmann JA, Ewbank JJ, Ferrandon D (2007) *A Model of Bacterial Intestinal Infections in Drosophila melanogaster*, PLoS Pathogens 3(11): 1694-1709, e173.

Nguyen LT, Haney AF, Vogel HJ (2011) *The Expanding Scope of Antimicrobial Peptide Structures and Their Modes of Action*, Trends in Biotechnology 29(9): 464-472.

Nwibo DD, Hamamoto H, Matsumoto Y, Kaito C, Sekimizu K (2015) *Current Use of Silkworm Larvae (Bombyx mori) as an Animal Model in Pharmaco-medical Research*, Drug Discoveries and Therapeutics 9(2): 133-135.

Nwibo DD, Matsumoto Y, Sekimizu K (2015) *Identification and Methods for Prevention of Enterococcus mundtii Infection in Silkworm Larvae, Bombyx mori, Reared on Artificial Diet*, Drug Discoveries & Therapeutics 9(3): 184-190.

Ochiai M, Ashida M (1988) *Purification of a β-1,3-Glucan Recognition Protein in the Prophenoloxidase Activating System from Hemolymph of the Silkworm, Bombyx mori*, Journal of Biological Chemistry 263(24): 12056-12062.

Ochiai M, Ashida M (2000) *A Pattern-Recognition Protein for β-1,3-glucan. The Binding Domain and the cDNA Cloning of β-1,3-glucan Recognition Protein from the Silkworm, Bombyx mori*, Journal of Biological Chemistry 275(7): 4995-5002.

Ohta M, Watanabe A, Mikami T, Nakajima Y, Kitami M, Tabunoki H, Ueda K, Sato R (2006) *Mechanism by which Bombyx mori Hemocytes Recognize Microorganisms: Direct and Indirect Recognition Systems for PAMPs*, Developmental and Comparative Immunology 30: 867-877.

Pasteur L (1870) *Etudes sur la Maladie des Vers a Soie, Moyen Pratique Assure de la Combattre et d'en Prevenir le Retour: la Pébrine et la Flacherie*, Gauthier-Villars. Paris, ed.

Pelte N, Robertson AS, Zou Z, Belorgey D, Dafforn TR, Jiang H, Lomas D, Reichhart J-M, Gubb D (2006) *Immune Challenge Induces N-terminal Cleavage of the Drosophila Serpin Necrotic*, Insect Biochemistry and Molecular Biology 36: 37–46.

Phoenix DA, Dennison SR, Harris F (2013) *Antimicrobial Peptides*, Wiley-VCH Verlag GmbH & Co. KGaA, Weinheim (Germany).

Ponnuvel KM, Subhasri N, Sirigineedi S, Murthy GN, Vijayaprakash NB (2010) *Molecular Evolution of the Cecropin Multigene Family in Silkworm Bombyx mori*, Bioinformation 5(3): 97-103.

Radzeka A and Wolfenden R (1988) *Comparing the Polarities of Amino Acids: Side-Chain Distribution Coefficients Between Vapor Phase, Cyclohexane, 1-Octanol and Neutral Aqueous Solution*, Biochemistry 27, 1664-1670.

Rämet M, Manfruelli P, Pearson A, Mathey-Prevot B, Ezekowitz RAB (2002) *Functional Genomic Analysis of Phagocytosis and Identification of a Drosophila Receptor for E. coli*, Nature 416: 644-648.

Rao X-J, Shahzad T, Liu S, Wu P, He Y-T, Sun W-J, Fan X-Y, Yang Y-F, Shi Q, Yu X-Q (2015) *Identification of C-type Lectin-Domain Proteins (CTLDPs) in Silkworm Bombyx mori*, Developmental and Comparative Immunology 53: 328-338.

Rasmuson T, Boman HG (1979) *Insect Immunity V. Purification and some Properties of Immune Protein P4 from Haemolymph of Hyalophora cecropia Pupae*, Insect Biochemistry 9: 259-270.

Ravaglioli L, Bombacci A (1997) *Meldola, il Baco e la Seta: Tradizione e Storia della Sericoltura nel Territorio*, Forlì: Edizioni Litocartotecnica Citienne.

Repizo GR, Espariz M, Blancato VS, Suàrez CA, Esteban L, Magni C (2014) *Genomic Comparative Analysis of the Environmental Enterococcus mundtii Against Enterococcal Representative Species*, BMC Genomics 15: 489.

Riddiford LM (2008) *Juvenile Hormone Action: a 2007 Perspective*, Journal of Insect Physiology 54: 895-901.

Santabárbara-Ruiz P, López-Santillán M, Martínez-Rodríguez I, Binagui-Casas A, Pérez L, Milán M, Corominas M, Serras F (2015) *ROS-Induced JNK and p38 Signaling Is Required for Unpaired Cytokine Activation during Drosophila Regeneration*, PLoS Genetics, doi: 10.1371/journal.pgen.1005595.

Schleifer KH, Kandler O (1972) *Peptidoglycan Types of Bacterial Cell Walls and Their Taxonomic Implications*, Bacteriological Reviews 36(4): 407–477.

Shao Q, Yang B, Xu Q, Li X, Lu Z, Wang C, Huang Y, Söderhäll K, Ling E (2012) *Hindgut Innate Immunity and Regulation of Fecal Microbiota through Melanization in Insects*, Journal of Biological Chemistry 28(17): 14270-14279.

Shelby KS, Cui L, Webb BA (1998) *Polydnavirus-Mediated Inhibition of Lysozyme Gene Expression and the Antibacterial Response*, Insect Molecular Biology 7(3): 265-272.

Stokes BA, Yadav S, Shokal U, Smith LC, Eleftherianos I (2015) *Bacterial and Fungal Pattern Recognition Receptors in Homologous Innate Signaling Pathways of Insects and Mammals*, Frontiers in Microbiology 6(19): 1-12.

Strand MR (2008) *The Insect Cellular Immune Response*, Insect Science 15: 1-14, 10.1111

Sugiyama M, Kuniyoshi H, Kotani E, Taniai K, Kadono.Okuda K, Kato Y, Yamamoto M, Shimabukuro M, Chowdhury S, Xu J, Choi SK, Kataoka H, Suzuki A, Yamakawa M (1995) *Characterization of a Bombyx mori cDNA Encoding a Novel Member of the Attacin Family of Insect Antibacterial Proteins*, Insect Biochemistry and Molecular Biology 3: 385-392.

Sun W, Yu HS, Shen YH, Banno Y, Xiang ZH, Zhand Z (2012) *Phylogeny and Evolutionary History of the Silkworm*, Life Sciences China 55(6): 483-496.

Suttmann H, Retz M, Paulsen F, Harder J, Zwerge U, Kamradt J, Wullich B, Unteregger G, Stöckle M, Lehmann J (2008) *Antimicrobial Peptides of the Cecropin-family Show Potent Antitumor Activity Against Bladder Cancer Cells*, BMC Urology 8:5, doi: 10.1186/1471-2490-8-5.

Takahasi K, Ochiai M, Horiuchi M, Kumeta H, Ogura K, Ashida M, Inagaki F (2009) *Solution Structure of the Silkworm GRP/GNBP3 N-terminal Domain Reveals the Mechanism for β-1,3-Glucan-Specific Recognition*, Proceedings of the National Academy of Science 106(28): 11679-11684.

Takase H, Watanabe A, Yoshizawa Y, Kitami M, Sato R (2009) *Identification and Comparative Analysis of Three Novel C-type Lectins from the Silkworm with Functional Implications in Pathogen Recognition*, Developmental and Comparative Immunology 33: 789-800.

Tamura T, Thibert C, Royer C, Kanda T, Abraham E, Kamba M, Kômoto N, Thomas JL, Mauchamp B, Chavancy G, Shirk P, Fraser M, Prudhomme JC, Couble P (2000) *GermLine Transformation of the Silkworm Bombyx mori L. Using a PiggyBac Transposon-derived Vector*, Nature Biotechnology 18: 81-84.

Tanaka H, Furukawa S, Nakazawa H, Sagisaka A, Yamakawa M (2005) *Regulation of Gene Expression of Attacin, an Antibacterial Protein in the Silkworm, Bombyx mori*, Journal of Insect Biotechnology and Sericology 74, 45-56.

Tanaka H, Ishibashi J, Fujita K, Nakajima Y, Sagisaka A, Tomimoto K, Suzuki N, Yoshimaya M, Kaneko Y, Iwasaki T, Sunagawa T, Yamaji K, Ashoka A, Mita K, Yamakawa M (2008) *A Genome-Wide Analysis of Genes and Gene Families Involved in Innate Immunity of Bombyx mori*, Insect Biochemistry and Molecular Biology 38: 1087-1110.

Tanaka H, Yamakawa M (2011) *Regulation of the Immune Responses in the Silkworm Bombyx mori*, Invertebrate Survival Journal 8: 59-69.

Teixeira V, Feio MJ, Bastos M (2012) *Role of Lipids in the Interaction of Antimicrobial Peptides with Membranes*, Progress in Lipid Research 51: 149-177.

Tennessen JA (2005) *Molecular evolution of animal antimicrobial peptides: widespread moderate positive selection*, Journal of Evolutionary Biology 18: 1387-1394.

Tian L, Guo E, Diao Y, Zhou S, Peng Q, Cao Y, Ling E, Li S (2010) *Genome-wide Regulation of Innate Immunity by Juvenile Hormone and 20-hydroxyecdysone in the Bombyx Fat Body*, BMC Genomics 11: 549.

Tokura A, Fu GS, Sakamoto M, Endo H, Tanaka S, Kikuta S, Tabunoki H, Sato R (2013) *Factors Functioning in Nodule Melanization of Insects and their Mechanisms of Accumulation in Nodules*, Journal of Insect Physiology 60: 40-49.

Torrent M, Di Tommaso P, Pulido D, Nogués MV, Notredame C, Boix E, AndreuD (2012) *AMPA: an Automated Web Server for Prediction of Protein Antimicrobial Regions,* Bioinformatics 28:130-131.

Unckless RL, Howick VM, Lazzaro BP (2016) *Convergent Balancing Selection on an Antimicrobial Peptide in Drosophila*, Current Biology 26, http://dx.doi.org/10.1016/j.cub.2015.11.063

Vasantharajan VN, Munirathnamm N (1978) *Studies on Silkworm Diseases-III Epizootiology of a Septicemic Disease of Silkworms caused by Serratia marcescens*, Journal of the Indian Institute of Science 60(4).

Vega FE, Kaya HK (2012) *Insect Pathology*, London (UK): Academic Press, Elsevier.

Velliyagounder K, Kaplan JB, Furgang D, Legarda D, Diamond G, Parkin RE, Fine DH (2003) *One of Two Human Lactoferrin Variants Exhibits Increased Antibacterial and Transcriptional Activation Activities and is Associated with Localized Juvenile Periodontitis*, Infection and Immunity:6141-6147.

Venken KJT, Bellen HJ (2007) *Transgenesis upgrades for Drosophila melanogaster*, Development 134: 3571-3584.

Waghu FH, Gopi L, Barai RS, Ramteke P, Nizami B, Idicula-Thomas S (2013) *CAMP: Collection of Sequences and Structures of Antimicrobial Peptides,* Nucleic Acids Research 42: D1154–D1158.

Wang G, Li X and Wang Z (2009) A*PD2: the Updated Antimicrobial Peptide Database and its Application in Peptide Design,* Nucleic Acids Research 37: D933-D937.

Wang G, Mishra B, Lau K, Lushnikova T, Gold R, Wang X (2015) *Antimicrobial Peptides in 2014*, Pharmaceuticals 8: 123-150.

Wang P, Granados RR (2001) *Molecular Structure of the Peritrophic Membrane (PM): Identification of Potential PM Target Sites for Insect Control*, Archives of Insect Biochemistry and Physiology 47: 110–118.

Wang Y, Cheng T, Rayaprolu S, Zou Z, Xia Q, Xiang Z, Jian H (2007) *Proteolytic Activation of Pro-Spätzle is Required for the Induced Transcription of Antimicrobial Peptide Genes in Lepidopteran Insects*, Developmental and Comparative Immunology 31: 1002–1012.

Watanabe A, Miyazawa S, Kitami M, Tabunoki H, Ueda K, Sato R (2006) *Characterization of a Novel C-Type Lectin, Bombyx mori Multibinding Protein, from the B. mori Hemolymph: Mechanism of Wide-Range Microorganism Recognition and Role in Immunity*, Journal of Immunology, 177: 4594-4604.

Wei ZJ, Liao AM, Zhang HX, Liu J, Jiang ST (2009) *Optimization of Supercritical Carbon Dioxide Extraction of Silkworm Pupal Oil Applying the Response Surface Methodology*, Bioresource Technology 100: 4214-4219.

Weis WI, Taylor ME, Drickamer K (1998) *The C-type Lectin Superfamily in the Immune System*, Immunological Reviews 163: 19-34.

Weiss BL, Savage AF, Griffith BC, Wu Y, Askoy S (2014) *The Peritrophic Matrix Mediates Differential Infection Outcomes in the Tsetse Fly Gut Following Challenge with Commensal, Pathogenic and Parasitic Microbes*, Journal of Immunology 193: 773-782.

Wen H, Lan X, Cheng T, He N, Shiomi K, Kajiura Z, Zhou Z, Xia Q, Xiang Z, Nakagaki M (2009) *Sequence Structure and Expression Pattern of a Novel Anionic Defensin-Like Gene from Silkworm (Bombyx mori)*, Molecular Biology Reports 36: 711-716.

Weng H, Pan A, Yang L, Zhang C, Liu Z, Zhang D (2004) *Estimating Number of Transgene Copies in Transgenic Rapeseed by Real-Time PCR Assay With HMG I/Y as an Endogenous Reference Gene*, Plant Molecular Biology Reporter 22: 289-300.

Werner T, Liu G, Kang D, Ekengren S, Steiner H, Hultmark D (2000) *A Family of Peptidoglycan Recognition Proteins in the Fruit Fly Drosophila melanogaster*, Proceedings of the National Academy of Science 97(25): 13772-13777.

Widdel F (2010) *Theory and Measurement of Bacterial Growth,* University Bremen. Available online at: www.mpi-bremen.de/Binaries/Binary13037/Wachstumsversuch.pdf

Wu JH, Wang Z, Xu SY (2007) *Preparation and Characterization of Sericin Powder Extracted from Silk Industry Wastewater*, Food Chemistry 103(4): 1255-1262.

Wu M, Maier E, Benz R, Hancock REW (1999) *Mechanism of Interaction of Different Classes of Cationic Antimicrobial Peptides with Planar Bilayers and with the Cytoplasmic Membrane of Escherichia coli,* Biochemistry 38:7235–7242.

Xia Q, Guo Y, Zhang Z, Li D, Xuan Z, Li Z, Dai F, Li Y, Cheng D, Li R et al (2009) *Complete Resequencing of 40 Genomes Reveals Domestication Events and Genes in Silkworm (Bombyx),* Science 326: 433-436.

Xu H (2014) *The Advances and Perspectives of Recombinant Protein Production in the Silk Gland of Silkworm Bombyx mori*, Transgenic Research 23: 697-706.

Yang W, Cheng T, Ye M, Deng X, Yi H, Huang Y, Tan X, Han D, Wang B, Xiang Z, Cao Y, Xia Q (2011) *Functional Divergence Among Silkworm Antimicrobial Peptide Paralogs by the Activities of Recombinant Proteins and the Induced Expression Profiles*, PLoS One 6(3):e18109.

Yano T, Mita S, Ohmori H, Oshima Y, Fujimoto Y, Ueda R, Takada H, Goldman WE, Fukase K, Silverman N, Yoshimori T, Kurata S (2008) *Autophagic Control of Listeria Through Intracellular Innate Immune Recognition in Drosophila*, Nature Immunology 9(8): 908-916.

Yeaman MR, Yount NY (2003) *Mechanism of Antimicrobial Peptide Action and Resistance*, Pharmacological Reviews 55:27-55.

Yi H-Y, Chowdhury M, Huang Y-D, Yu X-Q (2014) *Insect Antimicrobial Peptides and Their Applications*, Applied Microbiology and Biotechnology 98(13): 5807–5822.

Yi HY, Deng XJ, Yang WY, Zhou CZ, Cao Y, Yu XQ (2013) *Gloverins of the Silkworm Bombyx mori: Structural and Binding Properties and Activities*, Insect Biochemistry and Molecular Biology 43: 612-625.

Yoshida H, Ochiai M, Ashida M (1986) *β-1,3-glucan Receptor and Peptidoglycan Receptor are Present as Separate Entities within Insect Prophenoloxidase Activating System*, Biochemical and Biophysical Research Communications 141(3): 1177-1184.

Yu X-Q and Kanost MR (2000) *Immulectin-2, a Lipopolysaccharide-specific Lectin from an Insect, Manduca sexta, Is Induced in Response to Gram-negative Bacteria*, Journal of Biological Chemistry 275(48): 37373-37381.

Yu X-Q and Kanost MR (2002) *Binding of Hemolin to Bacterial Lipopolysaccharide and Lipoteichoic Acid. An Immunoglobulin Superfamily Member from Insects as a Pattern-Recognition Receptor,* European Journal of Biochemistry 269: 1827-1834.

Yu X-Q and Kanost MR (2003) *Manduca sexta Lipopolysaccharide-Specific Immulectin-2 Protects Larvae from Bacterial Infection*, Developmental and Comparative Immunology 27: 189-196.

Yu Y, Park JW, Kwon HM, Hwang HO, Jang IH, Masuda A, Kurokawa K, Nakayama H, Lee WJ, Dohmae N, Zhang J, Lee BL (2010) *Diversity of Innate Immune Recognition Mechanism for Bacterial Polymeric meso-Diaminopimelic Acid-type Peptidoglycan in Insects*, Journal of Biological Chemistry 285(43): 32937-32945.

Zanatta DB, Bravo JP, Barbosa JF, Munhoz REF, Fernandez MA (2009) *Evaluation of Economically Important Traits from Sixteen Parental Strains of the Silkworm Bombyx mori L (Lepidoptera: Bombycidae)*, Neotropical Entomology 38(3):327-331.

Zang G, Thomas A, Liu Z, Chen D, Ling H, Zhou L, Zhang F, Siu L, Zheng X (2013) *Preventing Breast Cancer Growth by Cationic Cecropin B,* Biological Systems 2:3, http://dx.doi.org/10.4172/2329-6577.1000112

Zasloff M (2002) *Antimicrobial Peptides of Multicellular Organisms*, Nature 415: 389-395.

Zhang J, Shen ZY, Tang XD, Tang XU, Xu L, Zhu F (2013) *Isolation and Identification of a Pathogen, Providencia rettgeri, in Bombyx mori,* Journal of Bacteriology Research 5(2): 22-28.

Zhang L, Wang YW, Lu ZQ (2015) *Midgut Immune Response Induced by Bacterial Infection in the Silkworm, Bombyx mori*, Biomedicine and Biotechnology 16(10): 875-882.